Thick Filament Protein Network, Functions, and Disease Association

Li Wang,[1] Janelle Geist,[1] Alyssa Grogan,[1] Li-Yen R. Hu,[1] and Aikaterini Kontrogianni-Konstantopoulos[1]*

ABSTRACT

Sarcomeres consist of highly ordered arrays of thick myosin and thin actin filaments along with accessory proteins. Thick filaments occupy the center of sarcomeres where they partially overlap with thin filaments. The sliding of thick filaments past thin filaments is a highly regulated process that occurs in an ATP-dependent manner driving muscle contraction. In addition to myosin that makes up the backbone of the thick filament, four other proteins which are intimately bound to the thick filament, myosin binding protein-C, titin, myomesin, and obscurin play important structural and regulatory roles. Consistent with this, mutations in the respective genes have been associated with idiopathic and congenital forms of skeletal and cardiac myopathies. In this review, we aim to summarize our current knowledge on the molecular structure, subcellular localization, interacting partners, function, modulation via posttranslational modifications, and disease involvement of these five major proteins that comprise the thick filament of striated muscle cells. © 2018 American Physiological Society. *Compr Physiol* 8:631-709, 2018.

Didactic Synopsis

Major teaching points

1. Sarcomeres consist of ordered arrays of thick myosin and thin actin filaments along with accessory proteins.

2. Myosin, the backbone of thick filaments, slides past actin filaments by hydrolyzing ATP to mediate muscle contraction.

3. Four other proteins that are bound to thick filaments play structural and regulatory roles.

   a. Myosin binding protein-C binds to myosin and actin filaments contributing to their stabilization and modulating cross-bridge cycling.

   b. Titin binds to myosin and functions as a scaffold, signaling mediator, and mechanosensor.

   c. Myomesin forms antiparallel homodimers, cross-linking myosin, and contributing to the elasticity of thick filaments.

   d. Obscurin wraps around myofilaments over M-bands, contributing to the maintenance and alignment of thick filaments with internal membranes.

4. The functions of myosin and its accessory proteins are regulated via alternative splicing and posttranslational modifications.

5. Mutations in the respective genes are causatively linked to the development of skeletal and cardiac myopathies.

Introduction

The sarcomere is the smallest contractile unit of the striated muscle cell that is repeated thousand of times to give rise to myofibrils, which assemble into myofibers that comprise the mature muscles (131, 495, 496). One of the most remarkable features of sarcomeres is their austere periodicity created by overlapping arrays of thick myosin and thin actin filaments occupying A- and I-bands, respectively (Fig. 1) (354).

A single thick filament contains >200 perfectly aligned myosin molecules assembled into highly ordered bundles in which the globular motor head domains face outward and the long rod regions face inward forming a bipolar filament (20, 176) (Fig. 1). The subregion of the A-band where thick and thin filaments overlap and actomyosin cross-bridges form is known as the overlap zone. The central subregion of the A-band that is devoid of thin filaments is referred to as the H-zone (223). Contrary to the A-band that remains constant during contraction, the H-zone shortens significantly when sarcomeres are activated and allowed to contract (the shortening distance is similar to that of the I-band). In the middle of the H-zone, there is a vertical line called M-line or M-band that is devoid of myosin heads, and contains accessory proteins that play scaffolding, cross-linking, and regulatory roles (223). For a more detailed description of the structure of thick

*Correspondence to akontrogianni@som.umaryland.edu

[1] Department of Biochemistry and Molecular Biology, University of Maryland, Baltimore, Maryland, USA

Janelle Geist, Alyssa Grogan, and Li-Yen R. Hu contributed equally to the work.

Published online, April 2018 (*comprehensivephysiology.com*)
DOI: 10.1002/cphy.c170023

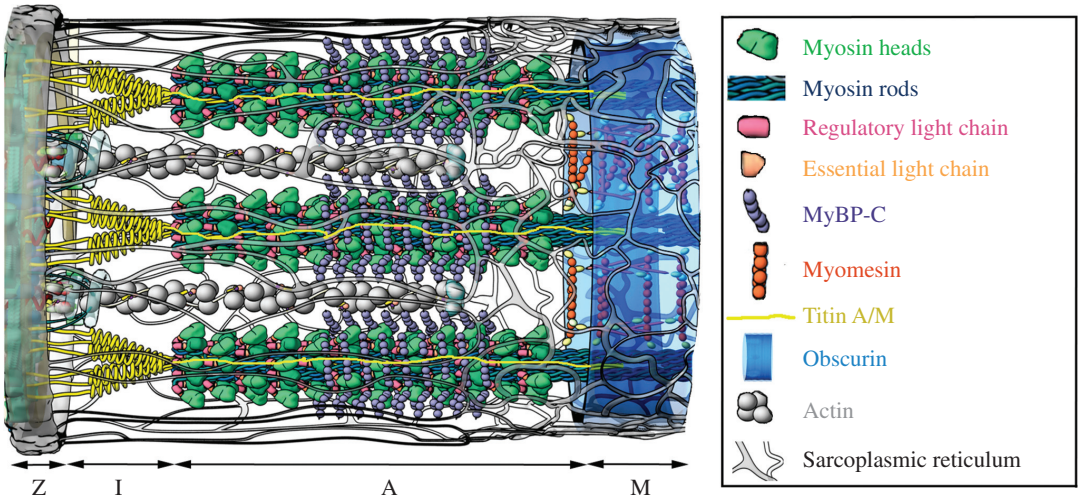

Figure 1 Schematic representation of a half sarcomere depicting the position of the Z-disk, I-band, A-band, and M-band. Myosin thick filaments and associated proteins are shown in color including myosin heads (green), myosin rods (petrol), regulatory light chains (magenta), essential light chains (peach), MyBP-C (purple), myomesin (orange), titin (yellow), and obscurin (light blue), while actin thin filaments and the surrounding sarcoplasmic reticulum are shown in different shades of grey; the structure of the half sarcomere was generated by *e-heart.org* bearing minor modifications.

filaments, readers are directed to two excellent recent reviews (530, 563).

In addition to myosin, a number of other proteins reside in the thick filament playing important structural and regulatory roles. These include: myosin binding protein-C (MyBP-C), titin, myomesin, and obscurin (Fig. 1). Myosin, the backbone of the thick filament, slides past actin thin filaments by hydrolyzing adenosine triphosphate (ATP) to mediate muscle contraction (255, 256). MyBP-C is tightly anchored to the thick filament through binding to both myosin and titin, and modulates the formation and cycling of actomyosin cross-bridges (160, 223, 420, 422). Titin, the largest known protein to date, is intimately bound to myosin along the length of the thick filament, and mainly functions as a scaffold for thick filament assembly (287, 356, 407). Myomesin forms antiparallel homodimers cross-linking myosin molecules within the M-band and contributing to the elasticity of the thick filament (17, 170, 171). Lastly, obscurin, the newest giant protein of muscle cells, contributes to the stabilization of thick filaments into mature A-bands and their alignment with internal membrane systems (287).

In this review, we provide a comprehensive, up-to-date description of the molecular structure and diversity, subcellular distribution, binding partners, functions, posttranslational modifications, and involvement in skeletal and cardiac myopathies of these five major proteins that make up the thick filament of striated muscle cells in vertebrates with an emphasis in mammals.

Myosin

Discovery

Myosin was the first protein purified from muscle cells, originally described as a "proteinous" complex in 1864 (297, 543). Following its original identification, extensive studies focused on its structural determination and physiological roles demonstrating its inherent ability to form thick filaments that slide past actin thin filaments by hydrolyzing ATP, thereby mediating muscle contraction (137, 255, 256, 534). To date, the myosin structure, isoform variability, regulated ATPase activity, and roles in contractility have been excessively interrogated yielding important information but also generating new questions. Below we present a comprehensive review of our current knowledge on mammalian (with an emphasis on human) sarcomeric myosin, its binding partners, and its causative involvement in the acquisition of hereditary myopathies.

Structure, localization, and isoforms

Sarcomeric myosin is a hexameric motor protein composed of two heavy chains (MyHC), two essential light chains (ELCs), and two regulatory light chains (RLCs). Each MyHC comprises a Src homology 3-like (SH3-like) domain, a globular motor "head" domain that bears ATPase activity and binds actin, a converter segment connecting the head domain to the lever arm that binds to ELC and RLC via isoleucine-glutamine (IQ) motifs, and a "tail" that consists of a coiled-coil α-helical region that homodimerizes to form rods, reviewed in (176) (Fig. 2A). Upon limited trypsin digestion, MyHC is fragmented into two parts, heavy meromyosin (HMM), which contains the head region, the converter segment, the lever arm and the NH_2-terminal portion of the α-helical rod domain, and light meromyosin (LMM), which contains the COOH-terminal half of the α-helical rod domain (Fig. 2A). Further cleavage of HMM by papain leads to generation of subfragments 1 (S1) and 2 (S2), with S1 comprising the head domain, the converter segment, and the lever arm, and S2 containing the NH_2-terminus of the α-helical rod domain (Fig. 2A). The

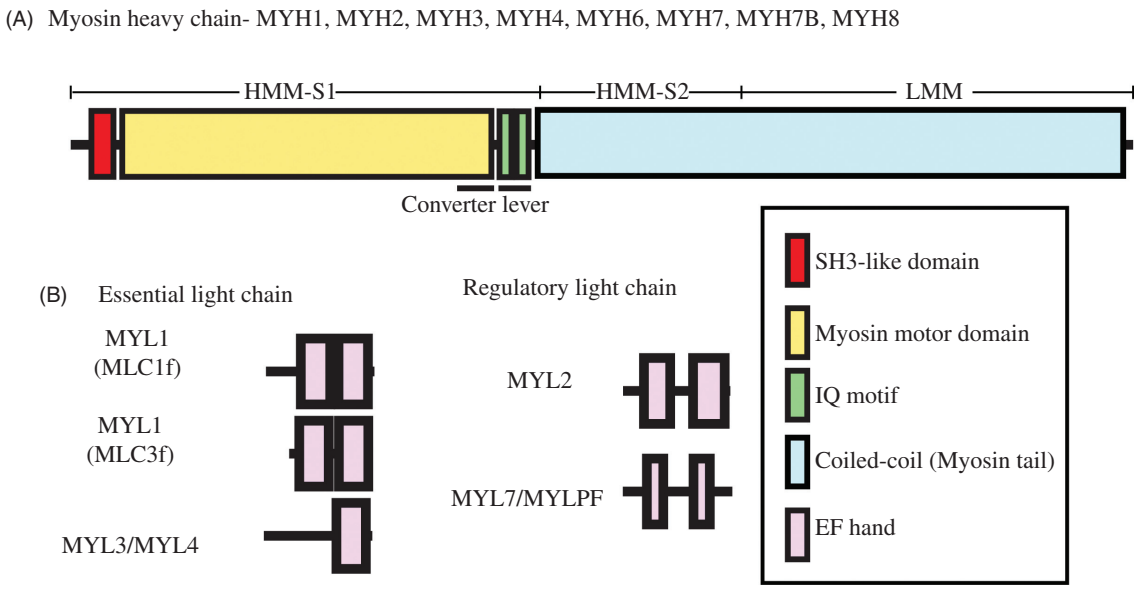

Figure 2 Domain organization of MyHC, ELC, and RLC. (A) The NH_2-terminus of sarcomeric MyHC contains an SH3-like domain, followed by the motor head domain containing the converter segment, a lever arm consisting of two IQ motifs, and a coiled-coil region. Proteolytic cleavage of MyHC yields three fragments: HMM-S1, HMM-S2, and LMM. The S1 segment contains the SH3-like domain, the motor head domain and the lever arm. The S2 and LMM fragments contain the NH_2- and COOH-terminal portions of the coiled-coil region, respectively. (B) Both ELC and RLC contain EF-hand motifs. ELC isoforms may contain two EF-hand motifs, such as MYL1, or one EF-hand motif, such as MYL3 and MYL4; however, all RLC isoforms carry two EF-hand motifs, with MYL2 containing longer EF-hand motifs compared to MYL7 and MYLPF.

head region contains the ATP binding site, and is composed of a core of seven-stranded β-sheets surrounded by 17 α-helices and 10 β-strands (105). ATP binding is mainly mediated by the central ~50 kDa region of the globular head, which is further divided into upper and lower subregions. The cleft that is formed between the upper and lower subregions contains the ATP binding site (393, 469). Importantly, ATP binding to the head domain is coupled with the opening of the actin binding cleft, described in detail in (279). The converter segment is connected to the head domain via a long α-helix, called relay helix. The interface of the converter segment and the relay α-helix is important in fine-tuning ATP binding and hydrolysis, as mutations in this region alter the kinetics of these events (58). Moreover, both ELC and RLC are primarily composed of α-helices and contain one or two EF-hand motifs mediating binding to the IQ motifs of MyHC (Fig. 2B) (476). While little is known about the regulation of ELC, RLC is regulated via complex phosphorylation/dephosphorylation events, which in turn influence the conformation of HMM and ELC, and therefore the catalytic and mechanical activities of myosin (413) and recently reviewed in (231, 232).

In striated muscle cells, myosin forms the backbone of the thick filaments, which are anchored within the M-band and extend bidirectionally toward the two opposite ends of the sarcomere (171, 247). Under the light microscope, myosin filaments appear as dark thick stripes, mainly due to their high degree of compactness, occupying A-bands. While A-bands contain HMM and part of the tail of myosin filaments including S1 and S2, M-bands are devoid of myosin heads and encompass overlapping arrays of antiparallel myosin rods making up LMM.

To date, 35 distinct myosin families have been characterized in mammalian genomes (581). Herein, we will focus on the myosin isoforms that are expressed in striated muscles and discuss their preferential expression during embryogenesis and at maturity.

MyHC isoforms

Eight different gene loci have been identified for MyHC across mammalian striated muscles during development and in adulthood (Table 1; Fig. 2A). Human cardiac muscle expresses two main types of MyHC, α and β, encoded by *MYH6* and *MYH7*, respectively. Recently though, an additional isoform was described that is encoded by the *MYH7b* gene (also called MYH14) (589); however, the expression profile and role of *MYH7b* in mediating cardiac contractility remain to be examined. MYH6 and MYH7 are expressed in embryonic human heart at 31 to 35 days *in utero* and persist during adulthood with MYH6 predominantly expressed in atria with minimal expression in ventricles (~7%), and MYH7 primarily expressed in ventricles (379, 474, 598), reviewed in (359). In developing mouse heart, both Myh6 and Myh7 are expressed evenly in ventricles at E11.5 (622); however, the expression of Myh6 is restricted to the right ventricle at E15.5 (622). At maturity, mouse hearts preferentially express Myh6 in both atria and ventricles (344, 519), whereas rat hearts express Myh6 and Myh7 in ventricles, and Myh6 in atria (123, 150).

Table 1 Predominant Myosin Isoforms Expressed in Human Striated Muscles

Type	Gene	Protein name	Predominant expression in muscle
Myosin heavy chain	MYH1	MyHC-2X	Fast-twitch skeletal muscle (Type IIx)
	MYH2	MyHC-2A	Fast-twitch skeletal muscle (Type IIx/IIa)
	MYH3	MyHC-embryonic	Embryo
	MYH4	MyHC-2B	Fast-twitch skeletal muscle (Type IIb)
	MYH6	α-MyHC	Atria
	MYH7	β-MyHC	Cardiac ventricles; slow-twitch skeletal muscle (Type I)
	MYH7B	MYH7b, MYH14	Heart
	MYH8	MyHC-perinatal	Fetal skeletal muscle
Essential light chain (Alkaline light chain)	MYL1	MLC1f; MLC3f	Fast-twitch skeletal muscle
	MYL3	VLC1; MLC1V	Cardiac ventricles; slow-twitch skeletal muscle
	MYL4	ALC1	Atria; embryonic cardiac ventricles and skeletal muscle
Regulatory light chain	MYL2	MLC-2	Heart; skeletal muscle
	MYL7	MYL7; MYL2A; MLC-2a	Atrial; embryo
	MYLPF	MYLPF; MRLC2; MLC2B; MYL11; MLC-2f	Fast-twitch skeletal muscle

Given that Myh6 confers faster contractions whereas Myh7 maintains tension more efficiently due to its slower ATPase activity (333, 346, 484), the faster heart rate in rodents unsurprisingly requires higher amounts of Myh6 in the ventricles. In human heart failure patients, the expression of MYH6 is greatly diminished to nearly undetectable levels, while the expression of MYH7 is significantly upregulated, possibly as a compensatory response (5, 334, 335, 379).

The MyHC expression profile is more complex in skeletal muscles (for a comprehensive review on the expression of myosins during muscle development readers are referred to reference (501). MYH3, referred to as the embryonic MyHC isoform, is encoded by *MYH3*. MYH3 is mainly expressed in human embryonic limb muscles as early as in week 8 of gestation, but disappears 2 weeks after birth (39, 100, 595). In addition to MYH3, MYH7 is also expressed in embryonic human skeletal muscles, as early as weeks 6 to 10 of gestation (39, 100, 254), along with perinatal MYH8, whose presence is detectable at week 9 postgestation (501). Similarly, in mouse, expression of Myh3, Myh7, and Myh8 has been reported at E10 (343, 579). Myh3 declines to undetectable levels by P21, whereas Myh8 is still expressed at this time, but disappears in adulthood (19). Contrary to Myh3 and Myh8, Myh7 is expressed throughout adulthood (19). Myh3 and Myh7 are expressed in primary myotubes, but Myh8 may replace Myh7 in secondary myotubes (107, 410, 482, 579).

In adulthood, skeletal muscles are classified as slow or fast depending on the predominant MyHC that they express, although additional MyHC isoforms may also be expressed, albeit in low amounts (403,536). Fast-twitch skeletal myofibers are subclassified as Type-IIx, -IIb, and -IIa, and primarily express MyHC-2X encoded by *MYH1*, MyHC-2B encoded by *MYH4*, and MyHC-2A encoded by *MYH2*, respectively, recently reviewed in (501, 581). Similar to cardiac ventricles, slow-twitch skeletal myofibers (Type-I) mainly express MYH7, along with low levels of MYH1, MYH2, MYH4, and MYH6 (403, 536). MYH7b is also expressed in skeletal muscles, but in low levels (479, 589).

Although sarcomeric MyHCs share >80% sequence identity, their enzymatic properties, including ATP consumption and hydrolysis rate, adenosine diphosphate (ADP) release rate, attachment time to actin, contraction rate, tension cost, and power output vary considerably (57, 70, 218, 226, 500, 518, 536, 581). Generally, fast-twitch muscles exhibit intense power output with high-contraction rate mediated by fast ATPase hydrolysis; they are therefore suitable for short bursts of contractility under anaerobic conditions (536, 581). Conversely, slow-twitch muscles display slow(er) shortening velocity and reduced ATP usage compared to fast-twitch muscles, thereby sustaining tension for longer periods of time (581).

ELC isoforms

Three different gene loci have been described for ELC in mammalian striated muscles. These include the fast ELC, the slow/ventricular ELC, and the atrial ELC encoded by *MYL1*, *MYL3*, and *MYL4*, respectively, Figure 2B; (138, 536). ELCs bind to the first IQ motif of MyHC present in the lever arm via their EF-hand motifs (73, 470). MYL1 and MYL3 are expressed in both fast- and slow-twitch skeletal muscles but at different ratios with MYL1 being the main isoform in fast-twitch muscles, and MYL3 in slow-twitch and ventricular muscles (536). Moreover, while MYL4 is the main isoform in atria, it is also expressed in skeletal muscles and ventricles during embryogenesis (343, 344, 452).

MYL1 is alternatively spliced giving rise to two variants, myosin light chain (MLC) 1f and MLC3f, which differ in their NH_2-termini mediating binding to the COOH-terminus of actin (Fig. 2B) (408,434,541,559). MYL3 and MYL4 share considerable homology (80.1% identity and 90.3% similarity); however, they exhibit distinct affinities to myosin and actin with MYL3 binding more efficiently to actin and MYL4 to MyHC (438, 439). MYL4 is upregulated in the ventricles of patients with tetralogy or trilogy of Fallot, double-outlet right ventricle disease, infundibular pulmonary stenosis, and

hypertrophic cardiomyopathy (HCM) or dilated cardiomyopathy (DCM) (30, 388, 390, 499). Skinned cardiac muscle fibers from these patients exhibit enhanced Ca^{2+} sensitivity, accelerated shortening velocity, and faster tension development (388, 390), similar to skinned ventricular fibers from transgenic mice overexpressing Myl4 (144). Consistently, overexpression of human MYL4 in rat hearts subjected to aortocaval shunt operation resulted in attenuation of heart failure (3), while replacement of Myl3 by human MYL4 in adult rat cardiomyocytes led to accelerated contractility kinetics without altering Ca^{2+} signaling (438). Thus, upregulation of MYL4 may serve as a compensatory mechanism to enhance cardiac contractility in patients with different types of cardiomyopathy possibly by reducing the binding affinity between ELC and actin therefore enabling faster actomyosin contractions.

RLC isoforms

There are three gene loci encoding RLC isoforms in mammalian striated muscles, including atrial, ventricular/slow skeletal, and fast skeletal encoded by the *MYL7*, *MYL2*, and *MYLPF* genes, respectively (Fig. 2B). RLCs bind to the second IQ motif present in the lever arm of MyHC via their EF-hand motifs (470).

MYL7 is ubiquitously expressed throughout the linear heart tube during development; however, in adulthood, its expression is restricted to the atria (296). Homozygous Myl7 knockout mice exhibit embryonic lethality at E10.5-E11.5 (251). Evaluation of isolated embryos revealed that they contain enlarged amorphous heart tubes at E8.5, which exhibit major defects in the atria manifested as impaired myofibrillar organization and reduced contraction by E9.5, underscoring the key role of Myl7 in cardiac atrial development (251).

MYL2 is expressed during early embryogenesis (i.e., E9.5), and persists at maturity preferentially localizing in the ventricular myocardium (158) and slow-twitch skeletal muscles (56, 319). Homozygous Myl2 knockout mice exhibit structural and contractile defects, and develop DCM, eventually dying at E12.5 (97). Although Myl7 is upregulated in the Myl2-null hearts, it does not compensate for the loss of Myl2 (97). Patients homozygous for frameshift mutations in *MYL2* exhibit sarcomeric disarray and miniaturized Type-I myofibers, but normal size Type-II myofibers, and die of cardiomyopathy (mainly DCM, but may carry features of other forms, such as HCM, restrictive or noncompaction cardiomyopathy) (599).

Lastly, myosin light chain phosphorylable fast skeletal muscle (MYLPF), also known as HUMMLC2B, is selectively expressed in fast skeletal muscles, although it is also present in slow skeletal and cardiac muscles, but in low amounts (500, 536). Homozygous *Mylpf* knockout mice fail to form functional skeletal muscles, and die immediately after birth, possibly due to abnormal diaphragm muscles and respiratory issues (588).

Binding partners

In addition to its well-characterized interaction with actin during the generation of power stroke (please see below), myosin forms stable or transient interactions with proteins involved in different molecular pathways. This section will focus on binding partners of myosin in striated muscles (Fig. 3), by grouping them according to their roles and/or subcellular location.

Proteins modulating contractility

Actin (~42 kDa). Actin makes up the thin filaments of striated muscle cells, recently reviewed in (171). It contains two domains, small and large, and an ATP binding pocket located in the cleft of the two domains (268). Each small and large actin domain consists of two subdomains; subdomains 1 and 2 are present in the small domain, and subdomains 3 and 4 are present in the large domain (268). Actin subdomains 1 and 3 bind to the myosin S1 fragment (48, 105, 323, 378, 540).

Actin also interacts with ELC isoforms via its COOH-terminus (389, 541, 559). Specifically, the NH_2-terminus of MLC1f contains a ~45-amino acid long insertion that is positively charged due to its high Lys content, which is absent from MLC3f (159, 225). The presence of this insertion enhances the binding affinity of MLC1f for actin (approximately fourfold) compared to MLC3f, and increases the catalytic efficiency (V_{max}/K_{ATPase}) of MyHC (approximately fourfold), but reduces the ATPase activity (V_{max}) of the S1 fragment (~60%) (212). Deletion or Ala substitution of this insertion leads to faster cross-bridge kinetics, resembling MLC3f (225, 542).

Similar to the MLC1f and MLC3f isoforms, the NH_2-termini of MYL3 and MYL4 also interact with actin, with MYL3 exhibiting a higher binding affinity than MYL4 (387, 439, 552, 553). Several studies reported that deletion of the first 43 amino acids of MYL3 results in reduced contractile force per cross-sectional area, diminished isometric tension and stiffness, and reduced length dependence of Ca^{2+} sensitivity in isolated papillary muscles (277, 371, 585). Other studies indicated that abrogation of the binding between the NH_2-terminus of MYL3 and actin leads to faster contractility kinetics in skinned human cardiomyocytes and mouse papillary muscle strips (389, 466, 585) or has no effect on shortening velocity in mouse papillary muscle strips (375). Thus, although the exact role of the interaction between actin and the different ELC isoforms is still elusive, it is apparent that it contributes to the regulation of actomyosin contractility as a function of the physiological demands of the muscle in which they are expressed.

MyBP-C (120-140 kDa) and MyBP-H (~52 kDa). MyBP-C and MyBP-H were first extracted from striated muscles in 1973 as impurities in myosin preparations (33, 420), whereas later studies demonstrated that they are interacting partners of sarcomeric myosin (119, 183, 386, 422). MyBP-C and MyBP-H are modular proteins consisting of tandem immunoglobulin (Ig) and fibronectin-III (FnIII) domains interspersed with unique sequences (134, 575, 576, 594). There are three

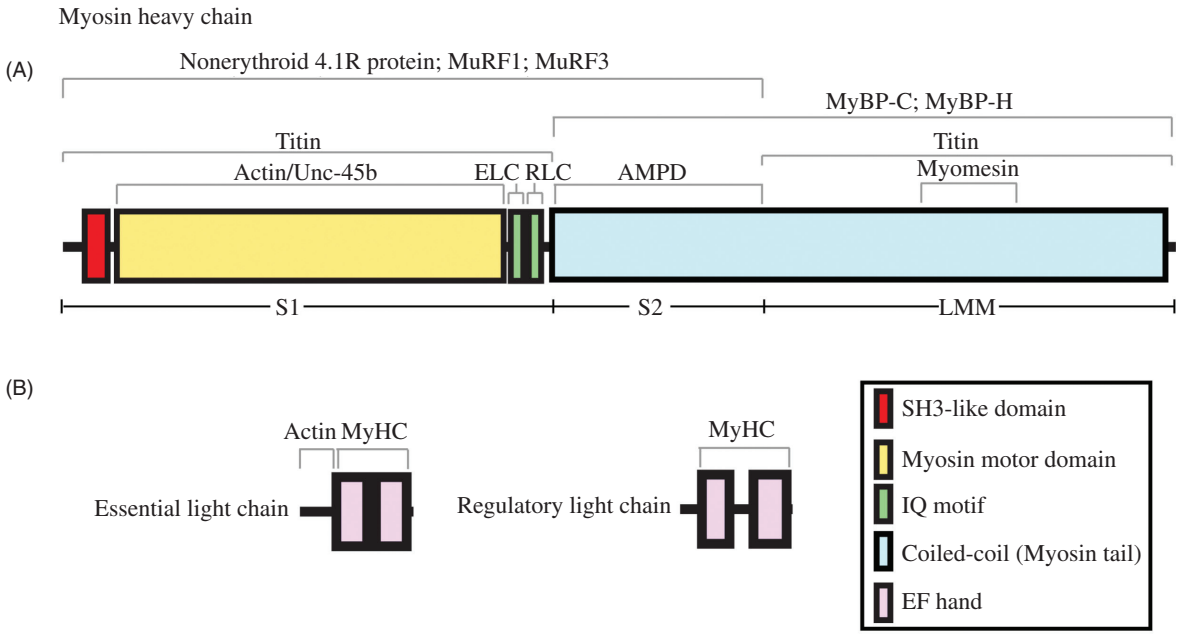

Figure 3 Binding partners of myosin heavy and light chains in striated muscles. (A) A number of interacting partners have been identified for MyHC, including actin binding to the motor head domain, MyBP-C and MyBP-H binding to the coiled-coil region containing both the S2 and LMM fragments, myomesin binding to the coiled-coil LMM region, titin binding to S1 and LMM, nonerythroid 4.1R, MuRF1 and MuRF3 binding to HMM, and AMPD binding to S2. ELC and RLC bind to the NH_2- and COOH-terminal IQ motifs of MyHC, respectively, via their EF-hand motifs. Although Akt2, HspB2, and caspase-3 interact with MyHC, the exact binding sites have not been characterized yet. (B) The binding partners of ELC and RLC are less studied; ELC interacts with actin via its nonmodular NH_2-terminus, and RLC interacts with cardiac MyBP-C, MuRF1, and MuRF2, however the exact binding sites have yet to be determined.

MyBP-C isoforms including cardiac, slow skeletal, and fast skeletal. While the cardiac isoform is restricted to cardiac muscle (172, 302), the skeletal isoforms may coexist in different skeletal muscles (9, 12, 172, 302, 326). The extreme COOH-terminal Ig8-FnIII9-Ig10 cassette of MyBP-C and MyBP-H supports binding to the LMM portion of MyHC (183, 422). Moreover, the NH_2-terminus of MyBP-C, specifically the Pro/Ala rich motif and M-motif flanking Ig domain C1, interacts with the S2 fragment of MyHC (153, 207, 208, 386). Unique to the cardiac isoform, Ig-C0 interacts specifically with MYL2 (467). While the interaction of the COOH-terminus of MyBP-C with LMM is constant, the interaction of the NH_2-terminus with myosin S2 is dynamic and regulated in a complex manner via phosphorylation (please see below).

Contrary to MyBP-C, little is known about MyBP-H. MyBP-H is preferentially expressed in fast-twitch skeletal muscles and the Purkinje fibers of cardiac muscle (21,33,50). Interestingly, the expression levels of MyBP-H are increased in the gracilis or vastus lateralis skeletal muscles of patients with amyotrophic lateral sclerosis (ALS), however the physiological significance of these observations are unknown (109). Recently, linkage disequilibrium analysis of MYH7 mutations associated with HCM and single nucleotide polymorphisms (SNP) in *MYBPH* described an association between increased left ventricular wall thickness in patients carrying the *MYH7* A797T mutation and the *MYBPH* SNP rs2250509 (396). However, the exact mechanism of how the *MYBPH* SNP rs2250509 exacerbates left ventricular wall thickness in patients containing the *MYH7* A797T mutation is currently unknown.

Cytoskeletal proteins

Myomesin and M-protein (165-188 kDa). Myomesin and M-protein consist of Ig and FnIII domains, and both localize at the sarcomeric M-band, reviewed in (247). Myomesin interacts with the central LMM region of myosin via its NH_2-terminal My1 domain (418), contributing to the assembly and incorporation of myosin into A-bands during myofibrillogenesis (163). It has been speculated that the disordered nature of My1 allows it to adopt an extended and flexible conformation that enables its interaction with the bulky myosin filaments. Consistent with this, myomesin anchors myosin filaments in an angular position and maintains the regularity of the A-band lattice (17). Although My1 binds specifically to myosin, it is not sufficient to target myomesin to M-bands (31). Indeed, ectopic expression of myomesin fragments in neonatal rat cardiomyocytes (NRCs) revealed that the Ig domain My2 is necessary (and sufficient) for the incorporation of myomesin into M-bands, likely due to its interaction with a yet unidentified M-band protein (31).

Contrary to myomesin that binds to LMM via My1, M-protein binds to LMM via Ig domains My2-My3 (419). Interestingly, the interaction between LMM and M-protein is negatively regulated by protein kinase A (PKA)-mediated

phosphorylation of Ser76 located in My1 (419). This finding suggests that My1 may also contribute to the interaction between M-protein and LMM (similar to myomesin) or that phosphorylation of My1 may induce a conformational change to the My2-My3 region precluding it from binding to LMM. Further evaluation of the ability of different portions of M-protein to target to M-bands indicated that My2-My3 (i.e., the LMM binding site) and My9-My13 independently mediate targeting of M-protein to M-bands (419).

Titin (~3-4 MDa). Titin is a giant protein with a molecular weight of 3 to 4 MDa. A single titin molecule spans a half sarcomere with its NH_2-terminus anchored to the Z-disk and its COOH-terminus to the M-band (164, 209, 287, 329). The A-band region of titin (~2 MDa) is composed of two types of super repeats made up of tandem Ig and FnIII domains (168, 287). The first super repeat contains seven domains, Ig-$(FnIII)_2$-Ig-$(FnIII)_3$, resides in the D-zone (comprising the ends of thick filaments), and is repeated six times, while the second super repeat contains 11 domains, Ig-$(FnIII)_2$-Ig-$(FnIII)_3$-Ig-$(FnIII)_3$, localizes in the C-zone (defined by the presence of MyBP-C), and is repeated 11 times (287, 306, 398). Interestingly, the 11-domain super repeat shows a ~43 nm periodicity, which corresponds well to the periodicity formed by myosin heads and MyBP-C in the C-zone (51, 287, 340). It has therefore been proposed that titin may serve as a blueprint to determine the regular organization of staggering myosin heads and MyBP-C. Consistent with this, the interaction between myosin and titin in the A-band takes place within minutes after they are synthesized, as shown by pulse-labeling and immunoprecipitation assays (259). Both the S1 and LMM regions of myosin interact with the FnIII domains of titin in the A-band, as demonstrated by cosedimentation and solid phase binding assays (51, 246, 259, 398, 586). The interaction between LMM and titin, however, is weaker than the interaction between the S1 fragment and titin (398). Accordingly, it has been postulated that the S1/titin interaction promotes the assembly and regular incorporation of thick filaments into A-bands, enhances the myosin ATPase activity *in vitro*, and contributes to the regulation of force production (280, 287, 398). Given that titin is a major structural component of the thick filament, it will also be discussed below in more detail.

Nonerythroid protein 4.1R (66-97 kDa). Protein 4.1R was originally identified as a peripheral protein in erythrocytes, but later it was shown that it is ubiquitously expressed in all tissues and organs (34). Protein 4.1R contains a nonmodular NH_2-terminus, a middle 4.1/ezrin/radixin/moesin (FERM) domain, a FERM-adjacent domain, and a COOH-terminal spectrin-actin binding domain (SAB) (34). In the heart, protein 4.1R localizes at the sarcolemma, is enriched at the intercalated disc, and is also present at Z-disks (444, 550). However, in skeletal muscles, protein 4.1R preferentially localizes to the C-zone of the A-band where it interacts with HMM via its SAB domain (292). Recently, it was shown that downregulation of protein 4.1R in mouse C2C12 skeletal myoblasts results in delayed myogenic differentiation and reduced levels of MyHC and light chains (252). However, the exact functional significance of the HMM/4.1R binding in skeletal muscles remains unknown.

Kinases

Protein kinase B (PKB)/Akt2 (49-56 kDa). PKB/Akt2 localizes in both the cytosol and the sarcolemma in rat skeletal myotubes (623). It contains a pleckstrin-homology (PH) domain at its NH_2-terminus and a kinase domain at its COOH-terminus. Akt2 directly binds to MyHC via its PH domain (546). In the presence of increasing amounts of phosphatidylinositol-4,5-bisphosphate ($PI(4,5)P_2$), myosin binding to Akt is competitively inhibited (546). Overexpression of a dominant negative form of Akt in chicken embryonic myoblasts demonstrated that Akt activity is required to induce myoblast differentiation and expression of MyHC (265). Although the interaction of Akt2 and myosin has been identified for nearly two decades, its exact physiological significance is still unknown.

Metabolic enzymes

Adenosine monophosphate deaminase 1 (*AMPD1, ~90 kDa)*. While the thick filament is home to many metabolic enzymes, recently reviewed in (247), AMPD1 is the only known metabolic enzyme that directly binds to myosin (28). AMPD1 binds to myosin during muscle contraction, and catalyzes the removal of an amine group from adenosine monophosphate (AMP) generating inosine monophosphate (IMP) (483). The central nonmodular region of AMPD1 (amino acids 178-333) mediates binding to the S2 fragment of myosin (28, 236). Since myosin ATPase requires large amounts of ATP to perform repetitive contractions, ATP is supplied by glycolysis, oxidative respiration, or adenylate kinase-mediated ATP synthesis at the M-band (310), reviewed in (247). Adenylate kinase mediates ATP synthesis by transferring a phosphate group from ADP to another ADP generating AMP and ATP as final products. Conversion of AMP to IMP by AMPD1 results in reduced AMP levels, allowing ATP synthesis to occur by adenylate kinase. Thus, the presence of AMPD1 is essential for maintaining the constant production of ATP via adenylate kinase during repeating contractions.

Molecular chaperones

Heat shock protein B2 (*HspB2, ~20 kDa)*. Molecular chaperones are proteins that promote refolding of denatured proteins (250), recently reviewed in (38). Among them, HspB2 was recently identified as an interacting partner of MYH6 and MYH7 in a yeast-two-hybrid screen (202). HspB2 mainly localizes at the interface of Z-disks and I-bands and the intercalated disc (185, 512). It is therefore likely that HspB2 binding to MYH6 and MYH7 is transient and takes place during stress to mediate myosin refolding. Conversely, it is possible that minute amounts of HspB2 are stably bound to myosin

filaments. Further work needs to be done to examine these possibilities.

Uncoordinated mutant number-45 (Unc-45, ~105 kDa). *Unc-45* is also a myosin chaperone first identified in *Caenorhabditis elegans* (*C. elegans*) that contains an NH_2-terminal tetratricopeptide repeat domain, a central domain, and a COOH-terminal UNC-45/CRO1/SHE4 (UCS) domain comprised of armadillo repeats (44, 317). Chaperones carrying the UCS domain are myosin-specific (22, 43), aiding the folding of the myosin head during differentiation and protecting myosin from denaturation during stress, such as heat-induced aggregation (317). While invertebrates express one *Unc-45* protein, vertebrates express two, *Unc-45a* that is present in general cell types and *Unc-45b* that is specifically expressed in striated muscle cells (453). Extensive biochemical and biophysical work has shown that *Unc-45b* binds to the myosin head domain via its central and UCS domains (72). Gain and loss of function experiments using *in vitro* and *in vivo* models demonstrated that while *Unc-45a* is critical for cell proliferation and fusion, *Unc-45b* is essential for myoblast fusion and sarcomeric organization (317,453,577,606). Consistent with the key role of *Unc-45b* in striated muscles, mice carrying loss-of-function *Unc-45b* mutations exhibit cardiac development arrest, heart failure, and embryonic lethality, despite the presence of normal levels of *Unc-45a*, likely due to decreased accumulation of myosins and thus defective contractility (96).

Ligases mediating proteasomal degradation

Muscle RING finger proteins (MuRFs, 40-60 kDa). MuRFs are E3 ubiquitin ligases preferentially expressed in striated muscles (59, 87, 524). They contain an NH_2-terminal really interesting new gene (RING) finger domain, a B-box zinc finger motif, a coiled-coil segment, and a nonmodular acidic COOH-terminus, reviewed in (361). By mediating substrate recognition and transferring ubiquitin chains to their substrates to mark them for proteasomal degradation, MuRFs are essential for maintaining the structural and molecular organization of sarcomeres (145,146,366). Coimmunoprecipitation and ubiquitination assays showed that MuRF1 and MuRF3 interact with both the S1 and S2 domains of MYH7 and MYH2, and mediate their degradation (145). Knockout mice deficient in both MuRF1 and MuRF3 develop myosin storage myopathy characterized by myosin accumulations and diminished force generation in skeletal muscles as well as HCM also presenting with myosin aggregates and disoriented thick filaments in the heart (145). Consistent with these findings, myosin accumulations were observed in a patient with compound mutations in *TRIM63* and *TRIM54* genes, encoding MuRF1 and MuRF3, respectively (424). A yeast-two-hybrid screen identified MuRF1 and MuRF2 as interacting partners of MYL2, too (605). Notably, MuRF1 and MuRF2 double knockout mice experience loss of type-II fibers accompanied by an increase in type-I fibers in soleus muscle, but not in tibialis anterior muscle (392). The increase in type-I and loss of type-II fibers may be due to accumulation of MYH7 and MYL2, which is consistent with MYH7 and MYL2 being the predominant MyHC and RLC isoforms, respectively, in type-I fibers (392, 403, 501, 536). Given that accumulation of myosin aggregates leads to myopathy (145), the association of the myosin hexamer with the MuRF family is essential for its regulated degradation, and thus for the maintenance of muscle structure and function.

Apoptotic proteins

Caspase-3 (~32 kDa). During apoptosis, cysteine proteases known as caspases dismantle subcellular structures by fragmenting individual proteins, recently reviewed in (498). Once the apoptotic cascade is initiated, caspase-3 is activated by cleavage and removal of its NH_2-terminal prodomain (219, 532). Activated caspase-3 in turn activates downstream caspases, resulting in massive proteolysis and DNA fragmentation (498). MYL3 is a substrate of caspase-3 in the heart, as evidenced by its caspase-3 mediated fragmentation in a rabbit heart failure model induced by rapid pacing (391). However, in heart failure patients MYL3 expression and cleavage were indistinguishable from controls, even though caspase-3 activity was significantly upregulated (67). Thus, further studies are required to elucidate whether cleavage of MYL3 by caspase-3 is experimentally induced and/or species specific.

Functions

Generation of power stroke

During muscle contraction, actin thin filaments slide past myosin thick filaments resulting in sarcomeric length shortening (527). This is a highly regulated process mediated by thin and thick filament accessory proteins. At rest, binding of tropomyosin (Tm) and troponin-I (TnI) to actin precludes its binding of myosin, while troponin-T (TnT) interlocks the Tn/Tm complex and actin, and contributes to the cooperative activation of thin filaments in response to Ca^{2+}, reviewed in (188) (186, 187, 348). In response to depolarization, Ca^{2+} released from the sarcoplasmic reticulum (SR) binds to troponin-C (TnC) resulting in displacement of TnI and Tm from the actin filament, and enabling its interaction with the motor head domain of myosin, reviewed in (350).

The conventional view of the actomyosin interaction postulates that it is solely induced by conformational changes of the thin filaments in response to increased sarcoplasmic Ca^{2+} levels, reviewed in (138, 188). However, recent studies suggest that both thin and thick filaments undergo structural alterations to accommodate actomyosin binding (please see below) (167, 327, 472, 612). During active contraction, ATP binding to HMM is coupled with the opening of the actin binding cleft, described in detail in (279), resulting in detachment of the globular myosin head domain from actin (108,239,376) (Fig. 4A). A recovery stroke takes place in response to the conformational strain imposed by ATP binding to myosin, leading to rotation of the converter domain by 65º (Fig. 4B)

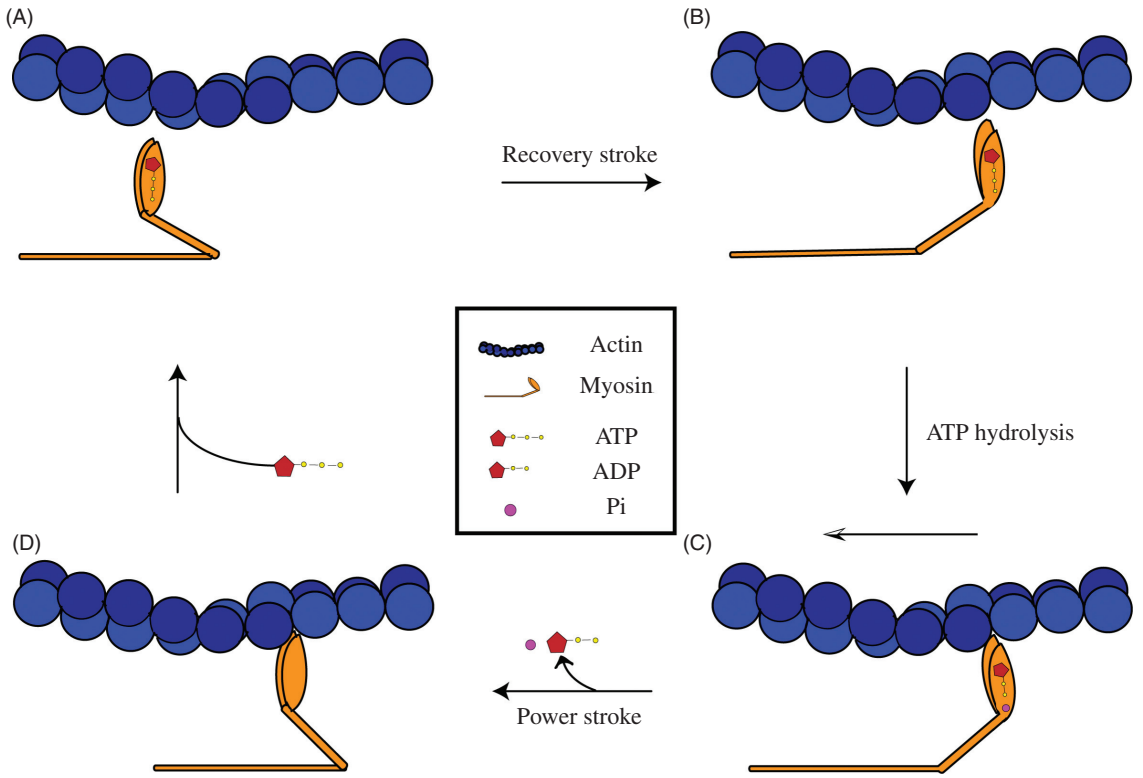

Figure 4 Schematic representation of the generation of power stroke. (A) Actomyosin interaction is inhibited upon binding of ATP to myosin. At this stage, the myosin ATPase site is partially open and inactive. (B) During recovery stroke, the converter segment of myosin is subjected to a 65° rotation resulting in closing of the myosin ATPase site and ATP hydrolysis. (C) While the hydrolysis products, ADP and inorganic phosphate, are still bound to the myosin globular head domain, the head domain weakly associates with actin and triggers the release of inorganic phosphate. Concomitantly, conformational changes of the head domain lead to enhanced actin binding, followed by release of ADP, the generation of power stroke, and muscle contraction. (D) The globular head domain of myosin is still attached to actin postpower stroke awaiting the addition of another ATP molecule and the initiation of a new cycle.

(279). This rotation allows ATP hydrolysis to take place due to closure of the ATP binding site, enabling the initial weak electrostatic association of actin and myosin (148,279). Once ATP is hydrolyzed and myosin is weakly bound to actin through the lower ~50 kDa domain (Fig. 4C) (48), HMM alters conformation triggering the release of inorganic phosphate (188). This results in a ~16° rotation of the upper ~50 kDa domain (48, 332) leading to enhanced actomyosin binding, mediated by both stereospecific and electrostatic interactions between the two filaments (332). Concomitant with the release of ADP, the lever arm undergoes a conformational change resulting to generation of power stroke and muscle contraction; it is worth noting, however, that recent studies debate whether inorganic phosphate is released before or after the generation of power stroke (78,79,118,245,373,401,402). Following ADP release, actomyosin is ready to undergo another round of cross-bridge cycling following binding and hydrolysis of a new molecule of ATP (Fig. 4D), recently reviewed in (211).

Recent studies have suggested that myosin exists in three states in skeletal muscle: activated, conventionally relaxed (CRX), and super-relaxed (SRX), recently reviewed in (368). In the SRX state, myosin heads are arranged almost parallel to the thick filament with a 14.34 nm periodicity, and exhibit a 10-fold lower ATPase activity compared to the CRX state (271,328,472,533,626). In the CRX state, myosin heads extend perpendicularly from the thick filament, but are blocked from interacting with actin due to the Tn/Tm complex (166). Notably, even when myosin filaments are in the SRX state, ~10% of myosin heads still adopt a CRX conformation (166,472). During unloaded (no mechanical force) or low load (small amount of mechanical force) shortening, only a subset of myosin heads supports contraction (327, 443), but their periodicity remains 14.34 nm as in resting states (327). Conversely, in response to high load (large amount of mechanical force), the thick filament helix switches to the activated state, and assumes a less-packed topography with myosin heads exhibiting a 14.57 nm periodicity (167, 327, 328). This periodicity shift from 14.34 nm (in the relaxed state) to 14.57 nm (in the activated state) is independent of Ca^{2+} concentration, and has been attributed to mechanical forces alone (167,327). Interestingly, activated skeletal muscle does not contain any myosin in the SRX state (110, 533). On the contrary, cardiac muscle always contains a subpopulation of myosin heads in the SRX conformation even during contraction (241), which may possibly have a cardioprotective role during stress (368).

Posttranslational modifications

Numerous studies have demonstrated that the myosin complex undergoes extensive posttranslational modifications (PTM) (Fig. 5, Tables 2-5), regulating its binding, enzymatic, and contractile properties. Below we provide a synopsis of the main PTM that myosin undergoes, and their effects (if known) on sarcomeric contractility. A listing of all (known) residues in MyHC, ELC, and RLC undergoing PTM is included in Tables 2 to 5; however, we only discuss select ones that have been biochemically or functionally studied.

Acetylation

Acetylation of myosin was first observed in 1983 (556). A number of acetylation sites have been identified on MyHC, ELC, and RLC (338, 487, 494), however little is known about their effects. Nevertheless, a recent study demonstrated that acetylation of purified Myh6 and Myh7 results in 20% and 36% increase in the sliding velocity of actin filaments in *in vitro* motility assays, respectively (494). Consistent with this, muscle disuse-induced atrophy of rat soleus and plantaris muscles leads to decreased acetylation of Myh7 and Myh2 (487). Taken together, these studies therefore suggest that acetylation of MyHC may enhance sarcomeric contractility.

Arginylation

Arginylation of sarcomeric components is essential for muscle formation and contractility; for a recent review, please see reference (321). Mass spectrometry has identified several arginylation sites in MYH2, MYH4, MYH6, and MYH7 (112, 303). Cardiac myofibrils prepared from ventricles of cardiac-specific knockout mice lacking arginyl-tRNA-transferase (Ate1), the enzyme responsible for arginylation, exhibited reduced active and passive force compared to wild type (303, 477). Similarly, myosin filaments isolated from muscles of skeletal muscle-specific Ate1 knockout mice displayed reduced force generation capacity *in vitro* when they were allowed to interact with actin filaments, likely due to loss of cross-bridges formation (112). This phenotype was rescued by arginylation of myosin filaments using purified Ate1 (112). Thus, it is possible that arginylation alters the conformation of MyHC, which may be essential for cross-bridges formation and force generation.

Phosphorylation

Biochemical and proteomics studies have documented that MyHC, ELC, and RLC are subjected to extensive phosphorylation; however, the physiological relevance of these events has only been scantily characterized (26, 184, 238, 337, 338). Phosphorylation of the ELC isoform MYL3 on Ser195 (26) has been proposed to be essential in regulating cardiac contractility. This notion was supported by *in vivo* overexpression studies in a zebrafish mutant line, *lazy susan* (*laz*), carrying COOH-terminal truncated MYL3 (cmlc-1 gene in zebrafish), which exhibits impaired cardiac contractility (369). Overexpression of phosphomimetic MYL3 (i.e., Ser195Asp), but not phosphoablated MYL3 (i.e., Ser195Ala), in the heart of *laz* zebrafish embryos restored cardiac contractility (369).

Contrary to the minimal information available on the effects of phosphorylation of MyHC and ELC, phosphorylation of RLC has been extensively studied. Structural studies have suggested that phosphorylation of RLC allows the head domain on MyHC to change orientation from parallel to the axis of the thick filament at the SRX state to perpendicular at the CRX state (271, 372). The effects of phosphorylation of RLC MYL2 at Ser15 by the cardiac and skeletal myosin light chain kinases (MLCK) have been extensively examined (89, 126, 624). Accordingly, it was demonstrated that it renders the lever arm of MyHC stiffer, potentiates isometric and concentric force production, and increases myofilament Ca^{2+} sensitivity in both cardiac and skeletal muscles, reviewed in (514, 573, 574, 618). Consistent with these findings, constitutive expression of phosphomimetic Myl2 (i.e., Ser15Asp) in myocardia prevented the development of HCM in transgenic mice carrying the HCM-linked Asp166Val *MYL2* missense mutation (620). In addition to being phosphorylated by the skeletal and cardiac MLCK, MYL2 is also a substrate of a novel MLCK, MLCK4 that is independent of Ca^{2+}/calmodulin regulation, although the specific residue and the effect of this PTM are still unknown (91).

Myl2 in mice and rats can be phosphorylated at both Ser14 and Ser15 contrary to human MYL2 that is only phosphorylated at Ser15, since it contains an Asn at position 14 (506). Substitution of Ser15 for Ala in mouse hearts (Ser15Ala) leads to increased phosphorylation of Ser14, as a compensatory response (515). Importantly, phosphoablated Ser15Ala mice show decreased DCM-induced mortality compared to double phosphoablated mice in which both Ser14 and Ser15 are substituted for Ala (515). Thus, it appears that although phosphorylation of Ser14 may not be essential, since it is not phosphorylated under normal conditions in the rodent heart (515), it can effectively compensate for the loss of Ser15 phosphorylation.

The dynamic versus constitutive nature of MYL2 phosphorylation in the heart following β1-adrenergic stimulation has led to conflicting reports in the literature. Scruggs et al. (2009) reported that the amount of phosphorylated Ser15 is increased upon β1-adrenergic stimulation, while Chang et al. (2015) indicated that there is no change in the phosphorylation levels of Ser15 upon dopamine infusion or propranolol treatment (90, 505). A possible explanation for this discrepancy may be that the phosphorylation levels of MYL2 in the heart follow a transmural gradient, with the highest in the epicardium and the lowest in the endocardium (515). Thus, the differential phosphorylation profile of MYL2 in response to β1-adrenergic stimulation may be due to the different regions examined in the two studies. Moreover, the phosphorylation status of MYL2 is not altered in response to α1-adrenergic signaling (200, 547).

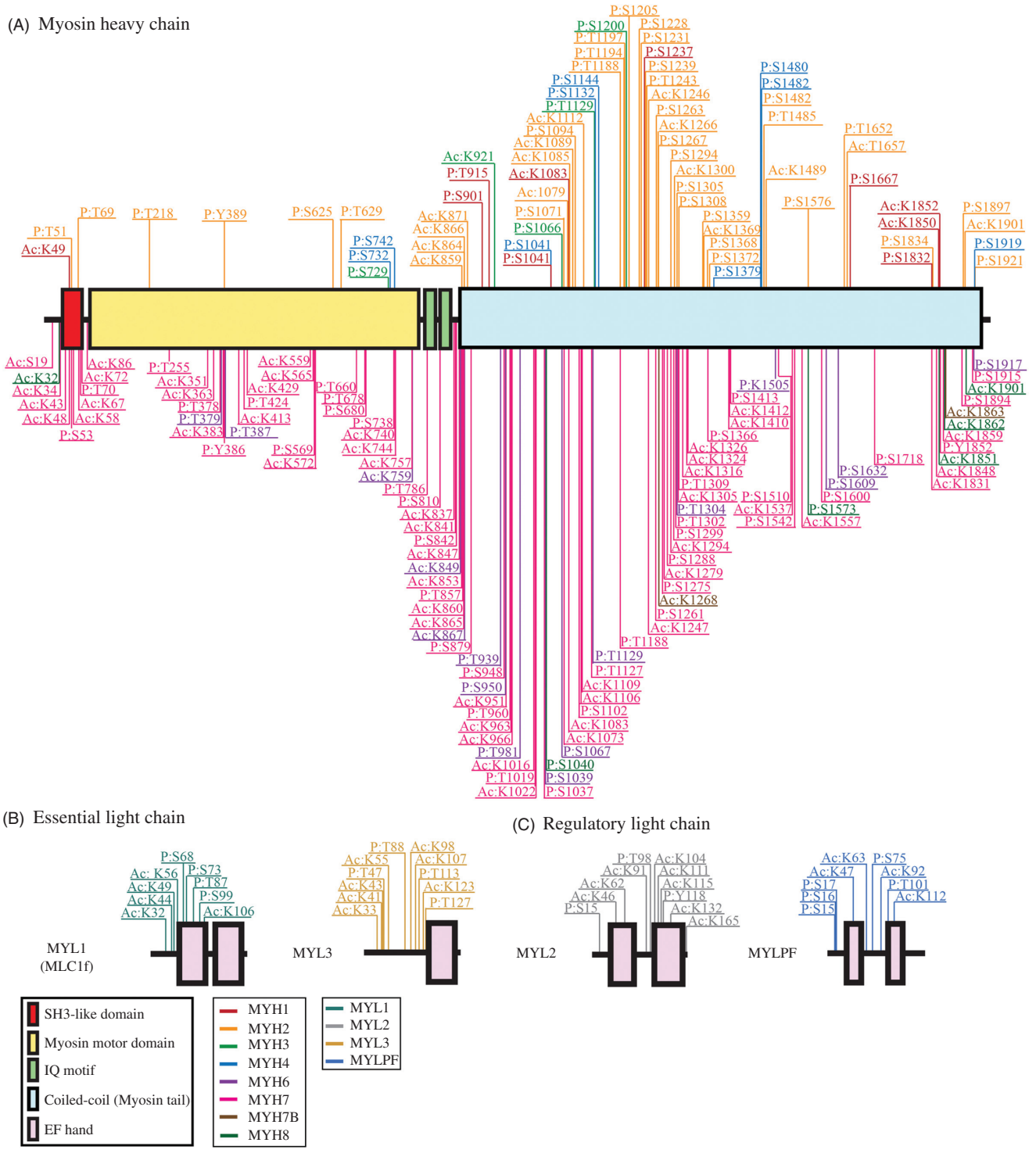

Figure 5 Posttranslational modifications of human myosin heavy and light chains. Given that only acetylation and phosphorylation sites are known for the human isoforms, the figure only denotes those; Tables 4 and 5 however includes additional modifications identified in other mammalian species. (A) Acetylation (Ac) and phosphorylation (P) sites of the human myosin heavy and light chains are depicted onto the myosin domains; color coding was used to note the different isoforms. With the exception of MYH7, acetylation and phosphorylation sites are mainly concentrated in the LMM coiled-coil region. In MYH7, however, acetylation and phosphorylation sites are present throughout the entire length of the protein. (B) Acetylation and phosphorylation sites are concentrated in the nonmodular NH_2-terminus and the first EF-hand motif of MYL1, but only in the nonmodular NH_2-terminus of MYL3; no posttranslational modifications have been identified for MYL4. (C) Acetylation and phosphorylation sites are scattered across the entire length of MYL2 and MYLPF; similar to MYL4, there are no known posttranslational modifications for MYL7.

Table 2 Acetylation Sites of Carcomeric Myosin Heavy and Light Chains

Gene name	Protein name	Accession #	Acetylation sites	Reference
MYH1	Myosin heavy chain-1	Human: NP_005954.3 Rat: NP_001128630.1	Human: K49, K1083, K1850, K1852 Rat: K1049, K1050	Lundby et al., 2012; Ryder et al., 2015
MYH2	Myosin heavy chain-2	Human: NP_001093582.1	Human: K859, K864, K866, K871, K1079, K1085, K1089, K1112, K1231, K1246, K1266, K1300, K1360, K1489, K1657, K1901	Lundby et al., 2012; Ryder et al., 2015
		Rat: NP_001128629.1	Rat: K35, K44, K55, K386, K726, K746, K883, K1033, K1080, K1301, K1323, K1361, K1466, K1838	
MYH3	Myosin heavy chain-3	Human: NP_002461.2 Mouse: NP_001093105.1	Human: K921 Mouse: K1317	Lundby et al., 2012; Yang et al., 2011
MYH4	Myosin heavy chain-4	Mouse: NP_034985.2	Mouse: K1561	Yang et al., 2011
MYH6	Myosin heavy chain-6	Human: NP_002462.2 Rat: NP_058935.2	Human: K759, K849, K862, K867, K1505 Rat: K1028, K1453, K1459	Lundby et al., 2012; Ryder et al., 2015
MYH7	Myosin heavy chain-7	Human: NP_000248.2	Human: K34, K43, K48, K58, K67, K72, K86, K351, K363, K383, K413, K429, K559, K565, K572, K740, K744, K757, K837, K841, K847, K853, K860, K865, K951, K963, K966, K1016, K1022, K1073, K1083, K1106, K1109, K1247, K1279, K1294, K1305, K1316, K1324, K1326, K1410, K1521, K1528, K1537, K1557, K1831, K1848, K1859	Lundby et al., 2012; Ryder et al., 2015; Yang et al., 2011
		Rat: NP_058936.1	Rat: K43, K48, K383, K397, K413, K942, K951, K1305, K1316, K1531, K1557, K1848, K1859	
		Mouse: NP_542766.1	Mouse: K1374	
MYH7B	Myosin heavy chain-7B	Human: NP_065935.3	Human: K1268, K1863	Lundby et al., 2012
MYH8	Myosin heavy chain 8	Human: NP_002463.2 Rat: NP_001093955.1	Human: K32, K1851, K1862, K1901 Rat: K1540, K1560, K1834	Lundby et al., 2012; Ryder et al., 2015
MYL1	Myosin light chain 1	Human: NP_524144.1 Rat: NP_001071124.1 Mouse: NP_067260.1	Human: K32, K44, K49, K56, K106 Rat: K51 Mouse: K50, K63, K135	Lundby et al., 2012; Ryder et al., 2015; Yang et al., 2011
MYL2	Myosin regulatory light chain 2	Human: NP_000423.2 Rat: NP_001030329.2	Human: K46, K62, K91, K104, K111, K115, K132, K165 Rat: K165	Lundby et al., 2012; Ryder et al., 2015
MYL3	Myosin light chain 3	Human: NP_000249.1 Rat: NP_036738.1 Mouse: NP_034989.1	Human: K33, K41, K43, K55, K98, K107, K123 Rat: K130 Mouse: K151	Lundby et al., 2012; Ryder et al., 2015; Yang et al., 2011
MYLPF	Fast skeletal myosin light chain	Human: NP_001311387.1 Rat: NP_036737.1 Mouse: XP_006507484.1	Human: K47, K63, K92, K105, K112 Rat: K47, K166 Mouse: K27, K146	Lundby et al., 2012; Ryder et al., 2015; Yang et al., 2011

In cardiac muscle, ~40% of MYL2 is constitutively phosphorylated in systole or diastole (90, 234, 270, 521). On the contrary, the extent of phosphorylation of MYL2 in skeletal muscles fluctuates significantly with ~10% being phosphorylated at rest and ~80% upon stimulation (270, 574). In both muscle types, myosin light chain phosphatase (MLCP) mediates dephosphorylation of MYL2 (194, 383). MLCP is a tripartite protein consisting of three components: protein phosphatase 1C delta (PP1cδ), myosin phosphatase targeting protein 2 (MYPT2), and a 20/21 kDa subunit (M20/M21) of unknown function (24, 161, 414, 423). Cardiac-specific overexpression of MYPT2 in a murine model resulted in upregulation of PP1cδ, which in turn led to reduced phosphorylation of Myl2 that was accompanied by decreased ejection fraction of whole hearts and Ca^{2+} desensitization of isolated ventricular fibers (380). Consistent with the important role of MLCP in regulating the phosphorylation levels of MYL2, treatment of paced ventricular cardiomyocytes with the MLCP inhibitor calyculin A resulted in ~90% of Myl2 being constitutively phosphorylated (90). Thus, MLCP is essential for maintaining the phosphorylation levels of Myl2 at ~40% in cardiac muscle for normal cardiac function.

Similar to MYL2, Mylpf is also phosphorylated on Ser15 in addition to Ser16 and Ser17 in human fast-twitch skeletal

Table 3 Phosphorylation Sites in Sarcomeric Myosin Heavy and Light Chains

Gene name	Protein name	Accession #	Phosphorylation sites	Reference
MYH1	Myosin heavy chain-1	Human: NP_005954.3 Rat: NP_001128630.1	Human: S901, T915, S1041, S1237, S1667, S1832 Rat: Y389, T419, Y424, Y622, S625, S900, S904, T986, T1000, S1044, S1072, T1073, T1189, T1195, S1240, S1246, T1258, S1264, T1281, T1289, S1291, Y1294, S1295, S1303, S1306, S1309, Y1467, S1545, S1557, S1717	Hojlund et al., 2009; Lundby et al., 2012; Zhao et al., 2011
MYH3	Myosin heavy chain-3	Human: NP_002461.2 Rat: NP_036736.1 Mouse: NP_001093105.1	Human: S729, S1066, T1129, S1200 Rat: S1066 Mouse: S54, S55	Lundby et al., 2012; Zhao et al., 2011; Lundby et al., 2013
MYH4	Myosin heavy chain-4	Human: NP_060003.2 Rat: NP_062198.1	Human: S732, S742, T992, S1041, S1132, S1144, Y1379, S1480, S1482, S1919 Rat: S79, Y389, T391, S392, T419, Y424, S625, T776, T983, T997, T1029, S1041, S1069, T1070, S1237, T1241, S1243, T1255, S1261, T1265, S1278, T1286, S1288, S1292, S1303, S1306, S1327, Y1351, S1413, Y1464, T1467, S1474, S1542, S1547, S1554, T1699, S1714	Hojlund et al., 2009; Zhao et al., 2011; Lundby et al., 2012
MYH6	Myosin heavy chain-6	Human: NP_002462.2 Rat: NP_058935.2 Mouse: NP_001157643.1	Human: T379, Y387, T939; S950, T981, S1039, S1067, T1129, T1304, S1609, S1632, S1917 Rat: T379, S417, S1090, S1139, S1149, Y1261, S1271, T1276, T1277, T1284, S1309, Y1310, T1311, S1512, T1515, T1681 Mouse: T379, S633, S645, S1090, S1094, Y1261, S1271, T1284, S1309, Y1310, S1512, S1639, Y1854	Lundby et al., 2012; 2013; Zhao et al., 2011
MYH7	Myosin heavy chain-7	Human: NP_000248.2 Rat: NP_058936.1 Mouse: NP_542766.1	Human: S19, S53, T70, T255, T378, Y386, T424, S569, T660, T678, S680, S738, T786, S810, S842, T857, S879, S948, T960, T1019, S1037, S1102, T1127, T1188, S1261, S1275, S1288, S1299, T1302, T1309, S1366, S1412, S1413, S1510, S1542, S1600, S1718, Y1852, S1894, S1915 Rat: S1510, S1518, S1645, S1648 Mouse: S643	Hojlund et al., 2009; Lundby et al., 2012; Zhao et al., 2011; Lundby et al., 2013
MYH8	Myosin heavy chain-8	Human: NP_002463.2	Human: S1040, S1573	Zhao et al., 2011
MYL1	Myosin light chain-1	Human: NP_524144.1 Rat: NP_001071124.1	Human: S68, S73, T87, S99 Rat: S41, T71, S73, T87, S99	Hojlund et al., 2009; Lundby et al., 2012
MYL2	Myosin regulatory light chain-2	Human: NP_000423.2 Rat: NP_001030329.2 Mouse: NP_034991.3	Human: S15, T98, Y118 Rat: S14, S15, T52, S113 Mouse: S14, S15, S113	Hojlund et al., 2009; Lundby et al., 2012; Zhou et al., 2011; Lundby et al., 2013
MYL3	Myosin light chain-3	Human: NP_000249.1 Rat: NP_036738.1 Mouse: NP_034989.1	Human: T47, T88, T113, T127 Rat: S45, T93, S127, T132, T134, Y135, S184 Mouse: S49, T73, S188	Lundby et al., 2012; Lundby et al., 2013
MYL7	Myosin light chain-7	Human: NP_067046.1 Rat: NP_001099487.1 Mouse: NP_075017.2	Mouse: S22, S23	Grimm et al., 2006; Lundby et al., 2013
MYLPF	Fast skeletal myosin light chain	Human: Q96A32 NP_001311387.1 Rat: NP_036737.1	Human: S15, S16, S17, S75, T101 Rat: S16, S20, T25	Hojlund et al., 2009; Lundby et al., 2012

Table 4 Arginylation Sites in Sarcomeric Myosin Heavy and Light Chains

Gene name	Protein name	Accession #	Acetylation sites	Reference
MYH2	Myosin heavy chain-2	Mouse: NP_001034634.2	Mouse: E1169	Cornachione et al., 2014
MYH4	Myosin heavy chain-4	Mouse: NP_034985.2	Mouse: E887, E1005, E1166, E1500	Cornachione et al., 2014
MYH6	Myosin heavy chain-6	Mouse: NP_034986.1	Mouse: L747, K999, L1001, V1027, L1486, Q1534, L1578, N1647	Kurosaka et al., 2012
MYH7	Myosin heavy chain-7	Mouse: NP_542766.1	Mouse: L745, K997, L999, V1025, L1484, L1576	Kurosaka et al., 2012
MYL3	Myosin light chain 3	Mouse: NP_034989.1	Mouse: A20, T81, M117	Kurosaka et al., 2012

muscles (238,338). Interestingly, a recent report demonstrated that aged rats suffering from sarcopenia exhibited reduced phosphorylation at both Ser15 and Ser16 of Mylpf in fast-twitch fibers of gastrocnemius muscle, along with decreased force production and myofilament Ca^{2+} sensitivity (196). Moreover, the atrial RLC isoform Myl7 is phosphorylated on Ser21 and Ser22 in mice (corresponding to human MYL7 Ser22 and Ser23) in response to stretch and α1-adrenergic signaling (201, 283). Given that treatment of atrial muscle strips with the MLCK ML-7 inhibitor decreased the extent of Myl7 phosphorylation considerably, it was proposed that Ser21 and Ser22 are substrates of MLCK (201). Consistent with this, inhibition of MLCK via ML-7 suppressed the phenylephrine-induced ionotropic effect in atria (201), and attenuated force production in response to stretch (283).

O-GlcNAcylation

MyHC, ELC, and RLC are also modified by O-GlcNAcylation (102, 229, 461). Accordingly, several sites of O-GlcNAcylation have been reported on Myh6, Myl2, and Myl3 (461, 462). Interestingly, Ser15 of Myl2 is subjected to both phosphorylation and O-GlcNAcylation, but the two posttranslational modifications are exclusive of each other (101).

O-GlcNAc transferase is the enzyme that mediates the covalent attachment of an acetyl-glucosamine moiety to a Ser or Thr residue, whereas O-GlcNAcase (OGA) is the enzyme that mediates its removal (229, 230, 461, 462). Incubation of skinned myofibers isolated from rat soleus muscle with β-N-acetyl-D-glucosamine (GlcNAc) or OGA inhibitors increased the O-GlcNAcylation levels of several contractile proteins, including Myl1, Myl2, and Mylpf, and led to enhanced Ca^{2+} myofilament sensitivity (102, 230). On the contrary, skinned trabeculae isolated from rat hearts exhibited decreased Ca^{2+} sensitivity following incubation with GlcNAc (461), while removal of GlcNAc restored Ca^{2+} sensitivity in diabetic rat hearts (462). These contradictory findings on the functional significance of O-GlcNAcylation with regards to myofilament Ca^{2+} sensitivity may be due to the inherent structural and regulatory differences between cardiac and skeletal muscles.

Mutations and myopathies

The aim of this section is to provide a brief synopsis on the mutational "hot spots" that are possibly present in the myosin complex and an updated list with the currently known mutations (Fig. 6 and Tables 6 and 7). We therefore kindly refer the readership to recent excellent reviews, summarizing the functional ramifications of select myosin mutations (105, 526, 545).

Table 5 Residues of Sarcomeric Myosin Heavy and Light Chains Modified by O-GlcNacylation

Gene name	Protein name	Accession #	Acetylation sites	Reference
MYH6	Myosin heavy chain-6	Rat: NP_058935.2	Rat: T35, T60, S173, T177, S180, S197, S241, S242, S393, S623, S627, S644, S645, S740, S750, S844, S881, S1039, S1149, S1160, T1190, S1201, S1301, T1304, S1309, S1337, S1368, S1414, S1415, S1437, S1465, S1467, S1471, S1472, S1598, T1601, S1602, T1607, S1639, T1697, T1711, S1712, T1777, S1778, S1838, S1917	Ramirez-Correa et al., 2008; 2015
MYL2	Myosin regulatory light chain-2	Rat: NP_001030329.2	Rat: S15	Ramirez-Correa et al., 2008
MYL3	Myosin light chain-3	Rat: NP_036738.1	Rat: S45, T93, T164	Ramirez-Correa et al., 2008; 2015

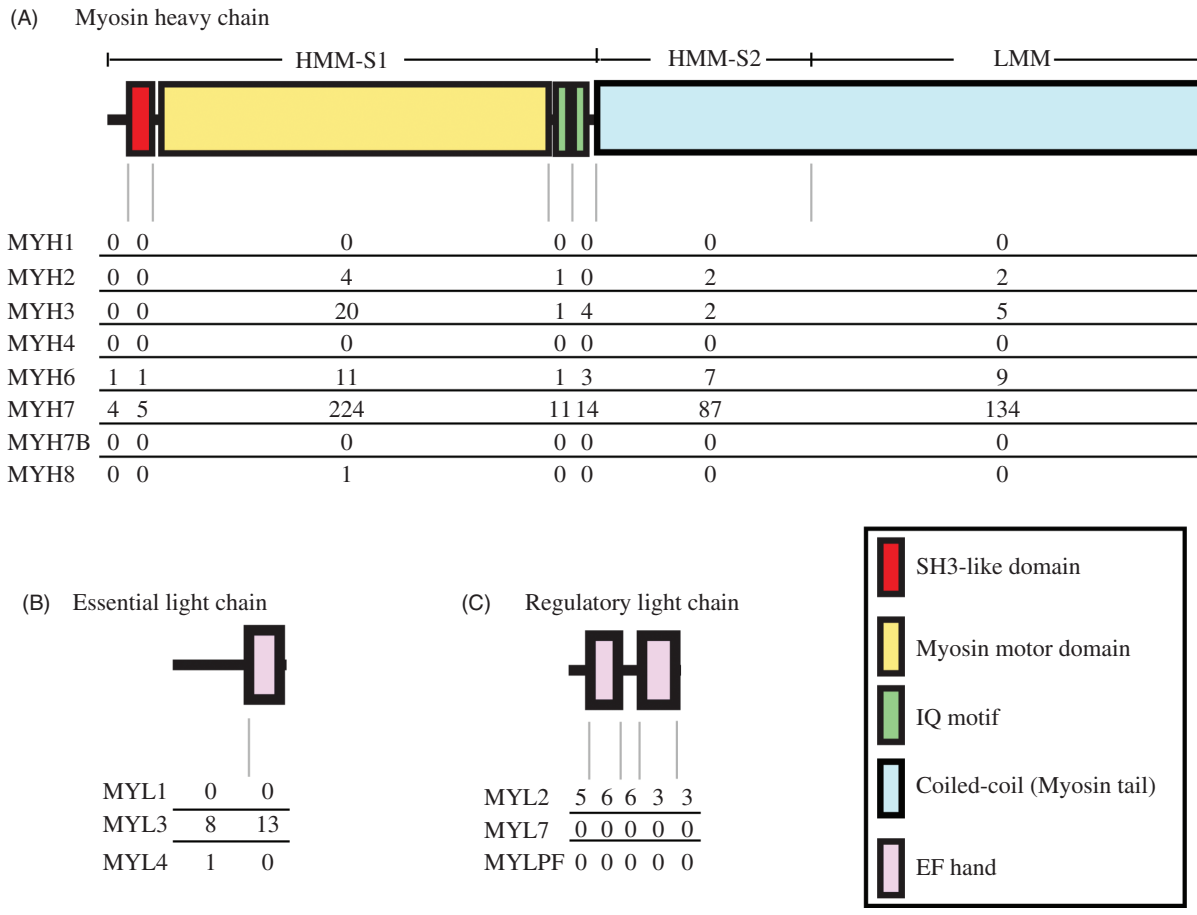

Figure 6 Number of mutations identified to date in individual domains of the myosin heavy (A) and light chain [(B) and (C)] isoforms expressed in human striated muscles. The total count noted includes missense mutations and single amino acid duplications and deletions, since these types of mutations account for >90% of the total number of mutations identified in the myosin family.

Although encoded by different genes, the MyHC isoforms are highly homologous, sharing 87% to 97.8% similarity. Mutations in conserved residues have been associated with the development of severe cardiac and skeletal myopathies. As such, more than ~700 mutations have been identified in the different MyHC isoforms. MYH7 contains the highest number of mutations with more than 600 mutations reported, whereas MYH2, MYH3, MYH6, and MYH8 contain 15, 33, 35, and 1 mutations, respectively. In contrast, no skeletal or cardiac myopathy causing mutations have been identified to date for MYH1, MYH4, and MYH7B.

The majority of the MYH7 HCM-causing mutations are present in the S1 and S2 fragments (105, 309). Consistent with this, a recent study highlighted the prevalence of MYH7 HCM-associated mutations in the converter region and the myosin mesa, a flat surface of the globular head domain (240). Conversely, the majority of the MYH7 skeletal myopathy-causing mutations reside in the coiled-coil LMM region (105, 240, 309). Thus, disease-linked mutations are scattered throughout the length of MYH7 although they appear segregated in terms of eliciting cardiac or skeletal muscle defects. Equivalent numbers of myopathic mutations have been identified in the motor head domain and the coiled-coil region of MYH2 and MYH6, while the majority of MYH3 mutations are present in the motor head domain. A somewhat paradoxical feature of HCM patients carrying MYH7 mutations is that they are asymptomatic until the third decade of their life or even later (526). Contrary to MYH7 mutations, MYH3 and MYH6 mutations are linked to developmental defects, and carriers with these mutations are often affected at an early age. Moreover, patients carrying the same missense mutation in a conserved residue within different myosin isoforms may present with different clinical phenotypes. An intriguing example of this is Thr177/178 that precedes the phosphate binding site in the motor head domain. Substitution of Thr177 for Ile (Thr177Ile) in MYH7 leads to development of HCM, substitution of Thr178 for Ile or Met in MYH3 (Thr178Ile and Thr178Met) leads to development of distal arthrogryposis, and substitution of Thr178 for Ile in MYH2 (Thr178Ile) leads to development of early-onset myopathy (105,544,558). It therefore appears that the differential expression profile of the MyHC isoforms is a major determining factor for the onset, severity, and tissue pathogenicity of their respective mutations.

Table 6 Mutations Identified in Myosin Heavy Chains

Mutation	Region	Disease	Reference
		MYH2	
		Missense mutations	
T178I	S1-myosin motor	Myopathy	Tajsharghi et al., 2014
A236T	S1-myosin motor	Myopathy	Tajsharghi et al., 2014
M531T	S1-myosin motor	Myopathy	Tajsharghi et al., 2014
E706K	S1-myosin motor	Inclusion body myopathy	Martinsson et al., 2000
V805A	S1	Inclusion body myositis	Cai et al., 2012
V970I	S2-coiled-coil	Inclusion body myopathy	Tajsharghi et al., 2005
L1061V	S2-coiled-coil	Inclusion body myopathy	Tajsharghi et al., 2005
L1870P	LMM-coiled-coil	Myopathy	D'Amico et al., 2013
L1877P	LMM-coiled-coil	Distal and proximal myopathy; ophthalmoplegia	Cabrera-Serrano et al., 2015
		Nonsense mutations	
E500Stop	S1-myosin motor	Proximal myopathy; ophthalmoplegia	Hernandez-Lain et al., 2016
R783Stop	S1	Myopathy	Tajsharghi et al., 2014
L802Stop	S1	Myopathy	Tajsharghi et al., 2014
		Frameshift mutations	
S337Lfs*11	S1-myosin motor	Myopathy; ophthalmoplegia	Willis et al., 2016
E801Sfs*28	S1	Myopathy; ophthalmoplegia	Lossos et al., 2013
V1451Sfs*40	LMM-coiled-coil	Myopathy; ophthalmoplegia	Tajsharghi et al., 2014
		MYH3	
		Missense mutations	
T178I	S1-myosin motor	DA, Type 2A	Toydemir et al., 2006
T178M	S1-myosin motor	DA, Type 2A	Tajsharghi et al., 2008
G184A	S1-myosin motor	DA, Type1	Beck et al., 2013
A234T	S1-myosin motor	DA, Type 1, 2B; myosin myopathy	Tajsharghi et al., 2008; Beck et al., 2013
G246A	S1-myosin motor	DA, Type 2B	Beck et al., 2013
S261F	S1-myosin motor	DA, Type 2B	Toydemir et al., 2006
S292C	S1-myosin motor	DA, Type 2B	Toydemir et al., 2006
T333R	S1-myosin motor	SCT	Carapito et al., 2016
L340Q	S1-myosin motor	DA, Type 2B	Beck et al., 2013
E375K	S1-myosin motor	DA, Type 2B	Toydemir et al., 2006
Y387C	S1-myosin motor	DA, Type 2A	Beck et al., 2014
F437I	S1-myosin motor	DA, Type 1	Alvarado et al., 2011
D462G	S1-myosin motor	DA Type 2B; myosin myopathy	Tajsharghi et al., 2008
F466C	S1-myosin motor	DA, Type 2B	Beck et al., 2013
E498G	S1-myosin motor	DA, Type 2A	Toydemir et al., 2006
K504N	S1-myosin motor	DA, Type 1	Beck et al., 2013
D517Y	S1-myosin motor	DA, Type 2B	Toydemir et al., 2006
Y583S	S1-myosin motor	DA, Type 2A	Toydemir et al., 2006
R672H	S1-myosin motor	DA, Type 2A; Freeman-Sheldon syndrome	Toydemir et al., 2006; Hague et al., 2016
R672C	S1-myosin Motor	DA, Type 2A	Toydemir et al., 2006

Table 6 (*Continued*)

Mutation	Region	Disease	Reference
G769V	S1	DA, Type 2B	Toydemir et al., 2006
V825D	S1-IQ motif	DA, Type 2A	Toydemir et al., 2006
K838E	S1	DA, Type 2B	Beck et al., 2013
Q1075P	S2-coiled-coil	DA, Type 8	Chong et al., 2015
L1320P	LMM-coiled-coil	Arthrogryposis multiplex congenita	Laquerriere et al., 2014
L1344P	LMM-coiled-coil	MPS	Carapito et al., 2016
D1622A	LMM-coiled-coil	DA, Type 2B	Toydemir et al., 2006
A1637V	LMM-coiled-coil	DA, Type 2B	Toydemir et al., 2006
A1752T	LMM-coiled-coil	DA, Type 1	Kimber et al., 2012
		Small deletions	
S243del	S1-myosin motor	DA, Type 8	Chong et al., 2015
F835del	S1	DA, Type 2B	Beck et al., 2013
L841del	S1	DA, Type 2B	Toydemir et al., 2006
		Small insertions	
N1072dup	S2-coiled-coil	DA, Type 8	Chong et al., 2015
		MYH6	
		Missense mutations	
R17H	S1	Atrial septal defect	Posch et al., 2011
G56R	S1-SH3-like	HCM	Santos et al., 2012
A230P	S1-myosin motor	Congenital heart defects	Granados-Riveron et al., 2010
H252Q	S1-myosin motor	Congenital heart defects	Granados-Riveron et al., 2010
I275N	S1-myosin motor	DCM	Hershberger et al., 2010
R443P	S1-myosin motor	Hypoplastic LV	Tomita-Mitchell et al., 2016
C539R	S1-myosin motor	Atrial septal defect	Posch et al., 2011
K543R	S1-myosin motor	Atrial septal defect	Posch et al., 2011
R568C	S1-myosin motor	DCM	Hershberger et al., 2010
D588A; E1207K	S1-myosin motor; S2-coiled-coil	Hypoplastic LV, reduced EF of RV	Theis et al., 2015
V700M	S1-myosin motor	Congenital heart defects	Granados-Riveron et al., 2010
I704N; T1379M	S1-myosin motor; LMM-coiled-coil	Hypoplastic LV, reduced EF of RV	Theis et al., 2015
R721W	S1-myosin motor	Sick sinus syndrome	Holm et al., 2011
R795Q	S1-IQ	HCM	Nimura et al., 2002
R809C	S1-IQ	HCM	Rubattu et al., 2016
I820N	S1-IQ	Atrial septal defect	Ching et al., 2005
P830L	S1-IQ	DCM	Carniel et al., 2005
A1004S	S2-coiled-coil	DCM	Carniel et al., 2005
R1047C	S2-coiled-coil	DCM	Zhao et al., 2015
Q1065H	S2-coiled-coil	HCM	Carniel et al., 2005
R1116S	S2-coiled-coil	Congenital heart defects	Granados-Riveron et al., 2010
R1177W	S2-coiled-coil	DCM	Hershberger et al., 2010

(*continued*)

Table 6 (*Continued*)

Mutation	Region	Disease	Reference
A1366D	LMM-coiled-coil	Congenital heart defects	Granados-Riveron et al., 2010
R1398Q	LMM-coiled-coil	Cardiac dysrhythmia	Gonzalez-Garay et al., 2013
A1440P	LMM-coiled-coil	DCM	Hershberger et al., 2010
A1443D	LMM-coiled-coil	Congenital heart defects	Granados-Riveron et al., 2010
E1457K	LMM-coiled-coil	DCM	Carniel et al., 2005
R1502Q	LMM-coiled-coil	DCM	Hershberger et al., 2010
R1865Q	LMM-coiled-coil	Congenital heart defects	Granados-Riveron et al., 2010
E1885K	LMM-coiled-coil	Wolff-Parkinson-White syndrome	Bowless et al., 2015
		Small deletions	
E933del	S2-coiled-coil	Sick sinus syndrome	Ishikawa et al., 2015
		Nonsense mutations	
E501Stop	S1-myosin motor	Congenital heart defects	Granados-Riveron et al., 2010
		Splicing mutations	
IVS37-2A>G	LMM-coiled-coil	ASD	Granados-Riveron et al., 2010
		*MYH7**	
		Missense mutations	
T70S	S1-SH3-like	HCM	Coppini et al., 2014
F95I	S1-myosin motor	HCM	Wang et al., 2014
Y117F	S1-myosin motor	HCM	Homburger et al., 2016
T135I	S1-myosin motor	HCM	Wang et al., 2014
V139L	S1-myosin motor	DCM	Mook et al., 2013
R147S	S1-myosin motor	HCM	Chiou et al., 2014
Q163P	S1-myosin motor	LVNC	Bainbridge et al., 2015
A200T	S1-myosin motor	HCM	Fujino et al., 2013
R204C	S1-myosin motor	HCM	Homburger et al., 2016
D218Y	S1-myosin motor	HCM	Wang et al., 2014
A226V	S1-myosin motor	HCM	Homburger et al., 2016
A226T	S1-myosin motor	HCM	Cecconi et al., 2016
T235N	S1-myosin motor	HCM	Wang et al., 2014
V236I	S1-myosin motor	DCM	Zimmerman et al., 2010
R243H	S1-myosin motor	LVNC	Klaassen et al., 2008
R249G	S1-myosin motor	LVNC	Tian et al., 2015
H251N	S1-myosin motor	HCM	Kaski et al., 2009
F252S	S1-myosin motor	HCM	Yu et al., 2014
F252L	S1-myosin motor	LVNC	Klaassen et al., 2008
Y283D	S1-myosin motor	LVNC; Ebstein's anomaly	Postma et al., 2011
I303M	S1-myosin motor	HCM	Homburger et al., 2016
P307H	S1-myosin motor	HCM	Homburger et al., 2016
D309G	S1-myosin motor	HCM	Sabater-Molina et al., 2013
E317G	S1-myosin motor	HCM	Coppini et al., 2014
A321V	S1-myosin motor	HCM	Fujino et al., 2013

Table 6 (*Continued*)

Mutation	Region	Disease	Reference
I323N	S1-myosin motor	HCM	Helms et al., 2014
V338A	S1-myosin motor	DCM	Zimmerman et al., 2010
Y350N	S1-myosin motor	LVNC	Postma et al., 2011
M362R	S1-myosin motor	LVNC; Ebstein's anomaly; VSD	Hirono et al., 2014
S384P	S1-myosin motor	HCM	Wang et al., 2014
L390P	S1-myosin motor	LVNC	Postma et al., 2011
G407C	S1-myosin motor	HCM	Guo et al., 2014
A426T	S1-myosin motor	HCM	Wang et al., 2014
R434T	S1-myosin motor	HCM	Wang et al., 2014
M435R	S1-myosin motor	HCM	Homburger et al., 2016
M439R	S1-myosin motor	LVNC; bicuspid aortic valve	Basu et al., 2014
M439T	S1-myosin motor	HCM	Wang et al., 2014
R442G	S1-myosin motor	HCM	Han et al., 2014
R442H	S1-myosin motor	Brugada syndrome	Di Resta et al., 2015
D461E	S1-myosin motor	HCM	Wang et al., 2014
F468L	S1-myosin motor	DCM	Lakdawala et al., 2012
M493V	S1-myosin motor	HCM	Meyer et al., 2013
Q498E	S1-myosin motor	LVNC	Yang et al., 2015
I506T	S1-myosin motor	HCM	Wang et al., 2014
I524L	S1-myosin motor	HCM	Wang et al., 2014
I530V	S1-myosin motor	HCM	Homburger et al., 2016
M531R	S1-myosin motor	LVNC	Kaneda et al., 2008
K542T	S1-myosin motor	LVNC	Nomura et al., 2015
K542R	S1-myosin motor	HCM	Coto et al., 2012
R567H	S1-myosin motor	DCM	Dalin et al., 2017
H581R	S1-myosin motor	HCM	Homburger et al., 2016
A583V	S1-myosin motor	HCM	Garcia-Castro et al., 2009
P600S	S1-myosin motor	DCM	Dalin et al., 2017
G607D	S1-myosin motor	HCM	Coppini et al., 2014
Y624C	S1-myosin motor	HCM	Coppini et al., 2014
S648L	S1-myosin motor	LVNC	Bainbridge et al., 2015
K657Q	S1-myosin motor	HCM	Hill et al., 2015
L658V	S1-myosin motor	LVNC	Hoedemaekers et al., 2010
T660N	S1-myosin motor	HCM	Curila et al., 2012
R671H	S1-myosin motor	HCM	Wang et al., 2015
M690T	S1-myosin motor	HCM	Coppini et al., 2014
E700G	S1-myosin motor	LVNC	Bainbridge et al., 2015
G701D	S1-myosin motor	HCM	Cecconi et al., 2016
I702N	S1-myosin motor	HCM	Alfares et al., 2015
G708A	S1-myosin motor	HCM	Helms et al., 2014
D717G	S1-myosin motor	HCM	Garcia-Giustiniani et al., 2015
I730N	S1-myosin motor	HCM	Garcia-Giustiniani et al., 2015

(*continued*)

Table 6 (*Continued*)

Mutation	Region	Disease	Reference
I730M	S1-myosin motor	HCM	Homburger et al., 2016
P731A	S1-myosin motor	HCM	Homburger et al., 2016
S738N	S1-myosin motor	HCM	Jaafar et al., 2016
K740N	S1-myosin motor	HCM	Wang et al., 2014
T761N	S1-myosin motor	HCM	Ntusi et al., 2016
K762R	S1-myosin motor	HCM	Alfares et al., 2015
L769P	S1	HCM	Homburger et al., 2016
R783C	S1-IQ	HCM	Homburger et al., 2016
L811P	S1	HCM	Homburger et al., 2016
A820D	S1	HCM	Okada et al., 2014
F834L	S1	HCM	Alfares et al., 2015
S842N	S1	HCM	Alfares et al., 2015
S842G	S1	HCM	Homburger et al., 2016
E848G	S2-coiled-coil	HCM	Pioner et al., 2016
K853Q	S2-coiled-coil	HCM	Wang et al., 2014
R858S	S2-coiled-coil	HCM	Captur et al., 2014
S866P	S2-coiled-coil	HCM	Fujino et al., 2013
M877I	S2-coiled-coil	HCM	Mattos et al., 2016
V878A	S2-coiled-coil	HCM	Ho et al., 2009
V878M	S2-coiled-coil	HCM	Wang et al., 2014
N885T	S2-coiled-coil	HCM	Zhao et al., 2016
E894K	S2-coiled-coil	HCM	Wang et al., 2014
E903Q	S2-coiled-coil	HCM	Coppini et al., 2014
R904C	S2-coiled-coil	DCM	Van der Zwaag et al., 2011
C905Y	S2-coiled-coil	HCM	Wang et al., 2014
I913T	S2-coiled-coil	HCM	Wang et al., 2014
L915P	S2-coiled-coil	HCM	Alfares et al., 2015
E929K	S2-coiled-coil	LVNC	Tian et al., 2015
E931A	S2-coiled-coil	HCM	Jaafar et al., 2016
E935V	S2-coiled-coil	HCM	Rubattu et al., 2016
L992M	S2-coiled-coil	HCM	Coppini et al., 2014
K994R	S2-coiled-coil	HCM	Wang et al., 2014
A1006T	S2-coiled-coil	HCM	Jaafar et al., 2016
R1050Q	S2-coiled-coil	HCM	Wang et al., 2014
E1119K	S2-coiled-coil	HCM	Wang et al., 2014
E1120K	S2-coiled-coil	HCM	Homburger et al., 2016
A1128T	S2-coiled-coil	HCM	Homburger et al., 2016
E1142K	S2-coiled-coil	HCM	Wang et al., 2014
S1199R	S2-coiled-coil	HCM	Homburger et al., 2016
N1209S	S2-coiled-coil	DCM	Zimmerman et al., 2010
L1297Q	LMM-coiled-coil	HCM	Wang et al., 2014
R1344Q	LMM-coiled-coil	HCM	Marsiglia et al., 2013

Table 6 (*Continued*)

Mutation	Region	Disease	Reference
Y1347C	LMM-coiled-coil	HCM	Cecconi et al., 2016
E1348Q	LMM-coiled-coil	HCM	Sabater-Molina et al., 2013
E1348K	LMM-coiled-coil	HCM	Wang et al., 2014
E1350K	LMM-coiled-coil	DCM	Miller et al., 2013
E1356Q	LMM-coiled-coil	HCM	Sabater-Moline et al., 2013
R1359C	LMM-coiled-coil	LVNC	Klaassen et al., 2008
V1360I	LMM-coiled-coil	HCM	Wang et al., 2014
Y1375H	LMM-coiled-coil	HCM	Homburger et al., 2016
V1404M	LMM-coiled-coil	HCM	Wang et al., 2014
R1434P	LMM-coiled-coil	LDM-like	Feinstein-Linial et al., 2016
S1435P	LMM-coiled-coil	Distal myopathy	Astrea et al., 2016
A1437P	LMM-coiled-coil	LDM-like	Feinstein-Linial et al., 2016
L1453P	LMM-coiled-coil	LDM	Lefter et al., 2015
E1468K	LMM-coiled-coil	HCM	Mattos et al., 2016
L1481P	LMM-coiled-coil	SM	Lamont et al., 2014
H1494L	LMM-coiled-coil	HCM	Berge and Leren 2014
Q1541P	LMM-coiled-coil	SM	Lamont et al., 2014
A1549P	LMM-coiled-coil	Laing myopathy	Ferbert et al., 2016
E1564K	LMM-coiled-coil	HCM	Cecconi et al., 2016
E1573K	LMM-coiled-coil	Ebstein's anomaly	Postma et al., 2011
N1589K	LMM-coiled-coil	HCM	Wang et al., 2014
L1597R	LMM-coiled-coil	SM	Clarke et al., 2013
T1599P	LMM-coiled-coil	SM	Lamont et al., 2014
R1606C	LMM-coiled-coil	HCM	Helms et al., 2014
L1612P	LMM-coiled-coil	SM	Lamont et al., 2014
A1636P	LMM-coiled-coil	SM	Lamont et al., 2014
L1646P	LMM-coiled-coil	SM	Lamont et al., 2014
R1662P	LMM-coiled-coil	SM	Lamont et al., 2014
N1664K	LMM-coiled-coil	HCM	Homburger et al., 2016
Q1719R	LMM-coiled-coil	HCM	Homburger et al., 2016
L1723P	LMM-coiled-coil	Eccentric core disease	Romero et al., 2014
E1752K	LMM-coiled-coil	HCM	Lee et al., 2014
K1757E	LMM-coiled-coil	HCM	Wang et al., 2014
A1766T	LMM-coiled-coil	LVNC	Klaassen et al., 2008
R1781H	LMM-coiled-coil	HCM	Homburger et al., 2016
M1782V	LMM-coiled-coil	HCM	Homburger et al., 2016
L1793P	LMM-coiled-coil	MSM, CM	Uro-Coste et al., 2009; Dye et al., 2006
Q1794K	LMM-coiled-coil	HCM	Xu et al., 2015
R1820W	LMM-coiled-coil	MSM	Yuceyar et al., 2015
S1836Q	LMM-coiled-coil	DCM	Marston et al., 2015
E1856K	LMM-coiled-coil	LVNC; MSM	Finisterer et al., 2014; Tajsharghi and Oldfors, 2013

(*continued*)

Table 6 (*Continued*)

Mutation	Region	Disease	Reference
D1869G	LMM-coiled-coil	HCM	Homburger et al., 2016
V1899A	LMM-coiled-coil	HCM	Homburger et al., 2016
A1906G	LMM-coiled-coil	DCM	Dalin et al., 2017
R1909P	LMM-coiled-coil	DCM	Dalin et al., 2017
E1914K	LMM-coiled-coil	DCM; SM	Lamont et al., 2014
N1918K	LMM-coiled-coil	LVNC	Postma et al., 2011
		Small deletions	
G10del	S1	HCM	Nakajima-Taniguchi et al., 1995
F155del	S1-myosin motor	LVNC; ASD; Ebstein's anomaly	Tian et al., 2015
G768_L770del	S1	HCM	Chida et al., 2016
E875del	S2-coiled-coil	HCM	Alfares et al., 2015
G1101_L1104del	S2-coiled-coil	DCM	Millat et al., 2011
E1220del	LMM-coiled-coil	Ebstein's anomaly; LVNC; VSD	Bettinelli et al., 2013
E1350del	LMM-coiled-coil	LVNC	Hoedemaekers et al., 2010
E1669del	LMM-coiled-coil	SM	Lamont et al., 2014
T1854_A1885del	LMM-coiled-coil	SM	Pajusalu et al., 2016
		Small insertions	
K1729dup	LMM-coiled-coil	SM	Lamont et al., 2014
		Nonsense mutations	
Y266Stop	S1-myosin motor	LVNC	Hoedemaekers et al., 2010
E1835Stop	LMM-coiled-coil	HCM	Wang et al., 2014
		Frameshift mutations	
F153Tfs*12	S1-myosin motor	DCM	Zimmerman et al., 2010
M493Vfs*17	S1-myosin motor	DCM	Zimmerman et al., 2010
L1629Pfs*54	LMM-coiled-coil	DCM	Dalin et al., 2017
S1924Afs*9	LMM-coiled-coil	HCM	Kassem et al., 2013
		Splicing mutations	
IVS4-7T>C	S1-myosin motor	HCM	Liu et al., 2013
IVS8+1G>A	S1-myosin motor	LVNC	Klassen et al., 2008
IVS8+3G>C	S1-myosin motor	LVNC	Klassen et al., 2008
IVS38+1G>A	LMM-coiled-coil	HCM	Wang et al., 2014
		MYH8	
		Missense mutations	
R674Q	S1-myosin motor	Trismus-pseudocamptodactyly syndrome	Veugelers et al., 2004

*This mutation list is supplemental to a previously compiled list by Colegrave and Peckham, 2014 (Ref # 99), which contains more than 400 mutations identified prior to December 2013.
Abreviations: S1, Subfragment 1; S2, Subfragment 2; LMM, light meromyosin; HCM, hypertrophic cardiomyopathy; DCM, dilated cardiomyopathy; LVNC, left ventricular noncompaction; VSD, ventricular septal defect; EF, ejection fraction; LV, left ventricle; RV, right ventricle; SCT, spondylocarpotarsal synostosis syndrome; SM, skeletal myopathy; LDM, Laing distal myopathy; MPS, multiple pterygium syndromes; MSM, myosin storage myopathy.

Table 7 Mutations Identified in Myosin Light Chains

Mutation	Domain	Disease	Reference
		MYL2	
		Missense mutations	
A2T		HCM	Wang et al., 2014
A13T		HCM	Poetter et al., 1996
F18L		HCM	Flavigny et al., 1998
M20L		HCM	Olivotto et al., 2008
E22K		HCM	Poetter et al., 1996
I35V	EF-hand	HCM	Berge and Leren, 2014
R40K	EF-hand	HCM	Berge and Leren, 2014
I44M	EF-hand	HCM	Santos et al., 2012
N47K	EF-hand	HCM	Anderson et al., 2001
R58Q	EF-hand	HCM	Flavigny et al., 1998
M69I	EF-hand	HCM	Wang et al., 2014
P74L		HCM	Wang et al., 2014
G87E		HCM	Zou et al., 2013
G87W		HCM	Wang et al., 2014
A93V		HCM	Berge and Leren, 2014
D94A		DCM	Huang et al., 2015
P95A		HCM	Poetter et al., 1996
A102T	EF-hand	HCM	Coppini et al., 2014
K104E	EF-hand	HCM	Anderson et al., 2001
E134A	EF-hand	HCM	Olivotto et al., 2008
H161R		HCM	Helms et al., 2014
G162R		HCM	Olivotto et al., 2008
D166V		HCM	Richard et al., 2003
		Nonsense mutations	
R58Stop	EF-hand	HCM	Berge and Leren, 2014
		Frameshift mutations	
P144Lfs*2; D145Tfs*2	EF-hand	CM; infantile type 1 muscle fiber disease	Wetermen et al., 2013
		MYL3	
		Missense mutations	
E56G		HCM	Richard et al., 2003
A57G		HCM	Lee et al., 2001
A57D		HCM	Rubattu et al., 2016
R63C		HCM	Chiou et al., 2015
V79I		HCM	Andersen et al., 2012
R94H		HCM	Fokstuen et al., 2008
D126G		DCM	Zhao et al., 2015
G128C		HCM	Garcia-Pavia et al., 2011
E143K	EF-hand	HCM	Olson et al., 2002
M149T	EF-hand	HCM	Zou et al., 2013
M149I	EF-hand	HCM	Wang et al., 2014
M149V	EF-hand	HCM	Poetter et al., 1996
E152K	EF-hand	HCM	Kaski et al., 2009
R154C	EF-hand	HCM	Zou et al., 2013
R154H	EF-hand	HCM	Poetter et al., 1996
H155D	EF-hand	HCM	Kaski et al., 2009
V156L	EF-hand	HCM	Wang et al., 2014
G161C	EF-hand	HCM	Wang et al., 2014
M173V	EF-hand	HCM	Morita et al., 2006
E177G	EF-hand	HCM	Jay et al., 2013
N180H	EF-hand	HCM	Wang et al., 2014
		MYL4	
		Missense mutations	
E11K		AF	Orr et al., 2016
		Frameshift mutations	
C78Wfs*29		AF	Gudbjartsson et al., 2015

Abbreviations: CM, cardiomyopathy; HCM, hypertrophic cardiomyopathy; DCM, dilated cardiomyopathy; AF, atrial fibrillation.

In addition to mutations in MyHC, mutations in ELC and RLC also lead to disease development (253,625). Intriguingly, mutations in MYL2 and MYL3 mainly underlie the development of cardiomyopathies, although they are expressed in both cardiac and skeletal muscles. Specifically, the majority of mutations in MYL2 and MYL3 are associated with HCM, and only single cases are linked to DCM. Mutations in MYL2 have been suggested to alter its structure, therefore impacting the kinetics of cross-bridges formation, while mutations in MYL3 affect actomyosin binding and alter myofilament Ca^{2+} sensitivity, recently reviewed in (253). Moreover, mutations in the atrial-specific MYL4 were recently associated with the development of atrial fibrillation (210, 426). Lastly, no myopathy-causing mutations have been identified in MYL1 and MYLPF, which are predominantly expressed in fast-twitch muscles.

Conclusions

Although more than a century has passed since the initial discovery of hexameric myosin, our understanding of its structure, isoform diversity, regulation, and functions is still ongoing. Given that myosins are the most heavily mutated proteins in congenital and somatic cardiac and skeletal

myopathies, further multidisciplinary studies are warranted aiming to comprehensively investigate their roles in muscle (patho)physiology.

Myosin Binding Protein-C

Discovery

MyBP-C was first discovered as a contaminant of skeletal muscle myosin preparations (531), but later characterized as a myosin binding protein with a molecular weight of 120 to 150 kDa depending on the muscle source (420). Much work has focused on the cardiac isoform, as mutations in cardiac MyBP-C are a leading cause of congenital cardiomyopathies. Recent work, however, has begun to investigate the roles and regulation of the skeletal isoforms, due to their direct involvement in hereditary myopathies, especially in the case of slow MyBP-C.

Structure, localization, and isoforms

MyBP-C comprises a family of accessory proteins with structural and regulatory roles that constitutes 2% to 4% of the myofibrillar mass (395). Three different isoforms have been described: cardiac (cMyBP-C), fast skeletal (fMyBP-C), and slow skeletal (sMyBP-C) (594), which play key roles in the assembly and stabilization of thick filaments, and regulate actomyosin cross-bridges via direct interactions with both myosin and actin (12, 13, 122, 262, 355, 363, 416). The three isoforms share similar structures consisting of seven (sMyBP-C and fMyBP-C) or eight (cMyBP-C) Ig and three FnIII modules numbered from the NH_2-terminus to the COOH-terminus as C1-C10 (113) (Fig. 7). The cardiac isoform includes an additional Ig domain at its extreme NH_2-terminus, referred to as C0 (174). All three isoforms contain a 50-amino acid long Pro/Ala rich region and a 100-amino acid long MyBP-C specific motif, termed M-motif, that flank Ig domain C1 (113, 489). Unique to cMyBP-C are a 9-amino acid long insert in the M-motif and a 28-amino acid long insert in the C5 domain, which is enriched in Pro and charged residues and potentially acts as an SH3-domain recognition site (151). The cardiac and fast skeletal isoforms also share a conserved linker region between Ig domains C4 and C5, which is absent from the slow skeletal isoform (151).

cMyBP-C is encoded by the *MYBPC3* gene located on human chromosome 11, has an apparent molecular mass of ~140 kDa, and is restricted to heart muscle (152, 156, 449). Structural information about cMyBP-C is limited to secondary structures of the NH_2-terminal C0-C2 region and the C5 domain (147, 489). Solution nuclear magnetic resonance (NMR) structures confirmed that C0 exhibits a canonical Ig topography forming a β-sandwich, and ^{15}N relaxation studies showed that its NH_2-terminus is highly disordered, whereas its COOH-terminus is ordered (147, 467). Moreover, crystallographic and NMR studies demonstrated that Ig domain C1 is more extended than other Ig domains, with its NH_2-terminus being structurally compact, but its COOH-terminus disordered and flexible (1), possibly enabling the proper positioning of the neighboring M-motif for interactions with other myofilament proteins (147). In contrast to data for C0 and C1, there is disagreement regarding the conformation of the M-motif, with some studies reporting that it assumes a compact conformation that is structurally related to an Ig β-fold (264), and others indicating that it is highly disordered in solution (223, 272). NMR studies did confirm that the M-motif is partially folded, however, no β-sheet composition was evident (149). Moreover, Ig domain C2 displays the expected β-sandwich topology of an Ig domain (2), and molecular modeling studies predicted that charge-charge interactions are crucial to the formation of the protein binding interface

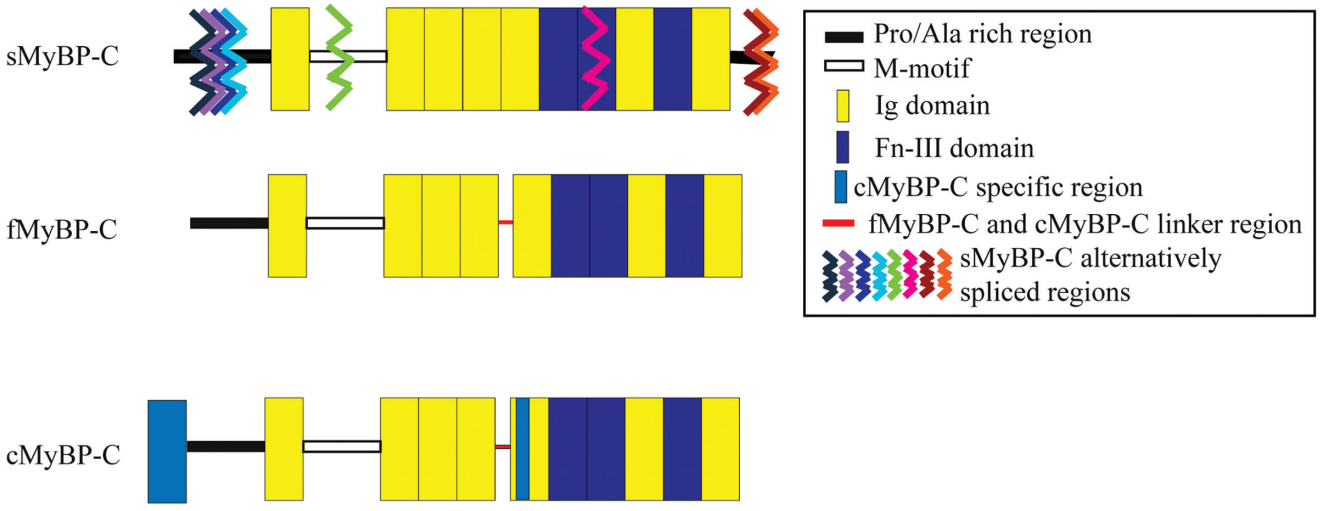

Figure 7 Schematic representation of the three MyBP-C isoforms. The black and white horizontal rectangles correspond to the Pro/Ala rich region and the M-motif, while the yellow and dark blue vertical rectangles represent Ig and FnIII domains, respectively. Colored zigzagged lines in sMyBP-C represent alternatively spliced insertions. fMyBP-C and cMyBP-C share a conserved linker region between C4 and C5, denoted in red. C0 and cardiac specific regions in cMyBP-C are shown in light blue.

between C2 and myosin S2 (147). Lastly, C5 exhibits a prominent β-bulge, formed by the 10-amino acid linker between C4 and C5 that stabilizes C5, and is only present in the cardiac and fast skeletal isoforms (86, 258).

In comparison to the cardiac isoform, much less is known about the skeletal isoforms. sMyBP-C and fMyBP-C are encoded by *MYBPC1* and *MYBPC2* located on human chromosomes 12 and 19, respectively (594). Similar to cMyBP-C, a single transcript has been described for fMyBP-C, which encodes a protein of ~130 kDa (614). sMyBP-C, however, is unique, as there are several variants that have been reported ranging in size from ~126 to ~131.5 kDa (15). The slow variants result from extensive alternative splicing of small amino acid segments within the Pro/Ala rich motif, the M-motif, Ig domain C7, and the extreme COOH-terminus (12). Accordingly, 14 sMyBP-C variants have been described in human skeletal muscles to date. The different sMyBP-C variants are coexpressed in variable amounts and combinations in both slow and fast-twitch skeletal muscles where they may coexist with fMyBP-C (11). However, there is no single mammalian muscle that expresses all known sMyBP-C proteins, which is indicative of their distinct structural and regulatory roles (7, 9-13).

cMyBP-C is expressed in embryonic, neonatal, and adult hearts (156, 172, 266, 594, 615). In mice, it is first detected at gestational day 8 coinciding with the appearance of titin (172). Expression of sMyBP-C succeeds the expression of titin and sarcomeric myosin by about 5 days, at approximately gestational day 14, while expression of fMyBP-C follows at gestational day 18 (172). Given the expression of sMyBP-C during early embryogenesis, it has been postulated that it has essential roles during myofibrillogenesis (4).

The location of MyBP-C in the thick filament was first shown by immuno-electron microscopy (immuno-EM), revealing its presence in 7 to 9 transverse stripes (C-zone) within the cross-bridge-bearing region of each half A-band (114,183). Early studies postulated that binding of the COOH-terminus of MyBP-C to titin determines its localization, given that titin is incorporated into sarcomeres prior to MyBP-C and exhibits the same periodic organization (152, 197). Notably, the distance between the MyBP-C stripes is ~43 nm, which is equal to the spacing of the myosin helix repeat (340). Different models have been proposed for the positioning and orientation of MyBP-C in the sarcomere to date, primarily focusing on cMyBP-C. These include the axial, the circumferential, the axial/radial, and the circumferential/radial models (304, 318). Early studies on MyBP-C localization using X-ray diffraction modeling suggested an axial arrangement of the entire molecule along the thick filament (257,528). Alternatively, the circumferential arrangement proposed that three molecules of cMyBP-C form collar-like rings every 43 nm around the thick filament, which are stabilized by intermolecular interactions mediated by the C5-C10 region, specifically between C5 and C8, and C7 and C10 (151, 152, 304, 382). Interestingly, binding interactions between the respective domains of fMyBP-C were also shown by surface plasmon resonance, suggesting that fMyBP-C may also wrap around the thick filament like a collar. Such interactions were considerably weaker between the corresponding domains of sMyBP-C with an estimated K_a at least 10-fold lower than that for the cMyBP-C domains (151). Lastly, the axial/radial and circumferential/radial models propose axial and circumferential orientation of the COOH-terminus of MyBP-C, respectively, with radial extension of the NH_2-terminus toward the thin filament (318). Consistent with an axial/radial arrangement of the protein, it was recently shown that the last three COOH-terminal domains (C8-C10) of cMyBP-C are located roughly parallel to the thick filament axis while the majority of the molecule (C0-C7) runs transversely to the thick filament (318). Notably, this orientation allows the NH_2-terminus to dynamically interact with both the thin and thick filaments (529).

Similar to the cardiac isoform, fMyBP-C and the majority of the sMyBP-C variants are targeted to the C-zone. However, select sMyBP-C variants (e.g., variants 1, 6, 7, 8, 9, 002, and 202) possess a unique COOH-terminal insertion of 26 residues and preferentially localize to the periphery of the M-band (7).

Binding partners

Based on its sarcomeric location, it is apparent that the main binding partners of MyBP-C are myosin, actin, and titin. Notably, later studies identified additional binding partners including obscurin, muscle-type creatine kinase, and myosin RLC (Fig. 8).

Actin (~42 kDa)

In addition to binding myosin (the interaction is described in the Myosin section above), cMyBP-C also binds actin (384, 385, 613). Early competition studies suggested that the binding between actin and cMyBP-C is specific, since it was abolished by myosin S1 (interacting with actin) in the absence of ATP, and cMyBP-C could displace myosin S1 from actin in the presence of ATP (385). A number of recent studies have attempted to precisely map the binding site of actin on cMyBP-C, occasionally yielding conflicting results. Several reports have identified the NH_2-terminal C0-C2 region as the actin binding site, although the interaction appears to be weak with an affinity in the μmol/L range (147, 336, 400, 486). In particular, sequences in C0 (298, 336, 425, 601), C1 (55, 511), the first 17 amino acids of the M-motif (597), and the folded tri-helix structure of the M-motif (54) were shown to support binding to actin, suggesting that there may be multiple (apparently weak) interaction sites dispersed throughout the NH_2-terminus of cMyBP-C. This was further supported by the ability of the C1-C2 region to cross-link F-actin filaments (400). Contrary to the above studies, Rybakova and colleagues reported that the COOH-terminal C5-C10 region confers binding to actin in a saturable and specific manner (486). Recent work on sMyBP-C has also located the actin binding site in the NH_2-terminus of the protein encompassing

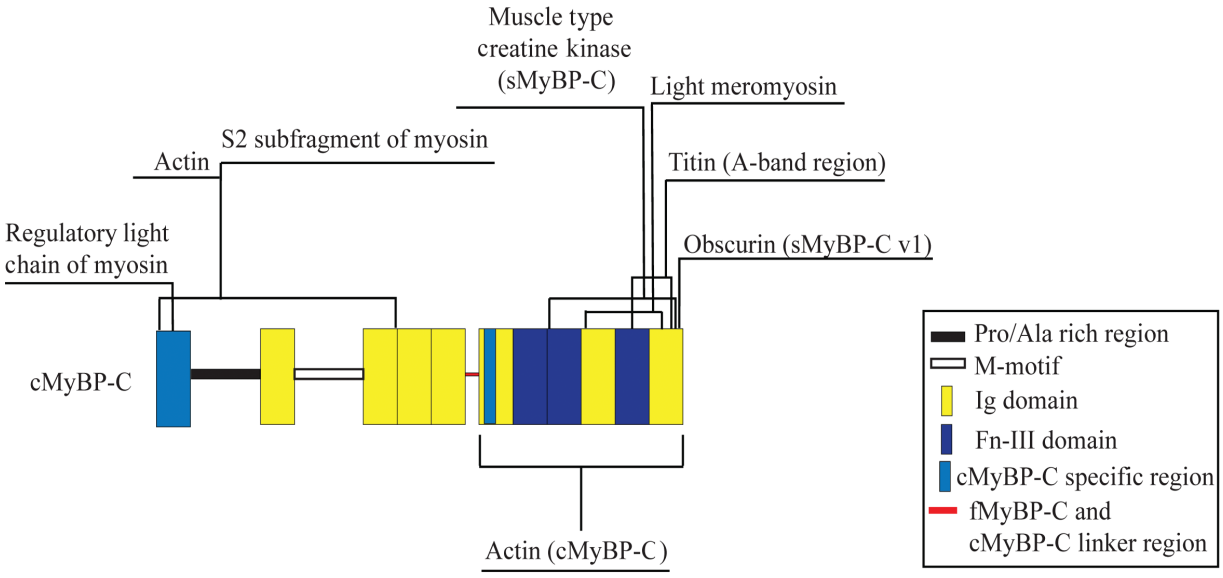

Figure 8 Binding partners of the three MyBP-C isoforms. Binding regions are shown on the cMyBP-C isoform to also include interactions mediated by C0. Binding to all partners has been determined for both cMyBP-C and sMyBP-C unless binding is located within a cardiac specific region (light blue) or noted only for sMyBP-C. Much less research has focused on confirming or identifying binding partners of fMyBP-C.

the Pro/Ala-C1-M-motif region, although the strength of the interaction appears to be variant-specific (13).

The ability of MyBP-C to bind both actin and myosin classifies it as the only myofilament protein that can link the thick and thin filaments within the region of active cross-bridge cycling (570).

Titin (3-4 MDa)

MyBP-C's other thick filament binding partner, titin, has been suggested to dictate its periodic positioning along the thick filament, as the region of titin that lies in the C-zone of the A-band also exhibits a periodicity of ~43 nm (306, 307). Early work had shown that radiolabeled skeletal MyBP-C binds strongly and specifically to the first Ig domain within titin's second set of super repeats, and binding was retained by a MyBP-C fragment lacking the NH_2-terminal 171 residues (165), suggesting that the COOH-terminus of the protein mediates binding to titin. Later studies using recombinant titin and cMyBP-C fragments mapped the titin binding site to domains C8-C10 (160). Although the interaction between MyBP-C and titin is relatively weak, the interaction between MyBP-C, myosin, and titin has been suggested to be instrumental in the ordered arrangement of the sarcomere (160).

Obscurin (~50-970 kDa)

Unique to sMyBP-C, the COOH-terminus of select slow variants (e.g., human variants 1, 6, 7, 8, 9, 002, and 202), contains a 26-amino acid long insertion that along with Ig domain C10 supports binding to the NH_2-terminal Ig2 repeat of the giant protein obscurin at the periphery of the sarcomeric M-band in both developing and adult skeletal myofibers (7). Overexpression of obscurins' Ig2 domain in primary cultures of skeletal myotubes disrupts the formation of M-bands and A-bands, and thereby the localization of sMyBP-C variants at M-bands, suggesting that obscurins play key roles in the stability and maintenance of thick filaments, and the targeting of select sMyBP-C variants to the periphery of M-bands (7,551).

Muscle-type creatine kinase (M-CK; ~43 kDa)

sMyBP-C directly binds to the M-CK (99). Using a combination of *in vitro* binding assays, it was shown that domains C6-C10 of sMyBP-C support binding to M-CK (99). The interaction has been suggested to be important, as Ig domain C10 also supports binding to myosin. In ATPase assays, ATP expenditure accelerated upon the association of the three proteins, and the apparent K_m value of myosin was therefore reduced (99). Thus, by functionally coupling myosin, sMyBP-C, and M-CK, sMyBP-C acts as an adaptor that connects the ATP consumer (myosin) and the ATP regenerator (M-CK) for efficient energy metabolism and homeostasis.

Myosin RLC (~18-19 kDa)

As discussed earlier, cMyBP-C contains an additional Ig domain, C0, and this domain binds to RLC (467). Although not proven yet, it has been postulated that C0 may be positioned between the two RLCs where it could influence the relative orientation of the myosin S1 heads (467).

Functions

Structural and regulatory roles have been suggested for the MyBP-C family in both cardiac and skeletal muscles

(4, 304, 322, 449, 604), although most of our knowledge stems from studies on cMyBP-C.

Structural roles

Early biochemical work demonstrated that MyBP-C plays key roles in the regular assembly of myofibrils, as the presence of normal MyBP-C levels is required for the regular assembly of synthetic myosin filaments in regards to thickness, length, formation of bare zone, and distribution of myosin heads (604). Consistent with this, Harris and colleagues showed that cMyBP-C null hearts (cMyBP-C$^{-/-}$) develop fibrosis, and contain misaligned (yet structurally intact) sarcomeres by 3 to 4 months of age (222). Ultrastructural evaluation of cMyBP-C$^{-/-}$ hearts further confirmed these findings revealing the presence of misaligned Z-disks. Functionally, the null hearts displayed significantly depressed indices of diastolic and systolic functions and reduced Ca^{2+} sensitivity of tension (222, 304, 367). Similarly, a second cMyBP-C null model generated by Carrier and colleagues also exhibits myocardial disarray with increased interstitial fibrosis, and additionally develops eccentric left ventricular hypertrophy characterized by depressed fractional shortening by 3 to 4 months of age and markedly impaired relaxation by 9 months of age (83, 222, 365, 427).

Much less is known about the structural roles of the skeletal isoforms. Early on, Davis and colleagues demonstrated that addition of purified rabbit skeletal MyBP-C reduces the critical concentration required for myosin polymerization *in vitro* (119). Moreover, Abdul-Hussain and colleagues reported that sMyBP-C is the major MyBP-C isoform expressed during early myofibrillogenesis in cultured primary human skeletal myotubes, suggesting that it may be essential for sarcomeric assembly and maintenance (4). Recently, Li and colleagues indicated that knockdown of fMyBP-C in zebrafish larvae leads to development of a myopathic phenotype, characterized by shorter sarcomeres, wider interfilament spacing, and muscle weakness (322). Muscle function was also significantly impaired, and was characterized by reduced force production, prolonged time between stimulus and onset of contraction, and slower rates of contraction and relaxation (322).

Regulatory roles

In addition to its proposed structural role, accumulating evidence has implicated MyBP-C in the regulation of cross-bridge cycling, myofilament Ca^{2+} sensitivity, and enzymatic activity of myosin.

Cross-bridge cycling. The first evidence that MyBP-C contributes to the regulation of cross-bridge cycling came from *in vitro* studies indicating that addition of purified rabbit skeletal MyBP-C in skinned myofibers slows down the shortening velocity of actomyosin cross-bridges (237). Despite this early work using skeletal MyBP-C, our current understanding of how MyBP-C modulates actomyosin cross-bridges comes from extensive *in vitro* and *in vivo* studies on cMyBP-C. Accordingly, it has been demonstrated that the first ~29 kDa of the NH_2-terminus of cMyBP-C, containing Ig domain C0, the Pro/Ala rich motif, Ig domain C1, and the first 17 amino acids of the M-motif has an inhibitory effect on thin filament sliding velocity along thick filaments at high Ca^{2+} concentrations (450). Interestingly, later studies further showed that cMyBP-C inhibits maximal sliding velocity of fully activated thin filaments at high Ca^{2+} concentration (i.e., pCa4), but activates actomyosin force generation and thin filament sliding at low Ca^{2+} concentration (i.e., pCa9) (449, 471). It has therefore been suggested that cMyBP-C may act both as a "brake" and an "accelerator," ultimately regulating the rate of formation of actomyosin cross-bridges as a function of Ca^{2+} levels.

Myofilament Ca^{2+} sensitivity. Moreover, cMyBP-C modulates myofilament Ca^{2+} sensitivity, as extraction of cMyBP-C from skinned rat cardiomyocytes and trabeculae results in dramatic increase of Ca^{2+} sensitivity, that is reversed by addition of μmol/L amounts of purified protein (237, 299, 351). Consistent with this, cMyBP-C null cardiomyocytes exhibit higher Ca^{2+} sensitivity than wild type (85, 98, 222, 427).

Myosin ATPase activity. Early studies had shown that MyBP-C modulates the actin activated, but not the intrinsic, ATPase activity of myosin (224, 384, 604, 613). Specifically, work from Yamamoto and colleagues as well as Winegrad and colleagues demonstrated that addition of purified cMyBP-C increases the enzymatic activity of cardiac myosin in the presence of actin independently of ionic strength (604,613). Given that cMyBP-C undergoes extensive phosphorylation within its NH_2-terminus (please see below), the effects of phosphorylation on the ATPase activity of myosin were evaluated, too. Although phosphorylated cMyBP-C also enhances the actin-activated ATPase activity of myosin, maximal activity was considerably lower (224). Moreover, work from Weisburg and colleagues further indicated that phosphorylation of cMyBP-C may differentially affect the actin-activated ATPase activity depending on the myosin isoform (596). Thus, PKA-mediated phosphorylation of cMyBP-C had no effect on the enzymatic activity of βMyHC, but significantly increased the enzymatic activity of αMyHC (596). Contrary to cMyBP-C, skeletal MyBP-C isolated from rabbit slow- and fast-twitch muscles has a biphasic effect on the ATPase activity of myosin that depends on ionic strength. At low ionic strength, it is strongly inhibitory, whereas at high ionic strength, it is moderately stimulatory (613). This inhibitory effect of skeletal MyBP-C at low ionic strength may result from competition with the S1 fragment of myosin for actin binding as it is not relieved by increasing actin concentration (384, 613).

Posttranslational modifications

The regulation of MyBP-C via PTM, and particularly phosphorylation, has been a major focus of several groups (199, 213, 347, 394, 451) (Fig. 9 and Table 8). In addition to phosphorylation, cMyBP-C undergoes acetylation, citrullination,

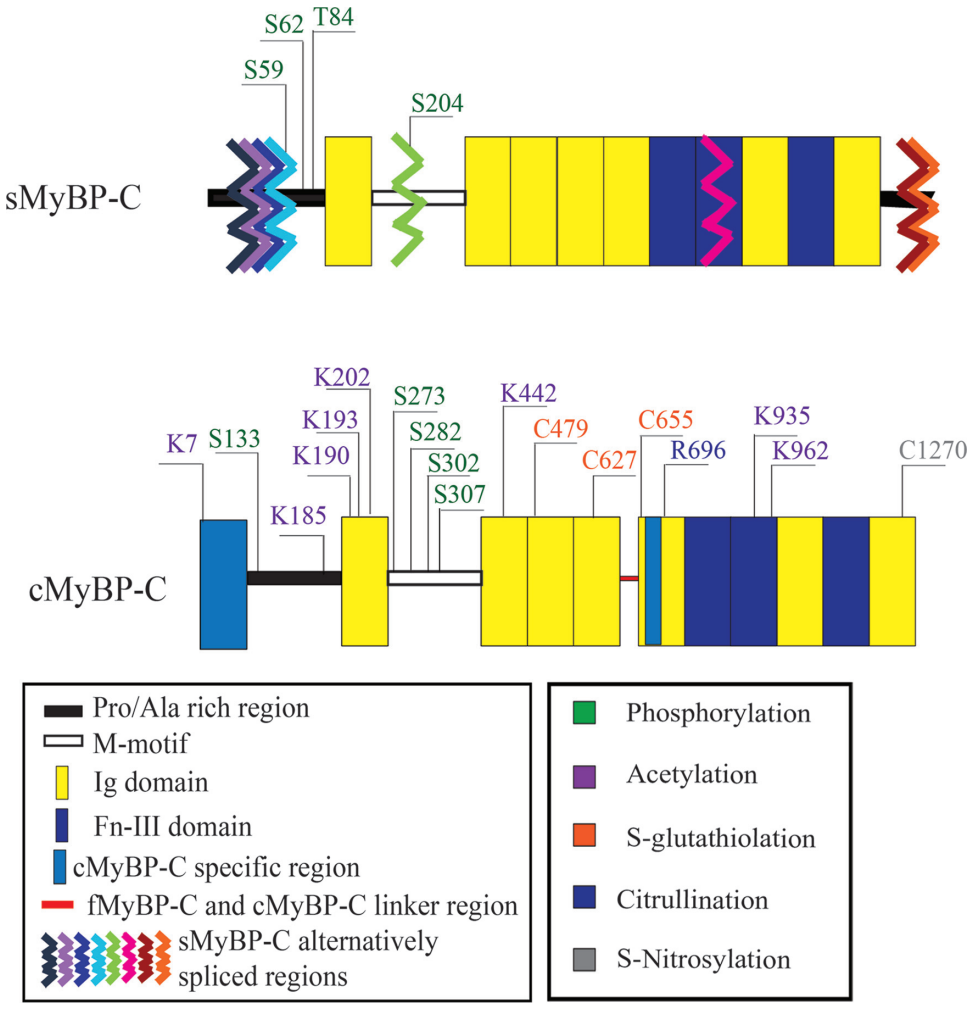

Figure 9 Posttranslational modifications identified in cMyBP-C and sMyBP-C. Phosphorylation sites in sMyBP-C and cMyBP-C (green) are located within their NH_2-terminal regions. Acetylation of lysine residues in cMyBP-C (purple) is primarily located in the NH_2-terminus and Ig domain C7. S-glutathiolation of cMyBP-C (orange) occurs in the central region of the protein within Ig domains C3-C5. One citrulination site (blue) and one S-nitrosylation site (gray) are located within the COOH-terminus of cMyBP-C. There are no known posttranslational modifications in fMyBP-C.

S-glutathiolation, S-nitrosylation, and carbonylation (84) (Fig. 9 and Table 8).

Phosphorylation

A great amount of literature has examined the effects of phosphorylation of cMyBP-C on actomyosin binding and contractile regulation (42, 451, 491). cMyBP-C is heavily phosphorylated within the NH_2-terminal M-motif at murine residues Ser273, Ser282, Ser302, and Ser307 (304). Protein kinase C (PKC) phosphorylates Ser273 and Ser302 (381), Ca^{2+}/calmodulin-dependent protein kinase II (CaMKII) and protein kinase D (PKD) primarily target Ser302 (40,174,490), ribosomal s6 kinase phosphorylates Ser282 (115, 142), and PKA is able to target all four residues. Ser307 has only been shown as a phosphorylatable residue in mice, as it is not conserved in humans (174, 381).

A hierarchy in the order of these phosphorylation events has been proposed from both *in vitro* and *in vivo* studies. Recombinant proteins encompassing the human C1-M-C2 region in which the three phosphorylatable serines (e.g., Ser273, Ser282, or Ser302) were individually mutated to Ala revealed that phosphorylation of Ser282 is required for Ser302 phosphorylation *in vitro* (488). Moreover, generation of three transgenic mouse lines expressing mutant cMyBP-C containing either Ser273-Ala282-Ser302 (cMyBP-C^{SAS}), Ala273-Asp282-Ala302 (cMyBP-C^{ADA}), or Asp273-Ala282-Asp302 (cMyBP-C^{DAD}) further demonstrated that Ser282 phosphorylation is critical, as loss of phosphorylation at Ser282 (cMyBP-C^{SAS} model) leads to decreased diastolic function at baseline, diminished β-adrenergic response, and reduced phosphorylation at Ser302 following stimulation (490). Similar to the cMyBP-C^{SAS} model, the cMyBP-C^{DAD} and cMyBP-C^{ADA} mice also showed diminished β-adrenergic response

Table 8 Posttranslational Modifications in MyBP-C Isoforms

Protein name	Accession #	Residue(s)	Reference
		MYBPC1 gene	
Myosin binding protein-C slow	Mouse: XM_006513045	Phosphorylation	
		Mouse: S59, S62, T84, S204	Ackermann et al., 2011
		MYBPC3 gene	
Myosin binding protein-C (cardiac isoform)	Human: NP_000247.2 Mouse: NP_032679.2	Phosphorylation	
		Human: S133 Mouse: S131	Kuster et al., 2013
		Human: S275, S304 Mouse: S273, S302	Mohamed et al., 1998 Gautel et al., 1995
		Human: S285 Mouse: S282	Ferrari et al., 1985 Cueoll et al., 2011
		Mouse: S307	Jia et al., 2010
		Acetylation	
		Mouse: K7, K185, K190, K193, K202	Govindan et al., 2012
		S-glutathiolation	
		Mouse: C479, C627, C655	Patell et al., 2013
		Citrullination	
		Human: R696	Fert-Bober & Sokolove, 2014
		S-nitrosylation	
		Mouse: C1270	Kohr et al., 2011

after dobutamine treatment, emphasizing the importance of phosphorylation at all three sites.

Early studies had shown that phosphorylation of Ser273, Ser282, and Ser302 accelerates contraction by disrupting the binding of the NH_2-terminus of cMyBP-C to myosin (596). Further experimentation confirmed these findings by describing an inverse relationship between the levels of unphosphorylated cMyBP-C and maximal Ca^{2+} activated force production in skinned rat trabeculae and skeletal muscle (301, 364). In later studies, measurements of cross-bridge cycle kinetics (i.e., rate constant of force development, k_{tr}) at submaximal Ca^{2+} activation were significantly elevated following PKA treatment in wild-type myocardia, however, this increase in kinetics was not observed in cMyBP-$C^{-/-}$ (null) myocardia (106). These studies were extended by measuring X-ray intensity ratios in trabeculae of wild type and cMyBP-$C^{-/-}$ mice under relaxed conditions to investigate the role of phosphorylation on the distribution of cross-bridge mass between thick and thin filaments. In resting myocardia, PKA-mediated phosphorylation of cMyBP-C resulted in a net transfer of mass from the thick to the thin filament by allowing myosin heads to move closer to the thin filament, therefore increasing the probability of actomyosin cross-bridges, and ultimately leading to acceleration of cooperative recruitment of additional cross-bridges (106).

Later studies further demonstrated that phosphorylation of cMyBP-C is essential for normal cardiac function and may be cardioprotective (478, 491, 492, 554). A phosphomimetic mouse model, in which all known phosphorylation sites were mutated to Asp (cMyBP-C^{AllP+}) showed no signs of cardiac hypertrophy or mortality (492). Notably, cMyBP-C^{AllP+} mice exhibited relatively conserved cardiac function and minimal cellular damage following ischemia/reperfusion injury (175, 492). Moreover, when the cMyBP-C^{AllP+} line was bred with a cMyBP-$C^{-/-}$ line, which displayed DCM, myocyte hypertrophy, fibrosis, and calcification (365), the cMyBP-C^{AllP+} allele was able to rescue the null phenotype, and the cMyBP-$C^{AllP+:null}$ hearts displayed normal structure and contractility (492).

cMyBP-C is dephosphorylated in heart failure (491), which correlates well with the reported increased levels of phosphatases (412). In support of the harmful effects of dephosphorylated cMyBP-C in heart failure, a transgenic mouse model in which all phosphorylation sites were mutated to nonphosphorylatable Ala (MyBP-C^{AllP-}) showed significantly decreased rates of contraction and relaxation, despite

the normal incorporation of mutant cMyBP-C into sarcomeres (478, 491). Moreover, the normal increase in twitch force resulting from increased pacing frequency was severely blunted in the MyBP-C^{AllP-} myocardia compared to wild type, even following β-adrenergic stimulation (555). Similarly, a non-PKA phosphorylatable cMyBP-C model exhibited systolic dysfunction due to decelerating cross-bridge kinetics (554). Notably, the phosphorylation levels of cMyBP-C were increased in a regionally stunned canine model, which mimics human coronary ischemic disease, possibly as a compensatory (cardioprotective) response (619). Consistent with this, phosphorylation of Ser288 (mouse Ser282) by CamKII was largely inhibited in a globally stunned rat model when stunning was prevented either by ischemic preconditioning or reperfusion, resulting in complete recovery of left-ventricular pressure (619).

Recent work using negative staining EM indicated that Ca^{2+} antagonizes the effects of phosphorylation. In particular, a recombinant NH_2-terminal cMyBP-C fragment containing the C0-C3 region adopts a compact conformation in the presence of phosphorylation (451). Addition of Ca^{2+} at peak contraction concentration reverses the impact of phosphorylation, altering the conformation of the C0-C3 region from compact to extended. This finding was further corroborated by *in vitro* motility assays demonstrating that wild-type recombinant C0-C3 and its phosphomimetic counterpart are functionally indistinguishable in the presence of physiological Ca^{2+} levels (0.5-1.2 μmol/L) (451). It therefore becomes apparent that phosphorylation and Ca^{2+} fine-tune the ability of cMyBP-C to modulate the formation and rate of actomyosin cross-bridges.

In addition to affecting the regulatory activities of cMyBP-C, phosphorylation also modulates its stability. In models of myocardial infarction, phosphorylation of cMyBP-C is significantly diminished, coinciding with increased degradation and release of NH_2-terminal fragments (124, 189).

Although cMyBP-C is primarily phosphorylated within the M-motif, a recent study reported the presence of glycogen synthase kinase β (GSKβ)-mediated phosphorylation of Ser133 located in the Pro/Ala rich region (539). The functional importance of this phosphorylation event has only been cursorily examined indicating that GSKβ treatment of permeabilized human cardiomyocytes enhances the maximal rate of tension development (305).

sMyBP-C is also subjected to phosphorylation within its NH_2-terminus (10). Contrary to cMyBP-C, however, sMyBP-C primarily undergoes phosphorylation in the Pro/Ala rich region and to a lesser extent in the M-motif (10). Three phosphorylation sites have been identified in the Pro/Ala rich region, including Ser59, Ser62, and Thr84, whereas one site, Ser204, has been reported in the M-motif. Ser59 and Ser62 are substrates of PKA, Thr84 is a substrate of PKC, and Ser204 is a substrate of both PKA and PKC (10). Interestingly, Ser62 and Thr84 reside in constitutively expressed exons, and are present in all slow variants, whereas Ser59 and Ser204 are located in alternatively spliced exons, and are present in select slow variants (12).

Although the effects of phosphorylation of sMyBP-C proteins are largely elusive, recent work has demonstrated that the levels of phosphorylation of sMyBP-C are altered in response to (patho)physiological stressors. Consistent with this, the overall phosphorylation levels of sMyBP-C are significantly reduced in both fast- (e.g., Flexor Digitorum Brevis) and slow-twitch (e.g., soleus) muscles as a function of aging, dystrophy, and distal arthrogryposis (15), but increased in slow-twitch muscles in response to fatigue (15). Thus, the phosphorylation profile of sMyBP-C is differentially altered depending on the muscle and the exerted stressor.

Other PTM present in cMyBP-C

In addition to phosphorylation, cMyBP-C undergoes additional PTM, including acetylation, citrullination, S-glutathiolation, S-nitrosylation, and carbonylation (84).

Eight acetylation sites have been identified within cMyBP-C, with six of them residing in the C0-C2 region, however, their exact effects are currently unknown (84). Interestingly, the presence of increased acetylation of a ~40 kDa proteolytic fragment of cMyBP-C suggested that acetylation may lead to decreased stability by promoting proteolysis, thereby acting opposite to phosphorylation (84).

Citrullination of cMyBP-C has also been reported at Arg696 in the myocardium of patients with rheumatoid arthritis, inflammatory myocarditis, and scleroderma (143), but the effects of this modification on the functional properties or stability of the protein are still unknown.

The presence and effects of S-glutathiolation of cMyBP-C have recently been described with the identification of three target sites; Cys-479, Cys-627, and Cys-655 (430). Isolated myofibrils and detergent-extracted fiber bundles treated with oxidized glutathione increased myofilament Ca^{2+} sensitivity compared to controls (430). Moreover, S-nitrosylation of Cys-1270 was found in murine hearts perfused with the S-nitrosylating agent S-nitroglutathione, but whether this modification occurs *in vivo* is currently unknown (84, 285). Lastly, in addition to undergoing reversible oxidative modifications (e.g., S-glutathiolation and S-nitrosylation), cMyBP-C is also subjected to irreversible oxidative modification via carbonylation in spontaneously hypertensive tumor-bearing rats after 14 days of doxycycline treatment (27).

Contrary to cMyBP-C, there is no information about the presence of additional PTM (with the exception of phosphorylation in sMyBP-C) in the skeletal isoforms. Thus, extensive work is required to decipher the roles of the different PTM in cMyBP-C, and examine their potential presence and effects in the skeletal isoforms.

Mutations and myopathies

More than 500 mutations have been reported in *MYBPC3* that are primarily associated with the development of HCM, and to

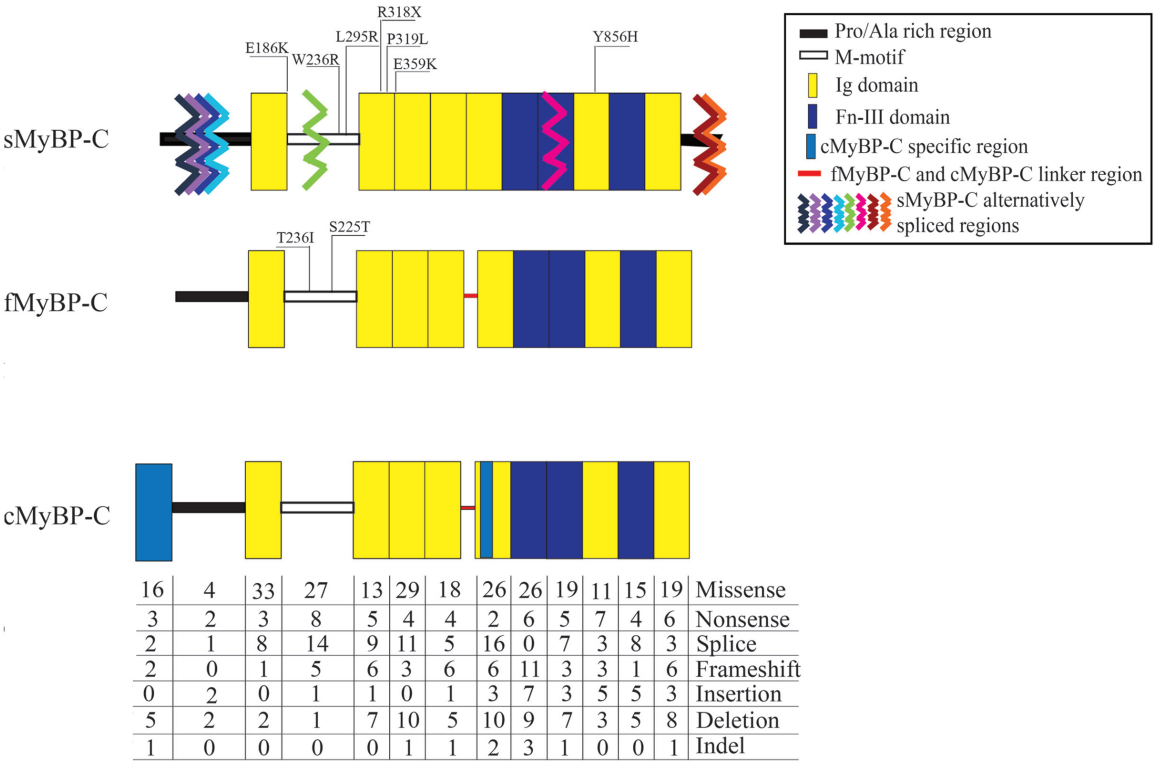

16	4	33	27	13	29	18	26	26	19	11	15	19	Missense
3	2	3	8	5	4	4	2	6	5	7	4	6	Nonsense
2	1	8	14	9	11	5	16	0	7	3	8	3	Splice
2	0	1	5	6	3	6	6	11	3	3	1	6	Frameshift
0	2	0	1	1	0	1	3	7	3	5	5	3	Insertion
5	2	2	1	7	10	5	10	9	7	3	5	8	Deletion
1	0	0	0	0	1	1	2	3	1	0	0	1	Indel

Figure 10 Illustration of the individual (sMyBP-C and fMyBP-C) or number and type (cMyBP-C) of mutations per domain that have been identified to date in the MyBP-C family.

a lesser extent with DCM and left ventricular noncompaction (LVNC) (61, 84, 304, 341, 593). Since two relatively recent reviews list known mutations until 2013 (223, 274), Table 9 includes additional mutations that were not included or identified since then, while Figure 10 indicates the total number of currently known mutations per domain.

HCM affects about 1:200 individuals (510), and is characterized primarily by left ventricular hypertrophy (LVH). Clinical presentation can vary between asymptomatic and progressive hypertrophy to heart failure (223). *MYBPC3* mutations that cause HCM have been identified in about 20% to 30% of all diagnosed HCM cases, second only to mutations in β-MyHC (611) (please see above). DCM is also a heterogeneous group of inherited and idiopathic disorders that is characterized by cardiac dilation and reduced systolic function (611). Gene mutations, including those found in *MYBPC3*, are a likely cause of DCM, as it is estimated that up to 35% of cases are familial (133). The clinical manifestations of individual *MYBPC3* mutations causing HCM and DCM are highly heterogeneous reflecting their widespread distribution throughout the entire gene (84, 223).

Dominant nonsense mutations or insertion/deletions are commonly found in *MYBPC3*, resulting in the generation of truncated proteins due to premature stop codons, exon skipping, or frameshifts. The majority of these mutations function via haploinsufficiency (41, 84, 304, 351). Consistent with this, the levels of mutant cMyBP-C proteins are commonly reduced in cardiac biopsies of affected individuals (480). Notably, both the ubiquitin-proteasomal axis and the nonsense-mediated mRNA decay pathway mediate degradation of mutant cMyBP-C proteins (351).

The mechanism through which haploinsufficiency of mutant *MYBPC3* underlies HCM has gained considerable interest. *In vitro* studies have shown that HCM-linked *MYBPC3* mutations cause increased Ca^{2+} sensitivity of contractile myofilaments, resulting in faster cross-bridge turnover rate and incomplete relaxation (353). As such, myocardia from HCM patients exhibit ~20% higher Ca^{2+} sensitivity compared to myocardia from normal subjects (244, 261, 351, 571). It has therefore been proposed that *MYBPC3* mutations increase myofibrillar Ca^{2+} sensitivity, which is necessary and sufficient to induce HCM (351). Notably, PKA-mediated phosphorylation of mutant cMyBP-C is significantly reduced in human mutant myocardia (111, 351, 370). Given that restoration of phosphorylation of mutant cMyBP-C returns myofilament Ca^{2+} sensitivity to nearly normal levels (351), it has been postulated that restoration of phosphorylation may be an effective treatment option for *MYBPC3*-linked HCM.

In addition to missense mutations, deletions have also been identified in *MYBPC3*. One mouse model of interest lacks exon 30, which results in frameshift and the generation of a truncated protein (365). Truncated cMyBP-C fails to incorporate into sarcomeres in murine myocardia, similar to myocardia from affected individuals that present with autosomal dominant familial HCM. Heterozygous mice

Table 9 Mutations Identified in MyBP-C Isoforms

Mutation	Domain	Disease	Reference
	MYBPC1		
	Missense mutations		
E186K	C1	AMC	Ekhilevitch et al., 2016
W236R	M-motif	DA-1	Gurnett et al., 2010
P319L	C2	DA-2	Li et al., 2015
E359K	C2	DA-2	Li et al., 2015
Y856H	C8	DA-1	Gurnett et al., 2010
	Nonsense mutations		
R318Stop	C2	LCCS-4	Markus et al., 2012
	MYBPC2		
	Missense mutations		
T236I	M-motif	Unclassified DA	Bayram et al., 2016
S255T	M-motif	Unclassified DA	Bayram et al., 2016
	MYBPC3		
	Large insertions or deletions		
Insertion of 1851 bp ex.13-27	Described at genomic DNA level	HCM	Herman et al., 2009
Duplication of 22 bp cd.740-747	Described at cDNA level	HCM	Richard et al., 2003
Duplication of 26 bp c.676_701	Described at genomic DNA level	HCM	Nannenberg et al., 2011
Gross deletion: 3505 bp c.2905+280_*485	Described at genomic DNA level	HCM	Chanavat et al., 2012
Gross deletion: 25 bp c.3628-41_3628-17	Described at genomic DNA level	HCM	Waldmuller et al., 2003
Gross deletion: ex. 25	Described at cDNA level	HCM	Jouven et al., 2002
Gross deletion: ex. 33	Described at cDNA level	HCM	Jouven et al., 2002
Incl. ex. 23-26	Described at genomic DNA level	HCM	Nannenberg et al., 2011
Del 215bp, ins 9bp	C8	HCM	Herman et al., 2009
	Small insertions and deletions		
Deletion: GGATCT^(79)TACGcAGTCATTGCT	Insertion: gag; C0	DCM	Lakdawala et al., 2012
Deletion: GGGCAG^(470)CGGGtgGAGTTTGAGT	Insertion: at; C3	HCM	Rodriguez-Garcia et al., 2010
Deletion: CCAAG^(647)ATCCAcctggaCTGCCCCAGGC	Insertion: t; linker between C4 and C5	HCM	Santos et al., 2012
Deletion: TGGAAAT^(666)AAGctACGTCTGGAC	Insertion: g; C5	DCM	Zimmerman et al., 2010
Deletion: GTCTG^(670)GACGTccctATCTCTGGGG	Insertion: gg; C5	HCM	Harris et al., 2011
Deletion: GAAGCG^(834)CGGCgcATGATCGAGG	Insertion: tt; C6	HCM	Otsuka et al., 2012
Deletion: CTACGCG^(849)GTCaacgccatcggcaTGTCCAGGC	Insertion: ggcg; C6	HCM	Zou et al., 2013
Deletion: TCAAC^(851)GCCATcgGCATGTCCAG	Insertion: tct; C6	HCM	Morner et al., 2003
Deletion: TCTGCCCAG_T25E26_GtcCC^(870)CCCAGCGA	Insertion: a; C7	HCM	Marston et al., 2009
Deletion: AATGGC^(1219)CTGGacctGGGAGAAGAC	Insertion: ttcaagaatgg; C10	HCM	Carrier et al., 1997

Table 9 (*Continued*)

Mutation	Domain	Disease	Reference
	Small insertions		
TGCCCCT^(111)GCTtGAGGCCACTG	P/A region	DCM	Zimmerman et al., 2010
CGATGCA^(153)CCCcATTGGCCTCT	P/A region	HCM	Millat et al., 2010
CTGCGC^(347)GGCAcggcaTGCTAAAGAG	M-motif	HCM	Xie et al., 2005
GTACATC^(412)TTTtGAGTCCATCG	C2	HCM	Bortot et al., 2011
AGGTC^(569)TCAGAaTGAGAATGTT	C4	HCM	Tanjore et al., 2008
CCAGAG^(704)GACAaCAGGTGACAG	C5	HCM	Page et al., 2012
CCGAGG(741)GCCgGGGTCCGCGT	C5	HCM	Liu et al., 2015
CGGTC^(752)ACAGTtGAAGAACCCT	C5	Increased LV wall thickness	Morita et al., 2006
CACAGTA^(791)CAGgTGGGAGCCGC	C6	HCM	Niimura et al., 1998
GGAGCTG^(830)AGTtCATGAAGCGC	C6	HCM	Van Driest et al., 2004
CGCATG^(837)ATCGgAGGGCGTGGT	C6	HCM	Lopes et al., 2013
GGCGTG^(841)GTGTtACGAGATGCG	C6	HCM	Lopes et al., 2013
TGGTG^(842)TACGAgaGATGCGCGTC	C6	HCM	García-Castro et al., 2009
TCAAC^(851)GCCATTcggcatgtcc	C6	HCM	Van Driest et al., 2004
CCCAG^(863)CCCTTgcctcccagcccttCATGCCTATC	C6	HCM	Caramins et al., 2003
CCCTC^(889)AAGTGGgcggcccccа	C7	HCM	García-Castro et al., 2009
CAGGA^(900)GGCCTgcctGGATGGCTAC	C7	HCM	Harris et al., 2011
CACAC^(948)AATATTggcagggcct	C7	HCM	Roncarati et al., 2011
AGCATC^(1022)CGCAAacagccccac	C8	HCM	Brito et al., 2005
CATTCA^(1041)GGCCAaaCTTACCAGGT	C8	HCM	Niimura et al., 1998
GAGGAC^(1055)AAGGgCCACGCTGGT	C8	DCM	Zimmerman et al., 2010
GTGCTG^(1061)CAGGgcaggTTGTTG_E29I29_GTGC	C8	HCM	Song et al., 2005
TCCCGCAG_T29E30_ACc^(1065)AAGCCAAGTC	C8	HCM	Girolami et al., 2006
CGGGTG^(1075)ACTGtACGCCTGGGG	C9	DCM	Zimmerman et al., 2010
TCTGGAG^(1086)TGGgAAGCCACCCC	C9	HCM	Nannenberg et al., 2011
TCTGGAG^(1086)TGGggAAGCCACCCC	C9	HCM	Christiaans et al., 2010
CCAG_T30E31_^(1111)GAGTGagtgGTTCACCGTC	C9	DCM	Zimmerman et al., 2010
TGAGCCA^(1170)CCCcAACTATAAGG	C9	HCM	Waldmüller et al., 2011
CGCATG^(1230)TTCAttccaGCAAGCAGGG	C10	HCM	Erdmann et al., 2001
CTATGTC^(1253)TGCgggggcatctatgtctgcAGGGCCACCA	C10	HCM	Watkins et al., 1995
	Small deletions		
GGTACCAAGTcctgtcaCCAACAG_T31E32_GCA	Noncoding region	HCM	Andersen et al., 2004
GCGGA^(46)GGCAGtGACATCAGCG	C0	HCM	Ehlermann et al., 2008
GCCTG^(58)GCCACagagggcacacGGCATACGCT	C0	DCM	Zimmerman et al., 2010
TGGCC^(59)ACAGAgggcacacggcATACGCTGAC	C0	HCM	Van Driest et al., 2004
GAAGTG^(72)GGCCcTGCCGACCAG	C0	HCM	Millat et al., 2010
GCCCT^(74)GCCGAccagggaTCTTACGCAG	C0	HCM	Richard et al., 2003
GACCTC^(93)AAGGtCATAGAGGCA	P/A region	HCM	Andersen et al., 2004
CCGAT^(152)GACCCcATTGGCCTCT	P/A region	HCM	Bashyam et al., 2011
CCTCCTA^(269)TCAgccttccGCCGCAC_E7I7_GTG	M-motif	HCM	Kaski et al., 2009

(*continued*)

Table 9 (*Continued*)

Mutation	Domain	Disease	Reference
GCTCA^(298)CTGCTgAAAAAGAG_E9I9_GT	M-motif	HCM	Nannenberg et al., 2011
TGCTG^(300)AAAAAgAG_E19I9_GTGAGTCC	M-motif	HCM	Ma et al., 2009
GAGCAG_I10E11_C^(304)AGTttCCGGACCCCG	M-motif	HCM	Olivotto et al., 2008
CCTACGG^(327)CAGgCACCCCCATC	M-motif	HCM	García-Castro et al., 2009
CAGGCA^(329)CCCCcATCTGAGTAC	M-motif	HCM	Nannenberg et al., 2011
TACGGC^(342)GTCAcTGACCTGCGC	M-motif	HCM	Erdmann et al., 2003
CAAGATC^(382)CGGctgaccgtggaactggCTGACCATGA	C2	HCM	Andersen et al., 2004
ACTGGCT^(389)GACcATGACGCTGA	C2	HCM	Erdmann et al., 2001
TGACCAT^(391)GACgCTGAGGTCAA	C2	HCM	Olivotto et al., 2008
CCAGGAG^(403)ATCcAGATGAGCGG	C2	HCM	García-Castro et al., 2009
AG_I14E15_GTAC^(411)ATCTttGAGTCCATCG	C2	HCM	Richard et al., 2003
GTACC^(421)CTGACcatcagccagtgctCATTGGCGGA	C2	HCM	Waldmüller et al., 2011
TACCAG^(436)TGCGtGGTGGGTGGC	C2	HCM	Richard et al., 2003
GCACG^(446)GAGCTcTTTGTGAAAG	C3	HCM	Richard et al., 2003
GGACAG_I15E16_AGCCccCT^(454)GTGCTCAT	C3	HCM	Waldmuller et al., 2003
TCACG^(458)CGCCCcTTGGAGGACC	C3	HCM	Lin et al., 2010
^(485)AAATG_E16I16_GTGAGttccagaagcacggggcatg GGTGTTGGGG	C3	DCM	Zimmerman et al., 2010
ATACCGG^(503)TTCaagAAGGACGGGC	C3	HCM	Richard et al., 2003
CCTGATC^(514)ATCaacGAGGCCATGC	C3	DCM	Waldmüller et al., 2011
GCACT^(530)AGCGGgGGCCAGGCGC	C3	HCM	García-Castro et al., 2009
GGGGC^(533)CAGGCgcTGGCTGAGCT	C3	HCM	Richard et al., 2003
CCTGCAG_I17E18_ AAAaG^(544)AAGCTGGAG	Linker between C3 and C4	HCM	Harris et al., 2011
AGCTG^(546)GAGGTgtACCAGAGCAT	Linker between C3 and C4	HCM	Van Driest et al., 2004
ACCAG^(550)AGCATcgcagACCTGATGGGT	Linker between C3 and C4	HCM	Waldmüller et al., 2011
GTTCAAA^(566)TGTgaGGTCTCAGAT	C4	HCM	Van Driest et al., 2004
CATAAAG^(592)GTGtCCCACATCGG	C4	HCM	Kimura et al., 1997
TAAAG^(592)GTGTCcCACATCGGGC	C4	HCM	Konno et al., 2005
AG_I18E19_GGTC^(599)CACAaACTGACCATT	C4	HCM	Richard et al., 2003
CACTTG^(632)ATGG_E19I19_gtgAGCCTGCTCC	C4	HCM	Otsuka et al., 2012
GGGGAAT^(692)AAGgCCCCAGCCAG	C5	HCM	Millat et al., 2010
CAGGCCA^(698)GCCcCAGATGCCCC	C5	HCM	Niimura et al., 1998
AG^(716)AAG_E22I22_GTGAGtgagACTGAGGTCA	C5	DCM	Zimmerman et al., 2010
GCACCCCCCCaG_I22E23_^(717)CTGCTGTGT	C5	HCM	Alders et al., 2003
AG_I22E23_CTG^(718)CTGTGtgAGACCGAGGG	C5	HCM	Iascone et al., 2009
GACCGC^(734)AGCAtcttcacggtcgaggggggcaGAGAA GGAAG	C5	HCM	Waldmüller et al., 2011
GGCAGAG^(743)AAGgAAGATGAGGG	C5	HCM	Millat et al., 2010
AGTGAAG^(755)AACcCTGTGGGCGA	C5	HCM	Moolman-Smook et al., 1999
CACAGTC^(767)AAGgtcatcg_E23I23_GTGAGGCCGG	C5	HCM	Olivotto et al., 2008
AGTGG^(793)GAGCCgCCTGCCTACG	C6	HCM	Van Driest et al., 2004
CATC^(804)CTGG_E24I24_GTgAGTGCAAGGG	C6	HCM	Zou et al., 2013
CTACCGG^(818)TGGatgcgGCTGAACTTC	C6	HCM	Van Driest et al., 2004
TACGAG^(844)ATGCgcgtcTACGCGGTCA	C6	HCM	Carrier et al., 1997

Table 9 (*Continued*)

Mutation	Domain	Disease	Reference
TACGAG^(844)ATGCgcgtctaCGCGGTCAAC	C6	HCM	Page et al., 2012
GCGCGTC^(847)TACGcggtcaacgc	C6	HCM	Song et al., 2005
TCAAC^(851)GCCATCggcatgtcca	C6	HCM	Richard et al., 2003
AACGCC^(852)ATCGGcatgtccagg	C6	HCM	Van Driest et al., 2004
CAG_I25E26_GT^(869)CCCCCcAGCGAACCCA	C6	HCM	Kaski et al., 2009
AGAGCGC^(896)GTGggagcaggagGCCTGGATGG	C7	HCM	Olivotto et al., 2008
CCTGGAT^(903)GGCTacagcgtgga	C7	HCM	Olivotto et al., 2008
CCAGAG^(912)GGCT_E26I26_gtGAGTGTCCCC	C7	HCM	Richard et al., 2003
GAG^(912)GGCT_E26I26_GTGagtgTCCCCGCCCC	C7	HCM	Waldmüller et al., 2011
ACAGAG^(926)CACAcaTCGATACTGG	C7	DCM	Zimmerman et al., 2010
TTTCCGA^(944)GTGcgGGCACACAAT	C7	HCM	Anan et al., 2002
CCTGGA^(954)GCCCctGTTACCACCA	C7	HCM	Niimura et al., 1998
ACCTG^(980)CGCCAgaccaTTCAGAAGAA	Linker between C7 and C8	DCM	Zimmerman et al., 2010
TGGACC^(1009)AAAGaGGGGCAGCCC	C8	HCM	Witjas-Paalberends et al., 2013
TACCAG^(1045)GTGAcGGTGCGCATT	C8	HCM	Zou et al., 2013
CCAGGTG^(1046)ACGGtgcgcattga	C8	HCM	Erdmann et al., 2001
GACGCC^(1078)TGGGGtcttaatgtg	C9	HCM	Waldmüller et al., 2011
GCAAC^(1095)ACGGAActctgggggt	C9	HCM	Lekanne Deprez et al., 2006
AGCTC^(1098)TGGGGGtacacagtgc	C9	HCM	Waldmüller et al., 2011
CCGCCGC^(1122)ACCcACTGCGTGGT	C9	HCM	Liu et al., 2013
CACCCAC^(1124)TGCgtggtgccagagctcATCATTGGCA	C9	HCM	Zou et al., 2013
GAGCCC^(1158)GTCTttATCCCCAGAC	Linker between C9 and C10	DCM	Zimmerman et al., 2010
CACCC^(1171)AACTATaaggccctgg	Linker between C9 and C10	HCM	Millat et al., 2010
CTCGGTC^(1193)ATCgcgggctacactGCTATGCTCT	Linker between C9 and C10	HCM?	Lopes et al., 2013
CTGCT^(1199)ATCGCTctgctgtgctGTCCGGGGTA	Linker between C9 and C10	DCM	Zimmerman et al., 2010
ATGCTC^(1201)TGCTGtgctgtccgg	C10	HCM	Richard et al., 2003
GCTGTC^(1205)CGGGgTAGCCCCAAG	C10	HCM	Witjas-Paalberends et al., 2013
CGGGGT^(1207)AGCCcCAGG_E32I32_GTAGGG	C10	HCM	Li et al., 2009
GTGTTG^(1237)ACTCtgGAGATTAGAA	C10	HCM	Ruppert et al., 2008
AGCCC^(1244)TGCCCcTTGACGGGG	C10	DCM	Zimmerman et al., 2010
CGCATG^(1245)TTCcAGCAAGCAGG	C10	HCM	Liu et al., 2015
ACCAAC^(1258)TTACaGGGCGAGGCA	C10	Cardiomyopathy, LVNC	Dellefave et al., 2009
	Splice mutations		
IVS1 as −2 A-G	C0	HCM	Van Driest et al., 2004
IVS4 ds +5 G-C	P/A	HCM	Lin et al., 2010
IVS5 as −1 G-A	C1	HCM	Millat et al., 2010
IVS5 as −1 G-A	C1	HCM	Millat et al., 2010
IVS7 ds +1 G-T	C1	HCM	Caramins et al., 2003

(*continued*)

Table 9 (*Continued*)

Mutation	Domain	Disease	Reference
IVS7 ds +5 G-A	C1	HCM	Carrier et al., 1997
IVS8 as −20 C-A	M-motif	HCM?	Andersen et al., 2004
IVS8 as −10 C-G	M-motif	HCM	Liu et al., 2013
IVS8 as −1 G-A	M-motif	HCM	Waldmüller et al., 2011
IVS9 as −36 G-A	M-motif	HCM	Frank-Hansen et al., 2008
IVS9 as −1 G-C	M-motif	HCM	Frank-Hansen et al., 2008
IVS11 as −2 A-G	M-motif	HCM	Niimura et al., 1998
IVS12 ds −1 G-A	M-motif	HCM	Roncarati et al., 2011
IVS12 ds +1 G-A	M-motif	HCM	Girolami et al., 2006
IVS12 ds +1 G-C	M-motif	HCM	Millat et al., 2010
IVS12 ds +1 G-T	M-motif	HCM	Otsuka et al., 2012
IVS13 ds +1 G-C	C2	HCM	Millat et al., 2010
IVS13 ds +1 G-T	C2	HCM	Waldmuller et al., 2008
IVS13 as −19 G-A	C2	HCM	Waldmuller et al., 2008
IVS13 as −2 A-G	C2	HCM	Richard et al., 2003
IVS14 as −13 G-A	C2	HCM	Jaaskelainen et al., 2002
IVS15 ds +1 G-A	C2	HCM	Ho et al., 2009
IVS15 as −1 G-A	C2	HCM	Song et al., 2005
IVS16 as −6 G-A	C3	HCM?	Andersen et al., 2004
IVS16 as −1 G-C	C3	HCM	van Dijk et al., 2012
IVS17 ds +1 G-A	C3	HCM	Lekanne Deprez et al., 2006
IVS17 ds +1 G-C	C3	HCM?	Brito et al., 2005
IVS17 ds +2 T-C	C3	HCM	Richard et al., 2003
IVS17 as −2 A-G	C3	HCM	Otsuka et al., 2012
IVS18 ds +1 G-C	C3	HCM	Brito et al., 2012
IVS19 as −1 G-A	C4	HCM	Zou et al., 2013
IVS21 ds +1 G-A	C4	HCM	Konno et al., 2006
IVS21 ds +2 T-G	C4	HCM	Golubenko et al., 2004
IVS22 as −80 G-A	C5	DCM	Waldmüller et al., 2011
IVS22 as −3 C-G	C5	HCM	Liu et al., 2013
IVS22 as −1 G-A	C5	HCM	Restrepo-Cordoba et al., 2017
IVS22 as −1 C-T	C5	HCM	Millat et al., 2010
IVS23 ds +1 G-A	C5	HCM	Carrier et al., 1997
IVS23 ds +1 G-C	C5	HCM	Zou et al., 2013
IVS23 ds +1 G-T	C5	HCM	Niimura et al., 1998
IVS23 as −26 A-G	C5	HCM	Carrier et al., 1997
IVS23 as −2 A-G	C5	HCM	Van Driest et al., 2004
IVS24 as −2 A-T	C5	HCM	Santos et al., 2012
IVS26 ds +12 C-T	C7	HCM	Liu et al., 2013
IVS26 as −3 C-G	C7	HCM	Niimura et al., 2002
IVS26 as −2 A-C	C7	HCM	Zou et al., 2013
IVS29 ds +1 G-A	C8	DCM	Hershberger et al., 2010
IVS29 ds +2 T-G	C8	HCM?	Valente et al., 2013

Table 9 (*Continued*)

Mutation	Domain	Disease	Reference
IVS30 ds +2 T-C	C9	HCM	Waldmuller et al., 2008
IVS30 ds +5 G-C	C9	HCM	Watkins et al., 1995
IVS31 ds +1 G-T	C9	DCM	Rottbauer et al., 1997
IVS31 ds −1 G-A	C9	HCM	Zou et al., 2013
IVS32 ds +1 G-A	C10	HCM	Niimura et al., 1998
IVS32 ds +2 T-A	C10	HCM	Frisso et al., 2009
	Missense mutations		
P2R	C0	HCM	Zou et al., 2013
K7R	C0	DCM	Waldmüller et al., 2011
S18L	C0	DCM	Waldmüller et al., 2011
A27V	C0	DCM	Waldmüller et al., 2011
V28M	C0	HCM	Waldmüller et al., 2011
A31P	C0	HCM	Van Dijk et al., 2016
T33A	C0	DCM	Waldmüller et al., 2011
E34D	C0	DCM	Waldmüller et al., 2011
I49S	C0	HCM	Liu et al., 2015
S52R	C0	HCM	Zou et al., 2013
T62P	C0	HCM	Millat et al., 2010
G84D	C0	DCM	Waldmüller et al., 2011
A140P	P/A region	HCM	Waldmüller et al., 2011
P147L	P/A region	HCM?	Jääskeläinen et al., 2002
L156P	C1	HCM	Waldmüller et al., 2011
R160W	C1	HCM	Anan et al., 2007
E165D	C1	HCM	Olivotto et al., 2008
R177H	C1	HCM	Yalcin et al., 2016
V178M	C1	HCM	Ho et al., 2009
P186L	C1	HCM	Millat et al., 2010
K202Q	C1	DCM?	Hershberger et al., 2010
S212R	C1	HCM	Olivotto et al., 2008
R215C	C1	HCM	Zou et al., 2013
A216T	C1	HCM?	Fokstuen et al., 2008
S217G	C1	HCM?	Roberts et al., 2010
V219F	C1	HCM	Millat et al., 2010
D228Q	C1	HCM	Andersen et al., 2001
Y237H	C1	HCM	Waldmüller et al., 2008
Y237C	C1	HCM	García-Castro et al., 2009
R238H	C1	DCM	Waldmüller et al., 2011
E240D	C1	HCM	Olivotto et al., 2008
S242P	C1	HCM	Curila et al., 2012
H257P	C1	HCM	Richard et al., 2003
E258K	M motif	HCM	Yalcin et al., 2016

(*continued*)

Table 9 (*Continued*)

Mutation	Domain	Disease	Reference
R272C	M-motif	DCM	Zeller et al., 2006
R273C	M-motif	HCM	Ingles et al., 2005
G278E	M-motif	HCM?	Richard et al., 2003
H287Y	M-motif	HCM	Millat et al., 2010
R282W	M-motif	HCM	Giuffre et al., 2016
S311L	M-motif	DCM	Waldmüller et al., 2011
V321M	M-motif	DCM	Waldmüller et al., 2011
R326Q	M-motif	HCM?	Maron et al., 2001
E334K	M-motif	HCM	Anan et al., 2007
I336V	M-motif	HCM	Ehlermann et al., 2008
G341R	M-motif	HCM	Page et al., 2012
V342D	M-motif	HCM	Garcia-Castro et al., 2005
L348P	M-motif	HCM	Mun et al., 2016
L352P	M-motif	HCM	Richard et al., 2003
P371R	M-motif	HCM	Girolami et al., 2010
H379P	M-motif	HCM	Kubo et al., 2011
V385M	C2	DCM	Waldmüller et al., 2011
G407S	C2	DCM	Waldmüller et al., 2011
S408Q	C2	HCM	Waldmüller et al., 2011
A429V	C2	HCM	Waldmüller et al., 2011
A433P	C2	HCM	Zou et al., 2013
V437M	C2	DCM	Waldmüller et al., 2011
E441K	C2	HCM	Olivotto et al., 2008
K442M	C2	HCM	Zou et al., 2013
F448S	C2	HCM	Kindel et al., 2012
T457M	C3	HCM?	Caramins et al., 2003
R470W	C3	HCM	Olivotto et al., 2008
W486G	C3	HCM	Lakdawala et al., 2011
G490V	C3	HCM	Wang et al., 2013
T494I	C3	DCM	Møller et al., 2009
R495Q	C3	HCM	Mattos et al., 2016
R502Q	C3	HCM	Niimura et al., 1998
R502G	C3	HCM	Richard et al., 2003
G507R	C3	HCM	Erdmann et al., 2003
A522T	C3	HCM?	Cardim et al., 2005
Y525S	C3	HCM	Girolami et al., 2006
Y525H	C3	HCM	Lopes et al., 2013
G531R	C3	HCM	Rubattu et al., 2016
E542Q	C3	HCM	Rubattu et al., 2016
M555T	C4	HCM	Girolami et al., 2006
A562V	C4	HCM	Aurensanz Clement et al., 2016
R589H	C4	HCM	Lekanne Deprez et al., 2006
R597Q	C4	HCM	Curila et al., 2012

Table 9 (*Continued*)

Mutation	Domain	Disease	Reference
I603V	C4	HCM	Liu et al., 2015
D605H	C4	HCM?	Roncarati et al., 2011
D605G	C4	DCM?	Hershberger et al., 2010
P608S	C4	HCM	Iascone et al., 2009
D610N	C4	HCM	Brito et al., 2012
D610H	C4	HCM	Olivotto et al., 2008
E611K	C4	DCM	Waldmüller et al., 2011
R654H	C5	DCM	Waldmüller et al., 2011
R654C	C5	DCM	Waldmüller et al., 2011
I659M	C5	HCM	Zou et al., 2013
V662A	C5	DCM	Waldmüller et al., 2011
R668C	C5	HCM	Roncarati et al., 2011
P679S	C5	HCM	Waldmüller et al., 2011
Q689H	C5	HCM	Brion et al., 2010
A693S	C5	HCM	Olivotto et al., 2008
A701T	C5	HCM	Millat et al., 2010
E710K	C5	HCM	Bashyam et al., 2012
R726C	C5	HCM	García-Castro et al., 2009
R733H	C5	HCM	García-Castro et al., 2009
R733C	C5	HCM	Van Driest et al., 2004
V762D	C5	Increased LV wall thickness	Hodatsu et al., 2012
D770N	C5	HCM	Van Driest et al., 2004
A774T	C6	HCM	Maron et al., 2012
V783L	C6	HCM?	Santos et al., 2012
V783L	C6	HCM	Brito et al., 2012
D786Y	C6	HCM	Olivotto et al., 2008
G805S	C6	HCM	Kubo et al., 2011
I807N	C6	HCM	Zou et al., 2013
R810L	C6	HCM	Millat et al., 2010
R810H	C6	HCM	Nanni et al., 2003
R820Q	C6	HCM	Rubattu et al., 2016
L825M	C6	HCM?	Santos et al., 2012)
R835L	C6	HCM	Millat et al., 2010
G853G (GGC-GGT)	C6	HCM	Waldmüller et al., 2011
P873L	C7	Cardiomyopathy, LVNC	Probst et al., 2011
P873H	C7	HCM	Nanni et al., 2003
T885M	C7	HCM	Millat et al., 2010
V896M	C7	HCM	Mattos et al., 2016
V906G	C7	HCM	Frisso et al., 2009
E907K	C7	SIDS	Brion et al., 2012
P910T	C7	HCM	Olivotto et al., 2008
Q921L	C7	HCM	Brito et al., 2012

(*continued*)

Table 9 (*Continued*)

Mutation	Domain	Disease	Reference
Q921E	C7	HCM	Maron et al., 2008
S928L	C7	HCM?	Brito et al., 2005
T936M	C7	HCM	Caramins et al., 2003
R939W	C7	HCM	Waldmüller et al., 2011
R943Q	C7	HCM	Zou et al., 2013
N948T	C7	DCM	Daehmlow et al., 2002
T957S	C7	HCM	Ehlermann et al., 2008
P961L	C7	HCM	Kaski et al., 2009
R970Q	Linker between C7 and C8	DCM	Lakdawala et al., 2012
P976R	Linker between C7 and C8	HCM	Waldmüller et al., 2011
Q998E	C8	HCM	Van driest et al., 2004
R1022S	C8	HCM	García-Castro et al., 2009
R1022P	C8	HCM?	Brito et al., 2005
R1033W	C8	HCM	Zou et al., 2013
R1073P	C9	HCM	Otsuka et al., 2012
G1079D	C9	DCM	Waldmüller et al., 2011
L1084P	C9	HCM	Roncarati et al., 2011
K1087E	C9	HCM	Waldmüller et al., 2011
E1096K	C9	HCM?	Santos et al., 2012
T1109I	C9	HCM	Maron et al., 2012
E1111G	C9	HCM	Christiaans et al., 2010
C1124R	C9	HCM	Otsuka et al., 2012
N1133D	C9	HCM	Zou et al., 2013
R1138H	C9	HCM	García-Castro et al., 2009
Y1172C	Linker between C9 and C10	HCM	Kaski et al., 2009
T1184N	Linker between C9 and C10	HCM	Olivotto et al., 2008
L1187R	Linker between C9 and C10	HCM	Olivotto et al., 2008
V1192D	Linker between C9 and C10	HCM	Zou et al., 2013
G1195V	Linker between C9 and C10	HCM?	Santos et al., 2012
G1206V	C10	HCM	Cardim et al., 2005
I1212M	C10	HCM	Rubattu et al., 2016
W1214R	C10	HCM	Christiaans et al., 2010
L1219P	C10	HCM	Bashyam et al., 2011
S1231G	C10	HCM	Waldmüller et al., 2011
L1238P	C10	HCM	Choi et al., 2010
P1245L	C10	HCM	Waldmüller et al., 2011
N1257K	C10	HCM	Lopes et al., 2013
G1260D	C10	DCM?	Hershberger et al., 2010
C1264F	C10	DCM	Hershberger et al., 2010
E1265V	C10	HCM	Maron et al., 2012
C1266R	C10	HCM	Maron et al., 2012
C1266Y	C10	HCM	Page et al., 2012
L1268Q	C10	HCM	Otsuka et al., 2012

Table 9 (*Continued*)

Mutation	Domain	Disease	Reference
	Nonsense mutations		
G37Stop	C0	HCM	Liu et al., 201
K185Stop	C1	HCM	Rubattu et al., 2016
Y237Stop	C1	HCM	Ehlermann et al., 2008
G263Stop	M-motif	HCM	García-Castro et al., 2009
S311Stop	M-motif	HCM	Waldmüller et al., 2011
Y340Stop	M-motif	HCM	Olivotto et al., 2008
L360Stop	M-motif	HCM	Zou et al., 2013
Q374Stop	M-motif	HCM	Rubattu et al., 2016
E386Stop	C2	HCM	Otsuka et al., 2012
W396Stop	C2	HCM	Zou et al., 2013
Q425 Stop	C2	HCM	Niimuraet al., 2002
Q463Stop	C3	HCM	Ma et al., 2009
E516Stop	C3	HCM	Millat et al., 2010
T525Stop	C3	HCM	Bortot et al., 2011
W577Stop	C4	HCM	Santos et al., 2011
C623Stop	C4	DCM	Waldmüller et al., 2011
Q642Stop	Linker between C4 and C5	HCM	Page et al., 2012
C788Stop	C6	HCM	Maron et al., 2012
L811Stop	C6	HCM	Curila et al., 2012
Y842Stop	C6	HCM	Andersen et al., 2004
Q965Stop	C7	HCM	Christiaans et al., 2010
Q998Stop	C8	HCM	Millat et al., 2010
Q1012Stop	C8	HCM	Rubattu et al., 2016
Q1044Stop	C8	HCM	Curila et al., 2012
K1055Stop	C8	HCM	Page et al., 2012
Q1061Stop	C8	HCM	Ojala et al., 2016
W1214Stop	C10	HCM	Bashyam et al., 2011
C1244Stop	C10	HCM	Millat et al., 2010
Y1251Stop	C10	HCM	Millat et al., 2010
Q1259Stop	C10	HCM	Rubattu et al., 2016

*This mutation list is supplemental to previously compiled lists by Harris et al., 2011 (217) and Kassem, 2013 (266), which together contain over 200 mutations linked to hypertrophic cardiomyopathy.
Abbreviations: DA-1, distal arthrogryposis-type 1; DA-2, distal arthrogryposis-Type 2; LCCS-4, lethal congential contractural syndrome-Type 4; HCM, hypertrophic cardiomyopathy; DCM, dilated cardiomyopathy; LVNC, left ventricular noncompaction; SIDS, sudden infant death syndrome.

Small indels: microindels (20 bp or less) are presented with the inserted/deleted bases in lower case plus 10 bp DNA sequence flanking both sides of the lesion in upper case. The numbered codon is preceded in the given sequence by the caret character (^).

Small insertions: microinsertions (20 bp or less) are presented with the inserted bases in lower case plus 10 bp DNA sequence flanking both sides of the lesion in upper case. The numbered codon is preceded in the given sequence by the caret character (^).

Small deletions: microdeletions (20 bp or less) are presented with the deleted bases in lower case plus 10 bp DNA sequence flanking both sides of the lesion in upper case. The numbered codon is preceded in the given sequence by the caret character (^).

Splice: mutations with consequences for mRNA splicing are presented in brief with information specifying the relative position of the lesion with respect to a numbered intron donor or acceptor splice site. Positions given as positive integers refer to a 3′ (downstream) location, while positions given as negative integers refer to a 5′ (upstream) location.

develop HCM by 2 to 3 months of age, whereas homozygous mice develop DCM, and display ventricular dysfunction at birth (365). Altered gene expression in homozygous murine myocardia is typical of that seen in other DCM models, including upregulation of embryonic or skeletal forms of actin, reversal of MyHC isoforms, and increased levels of B-type natriuretic peptide (365). The notion that force generation serves as a central signaling cue may explain the differential phenotypic manifestations of exon 30 skipping in heterozygous versus homozygous mice. Accordingly, in the heterozygous state impaired force production results in compensatory myocyte hypertrophy. In the homozygous state, however, force production remains insufficient despite myocyte growth, resulting in uncompensated hypertrophy, activation of myocyte apoptosis, excessive fibrosis, and ultimately dilation and heart failure. Moreover, a 25-base pair deletion in the branch point of intron 32 also leads to frameshift and the generation of a truncated protein (580). This deletion is highly prevalent in South Asian countries estimated to affect 55 million people (304), who present with HCM (125, 522, 578). Given that only one of the five key residues mediating binding of the COOH-terminus of cMyBP-C to LMM is conserved, it has been suggested that the decreased affinity of the truncated protein for LMM and failure to incorporate into sarcomeres may underlie the pathogenicity of this deletion (304, 377).

Recently, dominant missense mutations in *MYBPC1*, which encodes sMyBP-C, have been linked to both distal arthrogryposis type-1 (DA-1) and distal arthrogryposis type-2 (DA-2) (15,214,325). DA-1 affects approximately 1 in 10,000 individuals and results in contractures often limited to distal muscles of the hands and feet. These include clubfoot, verticle talus, camptodactyly, overriding fingers, and ulnar deviations of the fingers (214, 217, 282). Two autosomal dominant missense mutations, Trp236Arg and Tyr856His, located in the M-motif and Ig domain C8 domain, respectively, have been linked to DA-1 (214). Both mutations are present in constitutively expressed exons and thus are contained in all slow variants expressed in skeletal muscles (15,214). *In vitro* binding and motility assays have demonstrated that the Trp236Arg and Tyr856His mutations significantly diminish the ability of the NH_2- and COOH-termini of sMyBP-C, respectively, to bind actin and myosin and regulate the formation of actomyosin cross-bridges (13). Notably, the expression levels of mutant sMyBP-C are significantly reduced in human biopsies of abductor hallucis, but not gastrocnemius muscle (15). This is consistent with the selective effects of DA-1 on distal muscles, and the lack of a myopathic phenotype in proximal muscles. Similarly, the phosphorylation levels of mutant sMyBP-C are significantly decreased in abductor hallucis, varying between 30% and 70% for individual phosphosites, but not in gastrocnemius muscle (15).

Two novel autosomal dominant missense mutations residing in Ig domain C2, Pro319Leu and Glu359Lys, were also linked to DA-2 (325). DA-2 is a more severe form of DA, which is also characterized by contractures of the hands and feet, but is often accompanied by mild to severe craniofacial anomalies and/or scoliosis (35, 300). Even though the exact effects of the Pro319Leu and Glu359Lys mutations are still unknown, their location suggests that they may affect binding to the S2 portion of myosin and/or actin either by inducing an unfavorable conformation (Pro319Leu) or altering surface electrostatic interactions (Glu359Lys).

More recently, an autosomal recessive missense mutation, Glu186Lys, was identified in *MYBPC1* that is located on the border of Ig domain C1 and the M-motif, and is causatively linked to the development of arthrogryposis multiplex congenita (AMC) (136). Patients with the Glu186Lys mutation display phentoypes similar to DA patients along with speech impairment and seizures (136). Similar to the DA-2 mutations, little is known about the molecular mechanisms leading to disease development.

In addition to the aforementioned mutations, a recessive nonsense mutation has been described in Ig domain C2, Arg318X, resulting in the generation of a premature stop codon, and the development of neonatal lethal congenital contractural syndrome-4 (LCCS-4) (349). Given the recessive inheritance of LCCS-4, along with the absence of any phenotypic or functional abnormalities in the heterozygous carriers, it is highly likely that the Arg318X mutation results in loss of sMyBP-C rather than a poisonous truncated protein (7, 160, 422).

MYBPC2, encoding fMyBP-C, was also recently linked to an unclassified, neonatal lethal DA in the form of a compound heterozygote (46). Specifically, a patient presenting with narrow thorax, polyhydramnios during fetal development, and neonatal lethality was found to possess two missense mutations in *MYBPC2*, Thr236Ile and Ser255Thr, located in the M-motif. The same patient also contained an Arg7X homozygous mutation in the *GPR126* gene, which encodes a G-protein coupled receptor that regulates neural, cardiac, and ear development (46, 431). Although mutations in *GPR126* have been associated with isolated AMC (468), it is likely that the additional mutations in *MYBPC2* contribute to the postnatal lethality of the carrier due to accumulating anomalies in motor neurons and skeletal muscles (46).

Conclusions

Taken together, it is clear that the regulation and roles of MyBP-C proteins are complex, and that Ca^{2+} and phosphorylation (and possibly additional PTM) impact the proteins' ability to regulate actomyosin binding and sliding. In that respect, sMyBP-C regulation may prove to be even more intricate than that of cMyBP-C and fMyBP-C, as there are several slow variants that undergo constitutive and unique phosphorylation events. While *MYBPC3* has been extensively studied due to the overwhelming number of HCM- and DCM-linked mutations that have been identified, *MYBPC1* and *MYBPC2* have only recently garnered more attention given their involvement in severe and lethal forms of DA. Obviously, there is still a lot to learn about the biology of

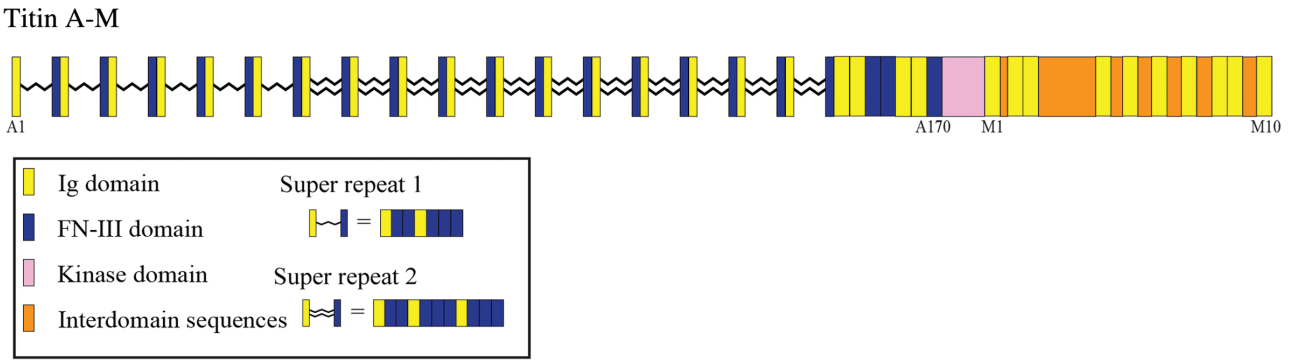

Figure 11 Domain schematic of titin within the thick filament. The various domains are depicted as differently colored rectangles with Ig domains shown in yellow, FnIII domains in dark blue, the kinase domain in pink, and interdomain sequences in orange. The two titin super repeats are also illustrated with the first one denoted by a single and the second one by a double zigzagged line connecting the respective Ig and FNIII domains.

the MyBP-C family. We expect that use of sophisticated molecular, biochemical, biophysical, and computational approaches alongside with the generation of the appropriate animal models will shed new light on the precise roles of this family of thick filament regulators in health and disease.

Titin (*aka* Connectin)

Discovery

Connectin was first identified as an elastic protein of skeletal muscle in 1976 (356) and of cardiac muscle in 1977 (357). Several years later, it was formally renamed titin after it was purified from chicken myofibrils and its sarcomeric localization and molecular composition were described, revealing that it is a giant filamentous protein and a major structural component of myofibrils (583, 584). Encoded by the single *TTN* gene located on human chromosome 2q31 and ranging from 27,000 to 35,000 amino acids in length, titins are the largest known proteins with a total mass of 3 to 4 MDa (36).

Structure, localization, and isoforms

Titin extends longitudinally across the sarcomere with its NH_2-terminus attached to the Z-disk and its COOH-terminus anchored in the M-band, thus spanning an entire half sarcomere (164). The region of titin that associates with the thick filament represents 2 MDa (A-band) and 200 kDa (M-band) of titin's total mass (36,417). The COOH-termini of two titin molecules overlap on either side of the M-band leading to a continuous titin filament that closely associates with myosin and other sarcomeric proteins (36,173,417). Unlike the NH_2-terminus and middle segment, the structure of titin within the A-band and M-band is relatively rigid, inelastic, and constitutively expressed among isoforms with the exception of M-band exon 5 (Mex5) (164, 286, 399, 600).

The region that spans the A-band, encoded by exons 252 to 357, is highly repetitive and composed entirely of Ig and FnIII domains that are organized in two types of super repeats (Fig. 11) (306, 561). The first super repeat, Ig-$(FnIII)_2$-Ig-$(FnIII)_3$, occurs six times in tandem and is located within the D-zone of the A-band. The second super repeat is located in the C-zone and contains 11 copies of the domain pattern Ig-$(FnIII)_2$-Ig-$(FnIII)_3$-Ig-$(FnIII)_3$. Importantly, the second set of super repeats are spaced every 43 to 45 nm, which matches the periodicity of MyBP-C that is tightly bound to myosin (please see above). This suggests that titin is highly associated with the thick filament and its binding partners, possibly acting as a scaffold or molecular blueprint for the assembly of A- and M-bands (51, 160, 168, 306, 398).

The most COOH-terminal portion of titin is localized to the M-band and is composed of a Ser/Thr kinase domain and 10 Ig-CII domains (referred to as M1-M10) that are interspersed by seven unique interdomain sequences (Is1-7) (Fig. 11) (173).

The titin kinase (TK) domain is related to the MLCK family, and is encoded by the first exon of the M-band portion of *TTN* (Mex1). MLCK kinases are typically regulated via binding of Ca^{2+}-calmodulin to their COOH-terminal regulatory tail, thereby displacing it from the ATP binding site (269, 537). TK is unique since it is only weakly regulated by Ca^{2+}-calmodulin binding. Instead, it undergoes an alternative activation mechanism that relieves the dual autoinhibition mediated by its regulatory tail and Tyr170 blocking the ATP binding site and catalytic Asp127, respectively (169, 195, 362, 454). Specifically, TK is activated upon exertion of mechanical force, which leads to unfolding of the regulatory autoinhibitory tail and displacement from the ATP binding site (169, 195, 454). Tyr170 is subsequently exposed and subjected to phosphorylation, possibly autophosphorylation, allowing ATP to bind to the catalytic Asp127 (169, 195, 454).

Recent studies have questioned the activity of TK, since phosphorylation of Tcap, the main substrate of TK, was found to be mediated by a different Ca^{2+}/calmodulin activated kinase that was present as a contaminant in the baculovirus expressed TK preparation (60). Furthermore, efforts to identify potential TK substrates in differentiating myocytes or adult gastrocnemius muscle were unsuccessful (60, 315).

The observed inactivity of TK was attributed to two residues present in the active site (Met34 and Glu147) that differ from canonical kinase sequences (60). It was therefore proposed that TK is a pseudokinase that may function as a binding scaffold for signaling proteins. Whether TK is an active or inactive kinase is still debatable, and requires further experimentation, especially because the zinc-finger proteins neighbor of BRCA1 gene 1 protein (Nbr1) and p62 have also been shown to be TK substrates at least *in vitro* (315); please see below.

Following the TK domain, there are 10 Ig-CII domains encoded by M-band exons 2-6 (Mex2-6). To date, Mex5, encoding Is7, is the only thick-filament associated titin exon known to be alternatively spliced (286). Skeletal muscles coexpress $Mex5^+$ and $Mex5^-$ isoforms in different ratios (286). Slow-twitch muscles typically contain higher levels of $Mex5^+$ titin, whereas fast-twitch muscles primarily express $Mex5^-$ titin (286). Similar to slow-twitch muscles, cardiac muscle predominantly contains $Mex5^+$ titin (286). $Mex5^-$ titin is only observed postnatally, and is absent during embryonic development, suggesting that its expression is developmentally regulated (286).

Binding partners

A number of binding partners have been identified within the A- and M-band portions of titin (Fig. 12). In particular, titin contains binding sites for myosin and MyBP-C (both of which were discussed earlier) within its A-band region, Ca^{2+}-calmodulin, Nbr1, and p62 within its TK domain, and muscle ring finger (MuRF) proteins, myomesin, M-protein, downregulated in rhabdomyosarcoma LIM protein/four and a half LIM domain-2 (DRAL/FHL-2), bridging integrator protein 1 (Bin1), calpain-3, myospryn, obscurin, and obscurin-like 1 (Obsl1) within its M-band region. Below, we describe these interactions and their functional relevance when known.

MuRFs (40-60 kDa)

Titin binds to members of the MuRF subfamily that consists of E3-ubiquitin ligases (342). Specifically, the most COOH-terminal Ig domains located within the A-band (A168-169) bind to the COOH-terminal helix of MuRF-1 *in vitro* (87,397). Interestingly, it was shown that constructs containing the region spanning A168 through the TK domain exhibited enhanced binding to MuRF-1, indicating that TK might also contribute to recruiting MuRF-1 to the A-band (60). The functional significance of this interaction has not been directly tested, although it has been speculated that as an E3-ligase linked to muscle atrophy, MuRF-1 is recruited to the A-band via its binding to titin where it may regulate the degradation and turnover of myofibrillar proteins (59, 198, 316, 342, 397).

Moreover, *in vitro* binding experiments have demonstrated that MuRF-2, which shares homology with MuRF-1, binds to the titin A164-169 region (447). MuRF-2 appears to interact transiently with titin, myosin, and the microtubule network during myofibrillogenesis (447). As such, MuRF-2 initially associates with detyrosinated microtubules at the onset of differentiation, and subsequently with the A-band region of titin and myosin during late sarcomerogenesis, possibly acting as an adaptor mediating the binding of titin and myosin

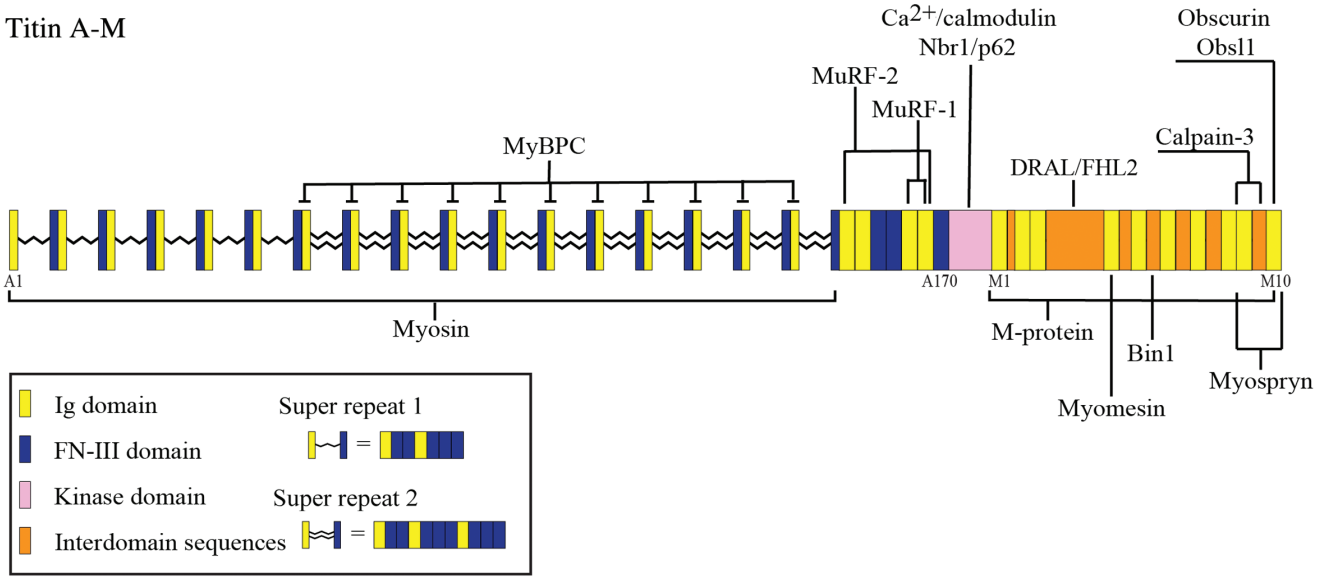

Figure 12 Binding partners of titin in the thick filament. In the A-band, the FnIII domains of titin's super repeats bind to the myosin S1 and LMM regions. Titin also provides regularly spaced binding sites for MyBPC in the first Ig domain of each second super repeat, leading to its periodic localization in the C-zone of the A-band. The Ig and FnIII domains located directly COOH terminally to the second super repeat mediate binding to MuRF-1 and -2. In the M-band, the titin kinase interacts with Ca^{2+}/calmodulin and Nbr1/p62. The rest of the M-band portion of titin provides binding sites for DRAL/FHL2, myomesin, Bin1, myospryn, calpain-3, obscurin, and obsl1. The exact binding site for M-protein in the COOH-terminus of titin has not yet been identified.

in developing myofibrils in a microtubule-dependent manner. However, upon transition of nascent myofibrils to mature myofibrils, MuRF-2 is no longer present in the sarcomere (433,447). The transient interaction between titin and MuRF-2 in the A-band is also regulated by mechanical stress (315). In the absence of a mechanical stimulus, MuRF-2 translocates from the A-band to the nucleus, where it regulates the transcription of myogenesis genes (further described below) (315).

Ca^{2+}-calmodulin (~17 kDa)

The TK domain contains binding sites for Ca^{2+}-calmodulin within its regulatory tail (362). Binding of Ca^{2+}-calmodulin was originally thought to contribute to activation of TK by leading to displacement of its regulatory tail from the ATP binding site, thereby relieving TK autoinhibition (362). However, extensive biophysical studies reported that the displacement of the inhibitory tail occurs by a mechanically induced conformational change (169, 195, 454). Thus, it appears that Ca^{2+}-calmodulin binding is actually only a weak activator of TK, whereas the exact functional significance of this interaction needs to be further assessed.

Nbr1 (~120 kDa) and p62 (~62 kDa)

Nbr1, a zinc-finger protein that acts as an adaptor to recruit polyubiquinated proteins for proteosomal degradation, also binds TK (267, 315, 591). Specifically, the NH_2-terminal Phox/Bem1p domain of Nbr1 that promotes the formation of homo- or heterodimeric signaling complexes interacts with the mechanically induced active conformation of TK (267, 308, 315, 509, 591). P62 is a related autophagic cargo receptor zinc-finger protein that binds TK via forming a signaling complex with Nbr1 (315). Both Nbr1 and p62 are substrates of TK and their phosphorylation has been demonstrated *in vitro* although the physiological significance of these events is still unknown (60, 315). In addition to regulating protein turnover via autophagy, p62 associates with a number of signaling proteins including members of the mitogen-activated protein kinase pathway, atypical PKCs, and MuRF family E3-ligases. Thus, the p62/TK interaction could facilitate the integration of different signaling pathways at the M-band, reviewed in (169).

Myomesin (~185 kDa) and M-protein (~165 kDa)

Myomesin and M-protein have similar domain compositions consisting of Ig and FnIII domains, and localize to the M-band where they bind both titin and myosin (415, 417, 418). Solid phase binding assays have demonstrated that myomesin binds to the M4 domain on titin via its FnIII domains My4-My6, therefore anchoring the COOH-terminus of titin to the M-band (417,418). This interaction is negatively regulated by PKA-mediated phosphorylation of Ser-482, a residue located in the linker region between myomesin domains My4 and My5 (418). Myomesin and titin incorporate into M-bands early in myofibrillogenesis and potentially serve as a scaffold for other sarcomeric proteins in the developing myofibril (80, 569). In support of this, it was shown that titin and myomesin together recruit obscurin and Obsl1 to the M-band (163). Similar to myomesin, M-protein binds titin (and myosin) at the M-band (80, 203-205). Contrary to myomesin however that is ubiquitously expressed among striated muscles, M-protein is only expressed in fast-twitch skeletal muscles and postnatal cardiac muscle (80, 203-205). Moreover, the interacting domains between titin and M-protein have yet to be identified.

DRAL/FHL-2 (~32 kDa)

DRAL/FHL-2, a member of the FHL protein family is primarily expressed in cardiac muscle, and binds titin at Is2 between Ig domains M3 and M4 (310). In addition to binding titin, DRAL/FHL-2 associates with various metabolic enzymes including CK, phosphofructokinase, and adenylate cyclase (310). Thus, it has been speculated that via its interaction with titin, DRAL/FHL-2 targets these enzymes to sarcomeric regions with high metabolic demands, like the M-band (310).

Bin1 (~65 kDa)

The SH3 domain of Bin1, a tumor suppressor protein that was originally identified as a binding partner of c-Myc, interacts with a set of phosphorylated Lys-Ser-Pro (KSP) motifs within the Is4 domain, which is localized between M5 and M6 (141). The phosphorylation of these Ser residues is developmentally regulated and is therefore thought to play an important role in myofibrillogenesis (further described below) (173). Bin1 is also suggested to regulate myofibrillogenesis, as it is primarily expressed in differentiating myoblasts, but not in developed myotubes (141). Moreover, Bin1 temporally associates with cyclin-dependent kinase 5 (Cdk5), which is potentially involved in the phosphorylation of Is4 (141). Thus, the interaction between Bin1 and titin could facilitate KSP phosphorylation via recruiting Cdk5 in the M-band during development (141).

Calpain-3 (~95 kDa)

Calpain-3, a Ca^{2+}-dependent cysteine protease, interacts with the Is7 region of titin and Ig domain M9 facilitating the cleavage of both titin (294, 548) and its interacting partner myospryn (please see below) in the M-band. Given that Mex5 encoding Is7 is alternatively spliced in a developmental- and muscle-specific manner (286), it has been proposed that titin cleavage may be regulated accordingly (93). Recent studies have localized the exact cleavage sites of titin to fragments TSLEKSIV and SFMGISNM within Is6 and Is7, respectively (93). Cleavage of these sites results in the production of COOH-terminal titin fragments ranging in size from 13 to 45 kDa (93). Although the effects of calpain-3 cleavage of

titin are not yet established, it has been suggested to contribute to sarcomeric remodeling by regulating the turnover rate of titin and its binding partners within the M-band (93).

Myospryn (~413 kDa)

Yeast two-hybrid screen identified myospryn, which is preferentially expressed in striated muscles, as a binding partner of both calpain-3 and M-band titin (52, 497). The COOH-terminal region of myospryn, composed of a Ser-Pro-Arg-Tyr domain and a partial FnIII motif, supports binding to the extreme COOH-terminus of titin region containing Ig domains M9 and M10 (497). In addition to binding titin, myospryn binds to and is a substrate of calpain-3. Therefore, binding of the COOH-terminus of titin to calpain-3 and myospryn may function to localize calpain-3 and myospryn in close proximity within the M-band thereby modulating the turnover rate of the latter (497).

Obscurin (50-960 kDa) and Obsl1 (130-230 kDa)

Titin's most COOH-terminal domain, Ig M10, binds to the most NH_2-terminal regions of both obscurin and Obsl1, as determined via yeast two-hybrid screen (163). Obscurin is a giant protein that is involved in sarcomeric organization, RhoA mediated signaling cascades, and cellular adhesion via its kinase domains (please see below) (287, 435). Obsl1 is smaller, but structurally similar to the NH_2-terminal portion of obscurin (177). Both obscurin and obscl1 bind to titin via their NH_2-terminal Ig1 domains and also contain binding sites for myomesin within their Ig3 domains (163). Thus, it has been proposed that titin facilitates the formation of a ternary complex between titin, myomesin, and obscurin/obsl1 in the M-band, and that this complex plays key structural roles (163). This notion was supported by the diffuse localization of endogenous obscurin and obsl1 when the minimal interacting domains of titin, myomesin, or obscurin/obsl1 were overexpressed in cultured cardiomyocytes (163). In addition, disruption of *de novo* sarcomeric organization was observed when these fragments were overexpressed in developing myoblasts (163). Because no apparent changes were observed in the localization of titin following overexpression of obscurin/obsl1 Ig1, it was suggested that titin (along with myomesin; please see below) functions to target obscurin/obsl1 to the M-band (158). Consistent with this, earlier work had demonstrated that obscurins accumulate at the M-band following the incorporation of titin's COOH-terminus and myomesin (281). Furthermore, homozygous deletion of titin's M-band region in mouse embryonic stem cells led to disruption of both obscurin and myomesin localization at the M-band (405). Taken together, this multiprotein complex consisting of the COOH-terminus of titin, myomesin, obscurin, and obsl1 appears to be important in the assembly and stabilization of the M-band.

Functions

As a giant filamentous protein that extends from the Z-disk to the M-band, titin plays multiple roles in the sarcomere. By harboring binding sites for a number of sarcomeric proteins, titin has been suggested to act as a scaffold for the assembly and stabilization of thick filaments (407). Moreover, it may function as a mechanosensor by participating in various signaling pathways via its COOH-terminal TK domain (295, 315). Lastly, titin may serve as a "molecular spring" via the extensive elastic elements located in its I-band region, therefore determining muscle elasticity and resting tension of sarcomeres (95, 178, 191-193, 562). Given the focus of this review on the thick filament, we will solely discuss the role of titin in the A- and M-band.

Structural roles

It was proposed early on that titin's inextensible region localized to the A- and M-band may act as a "molecular ruler" (600). According to the "molecular ruler" hypothesis, titin participates in the assembly of the sarcomere during myofibrillogenesis and acts as a scaffold to recruit myosin and other thick filament associated proteins. Specifically, this model indicates that during myofibrillogenesis, the NH_2-terminus of titin is first incorporated into primitive Z-disks while the COOH-terminus is cotranslationally integrated into A- and M-bands. Titin recruits myomesin to the developing M-band, and together act as a scaffold for the incorporation and regular organization of myosin thick filaments into A-bands, thereby establishing the dimensions of the forming sarcomeres (132, 163, 569). Thus, through its close association with the thick filament and anchorage in the Z-disk, titin could potentially set the length of sarcomeres and thick filaments. This model is supported by two lines of evidence: immunolocalization experiments monitoring the sequential incorporation of sarcomeric proteins in developing myocytes and embryonic chick hearts (132,569), and functional studies demonstrating disruption of thick filaments upon titin knockdown or targeted deletion of its M-band region in cultured myoblasts and embryonic stem cells (374, 405, 437, 568). Notably though, later studies pointed out the important roles of additional proteins in the regular assembly and maintenance of myosin thick filaments, including obscurin, which exists in a complex with titin and myomesin at M-bands (275, 290, 291, 460).

Later studies however proposed an alternative model, referred to as the "premyofibril" model suggesting that titin is not required for the initial assembly of sarcomeres (129, 407, 475). *In situ* examination of early myofibrillogenesis in embryonic avian hearts reported the assembly of short myosin rods that are not associated with titin, supporting the hypothesis that titin is not needed for the assembly of thick filaments (129). Consistent with this notion, knockdown of both titin orthologs in zebrafish embryos (*ttna* and *ttnb*) did not affect the initial assembly of myofibrils (507).

Similarly, zebrafish embryos harboring a truncating mutation in which the entire A-band region of the *ttna* ortholog was deleted displayed normal thick filament organization (406). This phenotype persisted even following knockdown of the second ortholog, *ttnb*, although, some sarcomeric disorganization was eventually observed in later stages of myofibrillogenesis (406). It has therefore been suggested that thick filament-associated titin is involved in the long-term stabilization of the myofibril rather than its assembly at least in zebrafish (407).

Regulatory roles

The TK domain is thought to function as a mechanosensor, linking changes in mechanical stress to various signaling pathways (169, 195, 295). Specifically, TK controls protein turnover and myogenic transcription by regulating the localization of the Nbr1/p62/MuRF-2 protein complex (315). Upon activation by mechanical stretch, the TK domain interacts with Nbr1, which acts as scaffold to target p62 and MuRF-2 to the M-band (315). In the absence of a mechanical signal, the Nbr1/p62/MURF-2 complex dissociates from TK and Nbr1/p62 and MuRF-2 translocate to the intercalated disc and the nucleus, respectively (315). Nuclear accumulation of MuRF-2 is correlated with reduction of the levels of nuclear serum response factor (SRF), thereby reducing SRF-mediated transcription of myogenic genes (315). In addition, Nbr1/p62, which are substrates of TK *in vitro*, function as adaptor proteins in degradation pathways by interacting with polyubiquitinated proteins and associating with the proteasome or the autophagosome (267, 315, 429, 508, 509, 591). Therefore, TK is implicated as a regulator of protein degradation and turnover and muscle remodeling in response to changes in mechanical stress (169).

Moreover, studies utilizing an inducible, cardiac-specific, knockout TK mouse model suggested a role for TK in Ca^{2+} cycling and PKC signaling (432). In particular, mice lacking TK exhibited reduced β-adrenergic response, and developed cardiac hypertrophy, fibrosis, and ultimately heart failure (432). This disease phenotype was associated with decreased expression of Ca^{2+} cycling proteins including calmodulin, SERCA2, and phospholamban, increased levels of PKCδ and its targets, and reduced Ca^{2+} transient amplitudes and kinetics (432). Although it has yet to be determined how deletion of TK mechanistically affects Ca^{2+} cycling and PKC signaling, it is intriguing to speculate that TK may act upstream of both processes mediating their cross-talk.

Posttranslational modifications

There are relatively few PTM currently identified within the A-band and M-band segments of titin (Fig. 13). Below, we briefly describe major PTM and their functional significance when known.

Phosphorylation

Early studies demonstrated that four KSP motifs located within Is4 in the M-band portion of titin are subjected to phosphorylation in all four Ser residues (Ser35236, Ser35243, Ser35249, and Ser35255; NP_001254479.2) in neonatal mouse cardiac and psoas muscle via cell-division cycle protein 2 (Cdc2) kinase (173). Interestingly, these phosphorylation events were primarily observed in lysates obtained from

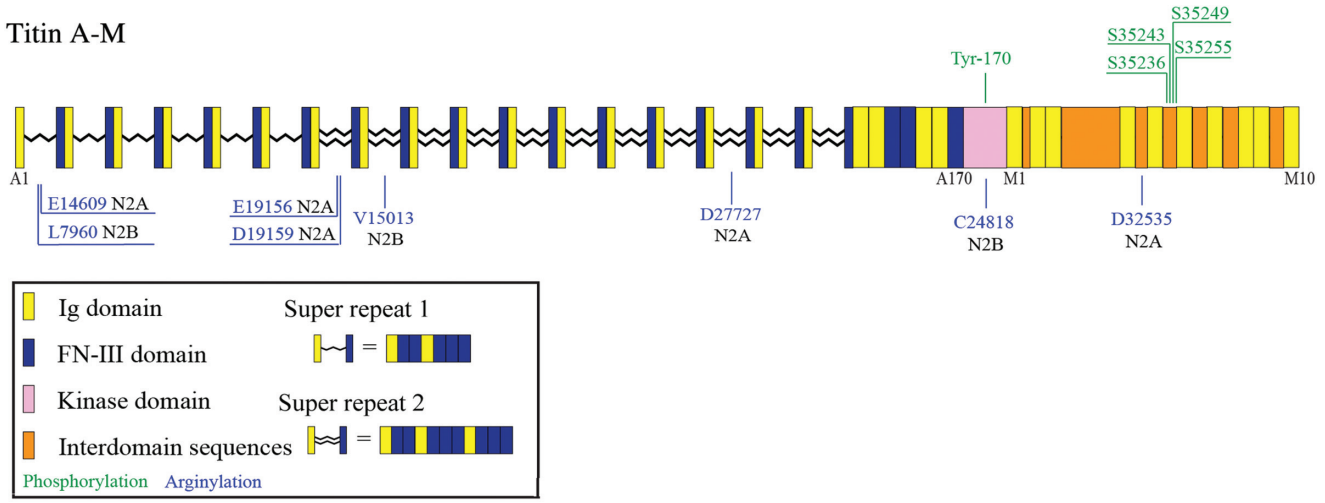

Figure 13 Posttranslational modifications of titin within the thick filament. The only known phosphorylation sites within this region are localized to the M-band, and include phosphorylation of the four Ser residues (Ser35236, Ser35243, Ser35249, and Ser35255; NP_001254479.2) located in the four KSP motifs present in Is4, and of Tyr-170 located in the P+1 loop of the titin kinase domain. Moreover, eight arginylation sites are spread throughout the A- and M-band portions of titin. Four of these sites (Glu14609, Glu19156, Asp19159, and Asp27727; NP_035782.3) are found within FnIII domains of the first and second super-repeat regions, while the fifth site (Asp32535; NP_035782.3) is located in Is3. The remaining three arginylation sites are present in Ig domains in the first and second super-repeat regions (L7960 and V15013; NP_082280.2) and the titin kinase (C24818; NP_082280.2).

neonatal, but not adult, muscles. Consistent with this, KSP motifs were highly phosphorylated in cultured differentiating myoblasts, but not in mature myotubes (173). Thus, KSP phosphorylation is developmentally regulated and possibly plays a role in myofbrillogenesis and myocyte differentiation (173). It is important to note that several phosphorylation sites have also been identified within the I-band portion of titin, which function to regulate passive tension by modulating the stiffness of titin's elastic elements; given that herein we focus on the thick filament-associated portion of titin, we refer the reader to an excellent review for the presence and role of phosphorylation events within the I-band protion of titin (235).

Arginylation

Five arginylation sites were recently found within the A- and M-band regions of titin in isolated mouse skeletal muscle myofibrils via mass spectrometry (321). Four of these sites are localized to FnIII domains in the A-band super repeats. Specifically, Glu14609 resides in the first FnIII domain of the seven-domain super repeat, Glu19156 and Asp19159 are present in the first FnIII domain of the 11-domain super repeat, and Asp27727 is localized in the ninth FnIII domain of the 11-domain super repeat (321). The fifth site, Asp32535, is present in the Is3 region between Ig domains M4 and M5 in the M-band (321). Similarly, several arginylation sites on titin were discovered in mouse heart lysates residing to Ig domains within its A-band portion and the TK domain in the M-band (320). In particular, Leu7960 resides in the first Ig domain of the seven-domain super repeat, Val15013 in the second Ig domain of the 11-domain super repeat, and Cys24818 in the TK domain (residues correspond to the N2B-titin sequence NP_082280.2). Arginylation-deficient mice, generated by the cardiac specific knockout of arginyl-transferase, develop dilated cardiomyopathy with age, and exhibit defects in myofibrillar ultrastructure and reduction in both active and passive force development (303). Similarly, isolated myofibrils from a skeletal muscle specific knockout of arginyl-transferase exhibit reduced passive force development (321). Given that titin is the primary regulator of passive force in the sarcomere, it is likely that titin arginylation contributes to the regulation of passive stiffness (320, 321). Since all of the arginylation sites localize to titin's inextensible region, and not the extensible I-band region, it was further proposed that titin arginylation regulates passive force possibly through modifying its anchorage to the thick filament (320, 321).

Mutations and myopathies

The majority of the mutations that have been identified in *TTN* to date are located within the A- and M-band regions, totaling 145 and 30 mutations, respectively (Fig. 14) (95). These mutations are commonly associated with either cardiac or skeletal myopathies, with only few linked to both types (6, 95, 411). Several of the identified mutations have been characterized as autosomal dominant, since patients develop the disease phenotype in the heterozygous state. However, there is also a number of mutations that are inherited in a recessive manner, and manifest a disease phenotype when homozygous or combined with additional mutations in the *TTN* gene as compound heterozygous (95). Since the functional implications of most of these mutations are unknown, only select mutations will be discussed below. Given that a recent review article reported all known *TTN* mutations up to 2014 (95), Table 10 only includes mutations within the thick filament associated portion of *TTN* identified after 2014.

An overwhelming number of mutations, totaling 132, has been identified in the A- and M-band regions of titin that are linked to DCM, HCM, and arrhythmogenic right ventricular cardiomyopathy (ARVC) (411). Approximately 126 of these mutations are associated with DCM, which

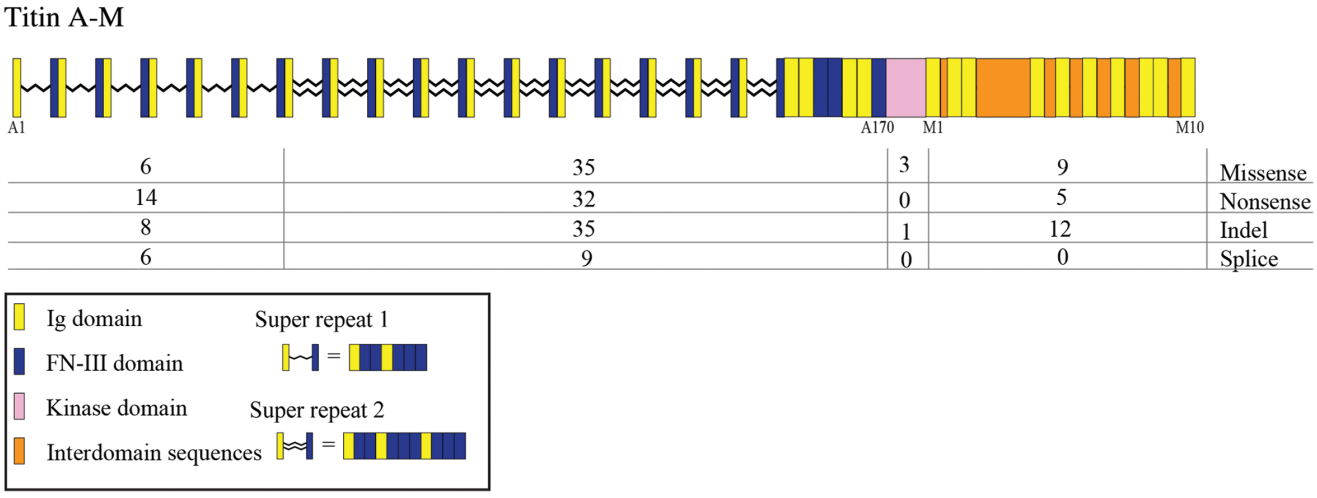

Figure 14 Number of mutations identified to date in individual domains of titin within the thick filament. The number of missense, nonsense, indel, or splice mutations present in each domain is depicted below the schematic.

Table 10 Mutations in the Thick Filament Associated Portion of Titin

Mutation	Domain	Region	Disease	Reference
		Missense mutations		
R17086H	FnIII 12	A-band (D-zone)	DCM	Begay et al., 2015
R19705C	FnIII 31	A-band (D-zone)	DCM	Begay et al., 2015
S20273Y	FnIII 34	A-band (D-zone)	DCM	Begay et al., 2015
L21176S	Ig 109	A-band (C-zone)	DCM	Begay et al., 2015
P21563A	FnIII 44	A-band (C-zone)	DCM	Begay et al., 2015
R22029H	FnIII 47	A-band (C-zone)	DCM	Begay et al., 2015
F22653L	FnIII 52	A-band (C-zone)	DCM	Begay et al., 2015
E23217G	FnIII 56	A-band (C-zone)	DCM	Begay et al., 2015
Y23494H	FnIII 58	A-band (C-zone)	DCM	Begay et al., 2015
A24343T	FnIII 65	A-band (C-zone)	DCM	Begay et al., 2015
V24516I	Ig 117	A-band (C-zone)	DCM	Begay et al., 2015
P25207R	FnIII 71	A-band (C-zone)	DCM	Begay et al., 2015
Y27008N	FnIII 84	A-band (C-zone)	DCM	Begay et al., 2015
R27563C	FnIII 88	A-band (C-zone)	DCM	Begay et al., 2015
S27585Y	FnIII 89	A-band (C-zone)	DCM	Begay et al., 2015
R28118H	FnIII 92	A-band (C-zone)	DCM	Begay et al., 2015
S29303G	FnIII 101	A-band (C-zone)	DCM	Begay et al., 2015
L29499R	Ig 130	A-band (C-zone)	DCM	Begay et al., 2015
G29562N	FnIII 103	A-band (C-zone)	DCM	Begay et al., 2015
E29590Q	FnIII 103	A-band (C-zone)	DCM	Begay et al., 2015
G30358E	FnIII 109	A-band (C-zone)	DCM	Begay et al., 2015
W30667R	FnIII 111	A-band (C-zone)	DCM	Begay et al., 2015
I31757T	FnIII 119	A-band (C-zone)	DCM	Begay et al., 2015
R31856G	FnIII 120	A-band (C-zone)	DCM	Begay et al., 2015
R33052H	FnIII 129	A-band (C-zone)	DCM	Begay et al., 2015
G33319R	FnIII 130	A-band (C-zone)	DCM	Begay et al., 2015
R33903L	Kinase	M-band	DCM	Begay et al., 2015
K34293E	M2	M-band	DCM	Begay et al., 2015
I34411N	M3	M-band	DCM	Begay et al., 2015
R34653L	Is2	M-band	DCM	Begay et al., 2015
W35930R	M10	M-band	LGMD2J	Zheng et al., 2016
		Nonsense mutations		
R17736Stop	Ig 99	A-band (D-zone)	DCM	Franaszczyk et al., 2017
P17886Stop	FnIII 18	A-band (D-zone)	DCM	Jansweijer et al., 2016
R18056Stop	Ig 100	A-band (D-zone)	DCM	Jansweijer et al., 2016
R21009Stop	FnIII 40	A-band (D-zone)	DCM	Franaszczyk et al., 2017
R21209Stop	Ig 109	A-band (C-zone)	DCM	Jansweijer et al., 2016
R22817Stop	FnIII 53	A-band (C-zone)	DCM	Franaszczyk et al., 2017
E23514Stop	FnIII 58	A-band (C-zone)	DCM	Franaszczyk et al., 2017

(*continued*)

Table 10 (*Continued*)

Mutation	Domain	Region	Disease	Reference
E25818Stop	Ig 121	A-band (C-zone)	DCM	Jansweijer et al., 2016
Q26147Stop	FnIII 78	A-band (C-zone)	DCM	Franaszczyk et al., 2017
R26562Stop	FnIII 81	A-band (C-zone)	DCM	Jansweijer et al., 2016
V26772Stop	FnIII 82	A-band (C-zone)	DCM	Jansweijer et al., 2016
Q27004Stop	FnIII 84	A-band (C-zone)	DCM	Franaszczyk et al., 2017
L27131Stop	FnIII 85	A-band (C-zone)	DCM	Franaszczyk et al., 2017
W27591Stop	FnIII 89	A-band (C-zone)	DCM	Jansweijer et al., 2016
E29772Stop	FnIII 105	A-band (C-zone)	DCM	Jansweijer et al., 2016
Y30384Stop	FnIII 109	A-band (C-zone)	DCM	Jansweijer et al., 2016
R31056Stop	FnIII 114	A-band (C-zone)	DCM	Franaszczyk et al., 2017
R31606Stop	FnIII 118	A-band (C-zone)	DCM	Jansweijer et al., 2016
Y35653Stop	M8	M-band	EDMD-like myopathy	De Cid et al., 2015
Q35660Stop	M8	M-band	EDMD-like myopathy	De Cid et al., 2015
		Indels/Frameshift mutations		
K17753Nfs*7	Ig 99	A-band (D-zone)	DCM	Jansweijer et al., 2016
E18113Dfs*10	FnIII 19	A-band (D-zone)	DCM	Jansweijer et al., 2016
K18487Sfs*3	FnIII 22	A-band (D-zone)	DCM	Jansweijer et al., 2016
G18918Vfs*17	FnIII 25	A-band (D-zone)	DCM	Franaszczyk et al., 2017
R19618Efs*6	FnIII 30	A-band (D-zone)	DCM	Jansweijer et al., 2016
E23066Gfs*8	FnIII 55	A-band (C-zone)	DCM	Jansweijer et al., 2016
A23647Lfs*19	Ig 115	A-band (C-zone)	DCM	Jansweijer et al., 2016
V25131Lfs*16	Ig 119	A-band (C-zone)	DCM	Jansweijer et al., 2016
I26829Mfs*15	FnIII 83	A-band (C-zone)	DCM	Franaszczyk et al., 2017
T27632Sfs*5	FnIII 89	A-band (C-zone)	DCM	Jansweijer et al., 2016
I28022Rfs*22	Ig 127	A-band (C-zone)	DCM	Jansweijer et al., 2016
T28262Kfs*39	FnIII 94	A-band (C-zone)	DCM	Jansweijer et al., 2016
S28693Ifs*2	FnIII 97	A-band (C-zone)	DCM	Franaszczyk et al., 2017
A29119Lfs*17	FnIII 100	A-band (C-zone)	DCM	Franaszczyk et al., 2017
P29241Lfs*24	FnIII 101	A-band (C-zone)	DCM	Jansweijer et al., 2016
S29255Afs*18	FnIII 101	A-band (C-zone)	DCM	Franaszczyk et al., 2017
N30367Kfs*3	FnIII 109	A-band (C-zone)	DCM	Jansweijer et al., 2016
G30648Vfs*	FnIII 111	A-band (C-zone)	DCM	Jansweijer et al., 2016
N30734Qfs*17	FnIII 112	A-band (C-zone)	DCM	Franaszczyk et al., 2017
V33646Hfs*26	Ig 142	A-band (C-zone)	DCM	Jansweijer et al., 2016
R35174Afs*4	M5	M-band	DCM	Jansweijer et al., 2016
T35304Cfs*3	M6	M-band	EDMD-like myopathy	De Cid et al., 2015
E35351Nfs*54	M6	M-band	EDMD-like myopathy	De Cid et al., 2015
F35475Sfs*4	M7	M-band	EDMD-like myopathy	De Cid et al., 2015

The listed titin mutations are supplemental to the previously compiled list of all known mutations in the *TTN* gene by Chauveau et al., 2014 (90). Residues are based upon the canonical full-length sequence (NP_001254479.2).
Abbreviations: DCM, dilated cardiomyopathy; LGMD2J, limb girdle muscular dystrophy type 2J; EDMD-like myopathy, emery-dreifuss muscular dystrophy-like myopathy.

is mainly characterized by pathological dilation of the left ventricle and impaired systolic function (77). Of these 126 mutations, 31 are missense mutations with 23 clustering in FnIII domains present in the C-zone (47, 182). Since these domains mediate binding to myosin, it has been speculated that they might lead to defects in contractility, however this has not yet been tested (47). The remaining DCM-associated mutations result from frameshift (37), nonsense (45), and splicing (13) mutations that typically lead to premature stop codons and truncations within the A- and M-band regions of titin (95, 157, 179, 180, 233, 263, 411, 572, 616). Truncated titin molecules missing COOH-terminal epitopes most likely lack sufficient interactions with thick filaments, and therefore, may be unable to appropriately span the sarcomere. This could potentially affect titin's stability/turnover and mechanosensing properties within the M-band (95, 233, 411).

Currently, there is no targeted treatment for titin-linked DCM. However, Gramlich and colleagues recently developed an antisense exon-skipping oligonucleotide approach as a potential therapy for treating truncating titin mutations (190). Importantly, this approach prevented the development of DCM in mice heterozygous for the frameshift mutation Ser14450fsX4, and partially restored sarcomeric organization in patient-derived cardiomyocytes (180, 190). Mechanistically, the exon skipping approach functions via splicing out exon 326 where a 2bp insertion leads to frameshift and the generation of a premature stop codon (180, 190). Exclusion of exon 326 recovers the reading frame and prevents truncation of the COOH-terminus of titin. The authors therefore propose exon skipping as a potential therapy for DCM truncating titinopathies.

A single frameshift mutation (Pro21689Profs*6) located in the A-band portion of titin has been associated with HCM, a disease mainly characterized by LVH, fibrosis, and diastolic dysfunction (77, 95, 233). Given that HCM-linked titinopathies are considerably less common than DCM-linked titinopathies, it has recently been suggested that titin is a disease modifier of HCM rather than the primary disease causing gene (178).

Moreover, five titin variants located within its A- and M-band regions have been found in individuals with ARVC (549). ARVC is a disease typically caused by mutations in proteins of the desmosomal complex, and is characterized by arrhythmia, right ventricular dilation, progressive fibroadiposis, and sudden death (411). Although ARVC-linked titin mutations that localize to the I-band have been shown to potentially affect titin stability, segregation analysis, and functional studies are currently lacking for those found in the A- and M-bands (411, 549).

Mutations in the A- and M-band regions of titin have also been linked to various skeletal myopathies. A number of mutations in the M-band that localize to Mex5 or Mex6 have been shown to segregate with tibial muscular dystrophy (TMD), a late-onset autosomal dominant muscle-weakening disease that preferentially affects the tibialis anterior muscle (564-566). These include frameshift (5), missense (3), nonsense (1), and in-frame indel (1) mutations (121, 140, 215, 216, 448, 567). The in-frame indel is an 11-base pair mutation commonly known as FINmaj resulting in substitution of four amino acids in Mex6 (216). FINmaj was identified in a Finnish population and is currently the most extensively studied titin mutation linked to a skeletal myopathy (216). Heterozygous individuals for the FINmaj mutation develop TMD, while homozygous individuals manifest a more severe muscular dystrophy, referred to as limb girdle muscular dystrophy type 2J (LGMD2J) (216). Consistent with this, the FINmaj mutation results in partial and complete loss of COOH-terminal titin epitopes in the heterozygous and homozygous states, respectively, along with a secondary deficiency in the levels of calpain-3, as reported in FINmaj knockin mice and LGMD2J muscle biopsies (92, 216, 220). Recent *in vitro* studies demonstrated that FINmaj leads to pathological titin cleavage patterns within Is4 and Is5, which is likely responsible for the loss of titin's COOH-terminus (93). Moreover, binding between titin M10 and obscurin Ig1 was reduced as a result of the FINmaj mutation *in vitro*, and the localization of obscurin to the M-band in LGMD2J muscle biopsies was disrupted (163). Thus, it is possible that FINmaj and other TMD/LGMD2J-linked mutations potentially disrupt M-band titin protein interactions.

Recently, five truncating mutations in Mex3 that are inherited in a recessive pattern were identified in patients with an Emery-Dreifuss muscular dystrophy (EDMD)-like phenotype (120). EDMD is a progressive, early onset muscular dystrophy that leads to limb-girdle weakness, joint contractures, and cardiomyopathy (135). The affected individuals develop a novel EDMD-like phenotype that display classical EDMD symptoms, yet have no effect on the heart (120). Muscle samples from all patients display rimmed vacuoles, disrupted M-band organization, and a secondary calpain-3 deficiency that likely results from the loss of its titin binding site in the M-band (120).

A total of nine missense mutations present in the 119th FnIII domain of the A-band and the TK domain have been identified in patients with hereditary myopathy with early respiratory failure (HMERF) (227, 260, 315, 421, 428, 441, 442, 557, 621). HMERF is characterized by severe weakening of the respiratory muscles that eventually leads to respiratory failure, as well as proximal and distal muscle weakness in the extremities (130). The majority (eight out of nine) of the mutations leading to HMERF localize to the 119th FnIII domain located within the second set of super repeats in the A-band portion of titin. These mutations are predicted to disrupt proper folding of the 119th FnIII domain, as evidenced by structural modeling analysis, and have been suggested to affect protein interactions mediated by it (95, 227, 228). Moreover, a point mutation, Arg25026Trp, located in the regulatory tail of the TK domain was identified in Swedish families with HMERF and found to disrupt Nbr1 binding *in vitro* (315). However, later studies showed that these individuals harbor a second missense mutation in the same *TTN* allele, Pro30091Leu, that is localized to the 119th FnIII "hot spot"

(227), therefore placing the pathogenicity of the Arg25026Trp TK mutation into question (95, 311, 440).

Six titin mutations in the A- or M-band regions were also identified in families with centronuclear myopathy (CNM), a disease characterized by centrally located myonuclei and muscle weakness that begins in childhood (88). These mutations, both frameshift and nonsense, are predicted to form truncated titin molecules (88). Consistent with this, immunofluorescence experiments of patient biopsies demonstrated the absence of titin's COOH-terminus and its COOH-terminal binding partner, calpain-3 (88). Importantly, the CNM-linked mutations are inherited in a recessive manner, and all affected individuals are compound heterozygotes bearing additional mutations in the titin gene (88, 95).

Lastly, nine titin mutations, eight of which are located within the A-and M-band portions of titin, have been linked to multiminicore disease with associated heart disease (82, 94). This disorder, also known as Salih myopathy, is characterized by congenital muscle weakness and early-onset fatal cardiomyopathy (493, 538). These mutations, both missense and frameshift, are the only known titin mutations to affect both skeletal and cardiac muscles. They are inherited recessively and only manifest the disease phenotype when homozygous or associated with additional titin mutations as compound heterozygous. Most of these mutations lead to premature stop codons and truncations, and often result in sarcomeric disarray and malfunction (82, 94).

Conclusions

As the largest known protein composed of 27,000 to 35,000 amino acids spanning the entire half sarcomere, titin plays key roles both as a scaffold and ruler for the regular assembly and maintenance of thick filaments, and as a signaling mediator. Consistent with this, hundreds of mutations have been identified within the thick filament associated region of titin that lead to both cardiac and skeletal muscle disorders. Due to titin's size and the fact that patients with *TTN* mutations frequently contain additional mutations in titin or other sarcomeric proteins, the effects of these mutations on muscle function have been difficult to study. Furthermore, other than utilizing exon skipping as a therapy for truncating titinopathies, the availability of targeted therapies is currently lacking. Future work should focus both on understanding the mechanisms of how *TTN* mutations lead to disease development as well as the establishment of targeted treatments for titin-linked myopathies.

Myomesin

Discovery

Myomesin was serendipitously discovered almost four decades ago during the characterization of M-protein in cross-striated muscles, as it was detected by monoclonal antibodies directed to M-protein (139, 206, 358, 535, 560). Following its molecular characterization, it was shown that myomesin encompasses a group of proteins that are expressed in striated muscles (16) where they cross-link myosin filaments (418, 419), and maintain their proper alignment particularly during eccentric contraction (17, 170, 171).

Structure, isoforms, and localization

The myomesin family consists of a group of modular proteins mainly composed of Ig and FnIII domains that reside in sarcomeric M-bands (16). Using comparative sequence analysis, three myomesin isoforms have been identified, including myomesin (myomesin-1), M-protein (myomesin-2), and myomesin-3, which are encoded by different *MYOM* isogenes (504). Myomesin (~185 kDa) is encoded by *MYOM1*, and is expressed in all vertebrate skeletal and cardiac muscles both during development and at maturity (16, 18). In contrast, M-protein (~165 kDa) encoded by *MYOM2* and myomesin-3 (~162 kDa) encoded by *MYOM3* exhibit muscle type and developmental stage specific distribution. Specifically, M-protein is predominantly expressed in adult cardiac and fast-twitch skeletal muscles with the highest expression in type-IIB fibers (80, 204, 504), while myomesin-3 is preferentially found in embryonic and postnatal skeletal muscles, and in adult slow-twitch and extraocular muscles with the highest expression in type IIA fibers (504).

All three myomesin isoforms have similar architectures, and are composed of 13 domains that include a nonmodular NH_2-terminal region My1, followed by an array of Ig and FnIII domains arranged in the following order 2Ig (My2-My3)-5FnIII (My4-My8)-5Ig (My9-My13) (Fig. 15) (504). Of the 13 domains, My1 is predicted to be intrinsically disordered, and is highly different among the three isoforms sharing a 25% to 28% homology, while the Ig and FnIII domains show significant similarity ranging between 38% to 51% and 40% to 52%, respectively (504).

A splicing variant of myomesin has also been identified, referred to as embryonic heart (EH)-myomesin, because it is the major isoform expressed during EH development, and its expression is rapidly downregulated after birth (16). EH-myomesin contains a unique unstructured ~100-residue long Ser/Pro-rich insertion between FnIII domains My6 and My7 (Fig. 15). Using biophysical tools, this insertion was shown to be intrinsically disordered and possess elastic properties similar to the extensible Pro-Glu-Val-Lys (PEVK) region of titin that resides in the I-band (502). In addition to its expression in EH, EH-myomesin is also found in adult slow-twitch skeletal myofibers, and its expression profile follows a reciprocal pattern to that of M-protein with fibers expressing EH-myomesin lacking M-protein, and *vice versa* (18).

Binding partners

The myomesin isoforms contain multiple Ig and FnIII domains, which may serve as binding sites for several

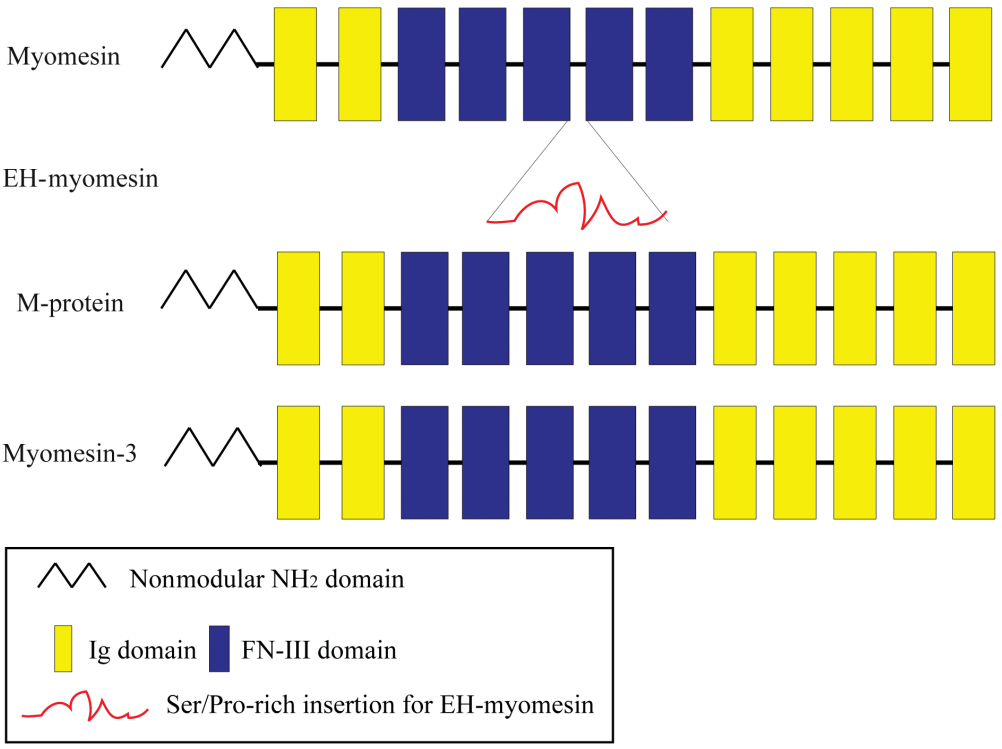

Figure 15 Schematic representation of the three myomesin isoforms: myomesin, M-protein, and myomesin-3. The yellow and dark blue rectangles correspond to Ig and FnIII domains, respectively, the black zigzagged line represents the nonmodular NH_2-terminal domain, and the red curvy line between domains My6 and My7 illustrates the Ser/Pro-rich insertion present in EH-myomesin.

proteins residing in thick filaments. Specifically, myomesin contains binding sites for myosin (discussed in the *Myosin* section), titin (discussed in the *Titin* section), obscurin and obsl1, M-CK, myofibrillogenesis regulator-1 (MR-1), and dysferlin (Fig. 16). Below we describe the main binding partners of the myomesin proteins and the potential significance of these interactions.

Obscurin (~50-960 kDa) and Obsl1 (~130-230 kDa)

Obscurin is the third member of the family of giant sarcomeric proteins expressed in vertebrate striated muscles (287), and plays both structural and regulatory roles (288). Given its tight association with the thick filament, a comprehensive description of obscurin is provided below. Recent work has shown that myomesin interacts with obscurin, and its close homologue, obsl-1 (163, 177). The linker region between FnIII domains My4 and My5 of myomesin binds to the NH_2-terminal Ig3 domain of obscurin and obsl1 (163). Notably, these interactions are specific for *MYOM1*, possibly due to the low homology that the linker regions of the three myomesin isoforms share, and are not regulated via phosphorylation (163).

Downregulation of myomesin in NRCs greatly affects the localization of endogenous obscurin and obsl-1, which appear diffuse in the cytoplasm (163). Overexpression of the myomesin, obscurin, or obsl-1 binding sites has similar effects in the distribution of endogenous obscurin and obsl-1, but not of myomesin (163). Among the three binding sites, overexpression of the myomesin My4-My5 linker has the most striking effect (163), suggesting that myomesin (along with titin as discussed above) facilitates the proper targeting and incorporation of obscurin and obsl-1 to M-bands (163). This is consistent with the sequential appearance of titin, myomesin, and obscurin at M-bands during myofibrillogenesis (62, 63, 289).

M-CK (~43 kDa)

CK is an enzyme involved in cellular energy metabolism that catalyzes the reversible conversion of creatine and ATP to phosphocreatine and ADP (278, 582). CK comprises a group of isoforms that express in a tissue-specific manner. In mature muscle, M-CK is the predominant isoform, 5% to 10% of which is bound to the myofibrillar M-band, whereas the remaining 90% to 95% is soluble in the sarcoplasm (243). Both myomesin and M-protein directly bind to M-CK that serves as an effective intramyofibrillar energy-generation system required to support the ATPase activity of MyHC (242). Four highly conserved Lys residues (i.e., Lys8, Lys24, Lys104, and Lys115) in M-CK are essential for its interaction with the central My7-My8 FnIII domains of myomesin and My6-My8 FnIII domains of M-protein (242). Interestingly

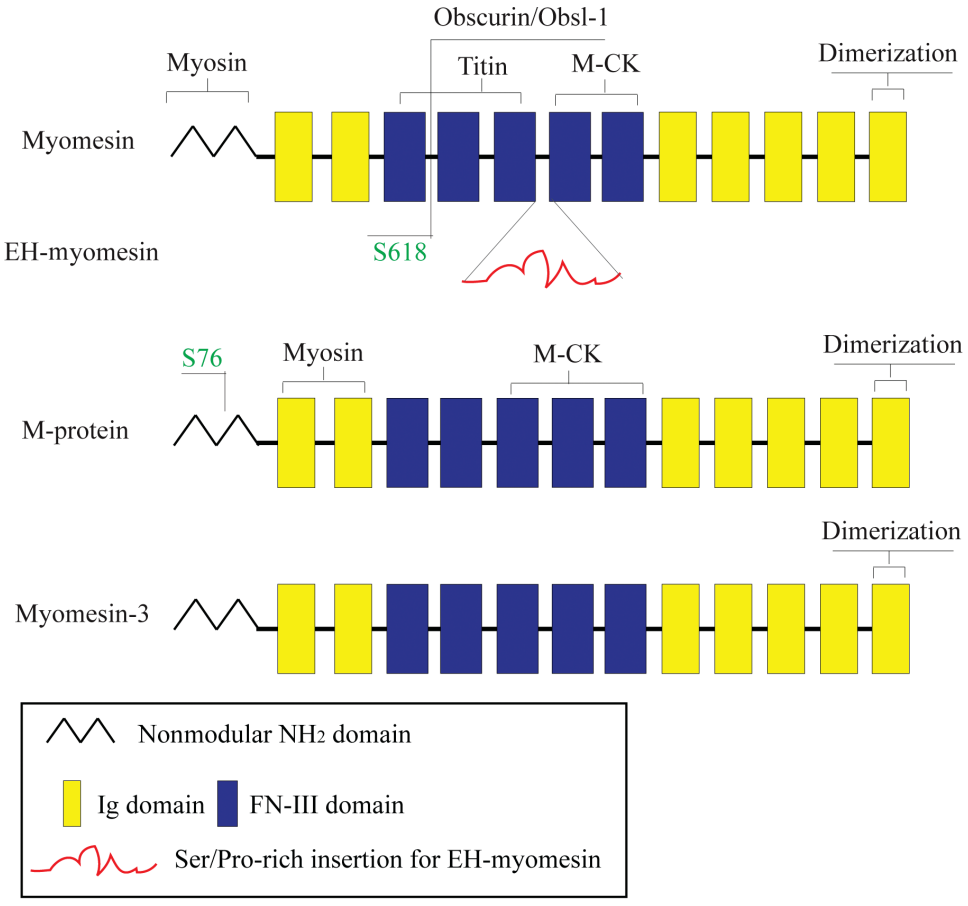

Figure 16 Interacting partners of the myomesin isoforms and their respective binding sites. All three proteins form homotypic dimers via their COOH-terminal Ig domain My13. Moreover, a number of binding sites have been identified primarily on myomesin that mediate binding to other M-band proteins. These include the nonmodular My1 region of myomesin and Ig domains My2-My3 of M-protein that bind to LMM, the FnIII domains My7-My8 of myomesin and My6-My8 of M-protein that interact with M-CK, the linker region between FnIII domains My4-My5 of myomesin that binds to the Ig3 domain of obscurin and obsl-1, and the FnIII My4-My6 region of myomesin that interacts with the Ig domain M4 of titin.

though, the binding affinities of the M-CK/myomesin and M-CK/M-protein interactions are distinct, as indicated by their K_d values calculated to be ~75 nmol/L and ~1μmol/L at pH 6.8, respectively (242). Both interactions are dynamic with a strong pH-dependence. Accordingly, M-CK binds stronger to either myomesin isoform when the pH is lowered from 7.0 to 6.7 (242). Given that under high workload such as muscle contraction, ATPases hydrolyze ATP to ADP+H^+, sequentially leading to a moderate acidic microenvironment, it is likely that the dynamic nature of the M-CK/myomesin and M-CK/M-protein interactions depends on the intramuscular pH, perhaps reflecting the changes in energy demand during contraction and relaxation (242).

MR-1 (~17 kDa)

MR-1 is expressed across different tissues with a greater abundance in striated muscles (324). MR-1 levels are significantly increased in hypertrophic rat myocardium induced by abdominal aortic stenosis and NRCs following angiotensin II stimulation, possibly playing a role in the pathogenesis of cardiac hypertrophy (331) by promoting sarcomere growth and remodeling (587). *In vitro* studies have demonstrated that MR-1 interacts directly with myomesin (324). Moreover, earlier work has shown that myomesin localizes to the nucleus in NRC contrary to mature cardiomyocytes where it resides in the cytoplasm occupying M-bands (473). Overexpression of MR-1 in NRC induced translocation of myomesin from the nucleus to the cytoplasm (587), which may explain the MR-1-promoted sarcomere reorganization seen in hypertrophic animal models. Sumoylation of myomesin by small ubiquitin-like modifier-1 (SUMO-1) has also been implicated in the cytosolic translocation of myomesin at maturity (473). Indeed, overexpression of SUMO-1 in NRC elicited the same effect on myomesin's localization as overexpression of MR-1. However, overexpression of SUMO-1 failed to induce cytoplasmic translocation of myomesin if MR-1 was downregulated, suggesting that MR-1 acts upstream of SUMO-1, although the exact mode of action requires further investigation (587).

Dysferlin (~237 KDa)

Dysferlin, encoded by the *DYSF* gene, is a major player in sarcolemma repair (37). Decreased or null expression of dysferlin due to mutations in the *DYSF* gene has been associated with the development of severe muscle disorders, called dysferlinopathies (45,330). Biochemical and imaging approaches have demonstrated that M-protein interacts directly with dysferlin (154), potentially contributing to the anchoring of the sarcolemma with superficial myofibrils, although further work is required to establish this.

Functions

Thick filament assembly and cross-linking

Several studies have indicated that myomesin has structural and cross-linking roles in striated muscles (62, 63, 163, 289, 312,418,419). Specifically, three lines of evidence have highlighted the essential role of myomesin in thick filament assembly and stabilization, including: (i) its early expression and incorporation into M-bands during myofibrillogenesis (62, 63, 289), (ii) its direct interaction with other M-band proteins and myosin (please see above) (163, 418, 419), and (iii) the presence of disorganized M- and A-bands in NRC following manipulation of its expression (i.e., overexpression of the My4-My5 linker or downregulation of the protein) (163). In addition to its structural role, myomesin serves as a cross-linker of neighboring myosin filaments (171). Based on sophisticated biochemical and biophysical methods, a three-dimensional model of the M-band has been proposed indicating that neighboring myosin filaments are connected by myomesin molecules that bind to myosin via the NH_2-terminal My1 domain (in the case of myomesin) or My2-My3 region (in the case of M-protein), which form antiparallel homotypic dimers via their COOH-terminal My13 domains (312, 445, 446). Notably, no heterotypic dimers have been observed even though the three isoforms share ~50% identity in their My13 domains (504). Therefore, myomesin is considered as the main thick filament cross-linker in the M-band, similar to α-actinin in the Z-disk (312). Consistent with the ability of myomesin to homodimerize, X-ray crystallography demonstrated that the COOH-terminal My12-My13 region self-assembles into an end-to-end dimer with a length of 14.3 nm (446). Similar structural examination of the My9-My13 region revealed that it adopts a unique arrangement referred to as "ball-and-spring," in which the Ig domains are interspersed by a long α-helix, thus forming an end-to-end dimer that is folded into an irregular superhelical coil (445).

Thick filament elasticity

Examination of the biophysical properties of the Ig and FnIII domains of myomesin demonstrated that they display similar unfolding and refolding properties as the respective domains of the I-band portion of titin (502). Moreover, the unique 100-amino acids long segment present between My6 and My7 in EH-myomesin exhibits a random coil conformation resembling an entropic chain (502), and may behave similar to the PEVK region of the I-band portion of titin (502). More importantly, X-ray crystallography and secondary structure prediction indicated that the linker regions between the COOH-terminal Ig domains My9-My13 are arranged as long α-helices (446) that can undergo rapid unfolding/refolding at relatively low forces (15-40 pN) (53, 445, 608). On the contrary, the forces required to unfold Ig domains (~80 pN) (502) or to dissociate myomesin dimers (>130 pN) (53, 445, 608) are comparatively higher. As a consequence of the reversible elongation of its linker regions, myomesin is capable of extending ~2.5-fold of its original length (445). Thus, the extensibility of the α-helical linkers protects the myomesin dimers from dissociating at physiological forces (53, 445), which is crucial for maintaining the stability of thick filaments during force production. Taken together, these studies highlight the role of myomesin as an elastic spring in the M-band, similar to titin in the I-band.

Mutations and myopathies

Given the essential role of myomesin in sarcomeres, the *MYOM1* gene has been screened for genetic variants associated with muscle disease, leading to the identification of three mutations that are linked to HCM, DCM, and myotonic dystrophy type 1 (DM1) (Fig. 17 and Table 11) (284, 352, 513, 520). Of note, it is surprising that although *MYOM1* plays key roles in sarcomeric structure and function, the number of mutations that have been identified to date are small.

Genomic DNA screening of 188 unrelated Caucasian HCM patients identified a missense mutation, Val1490Ile, in *MYOM1* located in My12 that cosegregates with congenital HCM (520). Evaluation of recombinant myomesin fragments containing the Val1490Ile mutation via circular dichroism revealed that although their secondary structure is indistinguishable from wild type, they unfold more rapidly, indicating that Val1490Ile promotes the dissociation of dimers, thereby reduces their thermal stability (520). Consistent with this finding, the K_d of mutant homodimers was modestly increased compared to wild type, although it still remained in the low micromolar range (520). Given the relatively reduced ability of mutant myomesin to form stable homodimers, it was postulated that the Val1490Ile mutation contributes to the pathogenesis of HCM by impacting the organization and stability of thick filaments during force development (520). Contrary to *MYOM1*, *MYOM2*, and *MYOM3* have not yet been screened for potential mutations in HCM patients.

Moreover, whole exon sequencing of 30 samples obtained from end-stage heart failure patients diagnosed with familial or idiopathic DCM identified a missense mutation, Glu247Lys, residing in the nonmodular NH_2-terminal My1 domain of myomesin in a patient with familial DCM (352). The functional ramifications of the Glu247Lys mutation

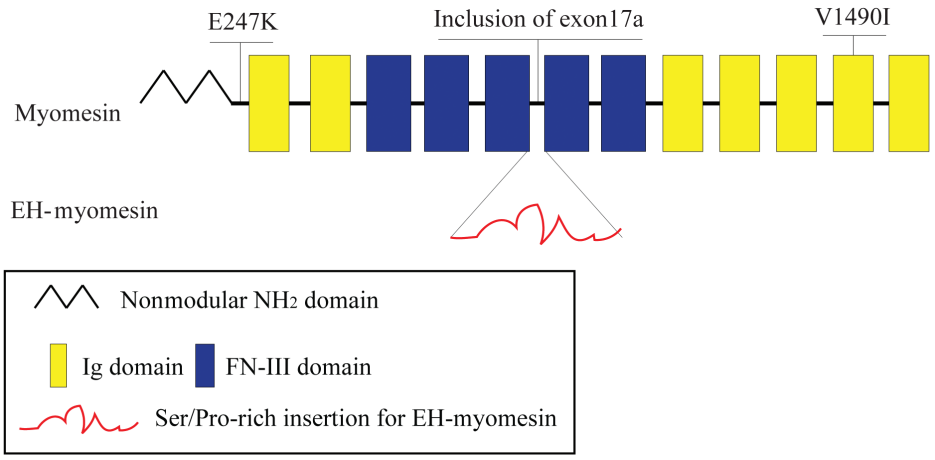

Figure 17 Illustration of the mutations that have been identified in *MYOM1* encoding myomesin and their location. There are no known myopathy-causing mutations for *MYOM2* encoding M-protein and *MYOM3* encoding myomesin-3.

however are currently elusive. Notably, similar screening was performed for *MYOM2*, but no mutations were identified.

In addition to the presence of mutations in *MYOM1*, the levels of EH-myomesin are significantly increased in biopsies from human failing hearts due to DCM (503). Importantly, upregulation of EH-myomesin coincides with upregulation of a longer, more compliant titin isoform (345, 409), suggesting that these alterations may be adaptive responses of the strained dilated myocardium (503).

Alterations in myomesin have been also described in skeletal muscles leading to DM1. DM1 is an autosomal dominant disease, which is caused by expansion of the CTG repeat in the 3′-UTR of the dystrophia myotonica protein kinase (*DMPK*) gene (29, 71, 76, 221). Aberrant alternative splicing is a distinctive feature of DM1 as the expanded CUG repeats bind and therefore sequester the muscleblind-like family of RNA splice regulators, resulting in deregulation of normal exon shuffling (127). More than 30 genes have been identified to be abnormally spliced in DM1 (465), including *MYOM1* (284). Specifically, inclusion of exon 17a was significantly increased in DM1 skeletal muscles, compared to wild type. Inclusion of exon 17a in DM1 muscles leads to insertion of a 60 to 100 amino acids long peptide between My6 and My7 of myomesin, the pathological significance of this insertion however is currently unknown (284).

Table 11 Mutations Identified in Myomesin

Mutation	Domain	Disease	Reference
	Missense mutations		
V1490I	My12 (Ig)	HCM	Siegert et al., 2011
E247K	My1 (nonmodular)	DCM	Marston et al., 2015
	Splicing mutations		
Inclusion of exon 17a	Between My6 (FnIII) and My7 (FnIII)	DM1	Koebis et al., 2011

Abbreviations: My, Myomesin; Ig, immunoglobulin; FnIII, fibronectin-III; HCM, hypertrophic cardiomyopathy; DCM, dilated cardiomyopathy; DM1, myotonic dystrophy type 1.

Conclusions

Mounting evidence has accumulated over the last decades indicating that myomesin plays key roles in thick filament assembly, cross-linking, and stability in addition to serving as elastic spring in M-bands. Thus, it is not surprising that similar to other thick filament associated proteins, myomesin is also causatively linked to hereditary myopathies. Actually, the small number of mutations that has been described in *MYOM1* alongside the lack of myopathy-causing mutations in *MYOM2* and *MYOM3* suggests that a focused interrogation of the involvement of the *MYOM* genes in the development of cardiac and skeletal myopathies is warranted. Alternatively, mutations in the *MYOM* genes may be embryonic lethal, which may preclude their identification. Consequently, early genetic screening may be highly informative for identifying novel disease-causing mutations in the *MYOM* genes.

Obscurin

Discovery

Obscurin is the most recently discovered, and the third member of the family of giant sarcomeric proteins expressed in vertebrate striated muscles, along with titin and nebulin (287). Obscurin was named after the adjective "obscure," meaning "difficult to see or make out," "not well known," and "not easily understood" due to its complexity (617). Similar to titin, obscurin is a modular protein composed of tandem adhesion

and signaling domains, and plays both structural and regulatory roles (288).

Structure, localization, and isoforms

Obscurin is encoded by the *OBSCN* gene, which is localized on human chromosome 1q42 (162). The *OBSCN* gene contains 117 exons that are subjected to extensive alternative splicing, giving rise to multiple protein isoforms, classified as giant (~720-970 kDa), intermediate (~290-550 kDa), and small (~50-250 kDa) obscurins (14, 162, 617). The prototypical obscurin, referred to as obscurin-A (~720 kDa), contains tandem Ig and FnIII domains followed by an array of signaling motifs (Fig. 18). In particular, the NH_2-terminus and middle of the molecule consists of 59 Ig and 3 FnIII domains, followed by an IQ rich domain that binds calmodulin, a SH3 domain, a rho guanine nucleotide exchange factor (Rho-GEF) motif, and a pleckstrin homology (PH) domain. The extreme COOH-terminus of obscurin-A contains a 417-amino-acid-long nonmodular region that carries binding sites for ankyrins (162,287,288,293,617). Obscurin-B (~870 kDa) is also a giant isoform originating from *OBSCN* that shares the same architecture with obscurin-A with the exception of its COOH-terminus that contains two Ser/Thr kinases, referred to as Kinase1 and Kinase2, which are preceded by Ig and Ig/FnIII domains, respectively (485) (Fig. 18). Kinase1 and Kinase2 belong to the MLCK subfamily, and can also be expressed as smaller isoforms that contain one or both domains, referred to as single (~55 kDa, containing only Kinase2) and double (~145 kDa, containing partial Kinase1 and Kinase2) kinase isoforms (65,69,485) (Fig. 18). Notably, the presence of multiple promoters and translation initiation sites in the *OBSCN* gene along with the fact that individual domains are encoded by single exons may give rise to a large number of alternatively spliced obscurin isoforms. Consistent with this, several immunoreactive obscurin bands have been identified in muscle and nonmuscle tissues that may contain distinct combinations of adhesion and signaling motifs (14, 69, 435). Along these lines a recent study reported the presence of two small obscurin isoforms in cardiac muscle, obscurin-40 and obscurin-80 that are enriched at the intercalated disc, bind specifically to phosphatidylinositol bisphosphates (PIP2s) via their PH domain, and contribute to the regulation of cardiomyocyte size and coupling by modulating the PI3K/AKT/mTOR pathway (8).

Initial studies on obscurins' localization in adult mouse myocardium revealed that they primarily concentrate at M-bands (32, 64, 163, 288, 617). Their distribution is more variable during cardiac development, however, with obscurin epitopes accumulating transiently at Z-disks early on (65). Subsequent studies of adult rat cardiac and skeletal muscles with antibodies to the COOH-terminus detected obscurins simultaneously at M-bands and Z-disks, whereas antibodies to the NH_2-terminus and the Rho-GEF domain localized obscurins at M-bands (288, 617), and antibodies to the Ig58/Ig59/FnIII60 cassette identified obscurins at the edge of the I-band and the Z-disk (36). Moreover, detailed examination of the distribution of obscurins in adult rat skeletal myofibers demonstrated that at resting sarcomere lengths obscurin-A primarily concentrates at M-bands, whereas obscurin-B localizes at M-bands and A/I junctions. Interestingly though, following stretch both giant obscurins are detected at M-bands and I-bands near A/I junctions, while obscurin-B is also found at the periphery of Z-disks near the Z/I junction (69). Thus, it is possible that stretching of the muscle may either result in redistribution of obscurins along the sarcomere or unmask previously hidden epitopes.

Later studies examined the subcellular localization of obscurins in humans (81). Obscurins showed a preferential concentration at M-bands in both developing and adult skeletal and cardiac human muscles. Interestingly, these studies further indicated the presence of obscurins at the sarcolemma and the postsynaptic region of the neuromuscular junction (81), although the exact molecular identity of these isoforms is still unknown.

Obscurins assume a reticular distribution in cross-sections of striated muscles, suggesting that they are positioned at the surface of the myofibril rather than within it (68,81,288,293). It has therefore been postulated that unlike titin and nebulin, which are integral components of sarcomeres, obscurins

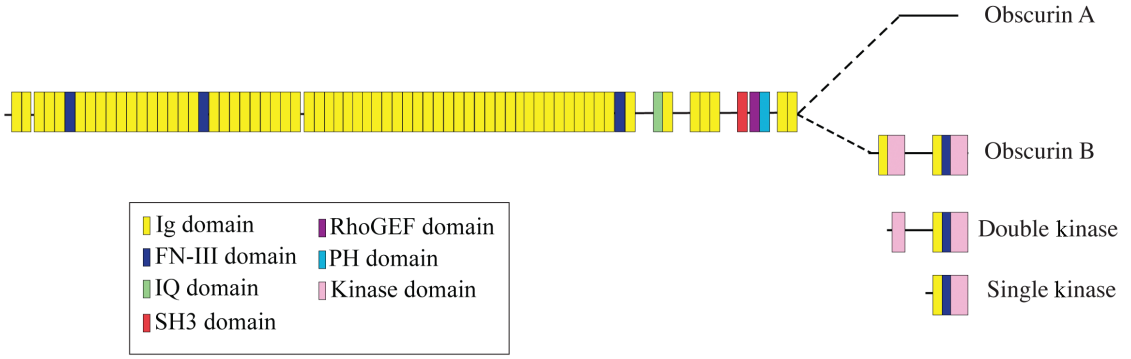

Figure 18 Schematic representation of giant obscurin-A and obscurin-B and small double kinase and single kinase. Domains are shown as colored rectangles: Ig (yellow), FnIII (dark blue), IQ (green), SH3 (red), RhoGEF (purple), PH (light blue), and kinase (pink). The nonmodular region at the extreme COOH-terminus of obscurin A is denoted as black line.

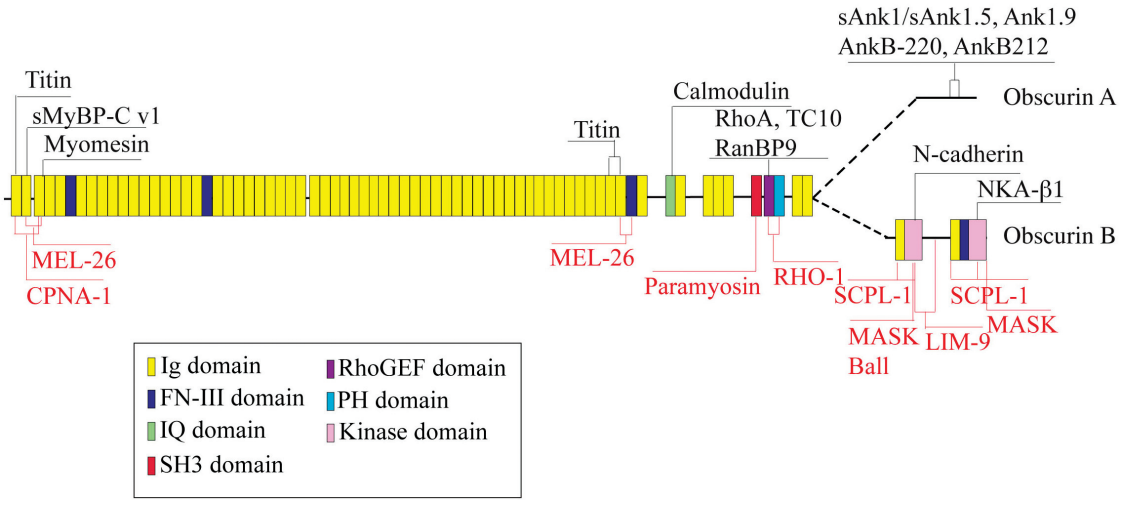

Figure 19 Interacting partners of obscurins in striated muscles. The NH_2-terminus of obscurins provides binding sites for several proteins residing in the M-band, including the extreme COOH-terminus of titin (obscurin Ig1/titin M10), sMyBP-C v1 (obscurin Ig2/sMyBP-C v1 C10) and myomesin (obscurin Ig3/My4-5). Obscurin Ig58/Ig59 domains also interact with titin Zlg9/Zlg10 domains at the level of Z/I junctions. Moreover, a number of binding partners have been identified for the obscurin signaling motifs. Accordingly, the obscurin RhoGEF motif mediates binding to GTPases RhoA and TC10 and the anchoring protein RanBP9, and the obscurin IQ domain binds calmodulin in a Ca^{2+}-independent manner. Notably, isoform-specific interactions have also been characterized, including the presence of multiple ankyrin binding sites in the nonmodular COOH-terminus of obscurin-A, and the ability of Kinase1 and Kinase2 of obscurin-B to interact with the cytoplasmic domain of N-cadherin and the extracellular domain of the NKA-β1 subunit, respectively. The binding partners of the invertebrate obscurin orthlogue UNC89 are also shown in red color, although these have not yet been confirmed in vertebrates; please note that the structural architecture of the invertebrate UNC-89 isoforms is different from the vertebrate obscurins, however the domains *per se* are conserved.

concentrate at the periphery of M-bands and Z-disks, possibly defining the diameter of myofibrils (1-2 μm; (288, 293)). Given the length of an individual obscurin molecule (~208 nm), it has been speculated that obscurins may form homooligomers or associate with other sarcomeric proteins to form a "ring" big enough to envelop myofibrils (288, 293). Although still speculative, such a scenario is tempting given the unique localization of obscurins at the perimeter of M-bands and Z-disks and their tandem adhesion and signaling domains that could provide binding sites for proteins located in different subcellular compartments.

Binding partners

Obscurins contain multiple adhesion and signaling motifs, which may function as binding sites for other proteins. Given their unique location, obscurins are well suited to connect the sarcomeric cytoskeleton with the surrounding myoplasm. Specifically, obscurins contain binding sites for sarcomeric (MyBP-C, titin, and myomesin; discussed in the relative sections above), membrane-associated (ankyrins, N-cadherin, and the β1 subunit of Na^+/K^+ ATPase; NKA-β1) and signaling (RhoA, Ran binding protein 9, and calmodulin) proteins. In addition, a number of binding partners have been identified for the nonvertebrate obscurin orthologue UNC-89, including sarcomeric (paramyosin) and signaling (RHO-1, small C-terminal domain phosphatase like-1; SCPL-1), LIM-9, copine domain protein atypical-1; CPNA-1, bällchen; Ball, and multiple ankyrin repeats single K-homology domain protein; MASK proteins and as well as ligases (bric-à-brac/tramtrack/broad complex (BTB)-domain protein maternal effect lethal-26; MEL-26) (Fig. 19). Below we describe the main binding partners of obscurins and the potential roles of these interactions, when known.

Membrane-associated proteins

Ankyrins (17.5-220 kDa). Early work had suggested that the SR is intimately associated with the nearby sarcomeric cytoskeleton; however, it was relatively recently that molecular links between the two compartments were identified. Two independent studies reported that the nonmodular COOH-terminus of obscurin-A directly interacts with small ankyrin 1 (sAnk1, also referred to as Ank1.5, encoded by *ANK1*), an integral protein of the SR membrane (32, 293). Immunofluorescence labeling of adult skeletal and cardiac muscles supported the physical proximity of the two proteins, as sAnk1/Ank1.5 exhibited a reticular distribution at the level of M-bands and Z-disks, similar to obscurin-A (293). Interestingly, two distinct binding sites for sAnk1/Ank1.5 have been identified in the COOH-terminus of obscurin. Kontrogianni-Konstantopoulos et al. found that a 120-residue long sequence of obscurin-A encompassing amino acids 6316 to 6436 (binding site 1, BS1) binds directly to a 70-residue long fragment in the cytoplasmic tail of sAnk1/Ank1.5 containing amino acids 61 to 130, with a K_d of ~130 nmol/L (293). BS1 is

composed of two positively charged regions containing high contents of Lys and Arg residues, referred to as ankyrin-like repeats, ALRs, located on the surface of the molecule (66). Conversely, Bagnato et al. showed that a 25-residue long sequence of obscurin-A including amino acids 6236 to 6260 (binding site 2, BS2), interacts with a 22-residue-long fragment in the cytoplasmic domain of sAnk1/Ank1.5 comprising amino acids 102 to 123 (32), with a K_d of ~380 nmol/L (75). A follow-up study further pinpointed the minimal binding region within BS1 to include amino acids 6316 to 6345 and to contain a high α-helical content (75). Four charged residues (Glu6327, Glu6329, Glu6330, and Lys6338) within the minimal obscurin BS1 region (74) and four hydrophobic residues (Val70, Phe71, Iso102, and Iso103) present in the ARL motifs of sAnk1/Ank1.5 mediate binding of the two proteins (602), highlighting the contribution of electrostatic interactions. Opposite to sAnk1/Ank1.5, *ANK1* splice variants Ank1.6 and Ank1.7 fail to bind obscurin-A *in vitro* (32), whereas Ank1.9 binds to obscurin-A with a lower affinity than sAnk1/Ank1.5 (25, 287).

The expression of sAnk1/Ank1.5 is significantly reduced in both skeletal and cardiac muscles from an obscurin null (obscn$^{-/-}$) mouse model suggesting that in the absence of obscurins sAnk1/Ank1.5 is subjected to faster turnover (313). Consistent with this, Lange and colleagues demonstrated that sAnk1/Ank1.5 associates with the E3 ligase cullin-3 residing at Z-disks via the adaptor protein potassium (K^+) channel tetramerization domain containing 6 (KCTD6), which targets it for ubiquitylation and degradation (314). When obscurin-A is present, it sequesters the sAnk1/Ank1.5-KCTD6 complex to the M-band (314). However, when obscurin-A is absent, the sAnk1/Ank1/5-KCTD6 complex is released from the M-band, translocating to the Z-disk where it associates with cullin-3 that mediates the increased degradation of sAnk1/Ank1.5 (314).

In addition to the *ANK1* splice variants, sAnk1/Ank1.5 and Ank1.9, *ANK2* (more commonly referred to as *ANKB*) splice variants also interact with obscurins (117, 607). The AnkB subfamily is important for normal cardiac physiology by targeting ion channels and transporters in excitable cells (116). The predominant cardiac isoform, AnkB-220, contains a unique COOH-terminal fragment encoded by a novel exon, referred to as exon 43′, which supports binding to the COOH-terminus of obscurin-A (117). Immunologogical and biochemical studies demonstrated that AnkB-220 is targeted to the M-band via its interaction with obscurin-A where it recruits protein phosphatase 2A (117). Similar to AnkB-220, AnkB-212 is targeted to the M-band via its association with the COOH-terminus of obscurin-A; however, the functional importance of the obscurin-A/AnkB-212 binding remains unclear (607).

N-cadherin (97-100 kDa). Recent work by Hu et al. showed that Kinase1 present at the COOH-terminus of obscurin-B undergoes autophosphorylation, and binds directly to and phosphorylates the cytoplasmic domain of N-cadherin (248). Although the physiological significance of this PTM is currently unknown, given that N-cadherin is a major component of adherens junctions, it is tempting to speculate that obscurin-B may play important roles in the regulation of cell adhesion and communication via its Kinase1 domain (248).

NKA-β1 (~35 kDa). Hu et al. also reported that Kinase2 binds to the extracellular domain of NKA-β1 (248). Although Kinase2 appears to be an active kinase since it also undergoes autophosphorylation, it failed to phosphorylate the NKA-β1 *in vitro* (248). Thus, it is possible that the Kinase2/NKA-β1 interaction may have important regulatory consequences on the activity of NKA-β1 by precluding its phosphorylation by other kinases.

Signaling proteins

RhoA (~22 kDa)

In addition to binding sarcomeric and membrane-associated proteins, obscurins interact with signaling proteins. Through their RhoGEF motif, obscurins selectively bind to and activate RhoA, but not rac1 or cdc-42, *in vitro* (155). This is consistent with the coincident distribution of obscurins and RhoA at the level of M-bands in both developing and mature myofibers (155). Overexpression of the obscurin RhoGEF motif in adult rat tibialis anterior muscle enhances RhoA expression and activity as evidenced by the increased levels of GTP-bound RhoA, and leads to redistribution of RhoA to Z-disks, I-bands, and Z/I junctions, in addition to M-bands (155). Increased RhoA activity (due to overexpression of the obscurin RhoGEF motif) alters the expression and localization of its downstream effectors, Rho-kinase 1 (ROCK1) and citron kinase (CRIK). Specifically, ROCK1 levels increase while CRIK levels decrease (155). Moreover, ROCK1 localizes to Z/I junctions, I-bands and minimally to M-bands following RhoGEF overexpression, instead of Z-disks, while CRIK is undetectable at A- and M-bands due to its diminished levels. These cellular alterations are reminiscent to those induced by large-strain lengthening contractions, suggesting that regulation of RhoA activity via the obscurin RhoGEF motif is essential in modulating contractility (155).

In addition to binding and activating RhoA, the obscurin RhoGEF motif interacts with and activates TC10 that also belongs to the Rho family of GTPases (104). TC10 appears after the fusion of myoblasts, and its expression is maintained in differentiating and mature myotubes (103). Downregulation or overexpression of a dominant-negative form of TC10 in human myotubes demonstrated that it is essential for myofibril assembly, indicating that the interaction of obscurin RhoGEF and TC10 may play key roles in sarcomerogenesis (104).

RanBP9 (~78 kDa)

RanBP9 is a modular scaffolding protein that interacts with a variety of signaling proteins (404). Bowman and colleagues identified RanBP9 as a binding partner of the RhoGEF motif

of obscurins (68). Kinetic evaluation of the RanBP9/obscurin-RhoGEF interaction indicated that is relatively weak and dynamic with a K_d of ~1.9 μmol/L. Consistent with their biochemical interaction, obscurins and RanBP9 colocalize in cultures of skeletal myotubes at the level of M-bands (68). Overexpression of the obscurin-RhoGEF motif or the RanBP9 obscurin-RhoGEF binding site in primary cultures of skeletal myotubes inhibited the incorporation of the NH_2-terminus of titin into developing Z-disks (68). Given that both recombinant proteins bind to the NH_2-terminal Z1/Z2 region of titin, it is likely that obscurin, titin, and RanBP9 form a complex that assists titin's integration into Z-disks (68).

Calmodulin (~17 kDa)

Yeast two-hybrid screening and *in vitro* binding assays indicated that calmodulin is a ligand for the obscurin IQ domain, and that their interaction is insensitive to the presence of Ca^{2+}. However, the functional significance of this interaction has not been explored yet (617).

Binding partners of nonvertebrate obscurins

Although this review primarily focuses on the mammalian thick filaments and associated proteins, a lot of work has been done on the nonvertebrate obscurin orthologue UNC-89, and mainly in *C. elegans* where it was first identified (49, 360, 455). We therefore provide a short description of the UNC-89 binding partners that have been identified today.

Sarcomeric proteins

Paramyosin (~100 kDa)

Paramyosin is orthologous to the rod portion of vertebrate MyHC, and is only found in invertebrate thick filaments. Yeast two-hybrid screening revealed that paramyosin binds to a segment of UNC-89 that includes the SH3-double homology (DH)-PH cassette (457). Further biochemical characterization of this interaction demonstrated that an α-helical segment (amino acids 294-376) of paramyosin interacts with the SH3 domain of UNC-89 with a K_d of ~1.1 μmol/L (457). Loss of giant UNC-89 isoforms or overexpression of the UNC-89 SH3 domain in body wall muscles of *C. elegans* leads to aggregation or mislocalization of paramyosin, respectively, suggesting that binding of paramyosin to UNC-89 is critical for its proper incorporation into sarcomeres (457).

Signaling proteins

RHO-1 (~22 kDa)

Similar to mammalian obscurins, the orthologous *C. elegans* UNC-89 DH-PH cassette binds to and activates RHO-1 (the *C. elegans* orthologue of RhoA), but not CED (the *C. elegans* orthologue of Rac), MIG-2 (the *C. elegans* orthologue of RhoG), or CDC-42 (the *C. elegans* orthologue of Cdc-42). Notably, the DH domain alone induces a comparable GTP/GDP exchange activity for RHO-1 (456). UNC-89 su75 mutant worms, lacking giant UNC-89 isoforms, contained severely disorganized thick filaments (523). Similarly, down-regulation of RHO-1 also resulted in disrupted thick filaments, indicating that the interaction between the UNC-89 DH-PH cassette and RHO-1 is important in thick filament formation and maintenance (456).

SCPL-1 (~54 kDa) and LIM-9 (~74 kDa)

SCPL-1 was identified as a novel binding partner of both Kinase1 (presumed to be catalytically inactive) and Kinase2 (presumed to be catalytically active) of the *C. elegans* UNC-89 protein (458). Interestingly though, both interactions require the presence of the preceding Ig and FnIII domains (458). SCPL-1 localizes to M-bands in body wall skeletal muscles, where UNC-89 also resides. In addition to binding SCPL-1, UNC-89 Kinase1 or interkinase region directly interacts with the cytoskeletal protein LIM-9, which is orthologous to the vertebrate FHL domain protein (609). LIM-9 resides partially at the M-band and was originally identified as a binding partner for UNC-97 and UNC-96 (459). It has been implicated in mediating cell-substratum attachments via indirectly associating with integrins, thus potentially playing a role in force transmission (459, 609). Although the ability of UNC-89 to dimerize has not been proven, it was proposed that the interactions of the COOH-terminal kinase domains with LIM-9 and SCPL-1 may function to stabilize UNC-89 dimers (609). Downregulation of SCPL-1 has no effect on the structure and function of body wall muscles (458), however overexpression of SCPL-1 results in dissolution of M-bands and loss of UNC-89 (609). Thus, it is possible that excessive levels of SCPL-1 may prevent the formation of the UNC-89/SCPL-1/LIM-9 ternary complex, thereby disrupting the normal linkages of UNC-89 via their kinase domains (609).

CPNA-1 (~125 kDa)

CPNA-1, containing a copine domain, is identified as a component of the integrin adhesion complex (590). CPNA-1 is present at M-bands and dense bodies (the analogous structure of the vertebrate Z-disk) of *C. elegans* body-wall muscles, and is implicated in thick filament stability during embryonic muscle development (590). The Ig1-Ig3 domains of UNC-89 bind to the copine domain of CPNA-1 (590). In addition to UNC-89, CPNA-1 interacts with other M-band proteins, such as SCPL-1, LIM-9, UNC-96, and PAT6 (the orthologue of vertebrate actopaxin), suggesting that it may function as a linker between the integrin complex and the sarcomeric cytoskeleton, therefore contributing to the proper localization and stability of the former (590).

Ball (~66 kDa) and MASK (~387 kDa)

Ball and MASK localize to M-bands and Z-disks, and were identified as binding partners of the Drosophila

UNC-89. Ball is an active Ser/Thr kinase that directly binds to Kinase1 domain of Drosophila UNC-89, while MASK is an ankyrin repeat protein that interacts with both UNC-89 kinase domains (276). Downregulation of Ball or MASK in indirect flight muscles (IFMs) causes major sarcomeric disorganization, manifested as fragmentation or aggregation of Z-disks, shifting of M-bands, and dissolution of H-zones (276). Interestingly, UNC-89 was still localized to M-bands in Ball or MASK knockdown IFM, suggesting that it mediates targeting of Ball and MASK to M-bands, but not *vice versa*. Consistent with this, Ball exhibited a diffuse distribution in the cytoplasm, and MASK was nearly lost with residual protein concentrating in puncta over M-bands in UNC-89 knockdown IFM (276).

E3 ubiquitin ligases

BTB-domain protein MEL-26 (~45 kDa). Yeast two-hybrid screen and *in vitro* binding assays showed that two regions of UNC-89, Ig2-Ig3 and Ig53-FNIII2, interact with the NH_2-terminal meprin associated Traf homology (MATH) domain of MEL-26, a substrate recognition protein for cullin 3. Cullins are conserved scaffolds mediating the assembly of the ubiquitin protein degradation machinery including E3 ubiquitin ligases (603). In addition to binding UNC-89, the MEL-26 MATH domain also binds to meiosis defective-1 (MEI-1) protein that is orthologous to the vertebrate microtubule-severing enzyme katanin, and plays key roles in meiotic spindle formation and the assembly of thick filaments (128,603). *C. elegans* mutants lacking giant UNC-89 proteins exhibit decreased levels of MEI-1 (603), suggesting a possible role for the UNC-89/MEL-26 interaction in preventing the degradation of MEI-1 via the MEL-26/cullin 3 ubiquitination complex (603).

Although none of the above interactions has been confirmed in vertebrates to date, the majority of the identified binding partners are highly conserved among species, suggesting that they may also interact with obscurins. In agreement with this, Lange et al. reported that degradation of sAnk1.5 is dependent upon obscurin, and is promoted by a cullin 3 substrate recognition protein, KCTD6 (314). Therefore, both invertebrate UNC-89 and vertebrate obscurin regulate ubiquitin-mediated protein degradation in striated muscles.

Along the same lines, a recent study focusing on breast epithelial cells demonstrated that the PH domain of obscurins binds directly to the SH3 domain of the p85-regulatory component of phosphatildyl inositol 3 kinase (PI3K) with a K_d of ~50 nmol/L (516). Loss of obscurins from breast epithelium results in increased activation of the PI3K cascade contributing to enhanced tumorigenicity and metastasis, suggesting that obscurins act upstream of the PI3K cascade regulating its activation (436, 516, 517). Given that the PI3K pathway is a major driver of growth and proliferation in multiple tissues, it is highly likely that obscurins modulate the activity of PI3K in cardiac and skeletal muscles, too.

Functions

Thick filament assembly

The essential role of obscurins in thick filament assembly and stabilization was suggested early on from *in vitro* developmental studies using mouse C2C12 skeletal myotubes and primary cultures of NRC (62, 63, 289). In both cell systems, myomesin, the COOH-terminus of titin, and obscurins are incorporated into developing M-bands (24-48 h postinitiation of differentiation) before sarcomeric myosin assembles into regular A-bands (72-96 h postinitiation of differentiation) (62, 63, 289). Later studies further underscored the essential roles of obscurins in thick filament assembly, as downregulation of obscurins or overexpression of the COOH-terminus of obscurin-A resulted in dissolute A- and M-bands or failure of myosin to assemble into periodic A-bands, respectively (290, 291). Consistent with these observations, coimmunoprecipitation experiments revealed that obscurins and myosin exist in a complex in adult skeletal muscles, although their direct interaction has not been confirmed yet (290). In addition to their roles in the formation and stability of A- and M-bands, obscurins are implicated in the fusion and lateral connection of myofibrils *in vitro* (62, 63). This notion is further supported by a study in zebrafish, which showed that depletion of obscurins by morpholino injection resulted in defective alignment of newly formed skeletal and cardiac myofibrils (460). Taken together, these studies suggest that obscurins play key scaffolding roles in the incorporation of myosin into A-bands, the assembly and maintenance of M-bands, and the lateral alignment of myofibrils.

Surprisingly, obscn$^{-/-}$ mice displayed a mild myopathic phenotype under sedentary conditions as evidenced by the presence of centralized myonuclei, primarily due to malformed and misaligned SR membranes (please see below) although sarcomeric organization and function were preserved (313). A possible explanation for the mild phenotype of the obscn$^{-/-}$ mice is the presence of nontargeted obscurin isoforms, such as the small kinases. Alternatively, it is likely that obsl1, an obscurin homologue that also consists of tandem Ig and FnIII domains and localizes to M-bands, may compensate for the loss of obscurins (14, 457). However, when obscn$^{-/-}$ mice were challenged with exhaustive exercise, their tolerance was markedly reduced compared to wild-type animals, as a function of the intensity of the running protocol and aging (463). Ultrastructural evaluation of obsc$^{-/-}$ diaphragm (but not hindlimb) muscles following intense exercise revealed that sarcomeric M-bands and H-zones appear wavy and less defined, suggesting that obscurins are essential to maintain the integrity of diaphragm muscle against damage induced by mechanical stress (463).

Contrary to the obscn$^{-/-}$ mouse model that exhibits no major structural alterations, spontaneous *C. elegans* null UNC-89 mutants display impaired locomotion and paralysis (592). Consistent with this phenotype, M- and A-bands fail to form and residual thick filaments are disorganized in the muscles of mutant worms (49, 458, 592). In agreement with

the phenotypic defects observed in the spontaneous UNC-89 mutant worms, downregulation of UNC-89 in adult *C. elegans* or Drosophila embryos yields similar effects (275, 523).

Sarcomeric anchoring and alignment of the sarcoplasmic reticulum

In addition to its essential role in thick filament assembly and stabilization, obscurin-A has an established role in anchoring the myofibrillar cytoskeleton with the SR membranes via its direct interaction with sAnk1/Ank1.5. Downregulation of obscurins in primary cultures of rat skeletal myotubes resulted in failure of sAnk1/Ank1.5 to integrate in the developing SR membranes and align over M-bands and Z-disks (291). Given that sAnk1/Ank1.5 is one of the first proteins to incorporate in the SR membranes (181), it becomes apparent that the sAnk1/Ank1.5-obscurin interaction is essential for the formation and myofibrillar anchoring of the SR network. In agreement with these findings, downregulation of obscurin-A in zebrafish embryos results in disorganized SR membranes in developing skeletal muscles (460). More importantly, the localization and expression levels of sAnk1/Ank1.5 are significantly altered in obscn$^{-/-}$ null skeletal muscles; instead of its typical concentration at the level of M-bands and Z-disks, sAnk1/Ank1.5 exhibits a diffuse cytosolic distribution with occasional accumulation over I-bands (313). In addition to its mislocalization, the amounts of sAnk1/Ank1.5 are markedly reduced in obscn$^{-/-}$ null skeletal and cardiac muscles due to its increased turnover mediated by the KCTD6/cullin-3 complex, as discussed above (313). Consistent with the key role of the sAnk1/Ank1.5-obscurin-A interaction in the formation and sarcomeric alignment of the SR *in vitro* (291), ultrastructural evaluation of obscn$^{-/-}$ null TA muscles showed that the morphology of the longitudinal, but not the junctional, SR is changed by displaying significantly reduced extension over sarcomeres (313). Similarly, depletion of UNC-89 in *C. elegans* results in mislocalized sarco/endoplasmic reticulum Ca^{2+}-ATPase (SERCA) and ryanodine receptor (RyR), and impaired Ca^{2+} cycling, as shown by the presence of reduced Ca^{2+} transients (525). Collectively, these studies suggest an important role for obscurin-A in the regular assembly and sarcomeric anchoring of the SR membranes via its interaction with sAnk1/Ank1.5.

Additional functions

While the roles of obscurins in thick filament assembly and the myofibrillar alignment of the SR membranes have been extensively studied, their roles in other cellular processes, such as maintenance of sarcolemma integrity and cell adhesion, have just started to emerge. Accordingly, a recent study proposed that in skeletal muscle obscurin-A binds to and targets AnkB to M-bands, where it interacts with dynactin4 to organize the underlying subsarcolemmal microtubule lattice (464). Remarkably, the entire subsarcolemmal microtubule network is severely disrupted in obscn$^{-/-}$ null skeletal muscles following exertion of physiological stress via exercise, and AnkB along with dystrophin fail to target to their typical locations at M-bands and costameres, respectively (464). Given that the microtubule network confers stability to sarcolemma allowing it to withstand the mechanical stress imposed during repeating cycles of contraction and relaxation, these findings suggest that loss of obscurins enhances sarcolemmal fragility (464).

Moreover, giant obscurin-B was recently involved in the regulation of cell adhesion via its kinase domains and their ability to phosphorylate N-cadherin in the case of Kinase1 and interact with NKA-β1 in the case of Kinase2, as discussed above (248). Although the functional significance of these interactions remains to be examined, work in breast epithelial cells has demonstrated that obscurins play major scaffolding roles in the membrane localization of the cadherin/catenin complex, while their loss leads to disintegration of adherens junctions (517).

Taken together, obscurins appear to have structural and regulatory roles in striated muscles mediated via their multiple adhesion and signaling motifs that provide binding sites for diverse proteins located in different subcellular compartments.

Posttranslational modifications

Little is known about the regulation of obscurins via PTM. We herein discuss early and recent findings indicating that obscurins may be regulated via phosphorylation (Fig. 20 and Table 12). It is important to note that both kinase domains present in obscurin-B undergo autophosphorylation *in vitro* (248), although the functional relevance of these events is currently unknown.

Phosphorylation

Early studies have pointed out the presence of several copies of the Ser-Pro-X-Arg consensus sequence in the nonmodular COOH-terminus of obscurin-A that serves as recognition site for extracellular signal-regulated kinase (617). Consistent with this, phosphoproteomic analysis of human skeletal muscles from healthy volunteers revealed the presence of several phosphorylation sites in obscurins (238). Similarly, using phosphoproteomic analysis a recent study also reported the presence of multiple phosphorylation sites throughout the length of giant obscurins in both rat and human skeletal muscles (339). Although these findings highlight the potential role of phosphorylation in the regulation of obscurins, the kinases and the biological significance of these PTM are still elusive (238, 339).

Interestingly, a recent study indicated that obscurins are substrates of GSK-3β, which phosphorylates residue Ser4829 (Accession #: Q5VST9, corresponding to Ser4809 in canine obscurin) residing between Ig47 and the IQ domains (281). This phosphorylation event appears to be of high-functional

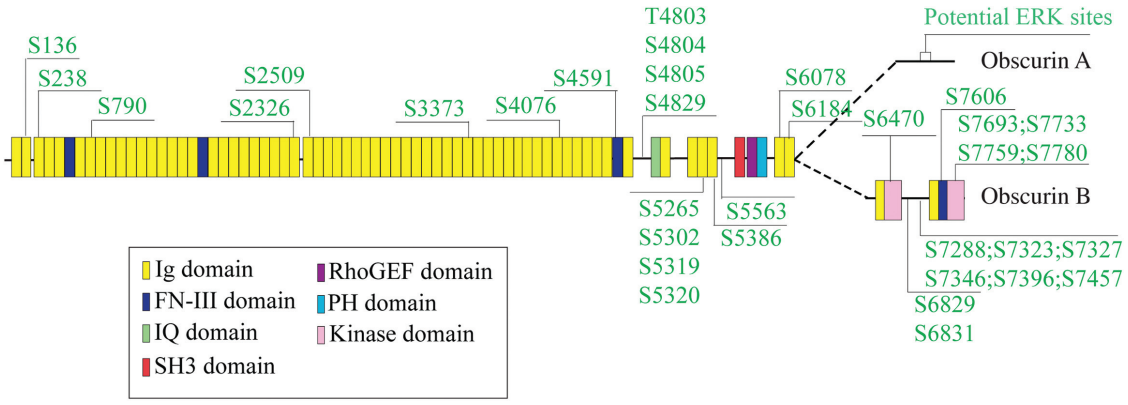

Figure 20 Posttranslational modifications of obscurins. To date, the only known modification that obscurins undergo is phosphorylation. A number of phosphorylation sites (shown in green) have been identified via phosphoproteomic analysis that exhibit a preferential accumulation within or proximal to the signaling motifs present in the COOH-terminus. However, these have not been confirmed via biochemical or molecular methods with the exception of a phosphorylation event involving Ser4829 that is mediated by GSK-3β and was identified in a tachypacing-induced heart failure model.

significance, as it was identified in a canine model subjected to tachypacing-induced heart failure concurrent with ventricular dyssynchrony (HF_{dys}) after cardiac resynchronization therapy (CRT) (281). HF_{dys} cardiac myofilaments display impaired maximal Ca^{2+}-activated force and reduced Ca^{2+} sensitivity, which are reversed by CRT that corrects discoordinate contraction via the application of biventricular stimulation (273). Molecularly, CRT appears to act (at least in part) via increased activation of GSK-3β that phosphorylates and therefore regulates several myofilament proteins (281). Thus, phosphorylation of obscurins by GSK-3β may contribute to restoring myofilament Ca^{2+} sensitivity in the HF_{dys} model (281).

Mutations and myopathies

The involvement of obscurins in myopathies has only been recently interrogated, leading to the identification of 15 mutations in the *OBSCN* gene that are linked to different forms of cardiomyopathy including HCM, DCM, and LVNC (Fig. 21 and Table 13) (23, 352, 481, 610).

The first disease-linked *OBSCN* mutations were identified in a patient with HCM (23). Specifically, two missense mutations, Arg4344Gln (c.13031 G > A in exon 51) and Ala4484Thr (c.13450 G > A in exon 52) were identified by linkage analysis (23). The Arg4344Gln and Ala4484Thr substitutions are located in Ig58 and Ig59, respectively, which have been reported to mediate binding to titin's Z9/Z10 region, as earlier discussed (617). *In vitro* binding studies, however, demonstrated that only the Arg4344Gln mutation diminishes, yet modestly, the obscurin/titin interaction (23). Notably, a knockin animal model containing the Arg4344Gln mutation was recently generated to examine the functional ramifications of this mutation; please note that the wild-type mouse genome contains the Ala4484Thr substitution, further suggesting that it is a polymorphism rather than a disease-driving mutation. The expression levels and localization of titin were indistinguishable between wild type and homozygous knockin animals. Interestingly, examination of homozygous knockin animals demonstrated that they develop arrhythmia by 1 year of age under sedentary conditions, accompanied by frequent episodes of premature ventricular contractions (249). Consistent with this, isolated cardiomyocytes exhibited enhanced Ca^{2+} transients and accelerated contractility kinetics due to increased levels and activity of SERCA2 pump (249). Detailed structural and biochemical work further indicated that the increased SERCA2 activity might result from sequestration of phospholamban, its major regulator in cardiac cells, due to enhanced binding of mutant obscurins to phospholamban (249). Moreover, young adult homozygous knockin animals subjected to pathological stress in the form of

Table 12 Phosphorylation Sites of Obscurins

Gene	Protein	Accession #	Phosphorylation sites	Reference
OBSCN	Obscurin-MLCK	Human: Q5VST9	S4076, T4803*, S4804, S4805, S5563, S6829, S6831	Hojlund et al., 2009
			S136, S238, S790, S2326, S2509, S3373, S4591, S5265, S5302, S5319, S5320, S5386, S6078, S6184, S6470, S7288, S7323, S7327, S7346, S7396, S7457, S7606, S7693, S7733, S7759, S7780	Lundby et al., 2012
			S4829	Kirk et al., 2014

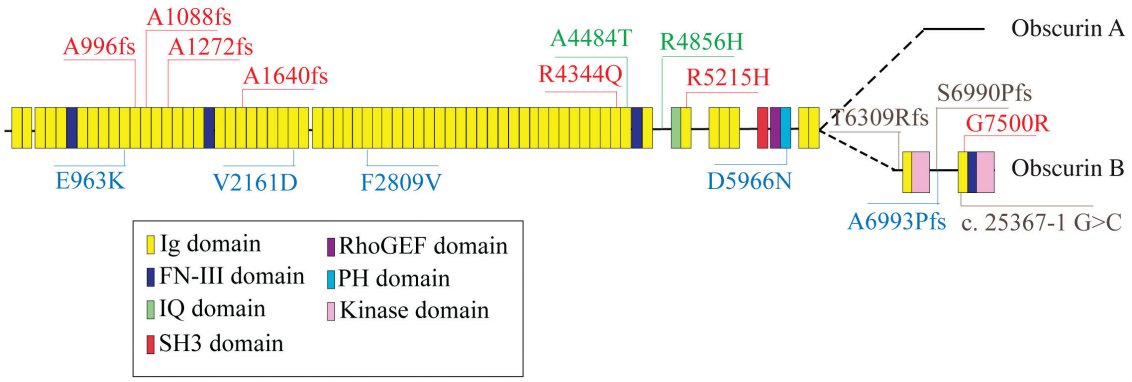

Figure 21 Illustration of the *OBSCN* mutations and their location that have been linked with the development of different forms of cardiomyopathy. Mutations associated with HCM are shown in red, mutations associated with DCM are shown in blue, and mutations associated with LVNC are shown in black. Three additional polymorphisms have been described as compound heterozygous, and are shown in green; fs: frameshift.

Table 13 Mutations Identified in Obscurins

OBSCN (NP-001092093)		*OBSCN* (NP-001258152)			
Mutation	Domain	Muation	Domain	Disease	Reference
		Missense mutations			
R4344Q	Ig47	R5304Q	Ig58	HCM	Arimura et al., 2007
A4484T	Ig48	A5441T	Ig59	Compound heterozygosity	Arimura et al., 2007
R5215H	Ig52	R6172H	Ig63	HCM	Xu et al., 2015
G7500R	Ig58	G8457R	Ig69	HCM	Xu et al., 2015
E963K	Ig10	E1055K	Ig11	DCM	Marston et al., 2015
V2161D	Ig23	V2536D	Ig27	DCM	Marston et al., 2015
F2809V	Ig29	F3238V	Ig34	Compound heterozygosity	Marston et al., 2015
R4856H	Between Ig50 and IQ	R5813H	Between Ig61 and Ig62	Compound heterozygosity	Marston et al., 2015
D5966N	PH	D6923N	PH	DCM	Marston et al., 2015
		Frameshift mutations			
A996fs	Ig11	A1088fs	Ig12	HCM	Xu et al., 2015
A1088fs	Ig12	A1180fs	Ig13	HCM	Xu et al., 2015
A1272fs	Ig14	A1364fs	Ig15	HCM	Xu et al., 2015
A1640fs	Ig18	A2015fs	Ig22	HCM	Xu et al., 2015
T6309Rfs*53	Between Ig56 and Ig57	T7266Rfs*53	Between Ig67 and Ig68	LVNC	Rowland et al., 2015
S6990Pfs*82	Between Kinase1 and Ig58	S7947Pfs*82	Between Kinase1 and Ig69	LVNC	Rowland et al., 2015
A6993Pfs*79	Between Kinase1 and Ig58	A7950Pfs*79	Between Kinase1 and Ig69	DCM	Rowland et al., 2015
		Splicing mutations			
c. 25367-1 G>C	Ig58	c. 25367-1 G>C	Ig69	LVNC	Rowland et al., 2015

Abbreviations: Ig, immunoglobulin; IQ, isoleucine/glutamine; PH, pleckstrin homology; Kinase1, the first kinase if counting from the NH_2-terminus; HCM, hypertrophic cardiomyopathy; DCM, dilated cardiomyopathy; LVNC, left ventricular noncompaction.

pressure overload developed a DCM-like phenotype characterized by cardiac remodeling (249). Thus, it becomes apparent that obscurins play important regulatory roles in cardiac muscle, which are compromised in disease, by contributing to the maintenance of Ca^{2+} homeostasis.

Almost a decade after the identification of the Arg4344Gln and Ala4484Thr mutations, the *OBSCN* was screened for the presence of additional HCM-linked mutations. Xu and colleagues performed whole exome sequencing in samples obtained from 74 Chinese patients presenting with sporadic HCM (610). *OBSCN* was identified in the top 10 putative HCM-associated genes out of 92 candidate genes (610). In particular, six rare pathogenic dominant mutations were described, including four frameshift (Ala996fs, Ala1088fs, Ala1272fs, and Ala1640fs) and two missense (Arg5215His and Gly7500Arg) mutations (610), although their specific mechanisms of action are currently unknown.

Moreover, whole exon sequencing of explanted heart samples obtained from 30 end-stage heart failure patients diagnosed with familial DCM and three HCM myectomy patients along with six control donor heart samples was used to identify possible disease-causing mutations in 58 genes previously associated with cardiomyopathy (352). Five missense mutations (Glu963Lys, Val2161Asp, Phe2809Val, Asp5966Asn, and Arg4856His) were identified in four DCM patients with two (V2161Asp and Phe2809Val) exhibiting compound heterozygosity. It is worth mentioning that Phe2809Val and Arg4856His are classified as nondisease-related due to high prevalence and lack of conservation among species, respectively (352). Interestingly, the expression levels of obscurin proteins were significantly decreased in DCM samples carrying the Glu963Lys, Val2161Asp/Phe2809Val and Asp5966Asn mutations compared to DCM samples without *OBSCN* mutations, HCM samples or healthy controls suggesting that these mutations may function via haploinsufficiency (352).

To further explore the presence of *OBSCN* mutations in patients with heart disease, Rowland and colleagues used the TruSight One-Sequence panel querying 4813 cardiomyopathic genes in a population of 335 patients diagnosed with DCM (325 patients) or LVNC (10 patients) (481). Four new dominant *OBSCN* variations were identified in four probands, including three frameshift mutations (Thr7266Argfs*ter53, Ser7947Profs*ter82, and Ala7950Profs*ter79) and one splicing variant (c. 25367-1 G>C) (481). Notably, among the four affected probands, only one was diagnosed with DCM (Ala7950Profs*ter79) while the other three suffered from LVNC (Thr7266Argfs*ter53, Ser7947Profs*ter82, and c. 25367-1 G>C). All four mutations affect residues located between Ig67 and Ig69 located in the COOH-terminus of obscurin-B, however their molecular manifestations are currently elusive. Given the prevalence of DCM samples in the panel (325 out of 335) compared to LVNC samples (10 out of 335), it is tempting to speculate that *OBSCN* mutations may be more commonly associated with the pathogenesis of LVNC rather than DCM or HCM (481).

Conclusions

Obscurins are the most recently discovered giant sarcomeric proteins. Although we still need to learn a lot about their molecular diversity, interacting partners, regulation, roles, and disease involvement, it is apparent that they play key roles in several processes, ranging from muscle assembly and maintenance to Ca^{2+} regulation and cellular adhesion. Consistent with their essential roles in striated muscles, accumulating evidence links mutations in *OBSCN* with different forms of cardiomyopathy although their molecular and cellular manifestations are currently elusive. Sophisticated biochemical and biophysical studies along with the generation of the appropriate animal models and the use of human biopsies (when available) are therefore needed to provide mechanistic insights on how individual mutations contribute to disease pathogenesis.

Acknowledgements

This work was supported by grants from American Heart Association (16GRNT31290010 to AKK), Muscular Dystrophy Association (313579 to AKK), and NIH/MIAMS (T32AR7592 to LW, JG, and AG). The authors would like to thank Dr. E. Rene Rodriguez and *e-heart.org* for the generation of Figure 1.

References

1. Ababou A, Gautel M, Pfuhl M. Dissecting the N-terminal myosin binding site of human cardiac myosin-binding protein C. Structure and myosin binding of domain C2. *J Biol Chem* 282: 9204-9215, 2007.
2. Ababou A, Rostkova E, Mistry S, Le Masurier C, Gautel M, Pfuhl M. Myosin binding protein C positioned to play a key role in regulation of muscle contraction: Structure and interactions of domain C1. *J Mol Biol* 384: 615-630, 2008.
3. Abdelaziz AI, Pagel I, Schlegel WP, Kott M, Monti J, Haase H, Morano I. Human atrial myosin light chain 1 expression attenuates heart failure. *Adv Exp Med Biol* 565: 283-292; discussion 292, 405-215, 2005.
4. Abdul-Hussein S, van der Ven PF, Tajsharghi H. Expression profiles of muscle disease-associated genes and their isoforms during differentiation of cultured human skeletal muscle cells. *BMC Musculoskelet Disord* 13: 262, 2012.
5. Abraham WT, Gilbert EM, Lowes BD, Minobe WA, Larrabee P, Roden RL, Dutcher D, Sederberg J, Lindenfeld JA, Wolfel EE, Shakar SF, Ferguson D, Volkman K, Linseman JV, Quaife RA, Robertson AD, Bristow MR. Coordinate changes in myosin heavy chain isoform gene expression are selectively associated with alterations in dilated cardiomyopathy phenotype. *Mol Med* 8: 750-760, 2002.
6. Ackermann M, Kontrogianni-Konstantopoulos A. Cardiomyopathies: When the goliaths of heart muscle hurt. In: Milei J, Ambrosio G, editors. *Cardiomyopathies*. London, United Kingdom: Intech, 2013.
7. Ackermann MA, Hu LY, Bowman AL, Bloch RJ, Kontrogianni-Konstantopoulos A. Obscurin interacts with a novel isoform of MyBP-C slow at the periphery of the sarcomeric M-band and regulates thick filament assembly. *Mol Biol Cell* 20: 2963-2978, 2009.
8. Ackermann MA, King B, Lieberman NAP, Bobbili PJ, Rudloff M, Berndsen CE, Wright NT, Hecker PA, Kontrogianni-Konstantopoulos A. Novel obscurins mediate cardiomyocyte adhesion and size via the PI3K/AKT/mTOR signaling pathway. *J Mol Cell Cardiol* 111: 27-39, 2017.
9. Ackermann MA, Kontrogianni-Konstantopoulos A. Myosin binding protein-C slow: An intricate subfamily of proteins. *J Biomed Biotechnol* 2010: 652065, 2010.
10. Ackermann MA, Kontrogianni-Konstantopoulos A. Myosin binding protein-C slow is a novel substrate for protein kinase A (PKA) and C (PKC) in skeletal muscle. *J Proteome Res* 10: 4547-4555, 2011.

11. Ackermann MA, Kontrogianni-Konstantopoulos A. Myosin binding protein-C: A regulator of actomyosin interaction in striated muscle. *J Biomed Biotechnol* 2011: 636403, 2011.
12. Ackermann MA, Kontrogianni-Konstantopoulos A. Myosin binding protein-C slow: A multifaceted family of proteins with a complex expression profile in fast and slow twitch skeletal muscles. *Front Physiol* 4: 391, 2013.
13. Ackermann MA, Patel PD, Valenti J, Takagi Y, Homsher E, Sellers JR, Kontrogianni-Konstantopoulos A. Loss of actomyosin regulation in distal arthrogryposis myopathy due to mutant myosin binding protein-C slow. *FASEB J* 27: 3217-3228, 2013.
14. Ackermann MA, Shriver M, Perry NA, Hu LY, Kontrogianni-Konstantopoulos A. Obscurins: Goliaths and Davids take over non-muscle tissues. *PLoS One* 9: e88162, 2014.
15. Ackermann MA, Ward CW, Gurnett C, Kontrogianni-Konstantopoulos A. Myosin binding protein-C slow phosphorylation is altered in Duchenne dystrophy and arthrogryposis myopathy in fast-twitch skeletal muscles. *Sci Rep* 5: 13235, 2015.
16. Agarkova I, Auerbach D, Ehler E, Perriard JC. A novel marker for vertebrate embryonic heart, the EH-myomesin isoform. *J Biol Chem* 275: 10256-10264, 2000.
17. Agarkova I, Perriard JC. The M-band: An elastic web that crosslinks thick filaments in the center of the sarcomere. *Trends Cell Biol* 15: 477-485, 2005.
18. Agarkova I, Schoenauer R, Ehler E, Carlsson L, Carlsson E, Thornell LE, Perriard JC. The molecular composition of the sarcomeric M-band correlates with muscle fiber type. *Eur J Cell Biol* 83: 193-204, 2004.
19. Agbulut O, Noirez P, Beaumont F, Butler-Browne G. Myosin heavy chain isoforms in postnatal muscle development of mice. *Biol Cell* 95: 399-406, 2003.
20. Al-Khayat HA. Three-dimensional structure of the human myosin thick filament: Clinical implications. *Glob Cardiol Sci Pract* 2013: 280-302, 2013.
21. Alyonycheva T, Cohen-Gould L, Siewert C, Fischman DA, Mikawa T. Skeletal muscle-specific myosin binding protein-H is expressed in Purkinje fibers of the cardiac conduction system. *Circ Res* 80: 665-672, 1997.
22. Ao W, Pilgrim D. *Caenorhabditis elegans* UNC-45 is a component of muscle thick filaments and colocalizes with myosin heavy chain B, but not myosin heavy chain A. *J Cell Biol* 148: 375-384, 2000.
23. Arimura T, Matsumoto Y, Okazaki O, Hayashi T, Takahashi M, Inagaki N, Hinohara K, Ashizawa N, Yano K, Kimura A. Structural analysis of obscurin gene in hypertrophic cardiomyopathy. *Biochem Biophys Res Commun* 362: 281-287, 2007.
24. Arimura T, Suematsu N, Zhou YB, Nishimura J, Satoh S, Takeshita A, Kanaide H, Kimura A. Identification, characterization, and functional analysis of heart-specific myosin light chain phosphatase small subunit. *J Biol Chem* 276: 6073-6082, 2001.
25. Armani A, Galli S, Giacomello E, Bagnato P, Barone V, Rossi D, Sorrentino V. Molecular interactions with obscurin are involved in the localization of muscle-specific small ankyrin1 isoforms to subcompartments of the sarcoplasmic reticulum. *Exp Cell Res* 312: 3546-3558, 2006.
26. Arrell DK, Neverova I, Fraser H, Marban E, Van Eyk JE. Proteomic analysis of pharmacologically preconditioned cardiomyocytes reveals novel phosphorylation of myosin light chain 1. *Circ Res* 89: 480-487, 2001.
27. Aryal B, Jeong J, Rao VA. Doxorubicin-induced carbonylation and degradation of cardiac myosin binding protein C promote cardiotoxicity. *Proc Natl Acad Sci U S A* 111: 2011-2016, 2014.
28. Ashby B, Frieden C. Interaction of AMP-aminohydrolase with myosin and its subfragments. *J Biol Chem* 252: 1869-1872, 1977.
29. Aslanidis C, Jansen G, Amemiya C, Shutler G, Mahadevan M, Tsilfidis C, Chen C, Alleman J, Wormskamp NG, Vooijs M, et al. Cloning of the essential myotonic dystrophy region and mapping of the putative defect. *Nature* 355: 548-551, 1992.
30. Auckland LM, Lambert SJ, Cummins P. Cardiac myosin light and heavy chain isotypes in tetralogy of Fallot. *Cardiovasc Res* 20: 828-836, 1986.
31. Auerbach D, Bantle S, Keller S, Hinderling V, Leu M, Ehler E, Perriard JC. Different domains of the M-band protein myomesin are involved in myosin binding and M-band targeting. *Mol Biol Cell* 10: 1297-1308, 1999.
32. Bagnato P, Barone V, Giacomello E, Rossi D, Sorrentino V. Binding of an ankyrin-1 isoform to obscurin suggests a molecular link between the sarcoplasmic reticulum and myofibrils in striated muscles. *J Cell Biol* 160: 245-253, 2003.
33. Bahler M, Eppenberger HM, Wallimann T. Novel thick filament protein of chicken pectoralis muscle: The 86 kd protein. I. Purification and characterization. *J Mol Biol* 186: 381-391, 1985.
34. Baines AJ, Lu HC, Bennett PM. The Protein 4.1 family: Hub proteins in animals for organizing membrane proteins. *Biochim Biophys Acta* 1838: 605-619, 2014.
35. Bamshad M, Van Heest AE, Pleasure D. Arthrogryposis: A review and update. *J Bone Joint Surg Am* 91 (Suppl 4): 40-46, 2009.
36. Bang ML, Centner T, Fornoff F, Geach AJ, Gotthardt M, McNabb M, Witt CC, Labeit D, Gregorio CC, Granzier H, Labeit S. The complete gene sequence of titin, expression of an unusual approximately 700-kDa titin isoform, and its interaction with obscurin identify a novel Z-line to I-band linking system. *Circ Res* 89: 1065-1072, 2001.
37. Bansal D, Campbell KP. Dysferlin and the plasma membrane repair in muscular dystrophy. *Trends Cell Biol* 14: 206-213, 2004.
38. Bar-Lavan Y, Shemesh N, Ben-Zvi A. Chaperone families and interactions in metazoa. *Essays Biochem* 60: 237-253, 2016.
39. Barbet JP, Thornell LE, Butler-Browne GS. Immunocytochemical characterisation of two generations of fibers during the development of the human quadriceps muscle. *Mech Dev* 35: 3-11, 1991.
40. Bardswell SC, Cuello F, Rowland AJ, Sadayappan S, Robbins J, Gautel M, Walker JW, Kentish JC, Avkiran M. Distinct sarcomeric substrates are responsible for protein kinase D-mediated regulation of cardiac myofilament Ca^{2+} sensitivity and cross-bridge cycling. *J Biol Chem* 285: 5674-5682, 2010.
41. Barefield D, Kumar M, Gorham J, Seidman JG, Seidman CE, de Tombe PP, Sadayappan S. Haploinsufficiency of MYBPC3 exacerbates the development of hypertrophic cardiomyopathy in heterozygous mice. *J Mol Cell Cardiol* 79: 234-243, 2015.
42. Barefield D, Sadayappan S. Phosphorylation and function of cardiac myosin binding protein-C in health and disease. *J Mol Cell Cardiol* 48: 866-875, 2010.
43. Barral JM, Bauer CC, Ortiz I, Epstein HF. Unc-45 mutations in *Caenorhabditis elegans* implicate a CRO1/She4p-like domain in myosin assembly. *J Cell Biol* 143: 1215-1225, 1998.
44. Barral JM, Hutagalung AH, Brinker A, Hartl FU, Epstein HF. Role of the myosin assembly protein UNC-45 as a molecular chaperone for myosin. *Science* 295: 669-671, 2002.
45. Bashir R, Britton S, Strachan T, Keers S, Vafiadaki E, Lako M, Richard I, Marchand S, Bourg N, Argov Z, Sadeh M, Mahjneh I, Marconi G, Passos-Bueno MR, Moreira Ede S, Zatz M, Beckmann JS, Bushby K. A gene related to *Caenorhabditis elegans* spermatogenesis factor fer-1 is mutated in limb-girdle muscular dystrophy type 2B. *Nat Genet* 20: 37-42, 1998.
46. Bayram Y, Karaca E, Coban Akdemir Z, Yilmaz EO, Tayfun GA, Aydin H, Torun D, Bozdogan ST, Gezdirici A, Isikay S, Atik MM, Gambin T, Harel T, El-Hattab AW, Charng WL, Pehlivan D, Jhangiani SN, Muzny DM, Karaman A, Celik T, Yuregir OO, Yildirim T, Bayhan IA, Boerwinkle E, Gibbs RA, Elcioglu N, Tuysuz B, Lupski JR. Molecular etiology of arthrogryposis in multiple families of mostly Turkish origin. *J Clin Invest* 126: 762-778, 2016.
47. Begay RL, Graw S, Sinagra G, Merlo M, Slavov D, Gowan K, Jones KL, Barbati G, Spezzacatene A, Brun F, Di Lenarda A, Smith JE, Granzier HL, Mestroni L, Taylor M, Registry FC. Role of titin missense variants in dilated cardiomyopathy. *J Am Heart Assoc* 4: 1-9, 2015.
48. Behrmann E, Muller M, Penczek PA, Mannherz HG, Manstein DJ, Raunser S. Structure of the rigor actin-tropomyosin-myosin complex. *Cell* 150: 327-338, 2012.
49. Benian GM, Tinley TL, Tang X, Borodovsky M. The *Caenorhabditis elegans* gene unc-89, required fpr muscle M-line assembly, encodes a giant modular protein composed of Ig and signal transduction domains. *J Cell Biol* 132: 835-848, 1996.
50. Bennett P, Craig R, Starr R, Offer G. The ultrastructural location of C-protein, X-protein and H-protein in rabbit muscle. *J Muscle Res Cell Motil* 7: 550-567, 1986.
51. Bennett PM, Gautel M. Titin domain patterns correlate with the axial disposition of myosin at the end of the thick filament. *J Mol Biol* 259: 896-903, 1996.
52. Benson MA, Tinsley CL, Blake DJ. Myospryn is a novel binding partner for dysbindin in muscle. *J Biol Chem* 279: 10450-10458, 2004.
53. Berkemeier F, Bertz M, Xiao S, Pinotsis N, Wilmanns M, Grater F, Rief M. Fast-folding alpha-helices as reversible strain absorbers in the muscle protein myomesin. *Proc Natl Acad Sci U S A* 108: 14139-14144, 2011.
54. Bezold KL, Shaffer JF, Khosa JK, Hoye ER, Harris SP. A gain-of-function mutation in the M-domain of cardiac myosin-binding protein-C increases binding to actin. *J Biol Chem* 288: 21496-21505, 2013.
55. Bhuiyan MS, Gulick J, Osinska H, Gupta M, Robbins J. Determination of the critical residues responsible for cardiac myosin binding protein C's interactions. *J Mol Cell Cardiol* 53: 838-847, 2012.
56. Bicer S, Reiser PJ. Myosin light chain isoform expression among single mammalian skeletal muscle fibers: Species variations. *J Muscle Res Cell Motil* 25: 623-633, 2004.
57. Bloemink MJ, Deacon JC, Resnicow DI, Leinwand LA, Geeves MA. The superfast human extraocular myosin is kinetically distinct from the fast skeletal IIa, IIb, and IId isoforms. *J Biol Chem* 288: 27469-27479, 2013.

58. Bloemink MJ, Melkani GC, Bernstein SI, Geeves MA. The relay/converter interface influences hydrolysis of ATP by skeletal muscle myosin II. *J Biol Chem* 291: 1763-1773, 2016.
59. Bodine SC, Latres E, Baumhueter S, Lai VK, Nunez L, Clarke BA, Poueymirou WT, Panaro FJ, Na E, Dharmarajan K, Pan ZQ, Valenzuela DM, DeChiara TM, Stitt TN, Yancopoulos GD, Glass DJ. Identification of ubiquitin ligases required for skeletal muscle atrophy. *Science* 294: 1704-1708, 2001.
60. Bogomolovas J, Gasch A, Simkovic F, Rigden DJ, Labeit S, Mayans O. Titin kinase is an inactive pseudokinase scaffold that supports MuRF1 recruitment to the sarcomeric M-line. *Open Biol* 4: 140041, 2014.
61. Bonne G, Carrier L, Bercovici J, Cruaud C, Richard P, Hainque B, Gautel M, Labeit S, James M, Beckmann J, Weissenbach J, Vosberg HP, Fiszman M, Komajda M, Schwartz K. Cardiac myosin binding protein-C gene splice acceptor site mutation is associated with familial hypertrophic cardiomyopathy. *Nat Genet* 11: 438-440, 1995.
62. Borisov AB, Kontrogianni-Konstantopoulos A, Bloch RJ, Westfall MV, Russell MW. Dynamics of obscurin localization during differentiation and remodeling of cardiac myocytes: Obscurin as an integrator of myofibrillar structure. *J Histochem Cytochem* 52: 1117-1127, 2004.
63. Borisov AB, Martynova MG, Russell MW. Early incorporation of obscurin into nascent sarcomeres: Implication for myofibril assembly during cardiac myogenesis. *Histochem Cell Biol* 129: 463-478, 2008.
64. Borisov AB, Raeker MO, Kontrogianni-Konstantopoulos A, Yang K, Kurnit DM, Bloch RJ, Russell MW. Rapid response of cardiac obscurin gene cluster to aortic stenosis: Differential activation of Rho-GEF and MLCK and involvement in hypertrophic growth. *Biochem Biophys Res Commun* 310: 910-918, 2003.
65. Borisov AB, Raeker MO, Russell MW. Developmental expression and differential cellular localization of obscurin and obscurin-associated kinase in cardiac muscle cells. *J Cell Biochem* 103: 1621-1635, 2008.
66. Borzok MA, Catino DH, Nicholson JD, Kontrogianni-Konstantopoulos A, Bloch RJ. Mapping the binding site on small ankyrin 1 for obscurin. *J Biol Chem* 282: 32384-32396, 2007.
67. Bott-Flugel L, Weig HJ, Uhlein H, Nabauer M, Laugwitz KL, Seyfarth M. Quantitative analysis of apoptotic markers in human end-stage heart failure. *Eur J Heart Fail* 10: 129-132, 2008.
68. Bowman AL, Catino DH, Strong JC, Randall WR, Kontrogianni-Konstantopoulos A, Bloch RJ. The rho-guanine nucleotide exchange factor domain of obscurin regulates assembly of titin at the Z-disk through interactions with Ran binding protein 9. *Mol Biol Cell* 19: 3782-3792, 2008.
69. Bowman AL, Kontrogianni-Konstantopoulos A, Hirsch SS, Geisler SB, Gonzalez-Serratos H, Russell MW, Bloch RJ. Different obscurin isoforms localize to distinct sites at sarcomeres. *FEBS Lett* 581: 1549-1554, 2007.
70. Brenner B, Hahn N, Hanke E, Matinmehr F, Scholz T, Steffen W, Kraft T. Mechanical and kinetic properties of beta-cardiac/slow skeletal muscle myosin. *J Muscle Res Cell Motil* 33: 403-417, 2012.
71. Brook JD, McCurrach ME, Harley HG, Buckler AJ, Church D, Aburatani H, Hunter K, Stanton VP, Thirion JP, Hudson T, et al. Molecular basis of myotonic dystrophy: Expansion of a trinucleotide (CTG) repeat at the 3′ end of a transcript encoding a protein kinase family member. *Cell* 68: 799-808, 1992.
72. Bujalowski PJ, Nicholls P, Oberhauser AF. UNC-45B chaperone: The role of its domains in the interaction with the myosin motor domain. *Biophys J* 107: 654-661, 2014.
73. Burke M, Sivaramakrishnam M, Kamalakannan V. On the mode of the alkali light chain association to the heavy chain of myosin subfragment 1. Evidence for the involvement of the carboxyl-terminal region of the heavy chain. *Biochemistry* 22: 3046-3053, 1983.
74. Busby B, Oashi T, Willis CD, Ackermann MA, Kontrogianni-Konstantopoulos A, Mackerell AD, Jr., Bloch RJ. Electrostatic interactions mediate binding of obscurin to small ankyrin 1: Biochemical and molecular modeling studies. *J Mol Biol* 408: 321-334, 2011.
75. Busby B, Willis CD, Ackermann MA, Kontrogianni-Konstantopoulos A, Bloch RJ. Characterization and comparison of two binding sites on obscurin for small ankyrin 1. *Biochemistry* 49: 9948-9956, 2010.
76. Buxton J, Shelbourne P, Davies J, Jones C, Van Tongeren T, Aslanidis C, de Jong P, Jansen G, Anvret M, Riley B, et al. Detection of an unstable fragment of DNA specific to individuals with myotonic dystrophy. *Nature* 355: 547-548, 1992.
77. Cahill TJ, Ashrafian H, Watkins H. Genetic cardiomyopathies causing heart failure. *Circ Res* 113: 660-675, 2013.
78. Caremani M, Dantzig J, Goldman YE, Lombardi V, Linari M. Effect of inorganic phosphate on the force and number of myosin cross-bridges during the isometric contraction of permeabilized muscle fibers from rabbit psoas. *Biophys J* 95: 5798-5808, 2008.
79. Caremani M, Melli L, Dolfi M, Lombardi V, Linari M. The working stroke of the myosin II motor in muscle is not tightly coupled to release of orthophosphate from its active site. *J Physiol* 591: 5187-5205, 2013.
80. Carlsson E, Grove BK, Wallimann T, Eppenberger HM, Thornell LE. Myofibrillar M-band proteins in rat skeletal muscles during development. *Histochemistry* 95: 27-35, 1990.
81. Carlsson L, Yu JG, Thornell LE. New aspects of obscurin in human striated muscles. *Histochem Cell Biol* 130: 91-103, 2008.
82. Carmignac V, Salih MA, Quijano-Roy S, Marchand S, Al Rayess MM, Mukhtar MM, Urtizberea JA, Labeit S, Guicheney P, Leturcq F, Gautel M, Fardeau M, Campbell KP, Richard I, Estournet B, Ferreiro A. C-terminal titin deletions cause a novel early-onset myopathy with fatal cardiomyopathy. *Ann Neurol* 61: 340-351, 2007.
83. Carrier L, Knoll R, Vignier N, Keller DI, Bausero P, Prudhon B, Isnard R, Ambroisine ML, Fiszman M, Ross J, Jr., Schwartz K, Chien KR. Asymmetric septal hypertrophy in heterozygous cMyBP-C null mice. *Cardiovasc Res* 63: 293-304, 2004.
84. Carrier L, Mearini G, Stathopoulou K, Cuello F. Cardiac myosin-binding protein C (MYBPC3) in cardiac pathophysiology. *Gene* 573: 188-197, 2015.
85. Cazorla O, Szilagyi S, Vignier N, Salazar G, Kramer E, Vassort G, Carrier L, Lacampagne A. Length and protein kinase A modulations of myocytes in cardiac myosin binding protein C-deficient mice. *Cardiovasc Res* 69: 370-380, 2006.
86. Cecconi F, Guardiani C, Livi R. Analyzing pathogenic mutations of C5 domain from cardiac myosin binding protein C through MD simulations. *Eur Biophys J* 37: 683-691, 2008.
87. Centner T, Yano J, Kimura E, McElhinny AS, Pelin K, Witt CC, Bang ML, Trombitas K, Granzier H, Gregorio CC, Sorimachi H, Labeit S. Identification of muscle specific ring finger proteins as potential regulators of the titin kinase domain. *J Mol Biol* 306: 717-726, 2001.
88. Ceyhan-Birsoy O, Agrawal PB, Hidalgo C, Schmitz-Abe K, DeChene ET, Swanson LC, Soemedi R, Vasli N, Iannaccone ST, Shieh PB, Shur N, Dennison JM, Lawlor MW, Laporte J, Markianos K, Fairbrother WG, Granzier H, Beggs AH. Recessive truncating titin gene, TTN, mutations presenting as centronuclear myopathy. *Neurology* 81: 1205-1214, 2013.
89. Chan JY, Takeda M, Briggs LE, Graham ML, Lu JT, Horikoshi N, Weinberg EO, Aoki H, Sato N, Chien KR, Kasahara H. Identification of cardiac-specific myosin light chain kinase. *Circ Res* 102: 571-580, 2008.
90. Chang AN, Battiprolu PK, Cowley PM, Chen G, Gerard RD, Pinto JR, Hill JA, Baker AJ, Kamm KE, Stull JT. Constitutive phosphorylation of cardiac myosin regulatory light chain in vivo. *J Biol Chem* 290: 10703-10716, 2015.
91. Chang AN, Mahajan P, Knapp S, Barton H, Sweeney HL, Kamm KE, Stull JT. Cardiac myosin light chain is phosphorylated by Ca^{2+}/calmodulin-dependent and -independent kinase activities. *Proc Natl Acad Sci U S A* 113: E3824-E3833, 2016.
92. Charton K, Danièle N, Vihola A, Roudaut C, Gicquel E, Monjaret F, Tarrade A, Sarparanta J, Udd B, Richard I. Removal of the calpain 3 protease reverses the myopathology in a mouse model for titinopathies. *Hum Mol Genet* 19: 4608-4624, 2010.
93. Charton K, Sarparanta J, Vihola A, Milic A, Jonson PH, Suel L, Luque H, Boumela I, Richard I, Udd B. CAPN3-mediated processing of C-terminal titin replaced by pathological cleavage in titinopathy. *Hum Mol Genet* 24: 3718-3731, 2015.
94. Chauveau C, Bonnemann CG, Julien C, Kho AL, Marks H, Talim B, Maury P, Arne-Bes MC, Uro-Coste E, Alexandrovich A, Vihola A, Schafer S, Kaufmann B, Medne L, Hübner N, Foley AR, Santi M, Udd B, Topaloglu H, Moore SA, Gotthardt M, Samuels ME, Gautel M, Ferreiro A. Recessive TTN truncating mutations define novel forms of core myopathy with heart disease. *Hum Mol Genet* 23: 980-991, 2014.
95. Chauveau C, Rowell J, Ferreiro A. A rising titan: TTN review and mutation update. *Hum Mutat* 35: 1046-1059, 2014.
96. Chen D, Li S, Singh R, Spinette S, Sedlmeier R, Epstein HF. Dual function of the UNC-45b chaperone with myosin and GATA4 in cardiac development. *J Cell Sci* 125: 3893-3903, 2012.
97. Chen J, Kubalak SW, Minamisawa S, Price RL, Becker KD, Hickey R, Ross J, Jr., Chien KR. Selective requirement of myosin light chain 2v in embryonic heart function. *J Biol Chem* 273: 1252-1256, 1998.
98. Chen PP, Patel JR, Rybakova IN, Walker JW, Moss RL. Protein kinase A-induced myofilament desensitization to Ca(2+) as a result of phosphorylation of cardiac myosin-binding protein C. *J Gen Physiol* 136: 615-627, 2010.
99. Chen Z, Zhao TJ, Li J, Gao YS, Meng FG, Yan YB, Zhou HM. Slow skeletal muscle myosin-binding protein-C (MyBPC1) mediates recruitment of muscle-type creatine kinase (CK) to myosin. *Biochem J* 436: 437-445, 2011.
100. Cho M, Webster SG, Blau HM. Evidence for myoblast-extrinsic regulation of slow myosin heavy chain expression during muscle fiber formation in embryonic development. *J Cell Biol* 121: 795-810, 1993.
101. Cieniewski-Bernard C, Dupont E, Richard E, Bastide B. Phospho-GlcNAc modulation of slow MLC2 during soleus atrophy through a multienzymatic and sarcomeric complex. *Pflugers Arch* 466: 2139-2151, 2014.

102. Cieniewski-Bernard C, Montel V, Berthoin S, Bastide B. Increasing O-GlcNAcylation level on organ culture of soleus modulates the calcium activation parameters of muscle fibers. *PLoS One* 7: e48218, 2012.
103. Coisy-Quivy M, Sanguesa-Ferrer J, Weill M, Johnson DS, Donnay JM, Hipskind R, Fort P, Philips A. Identification of Rho GTPases implicated in terminal differentiation of muscle cells in ascidia. *Biol Cell* 98: 577-588, 2006.
104. Coisy-Quivy M, Touzet O, Bourret A, Hipskind RA, Mercier J, Fort P, Philips A. TC10 controls human myofibril organization and is activated by the sarcomeric RhoGEF obscurin. *J Cell Sci* 122: 947-956, 2009.
105. Colegrave M, Peckham M. Structural implications of beta-cardiac myosin heavy chain mutations in human disease. *Anat Rec (Hoboken)* 297: 1670-1680, 2014.
106. Colson BA, Bekyarova T, Locher MR, Fitzsimons DP, Irving TC, Moss RL. Protein kinase A-mediated phosphorylation of cMyBP-C increases proximity of myosin heads to actin in resting myocardium. *Circ Res* 103: 244-251, 2008.
107. Condon K, Silberstein L, Blau HM, Thompson WJ. Development of muscle fiber types in the prenatal rat hindlimb. *Dev Biol* 138: 256-274, 1990.
108. Conibear PB, Bagshaw CR, Fajer PG, Kovacs M, Malnasi-Csizmadia A. Myosin cleft movement and its coupling to actomyosin dissociation. *Nat Struct Biol* 10: 831-835, 2003.
109. Conti A, Riva N, Pesca M, Iannaccone S, Cannistraci CV, Corbo M, Previtali SC, Quattrini A, Alessio M. Increased expression of myosin binding protein H in the skeletal muscle of amyotrophic lateral sclerosis patients. *Biochim Biophys Acta* 1842: 99-106, 2014.
110. Cooke R. The role of the myosin ATPase activity in adaptive thermogenesis by skeletal muscle. *Biophys Rev* 3: 33-45, 2011.
111. Copeland O, Sadayappan S, Messer AE, Steinen GJ, van der Velden J, Marston SB. Analysis of cardiac myosin binding protein-C phosphorylation in human heart muscle. *J Mol Cell Cardiol* 49: 1003-1011, 2010.
112. Cornachione AS, Leite FS, Wang J, Leu NA, Kalganov A, Volgin D, Han X, Xu T, Cheng YS, Yates JR, III, Rassier DE, Kashina A. Arginylation of myosin heavy chain regulates skeletal muscle strength. *Cell Rep* 8: 470-476, 2014.
113. Craig R, Lee KH, Mun JY, Torre I, Luther PK. Structure, sarcomeric organization, and thin filament binding of cardiac myosin-binding protein-C. *Pflugers Arch* 466: 425-431, 2014.
114. Craig R, Offer G. The location of C-protein in rabbit skeletal muscle. *Proc R Soc Lond B Biol Sci* 192: 451-461, 1976.
115. Cuello F, Bardswell SC, Haworth RS, Ehler E, Sadayappan S, Kentish JC, Avkiran M. Novel role for p90 ribosomal S6 kinase in the regulation of cardiac myofilament phosphorylation. *J Biol Chem* 286: 5300-5310, 2011.
116. Cunha SR, Le Scouarnec S, Schott JJ, Mohler PJ. Exon organization and novel alternative splicing of the human ANK2 gene: Implications for cardiac function and human cardiac disease. *J Mol Cell Cardiol* 45: 724-734, 2008.
117. Cunha SR, Mohler PJ. Obscurin targets ankyrin-B and protein phosphatase 2A to the cardiac M-line. *J Biol Chem* 283: 31968-31980, 2008.
118. Dantzig JA, Goldman YE, Millar NC, Lacktis J, Homsher E. Reversal of the cross-bridge force-generating transition by photogeneration of phosphate in rabbit psoas muscle fibres. *J Physiol* 451: 247-278, 1992.
119. Davis JS. Interaction of C-protein with pH 8.0 synthetic thick filaments prepared from the myosin of vertebrate skeletal muscle. *J Muscle Res Cell Motil* 9: 174-183, 1988.
120. De Cid R, Ben Yaou R, Roudaut C, Charton K, Baulande S, Leturcq F, Romero NB, Malfatti E, Beuvin M, Vihola A, Criqui A, Nelson I, Nectoux J, Ben Aim L, Caloustian C, Olaso R, Udd B, Bonne G, Eymard B, Richard I. A new titinopathy: Childhood-juvenile onset Emery-Dreifuss-like phenotype without cardiomyopathy. *Neurology* 85: 2126-2135, 2015.
121. de Seze J, Udd B, Vermersch P. Tibial muscular dystrophy. A rare form of distal myopathy. *Rev Neurol (Paris)* 155: 296-305, 1999.
122. de Tombe PP. Myosin binding protein C in the heart. *Circ Res* 98: 1234-1236, 2006.
123. Dechesne CA, Leger JO, Leger JJ. Distribution of alpha- and beta-myosin heavy chains in the ventricular fibers of the postnatal developing rat. *Dev Biol* 123: 169-178, 1987.
124. Decker RS, Decker ML, Kulikovskaya I, Nakamura S, Lee DC, Harris K, Klocke FJ, Winegrad S. Myosin-binding protein C phosphorylation, myofibril structure, and contractile function during low-flow ischemia. *Circulation* 111: 906-912, 2005.
125. Dhandapany PS, Sadayappan S, Xue Y, Powell GT, Rani DS, Nallari P, Rai TS, Khullar M, Soares P, Bahl A, Tharkan JM, Vaideeswar P, Rathinavel A, Narasimhan C, Ayapati DR, Ayub Q, Mehdi SQ, Oppenheimer S, Richards MB, Price AL, Patterson N, Reich D, Singh L, Tyler-Smith C, Thangaraj K. A common MYBPC3 (cardiac myosin binding protein C) variant associated with cardiomyopathies in South Asia. *Nat Genet* 41: 187-191, 2009.
126. Ding P, Huang J, Battiprolu PK, Hill JA, Kamm KE, Stull JT. Cardiac myosin light chain kinase is necessary for myosin regulatory light chain phosphorylation and cardiac performance in vivo. *J Biol Chem* 285: 40819-40829, 2010.
127. Dixon DM, Choi J, El-Ghazali A, Park SY, Roos KP, Jordan MC, Fishbein MC, Comai L, Reddy S. Loss of muscleblind-like 1 results in cardiac pathology and persistence of embryonic splice isoforms. *Sci Rep* 5: 9042, 2015.
128. Dow MR, Mains PE. Genetic and molecular characterization of the caenorhabditis elegans gene, mel-26, a postmeiotic negative regulator of mei-1, a meiotic-specific spindle component. *Genetics* 150: 119-128, 1998.
129. Du A, Sanger JM, Sanger JW. Cardiac myofibrillogenesis inside intact embryonic hearts. *Dev Biol* 318: 236-246, 2008.
130. Edström L, Thornell LE, Albo J, Landin S, Samuelsson M. Myopathy with respiratory failure and typical myofibrillar lesions. *J Neurol Sci* 96: 211-228, 1990.
131. Ehler E, Gautel M. The sarcomere and sarcomerogenesis. *Adv Exp Med Biol* 642: 1-14, 2008.
132. Ehler E, Rothen BM, Hämmerle SP, Komiyama M, Perriard JC. Myofibrillogenesis in the developing chicken heart: Assembly of Z-disk, M-line and the thick filaments. *J Cell Sci* 112 (Pt 10): 1529-1539, 1999.
133. Ehlermann P, Weichenhan D, Zehelein J, Steen H, Pribe R, Zeller R, Lehrke S, Zugck C, Ivandic BT, Katus HA. Adverse events in families with hypertrophic or dilated cardiomyopathy and mutations in the MYBPC3 gene. *BMC Med Genet* 9: 95, 2008.
134. Einheber S, Fischman DA. Isolation and characterization of a cDNA clone encoding avian skeletal muscle C-protein: An intracellular member of the immunoglobulin superfamily. *Proc Natl Acad Sci U S A* 87: 2157-2161, 1990.
135. Ekabe CJ, Kehbila J, Sama CB, Kadia BM, Abanda MH, Monekosso GL. Occurrence of Emery-Dreifuss muscular dystrophy in a rural setting of Cameroon: A case report and review of the literature. *BMC Res Notes* 10: 36, 2017.
136. Ekhilevitch N, Kurolap A, Oz-Levi D, Mory A, Hershkovitz T, Ast G, Mandel H, Baris HN. Expanding the MYBPC1 phenotypic spectrum: A novel homozygous mutation causes arthrogryposis multiplex congenita. *Clin Genet* 90: 84-89, 2016.
137. Engelhardt WA, Ljubimowa, MN. Myosine and adenosinetriphosphatase. *Nature* 144: 668-669, 1939.
138. England J, Loughna S. Heavy and light roles: Myosin in the morphogenesis of the heart. *Cell Mol Life Sci* 70: 1221-1239, 2013.
139. Eppenberger HM, Perriard JC, Rosenberg UB, Strehler EE. The Mr 165,000 M-protein myomesin: A specific protein of cross-striated muscle cells. *J Cell Biol* 89: 185-193, 1981.
140. Evilä A, Vihola A, Sarparanta J, Raheem O, Palmio J, Sandell S, Eymard B, Illa I, Rojas-Garcia R, Hankiewicz K, Negrão L, Löppönen T, Nokelainen P, Kärppä M, Penttilä S, Screen M, Suominen T, Richard I, Hackman P, Udd B. Atypical phenotypes in titinopathies explained by second titin mutations. *Ann Neurol* 75: 230-240, 2014.
141. Fernando P, Sandoz JS, Ding W, de Repentigny Y, Brunette S, Kelly JF, Kothary R, Megeney LA. Bin1 SRC homology 3 domain acts as a scaffold for myofiber sarcomere assembly. *J Biol Chem* 284: 27674-27686, 2009.
142. Ferrari R, Ceconi C, Curello S, Guarnieri C, Caldarera CM, Albertini A, Visioli O. Oxygen-mediated myocardial damage during ischaemia and reperfusion: Role of the cellular defences against oxygen toxicity. *J Mol Cell Cardiol* 17: 937-945, 1985.
143. Fert-Bober J, Sokolove J. Proteomics of citrullination in cardiovascular disease. *Proteomics Clin Appl* 8: 522-533, 2014.
144. Fewell JG, Hewett TE, Sanbe A, Klevitsky R, Hayes E, Warshaw D, Maughan D, Robbins J. Functional significance of cardiac myosin essential light chain isoform switching in transgenic mice. *J Clin Invest* 101: 2630-2639, 1998.
145. Fielitz J, Kim MS, Shelton JM, Latif S, Spencer JA, Glass DJ, Richardson JA, Bassel-Duby R, Olson EN. Myosin accumulation and striated muscle myopathy result from the loss of muscle RING finger 1 and 3. *J Clin Invest* 117: 2486-2495, 2007.
146. Fielitz J, van Rooij E, Spencer JA, Shelton JM, Latif S, van der Nagel R, Bezprozvannaya S, de Windt L, Richardson JA, Bassel-Duby R, Olson EN. Loss of muscle-specific RING-finger 3 predisposes the heart to cardiac rupture after myocardial infarction. *Proc Natl Acad Sci U S A* 104: 4377-4382, 2007.
147. Finley NL, Cuperman TI. Cardiac myosin binding protein-C: A structurally dynamic regulator of myocardial contractility. *Pflugers Arch* 466: 433-438, 2014.
148. Fischer S, Windshugel B, Horak D, Holmes KC, Smith JC. Structural mechanism of the recovery stroke in the myosin molecular motor. *Proc Natl Acad Sci U S A* 102: 6873-6878, 2005.
149. Fisher SJ, Helliwell JR, Khurshid S, Govada L, Redwood C, Squire JM, Chayen NE. An investigation into the protonation states of the C1

domain of cardiac myosin-binding protein C. *Acta Crystallogr D Biol Crystallogr* 64: 658-664, 2008.
150. Fitzsimons DP, Patel JR, Moss RL. Aging-dependent depression in the kinetics of force development in rat skinned myocardium. *Am J Physiol* 276: H1511-H1519, 1999.
151. Flashman E, Korkie L, Watkins H, Redwood C, Moolman-Smook JC. Support for a trimeric collar of myosin binding protein C in cardiac and fast skeletal muscle, but not in slow skeletal muscle. *FEBS Lett* 582: 434-438, 2008.
152. Flashman E, Redwood C, Moolman-Smook J, Watkins H. Cardiac myosin binding protein C: Its role in physiology and disease. *Circ Res* 94: 1279-1289, 2004.
153. Flashman E, Watkins H, Redwood C. Localization of the binding site of the C-terminal domain of cardiac myosin-binding protein-C on the myosin rod. *Biochem J* 401: 97-102, 2007.
154. Flix B, de la Torre C, Castillo J, Casal C, Illa I, Gallardo E. Dysferlin interacts with calsequestrin-1, myomesin-2 and dynein in human skeletal muscle. *Int J Biochem Cell Biol* 45: 1927-1938, 2013.
155. Ford-Speelman DL, Roche JA, Bowman AL, Bloch RJ. The rho-guanine nucleotide exchange factor domain of obscurin activates rhoA signaling in skeletal muscle. *Mol Biol Cell* 20: 3905-3917, 2009.
156. Fougerousse F, Delezoide AL, Fiszman MY, Schwartz K, Beckmann JS, Carrier L. Cardiac myosin binding protein C gene is specifically expressed in heart during murine and human development. *Circ Res* 82: 130-133, 1998.
157. Franaszczyk M, Chmielewski P, Truszkowska G, Stawinski P, Michalak E, Rydzanicz M, Sobieszczanska-Malek M, Pollak A, Szczygieł J, Kosinska J, Parulski A, Stoklosa T, Tarnowska A, Machnicki MM, Foss-Nieradko B, Szperl M, Sioma A, Kusmierczyk M, Grzybowski J, Zielinski T, Ploski R, Bilinska ZT. Titin truncating variants in dilated cardiomyopathy—Prevalence and genotype-phenotype correlations. *PLoS One* 12: e0169007, 2017.
158. Franco D, Markman MM, Wagenaar GT, Ya J, Lamers WH, Moorman AF. Myosin light chain 2a and 2v identifies the embryonic outflow tract myocardium in the developing rodent heart. *Anat Rec* 254: 135-146, 1999.
159. Frank G, Weeds AG. The amino-acid sequence of the alkali light chains of rabbit skeletal-muscle myosin. *Eur J Biochem* 44: 317-334, 1974.
160. Freiburg A, Gautel M. A molecular map of the interactions between titin and myosin-binding protein C. Implications for sarcomeric assembly in familial hypertrophic cardiomyopathy. *Eur J Biochem* 235: 317-323, 1996.
161. Fujioka M, Takahashi N, Odai H, Araki S, Ichikawa K, Feng J, Nakamura M, Kaibuchi K, Hartshorne DJ, Nakano T, Ito M. A new isoform of human myosin phosphatase targeting/regulatory subunit (MYPT2): cDNA cloning, tissue expression, and chromosomal mapping. *Genomics* 49: 59-68, 1998.
162. Fukuzawa A, Idowu S, Gautel M. Complete human gene structure of obscurin: Implications for isoform generation by differential splicing. *J Muscle Res Cell Motil* 26: 427-434, 2005.
163. Fukuzawa A, Lange S, Holt M, Vihola A, Carmignac V, Ferreiro A, Udd B, Gautel M. Interactions with titin and myomesin target obscurin and obscurin-like 1 to the M-band: Implications for hereditary myopathies. *J Cell Sci* 121: 1841-1851, 2008.
164. Fürst DO, Osborn M, Nave R, Weber K. The organization of titin filaments in the half-sarcomere revealed by monoclonal antibodies in immunoelectron microscopy: A map of ten nonrepetitive epitopes starting at the Z line extends close to the M line. *J Cell Biol* 106: 1563-1572, 1988.
165. Furst DO, Vinkemeier U, Weber K. Mammalian skeletal muscle C-protein: Purification from bovine muscle, binding to titin and the characterization of a full-length human cDNA. *J Cell Sci* 102 (Pt 4): 769-778, 1992.
166. Fusi L, Huang Z, Irving M. The Conformation of myosin heads in relaxed skeletal muscle: Implications for myosin-based regulation. *Biophys J* 109: 783-792, 2015.
167. Fusi L, Percario V, Brunello E, Caremani M, Bianco P, Powers JD, Reconditi M, Lombardi V, Piazzesi G. Minimum number of myosin motors accounting for shortening velocity under zero load in skeletal muscle. *J Physiol* 595: 1127-1142, 2017.
168. Gautel M. The super-repeats of titin/connectin and their interactions: Glimpses at sarcomeric assembly. *Adv Biophys* 33: 27-37, 1996.
169. Gautel M. Cytoskeletal protein kinases: Titin and its relations in mechanosensing. *Pflugers Arch* 462: 119-134, 2011.
170. Gautel M. The sarcomeric cytoskeleton: Who picks up the strain? *Curr Opin Cell Biol* 23: 39-46, 2011.
171. Gautel M, Djinovic-Carugo K. The sarcomeric cytoskeleton: From molecules to motion. *J Exp Biol* 219: 135-145, 2016.
172. Gautel M, Furst DO, Cocco A, Schiaffino S. Isoform transitions of the myosin binding protein C family in developing human and mouse muscles: Lack of isoform transcomplementation in cardiac muscle. *Circ Res* 82: 124-129, 1998.
173. Gautel M, Leonard K, Labeit S. Phosphorylation of KSP motifs in the C-terminal region of titin in differentiating myoblasts. *EMBO J* 12: 3827-3834, 1993.
174. Gautel M, Zuffardi O, Freiburg A, Labeit S. Phosphorylation switches specific for the cardiac isoform of myosin binding protein-C: A modulator of cardiac contraction? *EMBO J* 14: 1952-1960, 1995.
175. Ge Y, Rybakova IN, Xu Q, Moss RL. Top-down high-resolution mass spectrometry of cardiac myosin binding protein C revealed that truncation alters protein phosphorylation state. *Proc Natl Acad Sci U S A* 106: 12658-12663, 2009.
176. Geeves MA, Holmes KC. Structural mechanism of muscle contraction. *Annu Rev Biochem* 68: 687-728, 1999.
177. Geisler SB, Robinson D, Hauringa M, Raeker MO, Borisov AB, Westfall MV, Russell MW. Obscurin-like 1, OBSL1, is a novel cytoskeletal protein related to obscurin. *Genomics* 89: 521-531, 2007.
178. Gerull B. The rapidly evolving role of titin in cardiac physiology and cardiomyopathy. *Can J Cardiol* 31: 1351-1359, 2015.
179. Gerull B, Atherton J, Geupel A, Sasse-Klaassen S, Heuser A, Frenneaux M, McNabb M, Granzier H, Labeit S, Thierfelder L. Identification of a novel frameshift mutation in the giant muscle filament titin in a large Australian family with dilated cardiomyopathy. *J Mol Med (Berl)* 84: 478-483, 2006.
180. Gerull B, Gramlich M, Atherton J, McNabb M, Trombitas K, Sasse-Klaassen S, Seidman JG, Seidman C, Granzier H, Labeit S, Frenneaux M, Thierfelder L. Mutations of TTN, encoding the giant muscle filament titin, cause familial dilated cardiomyopathy. *Nat Genet* 30: 201-204, 2002.
181. Giacomello E, Sorrentino V. Localization of ank1.5 in the sarcoplasmic reticulum precedes that of SERCA and RyR: Relationship with the organization of obscurin in developing sarcomeres. *Histochem Cell Biol* 131: 371-382, 2009.
182. Gigli M, Begay RL, Morea G, Graw SL, Sinagra G, Taylor MR, Granzier H, Mestroni L. A review of the giant protein titin in clinical molecular diagnostics of cardiomyopathies. *Front Cardiovasc Med* 3: 21, 2016.
183. Gilbert R, Cohen JA, Pardo S, Basu A, Fischman DA. Identification of the A-band localization domain of myosin binding proteins C and H (MyBP-C, MyBP-H) in skeletal muscle. *J Cell Sci* 112 (Pt 1): 69-79, 1999.
184. Goel HL, Dey CS. Insulin-mediated tyrosine phosphorylation of myosin heavy chain and concomitant enhanced association of C-terminal SRC kinase during skeletal muscle differentiation. *Cell Biol Int* 26: 557-561, 2002.
185. Golenhofen N, Perng MD, Quinlan RA, Drenckhahn D. Comparison of the small heat shock proteins alphaB-crystallin, MKBP, HSP25, HSP20, and cvHSP in heart and skeletal muscle. *Histochem Cell Biol* 122: 415-425, 2004.
186. Gollapudi SK, Gallon CE, Chandra M. The tropomyosin binding region of cardiac troponin T modulates crossbridge recruitment dynamics in rat cardiac muscle fibers. *J Mol Biol* 425: 1565-1581, 2013.
187. Gollapudi SK, Mamidi R, Mallampalli SL, Chandra M. The N-terminal extension of cardiac troponin T stabilizes the blocked state of cardiac thin filament. *Biophys J* 103: 940-948, 2012.
188. Gordon AM, Homsher E, Regnier M. Regulation of contraction in striated muscle. *Physiol Rev* 80: 853-924, 2000.
189. Govindan S, McElligott A, Muthusamy S, Nair N, Barefield D, Martin JL, Gongora E, Greis KD, Luther PK, Winegrad S, Henderson KK, Sadayappan S. Cardiac myosin binding protein-C is a potential diagnostic biomarker for myocardial infarction. *J Mol Cell Cardiol* 52: 154-164, 2012.
190. Gramlich M, Pane LS, Zhou Q, Chen Z, Murgia M, Schotterl S, Goedel A, Metzger K, Brade T, Parrotta E, Schaller M, Gerull B, Thierfelder L, Aartsma-Rus A, Labeit S, Atherton JJ, McGaughran J, Harvey RP, Sinnecker D, Mann M, Laugwitz KL, Gawaz MP, Moretti A. Antisense-mediated exon skipping: A therapeutic strategy for titin-based dilated cardiomyopathy. *EMBO Mol Med* 7: 562-576, 2015.
191. Granzier H, Labeit S. Cardiac titin: An adjustable multi-functional spring. *J Physiol* 541: 335-342, 2002.
192. Granzier HL, Labeit S. The giant protein titin: A major player in myocardial mechanics, signaling, and disease. *Circ Res* 94: 284-295, 2004.
193. Granzier HL, Labeit S. The giant muscle protein titin is an adjustable molecular spring. *Exerc Sport Sci Rev* 34: 50-53, 2006.
194. Grassie ME, Moffat LD, Walsh MP, MacDonald JA. The myosin phosphatase targeting protein (MYPT) family: A regulated mechanism for achieving substrate specificity of the catalytic subunit of protein phosphatase type 1delta. *Arch Biochem Biophys* 510: 147-159, 2011.
195. Grater F, Shen J, Jiang H, Gautel M, Grubmuller H. Mechanically induced titin kinase activation studied by force-probe molecular dynamics simulations. *Biophys J* 88: 790-804, 2005.
196. Gregorich ZR, Peng Y, Cai W, Jin Y, Wei L, Chen AJ, McKiernan SH, Aiken JM, Moss RL, Diffee GM, Ge Y. Top-down targeted proteomics reveals decrease in myosin regulatory light-chain phosphorylation that

contributes to sarcopenic muscle dysfunction. *J Proteome Res* 15: 2706-2716, 2016.
197. Gregorio CC, Granzier H, Sorimachi H, Labeit S. Muscle assembly: A titanic achievement? *Curr Opin Cell Biol* 11: 18-25, 1999.
198. Gregorio CC, Perry CN, McElhinny AS. Functional properties of the titin/connectin-associated proteins, the muscle-specific RING finger proteins (MURFs), in striated muscle. *J Muscle Res Cell Motil* 26: 389-400, 2005.
199. Gresham KS, Stelzer JE. The contributions of cardiac myosin binding protein C and troponin I phosphorylation to beta-adrenergic enhancement of in vivo cardiac function. *J Physiol* 594: 669-686, 2016.
200. Grimm M, Haas P, Willipinski-Stapelfeldt B, Zimmermann WH, Rau T, Pantel K, Weyand M, Eschenhagen T. Key role of myosin light chain (MLC) kinase-mediated MLC2a phosphorylation in the alpha 1-adrenergic positive inotropic effect in human atrium. *Cardiovasc Res* 65: 211-220, 2005.
201. Grimm M, Mahnecke N, Soja F, El-Armouche A, Haas P, Treede H, Reichenspurner H, Eschenhagen T. The MLCK-mediated alpha1-adrenergic inotropic effect in atrial myocardium is negatively modulated by PKCepsilon signaling. *Br J Pharmacol* 148: 991-1000, 2006.
202. Grose JH, Langston K, Wang X, Squires S, Mustafi SB, Hayes W, Neubert J, Fischer SK, Fasano M, Saunders GM, Dai Q, Christians E, Lewandowski ED, Ping P, Benjamin IJ. Characterization of the cardiac overexpression of HSPB2 reveals mitochondrial and myogenic roles supported by a cardiac HspB2 interactome. *PLoS One* 10: e0133994, 2015.
203. Grove BK, Cerny L, Perriard JC, Eppenberger HM. Myomesin and M-protein: Expression of two M-band proteins in pectoral muscle and heart during development. *J Cell Biol* 101: 1413-1421, 1985.
204. Grove BK, Cerny L, Perriard JC, Eppenberger HM, Thornell LE. Fiber type-specific distribution of M-band proteins in chicken muscle. *J Histochem Cytochem* 37: 447-454, 1989.
205. Grove BK, Holmbom B, Thornell LE. Myomesin and M protein: Differential expression in embryonic fibers during pectoral muscle development. *Differentiation* 34: 106-114, 1987.
206. Grove BK, Kurer V, Lehner C, Doetschman TC, Perriard JC, Eppenberger HM. A new 185,000-dalton skeletal muscle protein detected by monoclonal antibodies. *J Cell Biol* 98: 518-524, 1984.
207. Gruen M, Gautel M. Mutations in beta-myosin S2 that cause familial hypertrophic cardiomyopathy (FHC) abolish the interaction with the regulatory domain of myosin-binding protein-C. *J Mol Biol* 286: 933-949, 1999.
208. Gruen M, Prinz H, Gautel M. cAPK-phosphorylation controls the interaction of the regulatory domain of cardiac myosin binding protein C with myosin-S2 in an on-off fashion. *FEBS Lett* 453: 254-259, 1999.
209. Guan K, Rohwedel J, Wobus AM. Embryonic stem cell differentiation models: Cardiogenesis, myogenesis, neurogenesis, epithelial and vascular smooth muscle cell differentiation in vitro. *Cytotechnology* 30: 211-226, 1999.
210. Gudbjartsson DF, Helgason H, Gudjonsson SA, Zink F, Oddson A, Gylfason A, Besenbacher S, Magnusson G, Halldorsson BV, Hjartarson E, Sigurdsson GT, Stacey SN, Frigge ML, Holm H, Saemundsdottir J, Helgadottir HT, Johannsdottir H, Sigfusson G, Thorgeirsson G, Sverrisson JT, Gretarsdottir S, Walters GB, Rafnar T, Thjodleifsson B, Bjornsson ES, Olafsson S, Thorarinsdottir H, Steingrimsdottir T, Gudmundsdottir TS, Theodors A, Jonasson JG, Sigurdsson A, Bjornsdottir G, Jonsson JJ, Thorarensen O, Ludvigsson P, Gudbjartsson H, Eyjolfsson GI, Sigurdardottir O, Olafsson I, Arnar DO, Magnusson OT, Kong A, Masson G, Thorsteinsdottir U, Helgason A, Sulem P, Stefansson K. Large-scale whole-genome sequencing of the Icelandic population. *Nat Genet* 47: 435-444, 2015.
211. Guellich A, Negroni E, Decostre V, Demoule A, Coirault C. Altered cross-bridge properties in skeletal muscle dystrophies. *Front Physiol* 5: 393, 2014.
212. Guhathakurta P, Prochniewicz E, Thomas DD. Amplitude of the actomyosin power stroke depends strongly on the isoform of the myosin essential light chain. *Proc Natl Acad Sci U S A* 112: 4660-4665, 2015.
213. Gupta MK, Robbins J. Post-translational control of cardiac hemodynamics through myosin binding protein C. *Pflugers Arch* 466: 231-236, 2014.
214. Gurnett CA, Desruisseau DM, McCall K, Choi R, Meyer ZI, Talerico M, Miller SE, Ju JS, Pestronk A, Connolly AM, Druley TE, Weihl CC, Dobbs MB. Myosin binding protein C1: A novel gene for autosomal dominant distal arthrogryposis type 1. *Hum Mol Genet* 19: 1165-1173, 2010.
215. Hackman P, Marchand S, Sarparanta J, Vihola A, Pénisson-Besnier I, Eymard B, Pardal-Fernández JM, Hammoudae-H, Richard I, Illa I, Udd B. Truncating mutations in C-terminal titin may cause more severe tibial muscular dystrophy (TMD). *Neuromuscul Disord* 18: 922-928, 2008.
216. Hackman P, Vihola A, Haravuori H, Marchand S, Sarparanta J, De Seze J, Labeit S, Witt C, Peltonen L, Richard I, Udd B. Tibial muscular dystrophy is a titinopathy caused by mutations in TTN, the gene encoding the giant skeletal-muscle protein titin. *Am J Hum Genet* 71: 492-500, 2002.
217. Hall JG. Genetic aspects of arthrogryposis. *Clin Orthop Relat Res*: 44-53, 1985.
218. Han YS, Geiger PC, Cody MJ, Macken RL, Sieck GC. ATP consumption rate per cross bridge depends on myosin heavy chain isoform. *J Appl Physiol (1985)* 94: 2188-2196, 2003.
219. Han Z, Hendrickson EA, Bremner TA, Wyche JH. A sequential two-step mechanism for the production of the mature p17:p12 form of caspase-3 in vitro. *J Biol Chem* 272: 13432-13436, 1997.
220. Haravuori H, Vihola A, Straub V, Auranen M, Richard I, Marchand S, Voit T, Labeit S, Somer H, Peltonen L, Beckmann JS, Udd B. Secondary calpain3 deficiency in 2q-linked muscular dystrophy: Titin is the candidate gene. *Neurology* 56: 869-877, 2001.
221. Harley HG, Brook JD, Rundle SA, Crow S, Reardon W, Buckler AJ, Harper PS, Housman DE, Shaw DJ. Expansion of an unstable DNA region and phenotypic variation in myotonic dystrophy. *Nature* 355: 545-546, 1992.
222. Harris SP, Bartley CR, Hacker TA, McDonald KS, Douglas PS, Greaser ML, Powers PA, Moss RL. Hypertrophic cardiomyopathy in cardiac myosin binding protein-C knockout mice. *Circ Res* 90: 594-601, 2002.
223. Harris SP, Lyons RG, Bezold KL. In the thick of it: HCM-causing mutations in myosin binding proteins of the thick filament. *Circ Res* 108: 751-764, 2011.
224. Hartzell HC. Effects of phosphorylated and unphosphorylated C-protein on cardiac actomyosin ATPase. *J Mol Biol* 186: 185-195, 1985.
225. Hayashibara T, Miyanishi T. Binding of the amino-terminal region of myosin alkali 1 light chain to actin and its effect on actin-myosin interaction. *Biochemistry* 33: 12821-12827, 1994.
226. He ZH, Bottinelli R, Pellegrino MA, Ferenczi MA, Reggiani C. ATP consumption and efficiency of human single muscle fibers with different myosin isoform composition. *Biophys J* 79: 945-961, 2000.
227. Hedberg C, Melberg A, Dahlbom K, Oldfors A. Hereditary myopathy with early respiratory failure is caused by mutations in the titin FN3 119 domain. *Brain* 137: e270, 2014.
228. Hedberg C, Toledo AG, Gustafsson CM, Larson G, Oldfors A, Macao B. Hereditary myopathy with early respiratory failure is associated with misfolding of the titin fibronectin III 119 subdomain. *Neuromuscul Disord* 24: 373-379, 2014.
229. Hedou J, Bastide B, Page A, Michalski JC, Morelle W. Mapping of O-linked beta-N-acetylglucosamine modification sites in key contractile proteins of rat skeletal muscle. *Proteomics* 9: 2139-2148, 2009.
230. Hedou J, Cieniewski-Bernard C, Leroy Y, Michalski JC, Mounier Y, Bastide B. O-linked N-acetylglucosaminylation is involved in the Ca^{2+} activation properties of rat skeletal muscle. *J Biol Chem* 282: 10360-10369, 2007.
231. Heissler SM, Sellers JR. Myosin light chains: Teaching old dogs new tricks. *Bioarchitecture* 4: 169-188, 2014.
232. Heissler SM, Sellers JR. Various themes of myosin regulation. *J Mol Biol* 428: 1927-1946, 2016.
233. Herman DS, Lam L, Taylor MR, Wang L, Teekakirikul P, Christodoulou D, Conner L, DePalma SR, McDonough B, Sparks E, Teodorescu DL, Cirino AL, Banner NR, Pennell DJ, Graw S, Merlo M, Di Lenarda A, Sinagra G, Bos JM, Ackerman MJ, Mitchell RN, Murry CE, Lakdawala NK, Ho CY, Barton PJ, Cook SA, Mestroni L, Seidman JG, Seidman CE. Truncations of titin causing dilated cardiomyopathy. *N Engl J Med* 366: 619-628, 2012.
234. Herring BP, England PJ. The turnover of phosphate bound to myosin light chain-2 in perfused rat heart. *Biochem J* 240: 205-214, 1986.
235. Hidalgo C, Granzier H. Tuning the molecular giant titin through phosphorylation: Role in health and disease. *Trends Cardiovasc Med* 23: 165-171, 2013.
236. Hisatome I, Morisaki T, Kamma H, Sugama T, Morisaki H, Ohtahara A, Holmes EW. Control of AMP deaminase 1 binding to myosin heavy chain. *Am J Physiol* 275: C870-C881, 1998.
237. Hofmann PA, Greaser ML, Moss RL. C-protein limits shortening velocity of rabbit skeletal muscle fibres at low levels of Ca^{2+} activation. *J Physiol* 439: 701-715, 1991.
238. Hojlund K, Bowen BP, Hwang H, Flynn CR, Madireddy L, Geetha T, Langlais P, Meyer C, Mandarino LJ, Yi Z. In vivo phosphoproteome of human skeletal muscle revealed by phosphopeptide enrichment and HPLC-ESI-MS/MS. *J Proteome Res* 8: 4954-4965, 2009.
239. Holmes KC, Angert I, Kull FJ, Jahn W, Schroder RR. Electron cryomicroscopy shows how strong binding of myosin to actin releases nucleotide. *Nature* 425: 423-427, 2003.
240. Homburger JR, Green EM, Caleshu C, Sunitha MS, Taylor RE, Ruppel KM, Metpally RP, Colan SD, Michels M, Day SM, Olivotto I, Bustamante CD, Dewey FE, Ho CY, Spudich JA, Ashley EA. Multidimensional structure-function relationships in human beta-cardiac myosin from population-scale genetic variation. *Proc Natl Acad Sci U S A* 113: 6701-6706, 2016.

241. Hooijman P, Stewart MA, Cooke R. A new state of cardiac myosin with very slow ATP turnover: A potential cardioprotective mechanism in the heart. *Biophys J* 100: 1969-1976, 2011.
242. Hornemann T, Kempa S, Himmel M, Hayess K, Furst DO, Wallimann T. Muscle-type creatine kinase interacts with central domains of the M-band proteins myomesin and M-protein. *J Mol Biol* 332: 877-887, 2003.
243. Hornemann T, Stolz M, Wallimann T. Isoenzyme-specific interaction of muscle-type creatine kinase with the sarcomeric M-line is mediated by NH(2)-terminal lysine charge-clamps. *J Cell Biol* 149: 1225-1234, 2000.
244. Hoskins AC, Jacques A, Bardswell SC, McKenna WJ, Tsang V, dos Remedios CG, Ehler E, Adams K, Jalilzadeh S, Avkiran M, Watkins H, Redwood C, Marston SB, Kentish JC. Normal passive viscoelasticity but abnormal myofibrillar force generation in human hypertrophic cardiomyopathy. *J Mol Cell Cardiol* 49: 737-745, 2010.
245. Houdusse A, Sweeney HL. How myosin generates force on actin filaments. *Trends Biochem Sci* 41: 989-997, 2016.
246. Houmeida A, Holt J, Tskhovrebova L, Trinick J. Studies of the interaction between titin and myosin. *J Cell Biol* 131: 1471-1481, 1995.
247. Hu LY, Ackermann MA, Kontrogianni-Konstantopoulos A. The sarcomeric M-region: A molecular command center for diverse cellular processes. *Biomed Res Int* 2015: 714197, 2015.
248. Hu LY, Kontrogianni-Konstantopoulos A. The kinase domains of obscurin interact with intercellular adhesion proteins. *FASEB J* 27: 2001-2012, 2013.
249. Hu LYR, Ackermann MA, Hecker PA, Prosser BL, King B, O' Connell KA, Grogan A, Meyer LC, Berndsen CE, Wright NT, Lederer WJ, Kontrogianni-Konstantopoulos A. Deregulated Ca^{2+} cycling underlies the development of arrhythmia and heart disease due to mutant obscurin. *Sci Adv* 3: e1603081, 2017.
250. Hu Z, Yang B, Lu W, Zhou W, Zeng L, Li T, Wang X. HSPB2/MKBP, a novel and unique member of the small heat-shock protein family. *J Neurosci Res* 86: 2125-2133, 2008.
251. Huang C, Sheikh F, Hollander M, Cai C, Becker D, Chu PH, Evans S, Chen J. Embryonic atrial function is essential for mouse embryogenesis, cardiac morphogenesis and angiogenesis. *Development* 130: 6111-6119, 2003.
252. Huang SC, Zhou A, Nguyen DT, Zhang HS, Benz EJ, Jr. Protein 4.1R influences myogenin protein stability and skeletal muscle differentiation. *J Biol Chem* 291: 25591-25607, 2016.
253. Huang W, Szczesna-Cordary D. Molecular mechanisms of cardiomyopathy phenotypes associated with myosin light chain mutations. *J Muscle Res Cell Motil* 36: 433-445, 2015.
254. Hughes SM, Cho M, Karsch-Mizrachi I, Travis M, Silberstein L, Leinwand LA, Blau HM. Three slow myosin heavy chains sequentially expressed in developing mammalian skeletal muscle. *Dev Biol* 158: 183-199, 1993.
255. Huxley AF, Niedergerke R. Structural changes in muscle during contraction; interference microscopy of living muscle fibres. *Nature* 173: 971-973, 1954.
256. Huxley H, Hanson J. Changes in the cross-striations of muscle during contraction and stretch and their structural interpretation. *Nature* 173: 973-976, 1954.
257. Huxley HE, Brown W. The low-angle x-ray diagram of vertebrate striated muscle and its behaviour during contraction and rigor. *J Mol Biol* 30: 383-434, 1967.
258. Idowu SM, Gautel M, Perkins SJ, Pfuhl M. Structure, stability and dynamics of the central domain of cardiac myosin binding protein C (MyBP-C): Implications for multidomain assembly and causes for cardiomyopathy. *J Mol Biol* 329: 745-761, 2003.
259. Isaacs WB, Kim IS, Struve A, Fulton AB. Association of titin and myosin heavy chain in developing skeletal muscle. *Proc Natl Acad Sci U S A* 89: 7496-7500, 1992.
260. Izumi R, Niihori T, Aoki Y, Suzuki N, Kato M, Warita H, Takahashi T, Tateyama M, Nagashima T, Funayama R, Abe K, Nakayama K, Aoki M, Matsubara Y. Exome sequencing identifies a novel TTN mutation in a family with hereditary myopathy with early respiratory failure. *J Hum Genet* 58: 259-266, 2013.
261. Jacques A, Hoskins AC, Kentish JC, Marston SB. From genotype to phenotype: A longitudinal study of a patient with hypertrophic cardiomyopathy due to a mutation in the MYBPC3 gene. *J Muscle Res Cell Motil* 29: 239-246, 2008.
262. James J, Robbins J. Signaling and myosin-binding protein C. *J Biol Chem* 286: 9913-9919, 2011.
263. Jansweijer JA, Nieuwhof K, Russo F, Hoorntje ET, Jongbloed JD, Lekanne Deprez RH, Postma AV, Bronk M, van Rijsingen IA, de Haij S, Biagini E, van Haelst PL, van Wijngaarden J, van den Berg MP, Wilde AA, Mannens MM, de Boer RA, van Spaendonck-Zwarts KY, van Tintelen JP, Pinto YM. Truncating titin mutations are associated with a mild and treatable form of dilated cardiomyopathy. *Eur J Heart Fail* 19(4): 512-521, 2017.
264. Jeffries CM, Whitten AE, Harris SP, Trewhella J. Small-angle X-ray scattering reveals the N-terminal domain organization of cardiac myosin binding protein C. *J Mol Biol* 377: 1186-1199, 2008.
265. Jiang BH, Aoki M, Zheng JZ, Li J, Vogt PK. Myogenic signaling of phosphatidylinositol 3-kinase requires the serine-threonine kinase Akt/protein kinase B. *Proc Natl Acad Sci U S A* 96: 2077-2081, 1999.
266. Jiang J, Burgon PG, Wakimoto H, Onoue K, Gorham JM, O'Meara CC, Fomovsky G, McConnell BK, Lee RT, Seidman JG, Seidman CE. Cardiac myosin binding protein C regulates postnatal myocyte cytokinesis. *Proc Natl Acad Sci U S A* 112: 9046-9051, 2015.
267. Johansen T, Lamark T. Selective autophagy mediated by autophagic adapter proteins. *Autophagy* 7: 279-296, 2011.
268. Kabsch W, Mannherz HG, Suck D, Pai EF, Holmes KC. Atomic structure of the actin:DNase I complex. *Nature* 347: 37-44, 1990.
269. Kamm KE, Stull JT. Dedicated myosin light chain kinases with diverse cellular functions. *J Biol Chem* 276: 4527-4530, 2001.
270. Kamm KE, Stull JT. Signaling to myosin regulatory light chain in sarcomeres. *J Biol Chem* 286: 9941-9947, 2011.
271. Kampourakis T, Sun YB, Irving M. Myosin light chain phosphorylation enhances contraction of heart muscle via structural changes in both thick and thin filaments. *Proc Natl Acad Sci U S A* 113: E3039-E3047, 2016.
272. Karsai A, Kellermayer MS, Harris SP. Mechanical unfolding of cardiac myosin binding protein-C by atomic force microscopy. *Biophys J* 101: 1968-1977, 2011.
273. Kass DA, Chen CH, Curry C, Talbot M, Berger R, Fetics B, Nevo E. Improved left ventricular mechanics from acute VDD pacing in patients with dilated cardiomyopathy and ventricular conduction delay. *Circulation* 99: 1567-1573, 1999.
274. Kassem H, Azer RS, Saber-Ayad M, Moharem-Elgamal S, Magdy G, Elguindy A, Cecchi F, Olivotto I, Yacoub MH. Early results of sarcomeric gene screening from the Egyptian National BA-HCM Program. *J Cardiovasc Transl Res* 6: 65-80, 2013.
275. Katzemich A, Kreiskother N, Alexandrovich A, Elliott C, Schock F, Leonard K, Sparrow J, Bullard B. The function of the M-line protein obscurin in controlling the symmetry of the sarcomere in the flight muscle of Drosophila. *J Cell Sci* 125: 3367-3379, 2012.
276. Katzemich A, West RJ, Fukuzawa A, Sweeney ST, Gautel M, Sparrow J, Bullard B. Binding partners of the kinase domains in Drosophila obscurin and their effect on the structure of the flight muscle. *J Cell Sci* 128: 3386-3397, 2015.
277. Kazmierczak K, Xu Y, Jones M, Guzman G, Hernandez OM, Kerrick WG, Szczesna-Cordary D. The role of the N-terminus of the myosin essential light chain in cardiac muscle contraction. *J Mol Biol* 387: 706-725, 2009.
278. Kenyon GL, Reed GH. Creatine kinase: Structure-activity relationships. *Adv Enzymol Relat Areas Mol Biol* 54: 367-426, 1983.
279. Kiani FA, Fischer S. ATP-dependent interplay between local and global conformational changes in the myosin motor. *Cytoskeleton (Hoboken)* 73: 643-651, 2016.
280. Kimura S, Maruyama K, Huang YP. Interactions of muscle beta-connectin with myosin, actin, and actomyosin at low ionic strengths. *J Biochem* 96: 499-506, 1984.
281. Kirk JA, Holewinski RJ, Kooij V, Agnetti G, Tunin RS, Witayavanitkul N, de Tombe PP, Gao WD, Van Eyk J, Kass DA. Cardiac resynchronization sensitizes the sarcomere to calcium by reactivating GSK-3beta. *J Clin Invest* 124: 129-138, 2014.
282. Klemp P, Hall JG. Dominant distal arthrogryposis in a Maori family with marked variability of expression. *Am J Med Genet* 55: 414-419, 1995.
283. Kockskamper J, Khafaga M, Grimm M, Elgner A, Walther S, Kockskamper A, von Lewinski D, Post H, Grossmann M, Dorge H, Gottlieb PA, Sachs F, Eschenhagen T, Schondube FA, Pieske B. Angiotensin II and myosin light-chain phosphorylation contribute to the stretch-induced slow force response in human atrial myocardium. *Cardiovasc Res* 79: 642-651, 2008.
284. Koebis M, Ohsawa N, Kino Y, Sasagawa N, Nishino I, Ishiura S. Alternative splicing of myomesin 1 gene is aberrantly regulated in myotonic dystrophy type 1. *Genes Cells* 16: 961-972, 2011.
285. Kohr MJ, Aponte AM, Sun J, Wang G, Murphy E, Gucek M, Steenbergen C. Characterization of potential S-nitrosylation sites in the myocardium. *Am J Physiol Heart Circ Physiol* 300: H1327-H1335, 2011.
286. Kolmerer B, Olivieri N, Witt CC, Herrmann BG, Labeit S. Genomic organization of M line titin and its tissue-specific expression in two distinct isoforms. *J Mol Biol* 256: 556-563, 1996.
287. Kontrogianni-Konstantopoulos A, Ackermann MA, Bowman AL, Yap SV, Bloch RJ. Muscle giants: Molecular scaffolds in sarcomerogenesis. *Physiol Rev* 89: 1217-1267, 2009.
288. Kontrogianni-Konstantopoulos A, Bloch RJ. Obscurin: A multitasking muscle giant. *J Muscle Res Cell Motil* 26: 419-426, 2005.
289. Kontrogianni-Konstantopoulos A, Catino DH, Strong JC, Bloch RJ. De novo myofibrillogenesis in C2C12 cells: Evidence for the independent

assembly of M bands and Z disks. *Am J Physiol Cell Physiol* 290: C626-C637, 2006.
290. Kontrogianni-Konstantopoulos A, Catino DH, Strong JC, Randall WR, Bloch RJ. Obscurin regulates the organization of myosin into A bands. *Am J Physiol Cell Physiol* 287: C209-C217, 2004.
291. Kontrogianni-Konstantopoulos A, Catino DH, Strong JC, Sutter S, Borisov AB, Pumplin DW, Russell MW, Bloch RJ. Obscurin modulates the assembly and organization of sarcomeres and the sarcoplasmic reticulum. *FASEB J* 20: 2102-2111, 2006.
292. Kontrogianni-Konstantopoulos A, Huang SC, Benz EJ, Jr. A nonerythroid isoform of protein 4.1R interacts with components of the contractile apparatus in skeletal myofibers. *Mol Biol Cell* 11: 3805-3817, 2000.
293. Kontrogianni-Konstantopoulos A, Jones EM, Van Rossum DB, Bloch RJ. Obscurin is a ligand for small ankyrin 1 in skeletal muscle. *Mol Biol Cell* 14: 1138-1148, 2003.
294. Kramerova I, Kudryashova E, Tidball JG, Spencer MJ. Null mutation of calpain 3 (p94) in mice causes abnormal sarcomere formation in vivo and in vitro. *Hum Mol Genet* 13: 1373-1388, 2004.
295. Kruger M, Kotter S. Titin, a central mediator for hypertrophic signaling, exercise-induced mechanosignaling and skeletal muscle remodeling. *Front Physiol* 7: 76, 2016.
296. Kubalak SW, Miller-Hance WC, O'Brien TX, Dyson E, Chien KR. Chamber specification of atrial myosin light chain-2 expression precedes septation during murine cardiogenesis. *J Biol Chem* 269: 16961-16970, 1994.
297. Kuhne W. *Untersuchungen uber das Protoplasma und die Contractilitat*. Leipzig: W. Engelmann, 1864.
298. Kulikovskaya I, McClellan G, Flavigny J, Carrier L, Winegrad S. Effect of MyBP-C binding to actin on contractility in heart muscle. *J Gen Physiol* 122: 761-774, 2003.
299. Kulikovskaya I, McClellan G, Levine R, Winegrad S. Effect of extraction of myosin binding protein C on contractility of rat heart. *Am J Physiol Heart Circ Physiol* 285: H857-H865, 2003.
300. Kulkarni KP, Panigrahi I, Ray M, Marwaha RK. Distal arthrogryposis syndrome. *Indian J Hum Genet* 14: 67-69, 2008.
301. Kunst G, Kress KR, Gruen M, Uttenweiler D, Gautel M, Fink RH. Myosin binding protein C, a phosphorylation-dependent force regulator in muscle that controls the attachment of myosin heads by its interaction with myosin S2. *Circ Res* 86: 51-58, 2000.
302. Kurasawa M, Sato N, Matsuda A, Koshida S, Totsuka T, Obinata T. Differential expression of C-protein isoforms in developing and degenerating mouse striated muscles. *Muscle Nerve* 22: 196-207, 1999.
303. Kurosaka S, Leu NA, Pavlov I, Han X, Ribeiro PA, Xu T, Bunte R, Saha S, Wang J, Cornachione A, Mai W, Yates JR, III, Rassier DE, Kashina A. Arginylation regulates myofibrils to maintain heart function and prevent dilated cardiomyopathy. *J Mol Cell Cardiol* 53: 333-341, 2012.
304. Kuster DW, Sadayappan S. MYBPC3's alternate ending: Consequences and therapeutic implications of a highly prevalent 25 bp deletion mutation. *Pflugers Arch* 466: 207-213, 2014.
305. Kuster DW, Sequeira V, Najafi A, Boontje NM, Wijnker PJ, Witjas-Paalberends ER, Marston SB, Dos Remedios CG, Carrier L, Demmers JA, Redwood C, Sadayappan S, van der Velden J. GSK3beta phosphorylates newly identified site in the proline-alanine-rich region of cardiac myosin-binding protein C and alters cross-bridge cycling kinetics in human: Short communication. *Circ Res* 112: 633-639, 2013.
306. Labeit S, Gautel M, Lakey A, Trinick J. Towards a molecular understanding of titin. *EMBO J* 11: 1711-1716, 1992.
307. Labeit S, Kolmerer B. Titins: Giant proteins in charge of muscle ultrastructure and elasticity. *Science* 270: 293-296, 1995.
308. Lamark T, Perander M, Outzen H, Kristiansen K, Øvervatn A, Michaelsen E, Bjørkøy G, Johansen T. Interaction codes within the family of mammalian Phox and Bem1p domain-containing proteins. *J Biol Chem* 278: 34568-34581, 2003.
309. Lamont PJ, Wallefeld W, Hilton-Jones D, Udd B, Argov Z, Barboi AC, Bonneman C, Boycott KM, Bushby K, Connolly AM, Davies N, Beggs AH, Cox GF, Dastgir J, DeChene ET, Gooding R, Jungbluth H, Muelas N, Palmio J, Penttilä S, Schmedding E, Suominen T, Straub V, Staples C, Van den Bergh PY, Vilchez JJ, Wagner KR, Wheeler PG, Wraige E, Laing NG. Novel mutations widen the phenotypic spectrum of slow skeletal/β-cardiac myosin (MYH7) distal myopathy. *Hum Mutat* 35: 868-879, 2014.
310. Lange S, Auerbach D, McLoughlin P, Perriard E, Schafer BW, Perriard JC, Ehler E. Subcellular targeting of metabolic enzymes to titin in heart muscle may be mediated by DRAL/FHL-2. *J Cell Sci* 115: 4925-4936, 2002.
311. Lange S, Edström L, Udd B, Gautel M. Reply: Hereditary myopathy with early respiratory failure is caused by mutations in the titin FN3 119 domain. *Brain* 137: e279, 2014.
312. Lange S, Himmel M, Auerbach D, Agarkova I, Hayess K, Furst DO, Perriard JC, Ehler E. Dimerisation of myomesin: Implications for the structure of the sarcomeric M-band. *J Mol Biol* 345: 289-298, 2005.
313. Lange S, Ouyang K, Meyer G, Cui L, Cheng H, Lieber RL, Chen J. Obscurin determines the architecture of the longitudinal sarcoplasmic reticulum. *J Cell Sci* 122: 2640-2650, 2009.
314. Lange S, Perera S, Teh P, Chen J. Obscurin and KCTD6 regulate cullin-dependent small ankyrin-1 (sAnk1.5) protein turnover. *Mol Biol Cell* 23: 2490-2504, 2012.
315. Lange S, Xiang F, Yakovenko A, Vihola A, Hackman P, Rostkova E, Kristensen J, Brandmeier B, Franzen G, Hedberg B, Gunnarsson LG, Hughes SM, Marchand S, Sejersen T, Richard I, Edstrom L, Ehler E, Udd B, Gautel M. The kinase domain of titin controls muscle gene expression and protein turnover. *Science* 308: 1599-1603, 2005.
316. Lecker SH, Jagoe RT, Gilbert A, Gomes M, Baracos V, Bailey J, Price SR, Mitch WE, Goldberg AL. Multiple types of skeletal muscle atrophy involve a common program of changes in gene expression. *FASEB J* 18: 39-51, 2004.
317. Lee CF, Melkani GC, Bernstein SI. The UNC-45 myosin chaperone: From worms to flies to vertebrates. *Int Rev Cell Mol Biol* 313: 103-144, 2014.
318. Lee K, Harris SP, Sadayappan S, Craig R. Orientation of myosin binding protein C in the cardiac muscle sarcomere determined by domain-specific immuno-EM. *J Mol Biol* 427: 274-286, 2015.
319. Lee KJ, Ross RS, Rockman HA, Harris AN, O'Brien TX, van Bilsen M, Shubeita HE, Kandolf R, Brem G, Price J, et al. Myosin light chain-2 luciferase transgenic mice reveal distinct regulatory programs for cardiac and skeletal muscle-specific expression of a single contractile protein gene. *J Biol Chem* 267: 15875-15885, 1992.
320. Leite FeS, Kashina A, Rassier DE. Posttranslational arginylation regulates striated muscle function. *Exerc Sport Sci Rev* 44: 98-103, 2016.
321. Leite FS, Minozzo FC, Kalganov A, Cornachione AS, Cheng YS, Leu NA, Han X, Saripalli C, Yates JR, III, Granzier H, Kashina AS, Rassier DE. Reduced passive force in skeletal muscles lacking protein arginylation. *Am J Physiol Cell Physiol* 310: C127-C135, 2016.
322. Li M, Andersson-Lendahl M, Sejersen T, Arner A. Knockdown of fast skeletal myosin-binding protein C in zebrafish results in a severe skeletal myopathy. *J Gen Physiol* 147: 309-322, 2016.
323. Li M, Zheng W. All-atom molecular dynamics simulations of actin-myosin interactions: A comparative study of cardiac alpha myosin, beta myosin, and fast skeletal muscle myosin. *Biochemistry* 52: 8393-8405, 2013.
324. Li TB, Liu XH, Feng S, Hu Y, Yang WX, Han Y, Wang YG, Gong LM. Characterization of MR-1, a novel myofibrillogenesis regulator in human muscle. *Acta Biochim Biophys Sin (Shanghai)* 36: 412-418, 2004.
325. Li X, Zhong B, Han W, Zhao N, Liu W, Sui Y, Wang Y, Lu Y, Wang H, Li J, Jiang M. Two novel mutations in myosin binding protein C slow causing distal arthrogryposis type 2 in two large Han Chinese families may suggest important functional role of immunoglobulin domain C2. *PLoS One* 10: e0117158, 2015.
326. Lin B, Govindan S, Lee K, Zhao P, Han R, Runte KE, Craig R, Palmer BM, Sadayappan S. Cardiac myosin binding protein-C plays no regulatory role in skeletal muscle structure and function. *PLoS One* 8: e69671, 2013.
327. Linari M, Brunello E, Reconditi M, Fusi L, Caremani M, Narayanan T, Piazzesi G, Lombardi V, Irving M. Force generation by skeletal muscle is controlled by mechanosensing in myosin filaments. *Nature* 528: 276-279, 2015.
328. Linari M, Piazzesi G, Dobbie I, Koubassova N, Reconditi M, Narayanan T, Diat O, Irving M, Lombardi V. Interference fine structure and sarcomere length dependence of the axial x-ray pattern from active single muscle fibers. *Proc Natl Acad Sci U S A* 97: 7226-7231, 2000.
329. Linke WA. Sense and stretchability: The role of titin and titin-associated proteins in myocardial stress-sensing and mechanical dysfunction. *Cardiovasc Res* 77: 637-648, 2008.
330. Liu J, Aoki M, Illa I, Wu C, Fardeau M, Angelini C, Serrano C, Urtizberea JA, Hentati F, Hamida MB, Bohlega S, Culper EJ, Amato AA, Bossie K, Oeltjen J, Bejaoui K, McKenna-Yasek D, Hosler BA, Schurr E, Arahata K, de Jong PJ, Brown RH, Jr. Dysferlin, a novel skeletal muscle gene, is mutated in Miyoshi myopathy and limb girdle muscular dystrophy. *Nat Genet* 20: 31-36, 1998.
331. Liu X, Li T, Sun S, Xu F, Wang Y. Role of myofibrillogenesis regulator-1 in myocardial hypertrophy. *Am J Physiol Heart Circ Physiol* 290: H279-H285, 2006.
332. Llinas P, Isabet T, Song L, Ropars V, Zong B, Benisty H, Sirigu S, Morris C, Kikuti C, Safer D, Sweeney HL, Houdusse A. How actin initiates the motor activity of myosin. *Dev Cell* 33: 401-412, 2015.
333. Locher MR, Razumova MV, Stelzer JE, Norman HS, Moss RL. Effects of low-level α-myosin heavy chain expression on contractile kinetics in porcine myocardium. *Am J Physiol Heart Circ Physiol* 300: H869-H878, 2011.
334. Lompre AM, Schwartz K, d'Albis A, Lacombe G, Van Thiem N, Swynghedauw B. Myosin isoenzyme redistribution in chronic heart overload. *Nature* 282: 105-107, 1979.

335. Lowes BD, Minobe W, Abraham WT, Rizeq MN, Bohlmeyer TJ, Quaife RA, Roden RL, Dutcher DL, Robertson AD, Voelkel NF, Badesch DB, Groves BM, Gilbert EM, Bristow MR. Changes in gene expression in the intact human heart. Downregulation of alpha-myosin heavy chain in hypertrophied, failing ventricular myocardium. *J Clin Invest* 100: 2315-2324, 1997.
336. Lu Y, Kwan AH, Trewhella J, Jeffries CM. The C0C1 fragment of human cardiac myosin binding protein C has common binding determinants for both actin and myosin. *J Mol Biol* 413: 908-913, 2011.
337. Lundby A, Andersen MN, Steffensen AB, Horn H, Kelstrup CD, Francavilla C, Jensen LJ, Schmitt N, Thomsen MB, Olsen JV. In vivo phosphoproteomics analysis reveals the cardiac targets of beta-adrenergic receptor signaling. *Sci Signal* 6: rs11, 2013.
338. Lundby A, Lage K, Weinert BT, Bekker-Jensen DB, Secher A, Skovgaard T, Kelstrup CD, Dmytriyev A, Choudhary C, Lundby C, Olsen JV. Proteomic analysis of lysine acetylation sites in rat tissues reveals organ specificity and subcellular patterns. *Cell Rep* 2: 419-431, 2012.
339. Lundby A, Secher A, Lage K, Nordsborg NB, Dmytriyev A, Lundby C, Olsen JV. Quantitative maps of protein phosphorylation sites across 14 different rat organs and tissues. *Nat Commun* 3: 876, 2012.
340. Luther PK, Bennett PM, Knupp C, Craig R, Padron R, Harris SP, Patel J, Moss RL. Understanding the organisation and role of myosin binding protein C in normal striated muscle by comparison with MyBP-C knockout cardiac muscle. *J Mol Biol* 384: 60-72, 2008.
341. Lynch TLt, Sivaguru M, Velayutham M, Cardounel AJ, Michels M, Barefield D, Govindan S, dos Remedios C, van der Velden J, Sadayappan S. Oxidative stress in dilated cardiomyopathy caused by MYBPC3 mutation. *Oxid Med Cell Longev* 2015: 424751, 2015.
342. Lyon RC, Lange S, Sheikh F. Breaking down protein degradation mechanisms in cardiac muscle. *Trends Mol Med* 19: 239-249, 2013.
343. Lyons GE, Ontell M, Cox R, Sassoon D, Buckingham M. The expression of myosin genes in developing skeletal muscle in the mouse embryo. *J Cell Biol* 111: 1465-1476, 1990.
344. Lyons GE, Schiaffino S, Sassoon D, Barton P, Buckingham M. Developmental regulation of myosin gene expression in mouse cardiac muscle. *J Cell Biol* 111: 2427-2436, 1990.
345. Makarenko I, Opitz CA, Leake MC, Neagoe C, Kulke M, Gwathmey JK, del Monte F, Hajjar RJ, Linke WA. Passive stiffness changes caused by upregulation of compliant titin isoforms in human dilated cardiomyopathy hearts. *Circ Res* 95: 708-716, 2004.
346. Malmqvist UP, Aronshtam A, Lowey S. Cardiac myosin isoforms from different species have unique enzymatic and mechanical properties. *Biochemistry* 43: 15058-15065, 2004.
347. Mamidi R, Gresham KS, Verma S, Stelzer JE. Cardiac myosin binding protein-C phosphorylation modulates myofilament length-dependent activation. *Front Physiol* 7: 38, 2016.
348. Mamidi R, Mallampalli SL, Wieczorek DF, Chandra M. Identification of two new regions in the N-terminus of cardiac troponin T that have divergent effects on cardiac contractile function. *J Physiol* 591: 1217-1234, 2013.
349. Markus B, Narkis G, Landau D, Birk RZ, Cohen I, Birk OS. Autosomal recessive lethal congenital contractural syndrome type 4 (LCCS4) caused by a mutation in MYBPC1. *Hum Mutat* 33: 1435-1438, 2012.
350. Marques MA, de Oliveira GA. Cardiac troponin and tropomyosin: Structural and cellular perspectives to unveil the hypertrophic cardiomyopathy phenotype. *Front Physiol* 7: 429, 2016.
351. Marston S, Copeland O, Gehmlich K, Schlossarek S, Carrier L. How do MYBPC3 mutations cause hypertrophic cardiomyopathy? *J Muscle Res Cell Motil* 33: 75-80, 2012.
352. Marston S, Montgiraud C, Munster AB, Copeland O, Choi O, Dos Remedios C, Messer AE, Ehler E, Knoll R. OBSCN mutations associated with dilated cardiomyopathy and haploinsufficiency. *PLoS One* 10: e0138568, 2015.
353. Marston SB. How do mutations in contractile proteins cause the primary familial cardiomyopathies? *J Cardiovasc Transl Res* 4: 245-255, 2011.
354. Martonosi AN. Animal electricity, Ca^{2+} and muscle contraction. A brief history of muscle research. *Acta Biochim Pol* 47: 493-516, 2000.
355. Martyn DA. Myosin binding protein-C: Structural and functional complexity. *J Mol Cell Cardiol* 37: 813-815, 2004.
356. Maruyama K. Connectin, an elastic protein from myofibrils. *J Biochem* 80: 405-407, 1976.
357. Maruyama K, Kimura S, Kuroda M, Handa S. Connectin, an elastic protein of muscle. Its abundance in cardiac myofibrils. *J Biochem* 82: 347-350, 1977.
358. Masaki T, Takaiti O. M-protein. *J Biochem* 75: 367-380, 1974.
359. Mascarello F, Toniolo L, Cancellara P, Reggiani C, Maccatrozzo L. Expression and identification of 10 sarcomeric MyHC isoforms in human skeletal muscles of different embryological origin. Diversity and similarity in mammalian species. *Ann Anat* 207: 9-20, 2016.
360. Mayans O, Benian GM, Simkovic F, Rigden DJ. Mechanistic and functional diversity in the mechanosensory kinases of the titin-like family. *Biochem Soc Trans* 41: 1066-1071, 2013.
361. Mayans O, Labeit S. MuRFs: Specialized members of the TRIM/RBCC family with roles in the regulation of the trophic state of muscle and its metabolism. *Adv Exp Med Biol* 770: 119-129, 2012.
362. Mayans O, van der Ven PF, Wilm M, Mues A, Young P, Furst DO, Wilmanns M, Gautel M. Structural basis for activation of the titin kinase domain during myofibrillogenesis. *Nature* 395: 863-869, 1998.
363. McClellan G, Kulikovskaya I, Flavigny J, Carrier L, Winegrad S. Effect of cardiac myosin-binding protein C on stability of the thick filament. *J Mol Cell Cardiol* 37: 823-835, 2004.
364. McClellan G, Kulikovskaya I, Winegrad S. Changes in cardiac contractility related to calcium-mediated changes in phosphorylation of myosin-binding protein C. *Biophys J* 81: 1083-1092, 2001.
365. McConnell BK, Jones KA, Fatkin D, Arroyo LH, Lee RT, Aristizabal O, Turnbull DH, Georgakopoulos D, Kass D, Bond M, Niimura H, Schoen FJ, Conner D, Fischman DA, Seidman CE, Seidman JG. Dilated cardiomyopathy in homozygous myosin-binding protein-C mutant mice. *J Clin Invest* 104: 1771, 1999.
366. McElhinny AS, Perry CN, Witt CC, Labeit S, Gregorio CC. Muscle-specific RING finger-2 (MURF-2) is important for microtubule, intermediate filament and sarcomeric M-line maintenance in striated muscle development. *J Cell Sci* 117: 3175-3188, 2004.
367. McGrath MJ, Cottle DL, Nguyen MA, Dyson JM, Coghill ID, Robinson PA, Holdsworth M, Cowling BS, Hardeman EC, Mitchell CA, Brown S. Four and a half LIM protein 1 binds myosin-binding protein C and regulates myosin filament formation and sarcomere assembly. *J Biol Chem* 281: 7666-7683, 2006.
368. McNamara JW, Li A, dos Remedios CG, Cooke R. The role of super-relaxed myosin in skeletal and cardiac muscle. *Biophysical Reviews* 7: 5-14, 2015.
369. Meder B, Laufer C, Hassel D, Just S, Marquart S, Vogel B, Hess A, Fishman MC, Katus HA, Rottbauer W. A single serine in the carboxyl terminus of cardiac essential myosin light chain-1 controls cardiomyocyte contractility in vivo. *Circ Res* 104: 650-659, 2009.
370. Messer AE, Jacques AM, Marston SB. Troponin phosphorylation and regulatory function in human heart muscle: Dephosphorylation of Ser23/24 on troponin I could account for the contractile defect in end-stage heart failure. *J Mol Cell Cardiol* 42: 247-259, 2007.
371. Michael JJ, Gollapudi SK, Ford SJ, Kazmierczak K, Szczesna-Cordary D, Chandra M. Deletion of 1-43 amino acids in cardiac myosin essential light chain blunts length dependency of Ca(2+) sensitivity and cross-bridge detachment kinetics. *Am J Physiol Heart Circ Physiol* 304: H253-H259, 2013.
372. Midde K, Rich R, Marandos P, Fudala R, Li A, Gryczynski I, Borejdo J. Comparison of orientation and rotational motion of skeletal muscle cross-bridges containing phosphorylated and dephosphorylated myosin regulatory light chain. *J Biol Chem* 288: 7012-7023, 2013.
373. Millar NC, Homsher E. Kinetics of force generation and phosphate release in skinned rabbit soleus muscle fibers. *Am J Physiol* 262: C1239-C1245, 1992.
374. Miller G, Musa H, Gautel M, Peckham M. A targeted deletion of the C-terminal end of titin, including the titin kinase domain, impairs myofibrillogenesis. *J Cell Sci* 116: 4811-4819, 2003.
375. Miller MS, Palmer BM, Ruch S, Martin LA, Farman GP, Wang Y, Robbins J, Irving TC, Maughan DW. The essential light chain N-terminal extension alters force and fiber kinetics in mouse cardiac muscle. *J Biol Chem* 280: 34427-34434, 2005.
376. Mitchell EJ, Jakes R, Kendrick-Jones J. Localisation of light chain and actin binding sites on myosin. *Eur J Biochem* 161: 25-35, 1986.
377. Miyamoto CA, Fischman DA, Reinach FC. The interface between MyBP-C and myosin: Site-directed mutagenesis of the CX myosin-binding domain of MyBP-C. *J Muscle Res Cell Motil* 20: 703-715, 1999.
378. Miyanishi T, Ishikawa T, Hayashibara T, Maita T, Wakabayashi T. The two actin-binding regions on the myosin heads of cardiac muscle. *Biochemistry* 41: 5429-5438, 2002.
379. Miyata S, Minobe W, Bristow MR, Leinwand LA. Myosin heavy chain isoform expression in the failing and nonfailing human heart. *Circ Res* 86: 386-390, 2000.
380. Mizutani H, Okamoto R, Moriki N, Konishi K, Taniguchi M, Fujita S, Dohi K, Onishi K, Suzuki N, Satoh S, Makino N, Itoh T, Hartshorne DJ, Ito M. Overexpression of myosin phosphatase reduces Ca(2+) sensitivity of contraction and impairs cardiac function. *Circ J* 74: 120-128, 2010.
381. Mohamed AS, Dignam JD, Schlender KK. Cardiac myosin-binding protein C (MyBP-C): Identification of protein kinase A and protein kinase C phosphorylation sites. *Arch Biochem Biophys* 358: 313-319, 1998.
382. Moolman-Smook J, Flashman E, de Lange W, Li Z, Corfield V, Redwood C, Watkins H. Identification of novel interactions between domains of Myosin binding protein-C that are modulated by hypertrophic cardiomyopathy missense mutations. *Circ Res* 91: 704-711, 2002.

383. Moorhead G, Johnson D, Morrice N, Cohen P. The major myosin phosphatase in skeletal muscle is a complex between the beta-isoform of protein phosphatase 1 and the MYPT2 gene product. *FEBS Lett* 438: 141-144, 1998.
384. Moos C. Fluorescence microscope study of the binding of added C protein to skeletal muscle myofibrils. *J Cell Biol* 90: 25-31, 1981.
385. Moos C, Mason CM, Besterman JM, Feng IN, Dubin JH. The binding of skeletal muscle C-protein to F-actin, and its relation to the interaction of actin with myosin subfragment-1. *J Mol Biol* 124: 571-586, 1978.
386. Moos C, Offer G, Starr R, Bennett P. Interaction of C-protein with myosin, myosin rod and light meromyosin. *J Mol Biol* 97: 1-9, 1975.
387. Morano I, Haase H. Different actin affinities of human cardiac essential myosin light chain isoforms. *FEBS Lett* 408: 71-74, 1997.
388. Morano I, Hadicke K, Haase H, Bohm M, Erdmann E, Schaub MC. Changes in essential myosin light chain isoform expression provide a molecular basis for isometric force regulation in the failing human heart. *J Mol Cell Cardiol* 29: 1177-1187, 1997.
389. Morano I, Ritter O, Bonz A, Timek T, Vahl CF, Michel G. Myosin light chain-actin interaction regulates cardiac contractility. *Circ Res* 76: 720-725, 1995.
390. Morano M, Zacharzowski U, Maier M, Lange PE, Alexi-Meskishvili V, Haase H, Morano I. Regulation of human heart contractility by essential myosin light chain isoforms. *J Clin Invest* 98: 467-473, 1996.
391. Moretti A, Weig HJ, Ott T, Seyfarth M, Holthoff HP, Grewe D, Gillitzer A, Bott-Flugel L, Schomig A, Ungerer M, Laugwitz KL. Essential myosin light chain as a target for caspase-3 in failing myocardium. *Proc Natl Acad Sci U S A* 99: 11860-11865, 2002.
392. Moriscot AS, Baptista IL, Bogomolovas J, Witt C, Hirner S, Granzier H, Labeit S. MuRF1 is a muscle fiber-type II associated factor and together with MuRF2 regulates type-II fiber trophicity and maintenance. *J Struct Biol* 170: 344-353, 2010.
393. Mornet D, Bertrand RU, Pantel P, Audemard E, Kassab R. Proteolytic approach to structure and function of actin recognition site in myosin heads. *Biochemistry* 20: 2110-2120, 1981.
394. Moss RL. Cardiac myosin-binding protein C: A protein once at loose ends finds its regulatory groove. *Proc Natl Acad Sci U S A* 113: 3133-3135, 2016.
395. Moss RL, Fitzsimons DP, Ralphe JC. Cardiac MyBP-C regulates the rate and force of contraction in mammalian myocardium. *Circ Res* 116: 183-192, 2015.
396. Mouton JM, van der Merwe L, Goosen A, Revera M, Brink PA, Moolman-Smook JC, Kinnear C. MYBPH acts as modifier of cardiac hypertrophy in hypertrophic cardiomyopathy (HCM) patients. *Hum Genet* 135: 477-483, 2016.
397. Mrosek M, Labeit D, Witt S, Heerklotz H, von Castelmur E, Labeit S, Mayans O. Molecular determinants for the recruitment of the ubiquitin-ligase MuRF-1 onto M-line titin. *FASEB J* 21: 1383-1392, 2007.
398. Muhle-Goll C, Habeck M, Cazorla O, Nilges M, Labeit S, Granzier H. Structural and functional studies of titin's fn3 modules reveal conserved surface patterns and binding to myosin S1—A possible role in the Frank-Starling mechanism of the heart. *J Mol Biol* 313: 431-447, 2001.
399. Müller S, Lange S, Gautel M, Wilmanns M. Rigid conformation of an immunoglobulin domain tandem repeat in the A-band of the elastic muscle protein titin. *J Mol Biol* 371: 469-480, 2007.
400. Mun JY, Previs MJ, Yu HY, Gulick J, Tobacman LS, Beck Previs S, Robbins J, Warshaw DM, Craig R. Myosin-binding protein C displaces tropomyosin to activate cardiac thin filaments and governs their speed by an independent mechanism. *Proc Natl Acad Sci U S A* 111: 2170-2175, 2014.
401. Muretta JM, Petersen KJ, Thomas DD. Direct real-time detection of the actin-activated power stroke within the myosin catalytic domain. *Proc Natl Acad Sci U S A* 110: 7211-7216, 2013.
402. Muretta JM, Rohde JA, Johnsrud DO, Cornea S, Thomas DD. Direct real-time detection of the structural and biochemical events in the myosin power stroke. *Proc Natl Acad Sci U S A* 112: 14272-14277, 2015.
403. Murgia M, Nagaraj N, Deshmukh AS, Zeiler M, Cancellara P, Moretti I, Reggiani C, Schiaffino S, Mann M. Single muscle fiber proteomics reveals unexpected mitochondrial specialization. *EMBO Rep* 16: 387-395, 2015.
404. Murrin LC, Talbot JN. RanBPM, a scaffolding protein in the immune and nervous systems. *J Neuroimmune Pharmacol* 2: 290-295, 2007.
405. Musa H, Meek S, Gautel M, Peddie D, Smith AJ, Peckham M. Targeted homozygous deletion of M-band titin in cardiomyocytes prevents sarcomere formation. *J Cell Sci* 119: 4322-4331, 2006.
406. Myhre JL, Hills JA, Prill K, Wohlgemuth SL, Pilgrim DB. The titin A-band rod domain is dispensable for initial thick filament assembly in zebrafish. *Dev Biol* 387: 93-108, 2014.
407. Myhre JL, Pilgrim D. A titan but not necessarily a ruler: Assessing the role of titin during thick filament patterning and assembly. *Anat Rec (Hoboken)* 297: 1604-1614, 2014.
408. Nabeshima Y, Fujii-Kuriyama Y, Muramatsu M, Ogata K. Alternative transcription and two modes of splicing results in two myosin light chains from one gene. *Nature* 308: 333-338, 1984.
409. Nagueh SF, Shah G, Wu Y, Torre-Amione G, King NM, Lahmers S, Witt CC, Becker K, Labeit S, Granzier HL. Altered titin expression, myocardial stiffness, and left ventricular function in patients with dilated cardiomyopathy. *Circulation* 110: 155-162, 2004.
410. Narusawa M, Fitzsimons RB, Izumo S, Nadal-Ginard B, Rubinstein NA, Kelly AM. Slow myosin in developing rat skeletal muscle. *J Cell Biol* 104: 447-459, 1987.
411. Neiva-Sousa M, Almeida-Coelho J, Falcao-Pires I, Leite-Moreira AF. Titin mutations: The fall of Goliath. *Heart Fail Rev* 20: 579-588, 2015.
412. Neumann J. Altered phosphatase activity in heart failure, influence on Ca^{2+} movement. *Basic Res Cardiol* 97 (Suppl 1): I91-I95, 2002.
413. Nieznanski K, Nieznanska H, Skowronek K, Kasprzak AA, Stepkowski D. Ca^{2+} binding to myosin regulatory light chain affects the conformation of the N-terminus of essential light chain and its binding to actin. *Arch Biochem Biophys* 417: 153-158, 2003.
414. Nishio H, Ichikawa K, Hartshorne DJ. Evidence for myosin-binding phosphatase in heart myofibrils. *Biochem Biophys Res Commun* 236: 570-575, 1997.
415. Noguchi J, Yanagisawa M, Imamura M, Kasuya Y, Sakurai T, Tanaka T, Masaki T. Complete primary structure and tissue expression of chicken pectoralis M-protein. *J Biol Chem* 267: 20302-20310, 1992.
416. Oakley CE, Chamoun J, Brown LJ, Hambly BD. Myosin binding protein-C: Enigmatic regulator of cardiac contraction. *Int J Biochem Cell Biol* 39: 2161-2166, 2007.
417. Obermann WM, Gautel M, Steiner F, van der Ven PF, Weber K, Furst DO. The structure of the sarcomeric M band: Localization of defined domains of myomesin, M-protein, and the 250-kD carboxy-terminal region of titin by immunoelectron microscopy. *J Cell Biol* 134: 1441-1453, 1996.
418. Obermann WM, Gautel M, Weber K, Furst DO. Molecular structure of the sarcomeric M band: Mapping of titin and myosin binding domains in myomesin and the identification of a potential regulatory phosphorylation site in myomesin. *EMBO J* 16: 211-220, 1997.
419. Obermann WM, van der Ven PF, Steiner F, Weber K, Furst DO. Mapping of a myosin-binding domain and a regulatory phosphorylation site in M-protein, a structural protein of the sarcomeric M band. *Mol Biol Cell* 9: 829-840, 1998.
420. Offer G, Moos C, Starr R. A new protein of the thick filaments of vertebrate skeletal myofibrils. Extractions, purification and characterization. *J Mol Biol* 74: 653-676, 1973.
421. Ohlsson M, Hedberg C, Brådvik B, Lindberg C, Tajsharghi H, Danielsson O, Melberg A, Udd B, Martinsson T, Oldfors A. Hereditary myopathy with early respiratory failure associated with a mutation in A-band titin. *Brain* 135: 1682-1694, 2012.
422. Okagaki T, Weber FE, Fischman DA, Vaughan KT, Mikawa T, Reinach FC. The major myosin-binding domain of skeletal muscle MyBP-C (C protein) resides in the COOH-terminal, immunoglobulin C2 motif. *J Cell Biol* 123: 619-626, 1993.
423. Okamoto R, Kato T, Mizoguchi A, Takahashi N, Nakakuki T, Mizutani H, Isaka N, Imanaka-Yoshida K, Kaibuchi K, Lu Z, Mabuchi K, Tao T, Hartshorne DJ, Nakano T, Ito M. Characterization and function of MYPT2, a target subunit of myosin phosphatase in heart. *Cell Signal* 18: 1408-1416, 2006.
424. Olive M, Abdul-Hussein S, Oldfors A, Gonzalez-Costello J, van der Ven PF, Furst DO, Gonzalez L, Moreno D, Torrejon-Escribano B, Alio J, Pou A, Ferrer I, Tajsharghi H. New cardiac and skeletal protein aggregate myopathy associated with combined MuRF1 and MuRF3 mutations. *Hum Mol Genet* 24: 3638-3650, 2015.
425. Orlova A, Galkin VE, Jeffries CM, Egelman EH, Trewhella J. The N-terminal domains of myosin binding protein C can bind polymorphically to F-actin. *J Mol Biol* 412: 379-386, 2011.
426. Orr N, Arnaout R, Gula LJ, Spears DA, Leong-Sit P, Li Q, Tarhuni W, Reischauer S, Chauhan VS, Borkovich M, Uppal S, Adler A, Coughlin SR, Stainier DY, Gollob MH. A mutation in the atrial-specific myosin light chain gene (MYL4) causes familial atrial fibrillation. *Nat Commun* 7: 11303, 2016.
427. Palmer BM, McConnell BK, Li GH, Seidman CE, Seidman JG, Irving TC, Alpert NR, Maughan DW. Reduced cross-bridge dependent stiffness of skinned myocardium from mice lacking cardiac myosin binding protein-C. *Mol Cell Biochem* 263: 73-80, 2004.
428. Palmio J, Evilä A, Chapon F, Tasca G, Xiang F, Brådvik B, Eymard B, Echaniz-Laguna A, Laporte J, Kärppä M, Mahjneh I, Quinlivan R, Laforêt P, Damian M, Berardo A, Taratuto AL, Bueri JA, Tommiska J, Raivio T, Tuerk M, Gölitz P, Chevessier F, Sewry C, Norwood F, Hedberg C, Schröder R, Edström L, Oldfors A, Hackman P, Udd B. Hereditary myopathy with early respiratory failure: Occurrence in various populations. *J Neurol Neurosurg Psychiatry* 85: 345-353, 2014.
429. Pankiv S, Clausen TH, Lamark T, Brech A, Bruun JA, Outzen H, Øvervatn A, Bjørkøy G, Johansen T. p62/SQSTM1 binds directly to

Atg8/LC3 to facilitate degradation of ubiquitinated protein aggregates by autophagy. *J Biol Chem* 282: 24131-24145, 2007.
430. Patel BG, Wilder T, Solaro RJ. Novel control of cardiac myofilament response to calcium by S-glutathionylation at specific sites of myosin binding protein C. *Front Physiol* 4: 336, 2013.
431. Patra C, Monk KR, Engel FB. The multiple signaling modalities of adhesion G protein-coupled receptor GPR126 in development. *Receptors Clin Investig* 1: 79, 2014.
432. Peng J, Raddatz K, Molkentin JD, Wu Y, Labeit S, Granzier H, Gotthardt M. Cardiac hypertrophy and reduced contractility in hearts deficient in the titin kinase region. *Circulation* 115: 743-751, 2007.
433. Perera S, Holt MR, Mankoo BS, Gautel M. Developmental regulation of MURF ubiquitin ligases and autophagy proteins nbr1, p62/SQSTM1 and LC3 during cardiac myofibril assembly and turnover. *Dev Biol* 351: 46-61, 2011.
434. Periasamy M, Strehler EE, Garfinkel LI, Gubits RM, Ruiz-Opazo N, Nadal-Ginard B. Fast skeletal muscle myosin light chains 1 and 3 are produced from a single gene by a combined process of differential RNA transcription and splicing. *J Biol Chem* 259: 13595-13604, 1984.
435. Perry NA, Ackermann MA, Shriver M, Hu LY, Kontrogianni-Konstantopoulos A. Obscurins: Unassuming giants enter the spotlight. *IUBMB Life* 65: 479-486, 2013.
436. Perry NA, Shriver M, Mameza MG, Grabias B, Balzer E, Kontrogianni-Konstantopoulos A. Loss of giant obscurins promotes breast epithelial cell survival through apoptotic resistance. *FASEB J* 26: 2764-2775, 2012.
437. Person V, Kostin S, Suzuki K, Labeit S, Schaper J. Antisense oligonucleotide experiments elucidate the essential role of titin in sarcomerogenesis in adult rat cardiomyocytes in long-term culture. *J Cell Sci* 113 (Pt 21): 3851-3859, 2000.
438. Petzhold D, Lossie J, Keller S, Werner S, Haase H, Morano I. Human essential myosin light chain isoforms revealed distinct myosin binding, sarcomeric sorting, and inotropic activity. *Cardiovasc Res* 90: 513-520, 2011.
439. Petzhold D, Simsek B, Meissner R, Mahmoodzadeh S, Morano I. Distinct interactions between actin and essential myosin light chain isoforms. *Biochem Biophys Res Commun* 449: 284-288, 2014.
440. Pfeffer G, Chinnery PF. Reply: Hereditary myopathy with early respiratory failure is caused by mutations in the titin FN3 119 domain. *Brain* 137: e280, 2014.
441. Pfeffer G, Elliott HR, Griffin H, Barresi R, Miller J, Marsh J, Evilä A, Vihola A, Hackman P, Straub V, Dick DJ, Horvath R, Santibanez-Koref M, Udd B, Chinnery PF. Titin mutation segregates with hereditary myopathy with early respiratory failure. *Brain* 135: 1695-1713, 2012.
442. Pfeffer G, Sambuughin N, Olivé M, Tyndel F, Toro C, Goldfarb LG, Chinnery PF. A new disease allele for the p.C30071R mutation in titin causing hereditary myopathy with early respiratory failure. *Neuromuscul Disord* 24: 241-244, 2014.
443. Piazzesi G, Reconditi M, Linari M, Lucii L, Bianco P, Brunello E, Decostre V, Stewart A, Gore DB, Irving TC, Irving M, Lombardi V. Skeletal muscle performance determined by modulation of number of myosin motors rather than motor force or stroke size. *Cell* 131: 784-795, 2007.
444. Pinder JC, Taylor-Harris PM, Bennett PM, Carter E, Hayes NV, King MD, Holt MR, Maggs AM, Gascard P, Baines AJ. Isoforms of protein 4.1 are differentially distributed in heart muscle cells: Relation of 4.1R and 4.1G to components of the Ca^{2+} homeostasis system. *Exp Cell Res* 318: 1467-1479, 2012.
445. Pinotsis N, Chatziefthimiou SD, Berkemeier F, Beuron F, Mavridis IM, Konarev PV, Svergun DI, Morris E, Rief M, Wilmanns M. Superhelical architecture of the myosin filament-linking protein myomesin with unusual elastic properties. *PLoS Biol* 10: e1001261, 2012.
446. Pinotsis N, Lange S, Perriard JC, Svergun DI, Wilmanns M. Molecular basis of the C-terminal tail-to-tail assembly of the sarcomeric filament protein myomesin. *EMBO J* 27: 253-264, 2008.
447. Pizon V, Iakovenko A, Van Der Ven PF, Kelly R, Fatu C, Furst DO, Karsenti E, Gautel M. Transient association of titin and myosin with microtubules in nascent myofibrils directed by the MURF2 RING-finger protein. *J Cell Sci* 115: 4469-4482, 2002.
448. Pollazzon M, Suominen T, Penttilä S, Malandrini A, Carluccio MA, Mondelli M, Marozza A, Federico A, Renieri A, Hackman P, Dotti MT, Udd B. The first Italian family with tibial muscular dystrophy caused by a novel titin mutation. *J Neurol* 257: 575-579, 2010.
449. Previs MJ, Beck Previs S, Gulick J, Robbins J, Warshaw DM. Molecular mechanics of cardiac myosin-binding protein C in native thick filaments. *Science* 337: 1215-1218, 2012.
450. Previs MJ, Michalek AJ, Warshaw DM. Molecular modulation of actomyosin function by cardiac myosin-binding protein C. *Pflugers Arch* 466: 439-444, 2014.
451. Previs MJ, Mun JY, Michalek AJ, Previs SB, Gulick J, Robbins J, Warshaw DM, Craig R. Phosphorylation and calcium antagonistically tune myosin-binding protein C's structure and function. *Proc Natl Acad Sci U S A* 113: 3239-3244, 2016.
452. Price KM, Littler WA, Cummins P. Human atrial and ventricular myosin light-chains subunits in the adult and during development. *Biochem J* 191: 571-580, 1980.
453. Price MG, Landsverk ML, Barral JM, Epstein HF. Two mammalian UNC-45 isoforms are related to distinct cytoskeletal and muscle-specific functions. *J Cell Sci* 115: 4013-4023, 2002.
454. Puchner EM, Alexandrovich A, Kho AL, Hensen U, Schäfer LV, Brandmeier B, Gräter F, Grubmüller H, Gaub HE, Gautel M. Mechanoenzymatics of titin kinase. *Proc Natl Acad Sci U S A* 105: 13385-13390, 2008.
455. Qadota H, Benian GM. Molecular structure of sarcomere-to-membrane attachment at M-Lines in *C. elegans* muscle. *J Biomed Biotechnol* 2010: 864749, 2010.
456. Qadota H, Blangy A, Xiong G, Benian GM. The DH-PH region of the giant protein UNC-89 activates RHO-1 GTPase in *Caenorhabditis elegans* body wall muscle. *J Mol Biol* 383: 747-752, 2008.
457. Qadota H, Mayans O, Matsunaga Y, McMurry JL, Wilson KJ, Kwon GE, Stanford R, Deehan K, Tinley TL, Ngwa VM, Benian GM. The SH3 domain of UNC-89 (obscurin) interacts with paramyosin, a coiled-coil protein, in *Caenorhabditis elegans* muscle. *Mol Biol Cell* 27: 1606-1620, 2016.
458. Qadota H, McGaha LA, Mercer KB, Stark TJ, Ferrara TM, Benian GM. A novel protein phosphatase is a binding partner for the protein kinase domains of UNC-89 (Obscurin) in *Caenorhabditis elegans*. *Mol Biol Cell* 19: 2424-2432, 2008.
459. Qadota H, Mercer KB, Miller RK, Kaibuchi K, Benian GM. Two LIM domain proteins and UNC-96 link UNC-97/pinch to myosin thick filaments in *Caenorhabditis elegans* muscle. *Mol Biol Cell* 18: 4317-4326, 2007.
460. Raeker MO, Su F, Geisler SB, Borisov AB, Kontrogianni-Konstantopoulos A, Lyons SE, Russell MW. Obscurin is required for the lateral alignment of striated myofibrils in zebrafish. *Dev Dyn* 235: 2018-2029, 2006.
461. Ramirez-Correa GA, Jin W, Wang Z, Zhong X, Gao WD, Dias WB, Vecoli C, Hart GW, Murphy AM. O-linked GlcNAc modification of cardiac myofilament proteins: A novel regulator of myocardial contractile function. *Circ Res* 103: 1354-1358, 2008.
462. Ramirez-Correa GA, Ma J, Slawson C, Zeidan Q, Lugo-Fagundo NS, Xu M, Shen X, Gao WD, Caceres V, Chakir K, DeVine L, Cole RN, Marchionni L, Paolocci N, Hart GW, Murphy AM. Removal of abnormal myofilament O-GlcNAcylation restores Ca^{2+} sensitivity in diabetic cardiac muscle. *Diabetes* 64: 3573-3587, 2015.
463. Randazzo D, Blaauw B, Paolini C, Pierantozzi E, Spinozzi S, Lange S, Chen J, Protasi F, Reggiani C, Sorrentino V. Exercise-induced alterations and loss of sarcomeric M-line organization in the diaphragm muscle of obscurin knockout mice. *Am J Physiol Cell Physiol* 312: C16-C28, 2017.
464. Randazzo D, Giacomello E, Lorenzini S, Rossi D, Pierantozzi E, Blaauw B, Reggiani C, Lange S, Peter AK, Chen J, Sorrentino V. Obscurin is required for ankyrinB-dependent dystrophin localization and sarcolemma integrity. *J Cell Biol* 200: 523-536, 2013.
465. Ranum LP, Cooper TA. RNA-mediated neuromuscular disorders. *Annu Rev Neurosci* 29: 259-277, 2006.
466. Rarick HM, Opgenorth TJ, von Geldern TW, Wu-Wong JR, Solaro RJ. An essential myosin light chain peptide induces supramaximal stimulation of cardiac myofibrillar ATPase activity. *J Biol Chem* 271: 27039-27043, 1996.
467. Ratti J, Rostkova E, Gautel M, Pfuhl M. Structure and interactions of myosin-binding protein C domain C0: Cardiac-specific regulation of myosin at its neck? *J Biol Chem* 286: 12650-12658, 2011.
468. Ravenscroft G, Nolent F, Rajagopalan S, Meireles AM, Paavola KJ, Gaillard D, Alanio E, Buckland M, Arbuckle S, Krivanek M, Maluenda J, Pannell S, Gooding R, Ong RW, Allcock RJ, Carvalho ED, Carvalho MD, Kok F, Talbot WS, Melki J, Laing NG. Mutations of GPR126 are responsible for severe arthrogryposis multiplex congenita. *Am J Hum Genet* 96: 955-961, 2015.
469. Rayment I, Holden, HM. Myosin subfragment-1: Structure and function of a molecular motor. *Currt Opin Struct Biol* 3: 944-952, 1993.
470. Rayment I, Rypniewski WR, Schmidt-Base K, Smith R, Tomchick DR, Benning MM, Winkelmann DA, Wesenberg G, Holden HM. Three-dimensional structure of myosin subfragment-1: A molecular motor. *Science* 261: 50-58, 1993.
471. Razumova MV, Shaffer JF, Tu AY, Flint GV, Regnier M, Harris SP. Effects of the N-terminal domains of myosin binding protein-C in an in vitro motility assay: Evidence for long-lived cross-bridges. *J Biol Chem* 281: 35846-35854, 2006.
472. Reconditi M, Brunello E, Linari M, Bianco P, Narayanan T, Panine P, Piazzesi G, Lombardi V, Irving M. Motion of myosin head domains during activation and force development in skeletal muscle. *Proc Natl Acad Sci U S A* 108: 7236-7240, 2011.
473. Reddy KB, Fox JE, Price MG, Kulkarni S, Gupta S, Das B, Smith DM. Nuclear localization of Myomesin-1: Possible functions. *J Muscle Res Cell Motil* 29: 1-8, 2008.

474. Reiser PJ, Portman MA, Ning XH, Schomisch Moravec C. Human cardiac myosin heavy chain isoforms in fetal and failing adult atria and ventricles. *Am J Physiol Heart Circ Physiol* 280: H1814-H1820, 2001.
475. Rhee D, Sanger JM, Sanger JW. The premyofibril: Evidence for its role in myofibrillogenesis. *Cell Motil Cytoskeleton* 28: 1-24, 1994.
476. Rhoads AR, Friedberg F. Sequence motifs for calmodulin recognition. *FASEB J* 11: 331-340, 1997.
477. Ribeiro PA, Ribeiro JP, Minozzo FC, Pavlov I, Leu NA, Kurosaka S, Kashina A, Rassier DE. Contractility of myofibrils from the heart and diaphragm muscles measured with atomic force cantilevers: Effects of heart-specific deletion of arginyl-tRNA-protein transferase. *Int J Cardiol* 168: 3564-3571, 2013.
478. Rosas PC, Liu Y, Abdalla MI, Thomas CM, Kidwell DT, Dusio GF, Mukhopadhyay D, Kumar R, Baker KM, Mitchell BM, Powers PA, Fitzsimons DP, Patel BG, Warren CM, Solaro RJ, Moss RL, Tong CW. Phosphorylation of cardiac myosin-binding protein-C is a critical mediator of diastolic function. *Circ Heart Fail* 8: 582-594, 2015.
479. Rossi AC, Mammucari C, Argentini C, Reggiani C, Schiaffino S. Two novel/ancient myosins in mammalian skeletal muscles: MYH14/7b and MYH15 are expressed in extraocular muscles and muscle spindles. *J Physiol* 588: 353-364, 2010.
480. Rottbauer W, Gautel M, Zehelein J, Labeit S, Franz WM, Fischer C, Vollrath B, Mall G, Dietz R, Kubler W, Katus HA. Novel splice donor site mutation in the cardiac myosin-binding protein-C gene in familial hypertrophic cardiomyopathy. Characterization of cardiac transcript and protein. *J Clin Invest* 100: 475-482, 1997.
481. Rowland TJ, Graw SL, Sweet ME, Gigli M, Taylor MR, Mestroni L. Obscurin variants in patients with left ventricular noncompaction. *J Am Coll Cardiol* 68: 2237-2238, 2016.
482. Rubinstein NA, Kelly AM. Development of muscle fiber specialization in the rat hindlimb. *J Cell Biol* 90: 128-144, 1981.
483. Rundell KW, Tullson PC, Terjung RL. AMP deaminase binding in contracting rat skeletal muscle. *Am J Physiol* 263: C287-C293, 1992.
484. Rundell VL, Manaves V, Martin AF, de Tombe PP. Impact of beta-myosin heavy chain isoform expression on cross-bridge cycling kinetics. *Am J Physiol Heart Circ Physiol* 288: H896-H903, 2005.
485. Russell MW, Raeker MO, Korytkowski KA, Sonneman KJ. Identification, tissue expression and chromosomal localization of human obscurin-MLCK, a member of the titin and Dbl families of myosin light chain kinases. *Gene* 282: 237-246, 2002.
486. Rybakova IN, Greaser ML, Moss RL. Myosin binding protein C interaction with actin: Characterization and mapping of the binding site. *J Biol Chem* 286: 2008-2016, 2011.
487. Ryder DJ, Judge SM, Beharry AW, Farnsworth CL, Silva JC, Judge AR. Identification of the acetylation and ubiquitin-modified proteome during the progression of skeletal muscle atrophy. *PLoS One* 10: e0136247, 2015.
488. Sadayappan S, de Tombe PP. Cardiac myosin binding protein-C: Redefining its structure and function. *Biophys Rev* 4: 93-106, 2012.
489. Sadayappan S, de Tombe PP. Cardiac myosin binding protein-C as a central target of cardiac sarcomere signaling: A special mini review series. *Pflugers Arch* 466: 195-200, 2014.
490. Sadayappan S, Gulick J, Osinska H, Barefield D, Cuello F, Avkiran M, Lasko VM, Lorenz JN, Maillet M, Martin JL, Brown JH, Bers DM, Molkentin JD, James J, Robbins J. A critical function for Ser-282 in cardiac myosin binding protein-C phosphorylation and cardiac function. *Circ Res* 109: 141-150, 2011.
491. Sadayappan S, Gulick J, Osinska H, Martin LA, Hahn HS, Dorn GW, II, Klevitsky R, Seidman CE, Seidman JG, Robbins J. Cardiac myosin-binding protein-C phosphorylation and cardiac function. *Circ Res* 97: 1156-1163, 2005.
492. Sadayappan S, Osinska H, Klevitsky R, Lorenz JN, Sargent M, Molkentin JD, Seidman CE, Seidman JG, Robbins J. Cardiac myosin binding protein C phosphorylation is cardioprotective. *Proc Natl Acad Sci U S A* 103: 16918-16923, 2006.
493. Salih MA, Al Rayess M, Cutshall S, Urtizberea JA, Al-Turaiki MH, Ozo CO, Straub V, Akbar M, Abid M, Andeejani A, Campbell KP. A novel form of familial congenital muscular dystrophy in two adolescents. *Neuropediatrics* 29: 289-293, 1998.
494. Samant SA, Pillai VB, Sundaresan NR, Shroff SG, Gupta MP. Histone deacetylase 3 (HDAC3)-dependent reversible lysine acetylation of cardiac myosin heavy chain isoforms modulates their enzymatic and motor activity. *J Biol Chem* 290: 15559-15569, 2015.
495. Sanger JW, Kang S, Siebrands CC, Freeman N, Du A, Wang J, Stout AL, Sanger JM. How to build a myofibril. *J Muscle Res Cell Motil* 26: 343-354, 2005.
496. Sanger JW, Wang J, Fan Y, White J, Sanger JM. Assembly and dynamics of myofibrils. *J Biomed Biotechnol* 2010: 858606, 2010.
497. Sarparanta J, Blandin G, Charton K, Vihola A, Marchand S, Milic A, Hackman P, Ehler E, Richard I, Udd B. Interactions with M-band titin and calpain 3 link myospryn (CMYA5) to tibial and limb-girdle muscular dystrophies. *J Biol Chem* 285: 30304-30315, 2010.
498. Savitskaya MA, Onishchenko GE. Mechanisms of apoptosis. *Biochemistry (Mosc)* 80: 1393-1405, 2015.
499. Schaub MC, Tuchschmid CR, Srihari T, Hirzel HO. Myosin isoenzymes in human hypertrophic hearts. Shift in atrial myosin heavy chains and in ventricular myosin light chains. *Eur Heart J* 5 (Suppl F): 85-93, 1984.
500. Schiaffino S, Reggiani C. Fiber types in mammalian skeletal muscles. *Physiol Rev* 91: 1447-1531, 2011.
501. Schiaffino S, Rossi AC, Smerdu V, Leinwand LA, Reggiani C. Developmental myosins: Expression patterns and functional significance. *Skelet Muscle* 5: 22, 2015.
502. Schoenauer R, Bertoncini P, Machaidze G, Aebi U, Perriard JC, Hegner M, Agarkova I. Myomesin is a molecular spring with adaptable elasticity. *J Mol Biol* 349: 367-379, 2005.
503. Schoenauer R, Emmert MY, Felley A, Ehler E, Brokopp C, Weber B, Nemir M, Faggian GG, Pedrazzini T, Falk V, Hoerstrup SP, Agarkova I. EH-myomesin splice isoform is a novel marker for dilated cardiomyopathy. *Basic Res Cardiol* 106: 233-247, 2011.
504. Schoenauer R, Lange S, Hirschy A, Ehler E, Perriard JC, Agarkova I. Myomesin 3, a novel structural component of the M-band in striated muscle. *J Mol Biol* 376: 338-351, 2008.
505. Scruggs SB, Hinken AC, Thawornkaiwong A, Robbins J, Walker LA, de Tombe PP, Geenen DL, Buttrick PM, Solaro RJ. Ablation of ventricular myosin regulatory light chain phosphorylation in mice causes cardiac dysfunction in situ and affects neighboring myofilament protein phosphorylation. *J Biol Chem* 284: 5097-5106, 2009.
506. Scruggs SB, Reisdorph R, Armstrong ML, Warren CM, Reisdorph N, Solaro RJ, Buttrick PM. A novel, in-solution separation of endogenous cardiac sarcomeric proteins and identification of distinct charged variants of regulatory light chain. *Mol Cell Proteomics* 9: 1804-1818, 2010.
507. Seeley M, Huang W, Chen Z, Wolff WO, Lin X, Xu X. Depletion of zebrafish titin reduces cardiac contractility by disrupting the assembly of Z-discs and A-bands. *Circ Res* 100: 238-245, 2007.
508. Seibenhener ML, Babu JR, Geetha T, Wong HC, Krishna NR, Wooten MW. Sequestosome 1/p62 is a polyubiquitin chain binding protein involved in ubiquitin proteasome degradation. *Mol Cell Biol* 24: 8055-8068, 2004.
509. Seibenhener ML, Geetha T, Wooten MW. Sequestosome 1/p62—More than just a scaffold. *FEBS Lett* 581: 175-179, 2007.
510. Semsarian C, Ingles J, Maron MS, Maron BJ. New perspectives on the prevalence of hypertrophic cardiomyopathy. *J Am Coll Cardiol* 65: 1249-1254, 2015.
511. Shaffer JF, Kensler RW, Harris SP. The myosin-binding protein C motif binds to F-actin in a phosphorylation-sensitive manner. *J Biol Chem* 284: 12318-12327, 2009.
512. Shama KM, Suzuki A, Harada K, Fujitani N, Kimura H, Ohno S, Yoshida K. Transient up-regulation of myotonic dystrophy protein kinase-binding protein, MKBP, and HSP27 in the neonatal myocardium. *Cell Struct Funct* 24: 1-4, 1999.
513. Shamseldin HE, Tulbah M, Kurdi W, Nemer M, Alsahan N, Al Mardawi E, Khalifa O, Hashem A, Kurdi A, Babay Z, Bubshait DK, Ibrahim N, Abdulwahab F, Rahbeeni Z, Hashem M, Alkuraya FS. Identification of embryonic lethal genes in humans by autozygosity mapping and exome sequencing in consanguineous families. *Genome Biol* 16: 116, 2015.
514. Sheikh F, Lyon RC, Chen J. Getting the skinny on thick filament regulation in cardiac muscle biology and disease. *Trends Cardiovasc Med* 24: 133-141, 2014.
515. Sheikh F, Ouyang K, Campbell SG, Lyon RC, Chuang J, Fitzsimons D, Tangney J, Hidalgo CG, Chung CS, Cheng H, Dalton ND, Gu Y, Kasahara H, Ghassemian M, Omens JH, Peterson KL, Granzier HL, Moss RL, McCulloch AD, Chen J. Mouse and computational models link Mlc2v dephosphorylation to altered myosin kinetics in early cardiac disease. *J Clin Invest* 122: 1209-1221, 2012.
516. Shriver M, Marimuthu S, Paul C, Geist J, Seale T, Konstantopoulos K, Kontrogianni-Konstantopoulos A. Giant obscurins regulate the PI3K cascade in breast epithelial cells via direct binding to the PI3K/p85 regulatory subunit. *Oncotarget* 7: 45414-45428, 2016.
517. Shriver M, Stroka KM, Vitolo MI, Martin S, Huso DL, Konstantopoulos K, Kontrogianni-Konstantopoulos A. Loss of giant obscurins from breast epithelium promotes epithelial-to-mesenchymal transition, tumorigenicity and metastasis. *Oncogene* 34: 4248-4259, 2015.
518. Sieck GC, Han YS, Prakash YS, Jones KA. Cross-bridge cycling kinetics, actomyosin ATPase activity and myosin heavy chain isoforms in skeletal and smooth respiratory muscles. *Comp Biochem Physiol B Biochem Mol Biol* 119: 435-450, 1998.
519. Siedner S, Kruger M, Schroeter M, Metzler D, Roell W, Fleischmann BK, Hescheler J, Pfitzer G, Stehle R. Developmental changes in contractility and sarcomeric proteins from the early embryonic to the adult stage in the mouse heart. *J Physiol* 548: 493-505, 2003.
520. Siegert R, Perrot A, Keller S, Behlke J, Michalewska-Wludarczyk A, Wycisk A, Tendera M, Morano I, Ozcelik C. A myomesin mutation associated with hypertrophic cardiomyopathy deteriorates dimerisation properties. *Biochem Biophys Res Commun* 405: 473-479, 2011.

521. Silver PJ, Buja LM, Stull JT. Frequency-dependent myosin light chain phosphorylation in isolated myocardium. *J Mol Cell Cardiol* 18: 31-37, 1986.
522. Simonson TS, Zhang Y, Huff CD, Xing J, Watkins WS, Witherspoon DJ, Woodward SR, Jorde LB. Limited distribution of a cardiomyopathy-associated variant in India. *Ann Hum Genet* 74: 184-188, 2010.
523. Small TM, Gernert KM, Flaherty DB, Mercer KB, Borodovsky M, Benian GM. Three new isoforms of *Caenorhabditis elegans* UNC-89 containing MLCK-like protein kinase domains. *J Mol Biol* 342: 91-108, 2004.
524. Spencer JA, Eliazer S, Ilaria RL, Richardson JA, Olson EN. Regulation of microtubule dynamics and myogenic differentiation by MURF, a striated muscle RING-finger protein. *J Cell Biol* 150: 771-784, 2000.
525. Spooner PM, Bonner J, Maricq AV, Benian GM, Norman KR. Large isoforms of UNC-89 (obscurin) are required for muscle cell architecture and optimal calcium release in *Caenorhabditis elegans*. *PLoS One* 7: e40182, 2012.
526. Spudich JA, Aksel T, Bartholomew SR, Nag S, Kawana M, Yu EC, Sarkar SS, Sung J, Sommese RF, Sutton S, Cho C, Adhikari AS, Taylor R, Liu C, Trivedi D, Ruppel KM. Effects of hypertrophic and dilated cardiomyopathy mutations on power output by human beta-cardiac myosin. *J Exp Biol* 219: 161-167, 2016.
527. Squire JM. Muscle contraction: Sliding filament history, sarcomere dynamics and the two Huxleys. *Glob Cardiol Sci Pract* 2016: 11, 2016.
528. Squire JM, Harford JJ, Edman AC, Sjostrom M. Fine structure of the A-band in cryo-sections. III. Crossbridge distribution and the axial structure of the human C-zone. *J Mol Biol* 155: 467-494, 1982.
529. Squire JM, Luther PK, Knupp C. Structural evidence for the interaction of C-protein (MyBP-C) with actin and sequence identification of a possible actin-binding domain. *J Mol Biol* 331: 713-724, 2003.
530. Squire JM, Paul DM, Morris EP. Myosin and actin filaments in muscle: Structures and interactions. *Subcell Biochem* 82: 319-371, 2017.
531. Starr R, Offer G. Polypeptide chains of intermediate molecular weight in myosin preparations. *FEBS Lett* 15: 40-44, 1971.
532. Stennicke HR, Jurgensmeier JM, Shin H, Deveraux Q, Wolf BB, Yang X, Zhou Q, Ellerby HM, Ellerby LM, Bredesen D, Green DR, Reed JC, Froelich CJ, Salvesen GS. Pro-caspase-3 is a major physiologic target of caspase-8. *J Biol Chem* 273: 27084-27090, 1998.
533. Stewart MA, Franks-Skiba K, Chen S, Cooke R. Myosin ATP turnover rate is a mechanism involved in thermogenesis in resting skeletal muscle fibers. *Proc Natl Acad Sci U S A* 107: 430-435, 2010.
534. Straub FB. Actin, II. *Stud Inst Med Chem Univ Szeged* III: 23-37, 1943.
535. Strehler EE, Pelloni G, Heizmann CW, Eppenberger HM. M-protein in chicken cardiac muscle. *Exp Cell Res* 124: 39-45, 1979.
536. Stuart CA, Stone WL, Howell ME, Brannon MF, Hall HK, Gibson AL, Stone MH. Myosin content of individual human muscle fibers isolated by laser capture microdissection. *Am J Physiol Cell Physiol* 310: C381-C389, 2016.
537. Stull JT, Lin PJ, Krueger JK, Trewhella J, Zhi G. Myosin light chain kinase: Functional domains and structural motifs. *Acta Physiol Scand* 164: 471-482, 1998.
538. Subahi SA. Distinguishing cardiac features of a novel form of congenital muscular dystrophy (Salih cmd). *Pediatr Cardiol* 22: 297-301, 2001.
539. Sumandea MP, Pyle WG, Kobayashi T, de Tombe PP, Solaro RJ. Identification of a functionally critical protein kinase C phosphorylation residue of cardiac troponin T. *J Biol Chem* 278: 35135-35144, 2003.
540. Sutoh K. An actin-binding site on the 20K fragment of myosin subfragment 1. *Biochemistry* 21: 4800-4804, 1982.
541. Sutoh K. Identification of myosin-binding sites on the actin sequence. *Biochemistry* 21: 3654-3661, 1982.
542. Sweeney HL. Function of the N terminus of the myosin essential light chain of vertebrate striated muscle. *Biophys J* 68: 112S-118S; discussion 118S-119S, 1995.
543. Szent-Gyorgyi AG. The early history of the biochemistry of muscle contraction. *J Gen Physiol* 123: 631-641, 2004.
544. Tajsharghi H, Hammans S, Lindberg C, Lossos A, Clarke NF, Mazanti I, Waddell LB, Fellig Y, Foulds N, Katifi H, Webster R, Raheem O, Udd B, Argov Z, Oldfors A. Recessive myosin myopathy with external ophthalmoplegia associated with MYH2 mutations. *Eur J Hum Genet* 22: 801-808, 2014.
545. Tajsharghi H, Oldfors A. Myosinopathies: Pathology and mechanisms. *Acta Neuropathol* 125: 3-18, 2013.
546. Tanaka M, Konishi H, Touhara K, Sakane F, Hirata M, Ono Y, Kikkawa U. Identification of myosin II as a binding protein to the PH domain of protein kinase B. *Biochem Biophys Res Commun* 255: 169-174, 1999.
547. Taniguchi M, Okamoto R, Ito M, Goto I, Fujita S, Konishi K, Mizutani H, Dohi K, Hartshorne DJ, Itoh T. New isoform of cardiac myosin light chain kinase and the role of cardiac myosin phosphorylation in alpha1-adrenoceptor mediated inotropic response. *PLoS One* 10: e0141130, 2015.
548. Taveau M, Bourg N, Sillon G, Roudaut C, Bartoli M, Richard I. Calpain 3 is activated through autolysis within the active site and lyses sarcomeric and sarcolemmal components. *Mol Cell Biol* 23: 9127-9135, 2003.
549. Taylor M, Graw S, Sinagra G, Barnes C, Slavov D, Brun F, Pinamonti B, Salcedo EE, Sauer W, Pyxaras S, Anderson B, Simon B, Bogomolovas J, Labeit S, Granzier H, Mestroni L. Genetic variation in titin in arrhythmogenic right ventricular cardiomyopathy-overlap syndromes. *Circulation* 124: 876-885, 2011.
550. Taylor-Harris PM, Keating LA, Maggs AM, Phillips GW, Birks EJ, Franklin RC, Yacoub MH, Baines AJ, Pinder JC. Cardiac muscle cell cytoskeletal protein 4.1: Analysis of transcripts and subcellular location—Relevance to membrane integrity, microstructure, and possible role in heart failure. *Mamm Genome* 16: 137-151, 2005.
551. Temple JE, Oehler MC, Wright NT. Chemical shift assignments for the Ig2 domain of human obscurin A. *Biomol NMR Assign* 10: 63-65, 2016.
552. Timson DJ, Trayer HR, Smith KJ, Trayer IP. Size and charge requirements for kinetic modulation and actin binding by alkali 1-type myosin essential light chains. *J Biol Chem* 274: 18271-18277, 1999.
553. Timson DJ, Trayer HR, Trayer IP. The N-terminus of A1-type myosin essential light chains binds actin and modulates myosin motor function. *Eur J Biochem* 255: 654-662, 1998.
554. Tong CW, Stelzer JE, Greaser ML, Powers PA, Moss RL. Acceleration of crossbridge kinetics by protein kinase A phosphorylation of cardiac myosin binding protein C modulates cardiac function. *Circ Res* 103: 974-982, 2008.
555. Tong CW, Wu X, Liu Y, Rosas PC, Sadayappan S, Hudmon A, Muthuchamy M, Powers PA, Valdivia HH, Moss RL. Phosphoregulation of cardiac inotropy via myosin binding protein-C during increased pacing frequency or beta1-adrenergic stimulation. *Circ Heart Fail* 8: 595-604, 2015.
556. Tong SW, Elzinga M. The sequence of the NH2-terminal 204-residue fragment of the heavy chain of rabbit skeletal muscle myosin. *J Biol Chem* 258: 13100-13110, 1983.
557. Toro C, Olivé M, Dalakas MC, Sivakumar K, Bilbao JM, Tyndel F, Vidal N, Farrero E, Sambuughin N, Goldfarb LG. Exome sequencing identifies titin mutations causing hereditary myopathy with early respiratory failure (HMERF) in families of diverse ethnic origins. *BMC Neurol* 13: 29, 2013.
558. Toydemir RM, Rutherford A, Whitby FG, Jorde LB, Carey JC, Bamshad MJ. Mutations in embryonic myosin heavy chain (MYH3) cause Freeman-Sheldon syndrome and Sheldon-Hall syndrome. *Nat Genet* 38: 561-565, 2006.
559. Trayer IP, Trayer HR, Levine BA. Evidence that the N-terminal region of A1-light chain of myosin interacts directly with the C-terminal region of actin. A proton magnetic resonance study. *Eur J Biochem* 164: 259-266, 1987.
560. Trinick J, Lowey S. M-protein from chicken pectoralis muscle: Isolation and characterization. *J Mol Biol* 113: 343-368, 1977.
561. Tskhovrebova L, Trinick J. Properties of titin immunoglobulin and fibronectin-3 domains. *J Biol Chem* 279: 46351-46354, 2004.
562. Tskhovrebova L, Trinick J. Roles of titin in the structure and elasticity of the sarcomere. *J Biomed Biotechnol* 2010: 612482, 2010.
563. Tskhovrebova L, Trinick J. Titin and nebulin in thick and thin filament length regulation. *Subcell Biochem* 82: 285-318, 2017.
564. Udd B, Haravuori H, Kalimo H, Partanen J, Pulkkinen L, Paetau A, Peltonen L, Somer H. Tibial muscular dystrophy—From clinical description to linkage on chromosome 2q31. *Neuromuscul Disord* 8: 327-332, 1998.
565. Udd B, Kääriänen H, Somer H. Muscular dystrophy with separate clinical phenotypes in a large family. *Muscle Nerve* 14: 1050-1058, 1991.
566. Udd B, Partanen J, Halonen P, Falck B, Hakamies L, Heikkilä H, Ingo S, Kalimo H, Kääriäinen H, Laulumaa V. Tibial muscular dystrophy. Late adult-onset distal myopathy in 66 Finnish patients. *Arch Neurol* 50: 604-608, 1993.
567. Van den Bergh PY, Bouquiaux O, Verellen C, Marchand S, Richard I, Hackman P, Udd B. Tibial muscular dystrophy in a Belgian family. *Ann Neurol* 54: 248-251, 2003.
568. van der Ven PF, Bartsch JW, Gautel M, Jockusch H, Furst DO. A functional knock-out of titin results in defective myofibril assembly. *J Cell Sci* 113 (Pt 8): 1405-1414, 2000.
569. Van der Ven PF, Ehler E, Perriard JC, Furst DO. Thick filament assembly occurs after the formation of a cytoskeletal scaffold. *J Muscle Res Cell Motil* 20: 569-579, 1999.
570. van Dijk SJ, Bezold KL, Harris SP. Earning stripes: Myosin binding protein-C interactions with actin. *Pflugers Arch* 466: 445-450, 2014.
571. van Dijk SJ, Dooijes D, dos Remedios C, Michels M, Lamers JM, Winegrad S, Schlossarek S, Carrier L, ten Cate FJ, Stienen GJ, van der Velden J. Cardiac myosin-binding protein C mutations and hypertrophic cardiomyopathy: Haploinsufficiency, deranged phosphorylation, and cardiomyocyte dysfunction. *Circulation* 119: 1473-1483, 2009.

572. van Spaendonck-Zwarts KY, Posafalvi A, van den Berg MP, Hilfiker-Kleiner D, Bollen IA, Sliwa K, Alders M, Almomani R, van Langen IM, van der Meer P, Sinke RJ, van der Velden J, Van Veldhuisen DJ, van Tintelen JP, Jongbloed JD. Titin gene mutations are common in families with both peripartum cardiomyopathy and dilated cardiomyopathy. *Eur Heart J* 35: 2165-2173, 2014.
573. Vandenboom R. Modulation of skeletal muscle contraction by myosin phosphorylation. *Compr Physiol* 7: 171-212, 2016.
574. Vandenboom R, Gittings W, Smith IC, Grange RW, Stull JT. Myosin phosphorylation and force potentiation in skeletal muscle: Evidence from animal models. *J Muscle Res Cell Motil* 34: 317-332, 2013.
575. Vaughan KT, Weber FE, Einheber S, Fischman DA. Molecular cloning of chicken myosin-binding protein (MyBP) H (86-kDa protein) reveals extensive homology with MyBP-C (C-protein) with conserved immunoglobulin C2 and fibronectin type III motifs. *J Biol Chem* 268: 3670-3676, 1993.
576. Vaughan KT, Weber FE, Ried T, Ward DC, Reinach FC, Fischman DA. Human myosin-binding protein H (MyBP-H): Complete primary sequence, genomic organization, and chromosomal localization. *Genomics* 16: 34-40, 1993.
577. Venolia L, Waterston RH. The unc-45 gene of *Caenorhabditis elegans* is an essential muscle-affecting gene with maternal expression. *Genetics* 126: 345-353, 1990.
578. Vignier N, Schlossarek S, Fraysse B, Mearini G, Kramer E, Pointu H, Mougenot N, Guiard J, Reimer R, Hohenberg H, Schwartz K, Vernet M, Eschenhagen T, Carrier L. Nonsense-mediated mRNA decay and ubiquitin-proteasome system regulate cardiac myosin-binding protein C mutant levels in cardiomyopathic mice. *Circ Res* 105: 239-248, 2009.
579. Vivarelli E, Brown WE, Whalen RG, Cossu G. The expression of slow myosin during mammalian somitogenesis and limb bud differentiation. *J Cell Biol* 107: 2191-2197, 1988.
580. Waldmuller S, Sakthivel S, Saadi AV, Selignow C, Rakesh PG, Golubenko M, Joseph PK, Padmakumar R, Richard P, Schwartz K, Tharakan JM, Rajamanickam C, Vosberg HP. Novel deletions in MYH7 and MYBPC3 identified in Indian families with familial hypertrophic cardiomyopathy. *J Mol Cell Cardiol* 35: 623-636, 2003.
581. Walklate J, Ujfalusi Z, Geeves MA. Myosin isoforms and the mechanochemical cross-bridge cycle. *J Exp Biol* 219: 168-174, 2016.
582. Wallimann T, Wyss M, Brdiczka D, Nicolay K, Eppenberger HM. Intracellular compartmentation, structure and function of creatine kinase isoenzymes in tissues with high and fluctuating energy demands: The 'phosphocreatine circuit' for cellular energy homeostasis. *Biochem J* 281 (Pt 1): 21-40, 1992.
583. Wang K, McClure J, Tu A. Titin: Major myofibrillar components of striated muscle. *Proc Natl Acad Sci U S A* 76: 3698-3702, 1979.
584. Wang K, Ramirez-Mitchell R, Palter D. Titin is an extraordinarily long, flexible, and slender myofibrillar protein. *Proc Natl Acad Sci U S A* 81: 3685-3689, 1984.
585. Wang L, Muthu P, Szczesna-Cordary D, Kawai M. Characterizations of myosin essential light chain's N-terminal truncation mutant Delta43 in transgenic mouse papillary muscles by using tension transients in response to sinusoidal length alterations. *J Muscle Res Cell Motil* 34: 93-105, 2013.
586. Wang SM, Jeng CJ, Sun MC. Studies on the interaction between titin and myosin. *Histol Histopathol* 7: 333-337, 1992.
587. Wang X, Liu X, Wang S, Luan K. Myofibrillogenesis regulator 1 induces hypertrophy by promoting sarcomere organization in neonatal rat cardiomyocytes. *Hypertens Res* 35: 597-603, 2012.
588. Wang Y, Szczesna-Cordary D, Craig R, Diaz-Perez Z, Guzman G, Miller T, Potter JD. Fast skeletal muscle regulatory light chain is required for fast and slow skeletal muscle development. *FASEB J* 21: 2205-2214, 2007.
589. Warkman AS, Whitman SA, Miller MK, Garriock RJ, Schwach CM, Gregorio CC, Krieg PA. Developmental expression and cardiac transcriptional regulation of Myh7b, a third myosin heavy chain in the vertebrate heart. *Cytoskeleton (Hoboken)* 69: 324-335, 2012.
590. Warner A, Xiong G, Qadota H, Rogalski T, Vogl AW, Moerman DG, Benian GM. CPNA-1, a copine domain protein, is located at integrin adhesion sites and is required for myofilament stability in *Caenorhabditis elegans*. *Mol Biol Cell* 24: 601-616, 2013.
591. Waters S, Marchbank K, Solomon E, Whitehouse C, Gautel M. Interactions with LC3 and polyubiquitin chains link nbr1 to autophagic protein turnover. *FEBS Lett* 583: 1846-1852, 2009.
592. Waterston RH, Thomson JN, Brenner S. Mutants with altered muscle structure of *Caenorhabditis elegans*. *Dev Biol* 77: 271-302, 1980.
593. Watkins H, Conner D, Thierfelder L, Jarcho JA, MacRae C, McKenna WJ, Maron BJ, Seidman JG, Seidman CE. Mutations in the cardiac myosin binding protein-C gene on chromosome 11 cause familial hypertrophic cardiomyopathy. *Nat Genet* 11: 434-437, 1995.
594. Weber FE, Vaughan KT, Reinach FC, Fischman DA. Complete sequence of human fast-type and slow-type muscle myosin-binding-protein C (MyBP-C). Differential expression, conserved domain structure and chromosome assignment. *Eur J Biochem* 216: 661-669, 1993.
595. Webster C, Silberstein L, Hays AP, Blau HM. Fast muscle fibers are preferentially affected in Duchenne muscular dystrophy. *Cell* 52: 503-513, 1988.
596. Weisberg A, Winegrad S. Alteration of myosin cross bridges by phosphorylation of myosin-binding protein C in cardiac muscle. *Proc Natl Acad Sci U S A* 93: 8999-9003, 1996.
597. Weith AE, Previs MJ, Hoeprich GJ, Previs SB, Gulick J, Robbins J, Warshaw DM. The extent of cardiac myosin binding protein-C phosphorylation modulates actomyosin function in a graded manner. *J Muscle Res Cell Motil* 33: 449-459, 2012.
598. Wessels A, Vermeulen JL, Viragh S, Kalman F, Lamers WH, Moorman AF. Spatial distribution of "tissue-specific" antigens in the developing human heart and skeletal muscle. II. An immunohistochemical analysis of myosin heavy chain isoform expression patterns in the embryonic heart. *Anat Rec* 229: 355-368, 1991.
599. Weterman MA, Barth PG, van Spaendonck-Zwarts KY, Aronica E, Poll-The BT, Brouwer OF, van Tintelen JP, Qahar Z, Bradley EJ, de Wissel M, Salviati L, Angelini C, van den Heuvel L, Thomasse YE, Backx AP, Nurnberg G, Nurnberg P, Baas F. Recessive MYL2 mutations cause infantile type I muscle fibre disease and cardiomyopathy. *Brain* 136: 282-293, 2013.
600. Whiting A, Wardale J, Trinick J. Does titin regulate the length of muscle thick filaments? *J Mol Biol* 205: 263-268, 1989.
601. Whitten AE, Jeffries CM, Harris SP, Trewhella J. Cardiac myosin-binding protein C decorates F-actin: Implications for cardiac function. *Proc Natl Acad Sci U S A* 105: 18360-18365, 2008.
602. Willis CD, Oashi T, Busby B, Mackerell AD, Jr., Bloch RJ. Hydrophobic residues in small ankyrin 1 participate in binding to obscurin. *Mol Membr Biol* 29: 36-51, 2012.
603. Wilson KJ, Qadota H, Mains PE, Benian GM. UNC-89 (obscurin) binds to MEL-26, a BTB-domain protein, and affects the function of MEI-1 (katanin) in striated muscle of *Caenorhabditis elegans*. *Mol Biol Cell* 23: 2623-2634, 2012.
604. Winegrad S. Cardiac myosin binding protein C. *Circ Res* 84: 1117-1126, 1999.
605. Witt SH, Granzier H, Witt CC, Labeit S. MURF-1 and MURF-2 target a specific subset of myofibrillar proteins redundantly: Towards understanding MURF-dependent muscle ubiquitination. *J Mol Biol* 350: 713-722, 2005.
606. Wohlgemuth SL, Crawford BD, Pilgrim DB. The myosin co-chaperone UNC-45 is required for skeletal and cardiac muscle function in zebrafish. *Dev Biol* 303: 483-492, 2007.
607. Wu HC, Yamankurt G, Luo J, Subramaniam J, Hashmi SS, Hu H, Cunha SR. Identification and characterization of two ankyrin-B isoforms in mammalian heart. *Cardiovasc Res* 107: 466-477, 2015.
608. Xiao S, Grater F. Molecular basis of the mechanical hierarchy in myomesin dimers for sarcomere integrity. *Biophys J* 107: 965-973, 2014.
609. Xiong G, Qadota H, Mercer KB, McGaha LA, Oberhauser AF, Benian GM. A LIM-9 (FHL)/SCPL-1 (SCP) complex interacts with the C-terminal protein kinase regions of UNC-89 (obscurin) in *Caenorhabditis elegans* muscle. *J Mol Biol* 386: 976-988, 2009.
610. Xu J, Li Z, Ren X, Dong M, Li J, Shi X, Zhang Y, Xie W, Sun Z, Liu X, Dai Q. Investigation of pathogenic genes in Chinese sporadic hypertrophic cardiomyopathy patients by whole exome sequencing. *Sci Rep* 5: 16609, 2015.
611. Xu Q, Dewey S, Nguyen S, Gomes AV. Malignant and benign mutations in familial cardiomyopathies: Insights into mutations linked to complex cardiovascular phenotypes. *J Mol Cell Cardiol* 48: 899-909, 2010.
612. Yagi N. An x-ray diffraction study on early structural changes in skeletal muscle contraction. *Biophys J* 84: 1093-1102, 2003.
613. Yamamoto K. The binding of skeletal muscle C-protein to regulated actin. *FEBS Lett* 208: 123-127, 1986.
614. Yasuda M, Koshida S, Sato N, Obinata T. Complete primary structure of chicken cardiac C-protein (MyBP-C) and its expression in developing striated muscles. *J Mol Cell Cardiol* 27: 2275-2286, 1995.
615. Yin Z, Ren J, Guo W. Sarcomeric protein isoform transitions in cardiac muscle: A journey to heart failure. *Biochim Biophys Acta* 1852: 47-52, 2015.
616. Yoskovitz G, Peled Y, Gramlich M, Lahat H, Resnik-Wolf H, Feinberg MS, Afek A, Pras E, Arad M, Gerull B, Freimark D. A novel titin mutation in adult-onset familial dilated cardiomyopathy. *Am J Cardiol* 109: 1644-1650, 2012.
617. Young P, Ehler E, Gautel M. Obscurin, a giant sarcomeric Rho guanine nucleotide exchange factor protein involved in sarcomere assembly. *J Cell Biol* 154: 123-136, 2001.
618. Yu H, Chakravorty S, Song W, Ferenczi MA. Phosphorylation of the regulatory light chain of myosin in striated muscle: Methodological perspectives. *Eur Biophys J* 45: 779-805, 2016.
619. Yuan C, Guo Y, Ravi R, Przyklenk K, Shilkofski N, Diez R, Cole RN, Murphy AM. Myosin binding protein C is differentially phosphorylated upon myocardial stunning in canine and rat hearts—Evidence for novel phosphorylation sites. *Proteomics* 6: 4176-4186, 2006.

620. Yuan CC, Muthu P, Kazmierczak K, Liang J, Huang W, Irving TC, Kanashiro-Takeuchi RM, Hare JM, Szczesna-Cordary D. Constitutive phosphorylation of cardiac myosin regulatory light chain prevents development of hypertrophic cardiomyopathy in mice. *Proc Natl Acad Sci U S A* 112: E4138-E4146, 2015.
621. Yue D, Gao M, Zhu W, Luo S, Xi J, Wang B, Li Y, Cai S, Li J, Wang Y, Lu J, Zhao C. New disease allele and de novo mutation indicate mutational vulnerability of titin exon 343 in hereditary myopathy with early respiratory failure. *Neuromuscul Disord* 25: 172-176, 2015.
622. Zammit PS, Kelly RG, Franco D, Brown N, Moorman AF, Buckingham ME. Suppression of atrial myosin gene expression occurs independently in the left and right ventricles of the developing mouse heart. *Dev Dyn* 217: 75-85, 2000.
623. Zheng X, Cartee GD. Insulin-induced effects on the subcellular localization of AKT1, AKT2 and AS160 in rat skeletal muscle. *Sci Rep* 6: 39230, 2016.
624. Zhi G, Ryder JW, Huang J, Ding P, Chen Y, Zhao Y, Kamm KE, Stull JT. Myosin light chain kinase and myosin phosphorylation effect frequency-dependent potentiation of skeletal muscle contraction. *Proc Natl Acad Sci U S A* 102: 17519-17524, 2005.
625. Zhou Z, Huang W, Liang J, Szczesna-Cordary D. Molecular and functional effects of a splice site mutation in the MYL2 gene associated with cardioskeletal myopathy and early cardiac death in infants. *Front Physiol* 7: 240, 2016.
626. Zoghbi ME, Woodhead JL, Moss RL, Craig R. Three-dimensional structure of vertebrate cardiac muscle myosin filaments. *Proc Natl Acad Sci U S A* 105: 2386-2390, 2008.